

# **GEOLOGY FOR SOCIETY**

SINCE 1858



**GEOLOGICAL  
SURVEY OF  
NORWAY**

· NGU ·

**NGU REPORT  
2022.021**

---

Mineral soil  
geochemistry in  
Hedmark







<b>Report no.:</b> 2022.021	<b>ISSN:</b> 0800-3416 (print) ISSN: 2387-3515 (online)	<b>Grading:</b> Open	
<b>Title:</b> Mineral soil geochemistry in Hedmark			
<b>Authors:</b> Belinda Flem, Pedro Acosta-Gongora, Tor Erik Finne, Martin Klug		<b>Client:</b> NGU	
<b>County:</b> Innlandet		<b>Municipalities:</b> Kongsvinger, Hamar, Lillehammer, Gjøvik, Ringsaker, Løten, Stange, Nord-Odal, Sør-Odal, Eidskog, Grue, Åsnes, Våler, Elverum, Trysil, Åmot, Stor-Elvdal, Rendalen, Engerdal, Tolga, Tynset, Alvdal, Follidal, Os	
<b>Map-sheet name (M=1:250.000):</b> Røros, Lillehammer, Hamar, Sveig, Orsa, Torsby		<b>Map-sheet no. &amp; name (M1:50.000):</b>	
<b>Deposit name and grid-reference:</b>		<b>Number of pages:</b> 155 <b>Price (NOK):</b> 470 <b>Map enclosures:</b>	
<b>Fieldwork carried out:</b> 2019 - 2021	<b>Date of report:</b> xxx	<b>Project no.:</b> 351700	<b>Person responsible:</b> <i>Siw Taftø</i> Siw Taftø

## Summary

This report present results from mineral soil geochemistry from a survey of former Hedmark county, now part of Innlandet county. It is a continuation of corresponding surveys undertaken in the counties Finnmark, Troms, Nordland, and Trøndelag. During the main field work in 2019 and 2020, and complementary field work in 2021, 787 locations where visited. The mineral soil samples were collected based on a loose 6x6 km grid. The <2 mm dried grain size fraction of these samples were analysed by ICPMS for 53 elements following an Aqua Regia digestion. Results are documented with respect to quality of data in tables with descriptive statistics, random plots, X-charts, and correlation plots, in addition to EDA geochemical maps of single elements. For the first time magnetic susceptibility is measured and made available for the samples collected by the national geochemical mapping program of mineral soil.

## Keywords

Till	geochemistry	Hedmark
Mineral soil	Aqua Regia	Magnetic susceptibility
Regional mapping		





## Table of contents

1. INTRODUCTION	6
2 DESCRIPTION OF THE SURVEY AREA	7
2.1 Bedrock and quaternary deposits	7
2.2 Known mineral deposits	10
3 METHODS	12
3.1 Field work	12
3.2 Sample preparation and quality control	15
3.3 Laboratory analyses	15
3.4 Magnetic susceptibility	16
4 RESULTS	19
4.1 Method detection limits	19
4.2 Analytical quality control, QC	22
4.2.1 NGU project standard, MINS	22
4.2.2 NGU standard, MINN	23
4.2.2 Samples re-analysed from previous surveys	23
4.3 Precision and Analysis of variance (ANOVA)	24
4.4 Survey data and maps	25
5 Preliminary interpretation OF the results	26
6 Summary	28
Acknowledgments	29
References	30
TABLES	33
Table A1 The MINS Project standard (Sagelva).	34
Table A2 Bureau Veritas (ACME) standard DS11	36
Table A3 Bureau Veritas (ACME) standard OREAS262	38
Table A4 The MINN Project standard.	40
Table A5 Precision of duplicates	42
Table A6 ANOVA	44
Table A7 Survey data	45
APPENDIXES	49
Appendix 1: Random plots	
Appendix 2: X-charts including analysis of splits with the MINN in-house standard from 2019 and 2022	
Appendix 3: Samples re-analysed from previous surveys	
Appendix 4: Correlation plots field duplicates and analytical duplicates	
Appendix 5: ECDF-PLOTS	
Appendix 6: Geochemical maps	



## 1. INTRODUCTION

As part of the national geochemical mapping program of soil, mineral soil, mainly till, were collected in Hedmark during the field seasons 2019-2021 at a density of 1 sample/ 36 km<sup>2</sup>. An overview of the mapping progress is given in Table 1.1.

**Table 1.1 Progress in the national geochemical mapping program of Norway.**

Survey	Year	Sampling density	Soil	Analysed fraction	Lab
Finnmark and Troms <sup>1)</sup>	2011	1/40 km <sup>2</sup>	Till	<0.063mm	ACME <sup>*)</sup>
Nordland <sup>1)</sup>	2011	1/40 km <sup>2</sup>	Till	<2mm	ACME <sup>*)</sup>
North-Trøndelag and Fosen <sup>2, 3)</sup>	2013	1/36 km <sup>2</sup>	Till Humus	<2mm	ACME <sup>*)</sup>
Southern Trøndelag <sup>4, 5)</sup>	2018/2019	1/36 km <sup>2</sup>	Till Humus	<2mm	ACME <sup>*)</sup>

<sup>1)</sup>Reimann et al., 2011

<sup>2)</sup>Finne et al., 2014

<sup>3)</sup>Finne and Eggen, 2015

<sup>4)</sup>Flem et al., 2020

<sup>5)</sup>Flem et al., 2021

<sup>\*)</sup> At present, operating as Bureau Veritas Commodities Canada Ltd.

The data from Trøndelag county have been further documented and investigated by Reimann et al., (2015; 2016; 2019), Fabian et al., (2017), Acosta-Gongora et al., (2021), Flem et al., (2022), and others. Based on the benefit and increased possibility to interpret possible areas of interest for mineral exploration and anthropogenic influence NGU decided to continue to sample both organic and bottom soil in the continuation of the national geochemical mapping program. This report presents the quality of the mineral soil samples and their analysis. Sampling and geochemical analysis of humus will be presented in a separate quality control report (QC-report). The analytical data is available at <https://www.ngu.no/> or by request to NGU. The photos from each sample location are available at [https://geo.ngu.no/kart/geokjemi\\_mobil/](https://geo.ngu.no/kart/geokjemi_mobil/).

## 2 DESCRIPTION OF THE SURVEY AREA

### 2.1 Bedrock and quaternary deposits

Hedmark can be divided into four main bedrock areas (Fig. 2.1). The southernmost area is part of the basement, dominated by gneisses and granites. The topography of this area is relatively uniform with low altitudes < 500 m. Towards the north, the bedrock changes to deposits of Cambro-Silurian age, limestone, and clay slate in alternating layers. Further north, the bedrock consists of staurolite from the late Precambrian, which extends far north and covers the majority of Hedmark. In the northernmost part of Hedmark, the area belongs to the Caledonian mountain range with elevations from 600 to > 2000 m. This area is dominated by the Trondheim fields, heavily converted Cambro-Silurian slate, penetrated by magmatic rocks in connection with the Caledonian mountain range folding (e.g., Dahl et al., 2017; Ramberg et al., 2008). Figure 2.1 and Appendix 6 shows the bedrock map of Hedmark, with adjacent areas, based on the NGU bedrock map of Norway with scale 1:1 350 000 (Geological Survey of Norway, 2021).

Quaternary deposits in Hedmark are well described by Olsen et al. (2017). With some known exceptions, the loose deposits in Hedmark formed during the last ice age and during the melting phase of the great inland ice which at its largest reached all the way to the continental shelf. The ice edge retreated from the coast in the west and in the south inland, the entire Hedmark was ice-free for approx. 9500 years ago (Olsen et al., 2017). Moraine material was deposited by the ice and covers approximately 74% of the surface. Glaciofluvial deposits and river material (block, stone, gravel, and sand), sea and fjord deposits (marine sediments: silt and clay), including beach material (stone, gravel, and sand), and marsh soil (peat), together with lakes cover almost 22% of the area. Other deposits cover only small fields, and bare rock only 4.1% of the county. Quaternary geological map of Hedmark is available at [https://geo.ngu.no/kart/kartkatalog\\_mobil/](https://geo.ngu.no/kart/kartkatalog_mobil/).



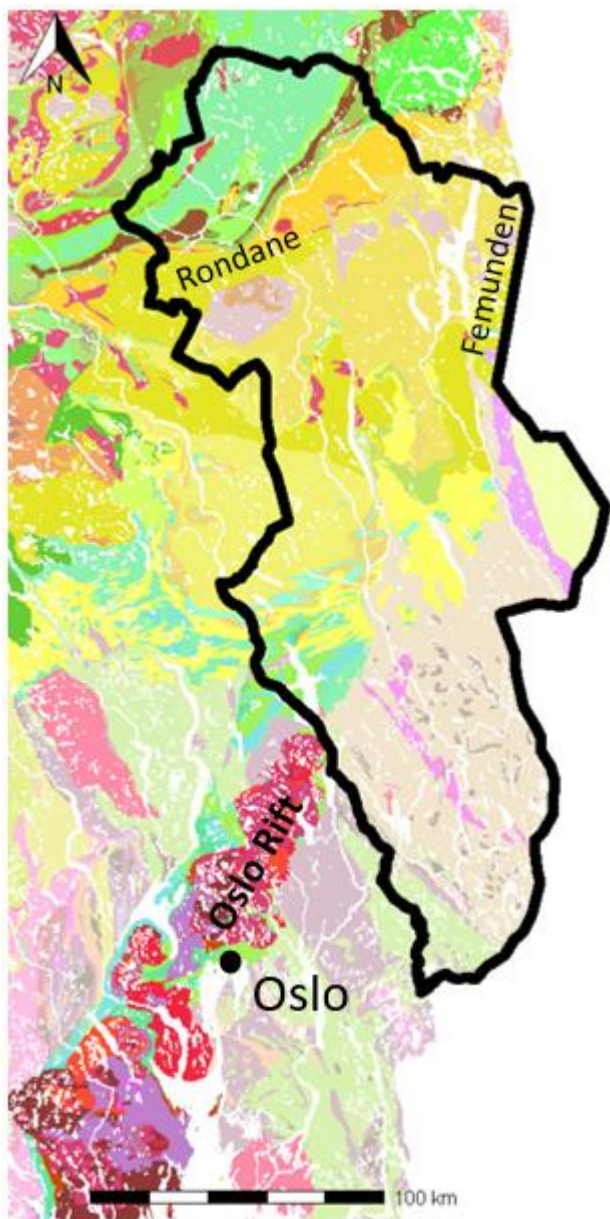


Figure 2.1 *Bedrock of survey area. The former county Hedmark, which is sampled, is marked with a black line. Bedrock units are from NGUs 1:1 350 000 scale bedrock map of Norway (Geological Survey of Norway, 2021).*













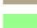
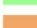


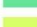



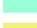


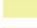


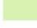


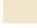
	Quartz alkali-feldspar syenite to nepheline syenite, in places porphyritic; 295–255 Ma
	Monzonite (larvikite), monzodiorite (kjelsåsite), in places syenite; 300–265 Ma
	Rhyolite and trachyte, in places ignimbrite, subordinate latite and basalt; 280–270 Ma
	Latite, porphyritic (rhomb porphyry), subordinate sedimentary rocks; 300–280 Ma
	Basalt; 300–295 Ma, and underlying sedimentary rocks; 320–295 Ma
	Gabbro, diorite, tonalite, ultramafic rocks and granite; 440–430 Ma
	Metabasalt, subordinate felsic volcanic rocks, conglomerate and breccia; 475–460 Ma
	Metabasalt and metagabbro, subordinate ultramafic rocks, in places felsic rocks; 500–475 Ma
	Metabasalt, subordinate intermediate and felsic volcanic rocks; antatt 1000–420 Ma
	Calcareous mica schist, calc-silicate schist and amphibole schist, subordinate marble; antatt 1000–420 Ma
	Metagabbro and metamonzonite, orthopyroxene-bearing; 1660–1230 Ma
	Mica schist and phyllite, subordinate peridotite and serpentinite; 500–470 Ma
	Metabasalt, subordinate serpentinite and soapstone; 500–470 Ma
	Mica gneiss and mica schist, subordinate marble and amphibolite; 1000–900 Ma or younger
	Amphibolite and gabbro, in places anorthosite and ultramafic rocks; 1670–420 Ma
	Granitic to tonalitic gneiss, in places mylonitic; north: 2850–1600 Ma, south: 1660–940 Ma
	Limestone and slate (lower part), sandstone and conglomerate (upper part); 440–420 Ma
	Sandstone, subordinate conglomerate and phyllite; 470–440 Ma
	Limestone, slate, alum shale and sandstone, in places conglomerate; 540–470 Ma
	Tillite and slate; 630–580 Ma
	Limestone and slate; 650–600 Ma
	Sandstone alternating with shale, in places conglomerate; 750–600 Ma
	Metarhyolite and metadacite; 1680–1600 Ma
	Granitic to dioritic gneiss, in places augen gneiss, in places migmatitic; 1680–1600 Ma
	Quartzite, metasandstone and mica gneiss, subordinate amphibolite; 1520–1350 Ma
	Granitic to tonalitic gneiss, augen gneiss, in places migmatitic; 1520–1480 Ma
	Granitic to dioritic gneiss and mica gneiss, mainly banded; 1560–1000 Ma
	Mica gneiss, metagreywacke and amphibolite, in places migmatitic; 1740–1520 Ma
	Tonalitic to granitic and quartz-dioritic gneiss, in places migmatitic; 1660–1520 Ma
	Metarhyolite and metatuff; 1740–1660 Ma
	Granitic to monzonitic and granodioritic gneiss, subordinate augen gneiss; 1740–1660 Ma
	Sandstone, subordinate basalt and dolerite; 1580–1260 Ma

Figure 2.2 Legend giving the lithological units of the bedrock map in Figure 2.1



## 2.2 Known mineral deposits

There are few known mineral deposits in Hedmark except from those south of the historical mining fields in and around Røros with occurrences of major base metal sulphide (VMS) deposits. Figure 2.3 shows deposits of industrial minerals, natural stones, and metals in south Norway, while Figure 2.4 show known deposits of ferro alloys metals, ferrous metals, and base metals in the northern part of Hedmark. More information can be obtained from the open access database [https://geo.ngu.no/kart/mineralressurser\\_mobil/](https://geo.ngu.no/kart/mineralressurser_mobil/).

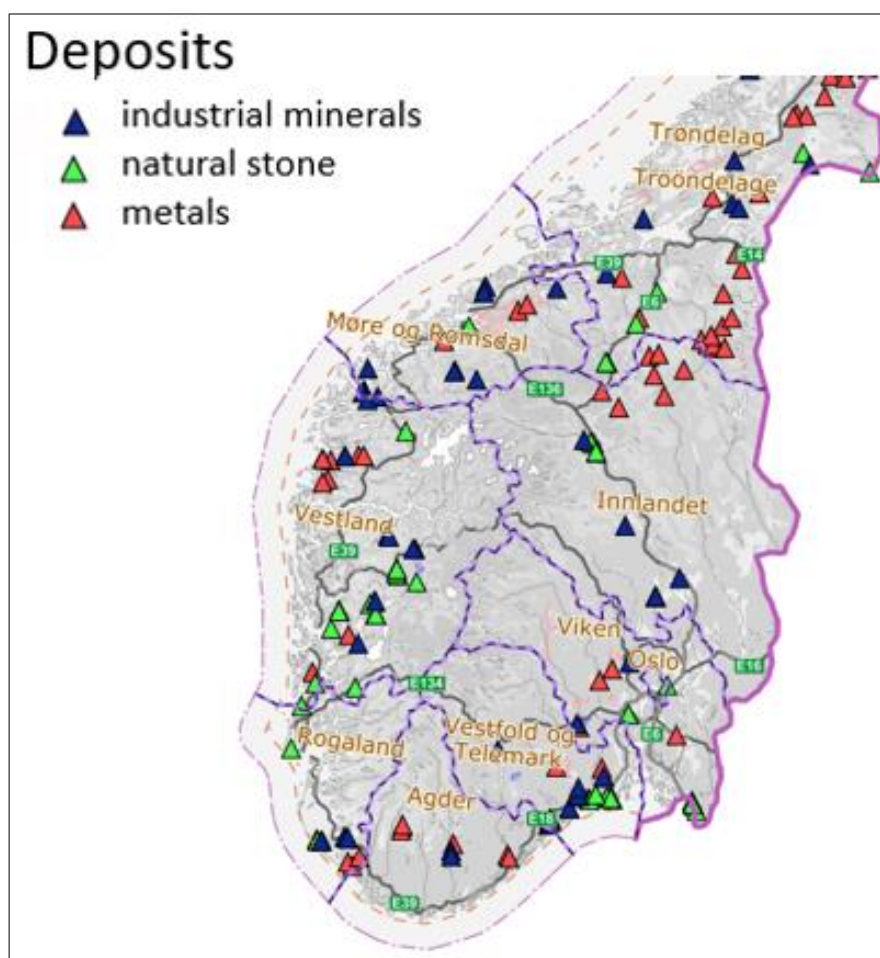


Figure 2.3 *Known deposits of industrial minerals, natural stones, and metals in southern Norway.* [https://geo.ngu.no/kart/mineralressurser\\_mobil/](https://geo.ngu.no/kart/mineralressurser_mobil/).

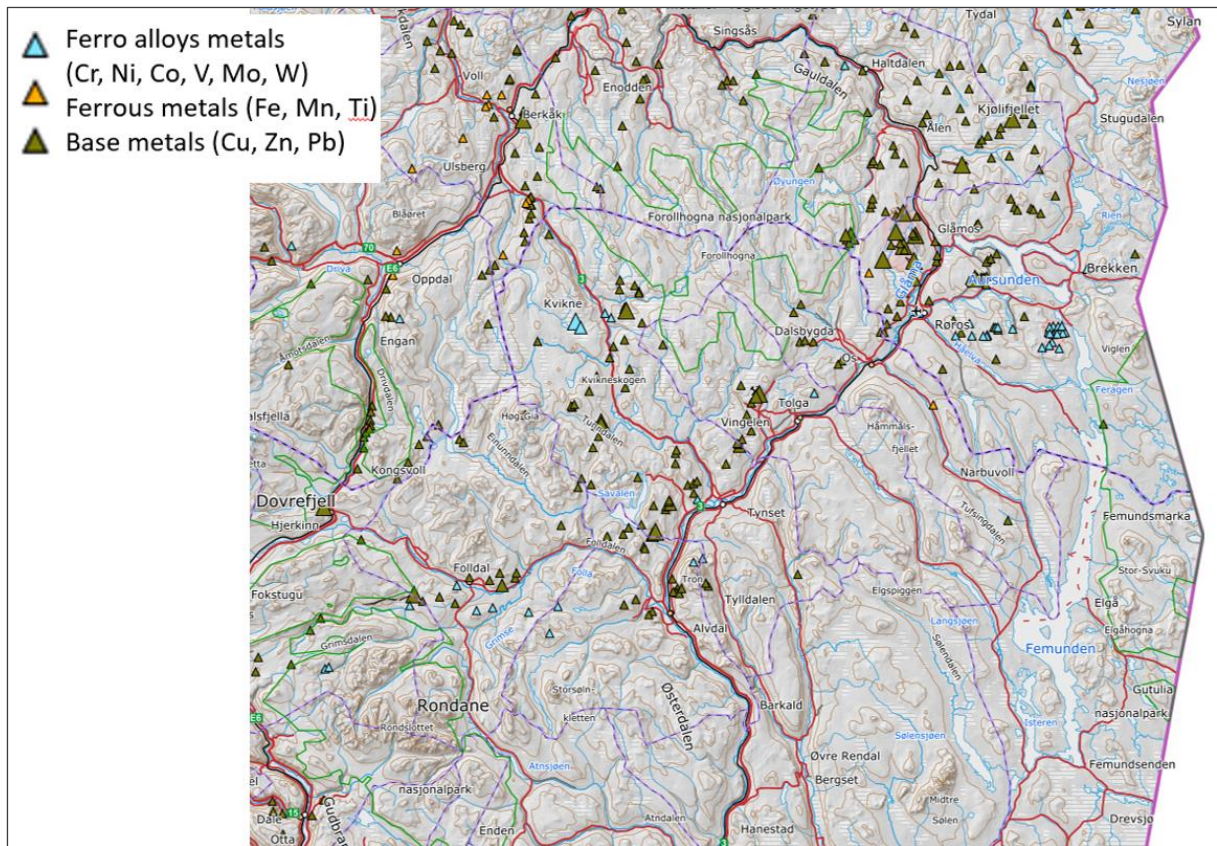


Figure 2.4 Known deposits of ferro alloys metals, ferrous metals, and base metals in the northern part of Hedmark, [https://geo.ngu.no/kart/mineralressurser\\_mobil/](https://geo.ngu.no/kart/mineralressurser_mobil/).

### 3 METHODS

#### 3.1 Field work

This survey is a continuation of the geochemical soil survey undertaken in North-Trøndelag and Fosen in 2013-2014 (Finne et al., 2014), and in the southern Trøndelag in 2018-2019 (Flem et al. 2020).

Grids of 6km x 6km were marked on topographical maps along with the highest marine level, polygons delineating glaciofluvial deposits and areas with marine deposits. These areas were excluded from sampling. In addition, national parks and protected areas were marked to remind the field workers to take extra precautions and, if possible, avoid these areas as there may be special rules for thoroughfare and sampling. Field workers were free to find a suitable location within each grid cell with a minimum distance of 10-100 m from abandoned to high traffic roads. Sample pits were dug by paint-free steel shovels down to the mineral soil layer, preferably to C-horizon in podzols. If till was not available, weathered soil was collected. Samples were transferred into Rilsan® plastic bags using a small steel shovel (Flem et al., 2020). Sample locations and sample IDs were given numbers in the range 3201 to 3999.

At approximately every twentieth sampling site a field duplicate sample was collected, resulting in 40 field duplicate pairs from the survey area. In total 787 mineral soil samples were collected.

However, apart from similar sample density and sampling procedure field registrations was done on mobile devices such as smartphones or tablets by the ArcGis Collector for Android and iOS apps. Previously this has been done by handheld GPS devices and “manual” notebooks. Figure 3.1 shows all attributes that was registered at each sample site. The attribute “jordTopp” is the measured distance from the bottom of the humus layer to the top of the mineral soil layer where soil is sampled (Fig. 3.2).

<u>Attributes</u>	Geometry	Attachments (4)
OBJECTID	593	
Initialer	BF	
proveDato	08.09.2020 10:24:43	
lokalitetNr	3780	
lokalitetNavn	3780	
jordTopp (cm)	30	
jordtype1	Morene	
jordtype2	<Null>	
jordNotater	Podzol, C-Horizon	
humusMin (cm)	5	
humusMax (cm)	10	
humusTypisk (cm)	8	
subSamp	5	
skogstype	Mix-skog	
bakkevegetasjon1	Lyng	
bakkevegetasjon2	Mose	
humusNotater	Fine humustuer	
rutelD	<Null>	
PROSJEKTNR	351700	

Figure 3.1 *Attributes registered at each sample site by the field worker in ArcGis Collector*



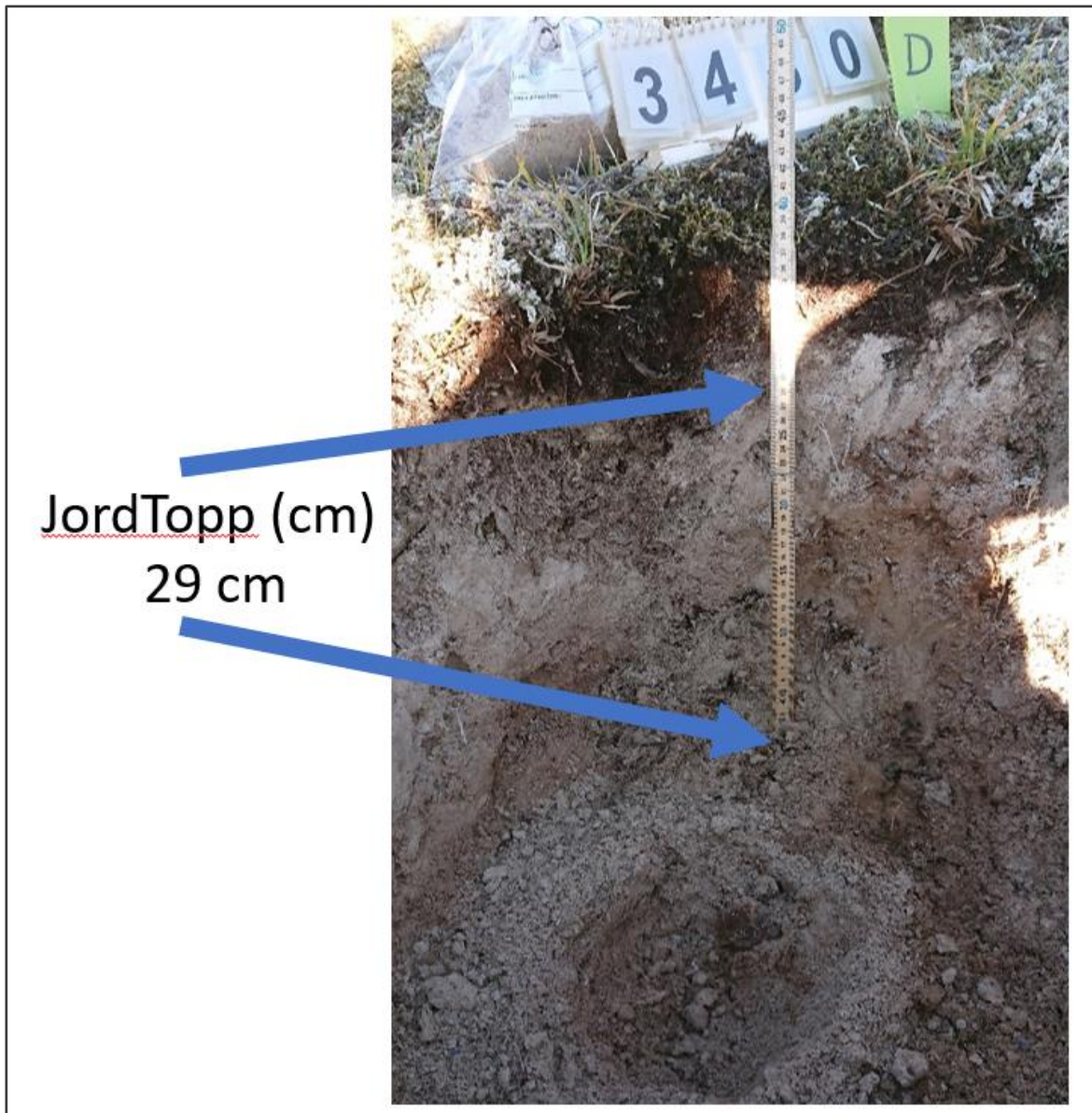


Figure 3.2 *JordTopp (cm)* or *Soil Top (cm)* is the measured distance between the bottom of the humus layer to the top of the mineral soil layer where the soil sample is collected.

### 3.2 Sample preparation and quality control

The sample procedure and equipment as reported for the southern Trøndelag survey (Flem et al. 2020) were used during the field work. Sampling was conducted by digging soil pits at representative sites. To avoid contamination pit walls were cleaned and samples retrieved into labelled sample bags. After returning to NGU wet weight was recorded before the samples were air-dried at temperatures 20 - 40 °C for more than 3 months. The soil samples were subsequently dry-sieved using a 2 mm nylon mesh. For each sample two 50 ml Kautex boxes and one 100 ml Kautex box was filled using a stainless-steel spoon. The remaining < 2mm sieved fraction was filled back into the sample bag and stored for future use. From each field duplicate sample (40 in number), an analytical split was prepared in an additional 50 ml Kautex box. The >2 mm fraction was discarded. To enable comparison with the previous surveys in Trøndelag (Finne et al., 2014; Flem et al., 2020), and in the three northernmost counties (Reimann et al. 2011), in total 20 samples from the Nordland/Troms sample collection were evenly distributed into the sample series and remeasured following the same procedure. In addition, 19 samples of the MINN in-house project standard and 39 samples of the MINS in-house project standard were included. The sampling and analytical design followed the same unbalanced ANOVA design as used in earlier surveys (e.g., Eggen and Finne, 2014; Eggen et al., 2017; Flem et al 2020). All samples, field duplicates, analytical duplicates of the field duplicate, and quality control samples (MINN and MINS project standards) were randomized after the procedure described by Eggen et al., (2019). Randomisation numbers from 14001 upwards were used.

### 3.3 Laboratory analyses

The randomized sample series of the <2-mm fraction was shipped to Bureau Veritas Minerals (previously ACME Labs) in Vancouver Canada. The mineral soil samples were analysed using the laboratory standard package ‘AQ251-EXT 53 element 15g’, which uses a sample split of 15 g for the extraction. The analytical package involves a modified aqua regia digestion, which consists of 1:1:1 v/v concentrated ACS grade HCl, HNO<sub>3</sub>, and de-mineralized H<sub>2</sub>O. The analyses were performed by using a Spectro Ciros Vision emission spectrometer (ICP-AES) and a Perkin Elmer Elan 6000/9000 inductively coupled plasma mass spectrometer (ICP-MS) for 53 elements. Details on the analytical procedure can be found on Acme Labs home page, <http://acmelab.com/>. Results reported by the laboratory Bureau Veritas Minerals include

measurements below the method detection limit, MDL (Table 3.1), blank measurements, and measurements of in-house reference materials.

Table 3.1 *Bureau Veritas official MDL*

Element	mg/kg	Element	mg/kg	Element	mg/kg	Element	mg/kg
Ag	0.002	Cu	0.01	Nb	0.02	Ta	0.05
Al	100	Fe	100	Ni	0.1	Te	0.02
As	0.1	Ga	0.1	P	10	Th	0.1
Au	0.0002	Ge	0.1	Pb	0.01	Ti	10
B	1	Hf	0.02	Pd	0.01	Tl	0.02
Ba	0.5	Hg	0.005	Pt	0.002	U	0.05
Be	0.1	In	0.02	Rb	0.1	V	1
Bi	0.02	K	100	Re	0.001	W	0.05
Ca	100	La	0.5	S	200	Y	0.01
Cd	0.01	Li	0.1	Sb	0.02	Zn	0.1
Ce	0.1	Mg	100	Sc	0.1	Zr	0.1
Co	0.1	Mn	1	Se	0.1		
Cr	0.5	Mo	0.01	Sn	0.1		
Cs	0.02	Na	10	Sr	0.5		

### 3.4 Magnetic susceptibility

The magnetic susceptibility measurements were carried out with a Bartington MS3/MS2K system, which has a resolution (lowest measurement capable of recording) of  $1 \times 10^{-6}$  SI. This sensor is designed to take measurements on flat and smooth surface and has a surface of integration (spot size) of ca. 25.4 mm diameter. The measurements were made at NGU's laboratory facilities directly on the sieved soil material contained in the Kautex boxes. Amplitude changes of a low-frequency magnetic field measured by the MS3 with a magnetic susceptibility (MS) achieve a resolution of 2  $\mu$ SI (Deng, 2015). To avoid cross-contamination, the sensor was covered with a ca. 7  $\mu$ m thick plastic sheet, which was replaced after each measurement. Each sample measurement was conducted as follows: 1-3 analysis of a disk-shaped MS reference material was performed every ten samples. MS analyses of this reference material yield average and median values of  $404 \times 10^{-5}$   $\mu$ SI and  $405 \times 10^{-5}$   $\mu$ SI (standard deviation of  $2 \times 10^{-5}$   $\mu$ SI; only 1.0% offset from manufacturer reference value). Then, 1-3 successive analyses of the sample lasting 0.1 s each were bracketed by two 0.1 s analyses of blank (gun targeting the air) for instrument drift correction.

A subset of the sample suite was measured using a Bartington MS3 susceptibility meter linked to MS2B sensor. This sensor is often used for soil measurements. However, the logistics associated with the sample preparation significantly increases the time and cost of the survey. Thus, we aimed to compare data trends and absolute values between both instruments to assess the viability of the MS2K sensor for soil measurements. For this study, soil material was placed in 2 x 2 x 1.6 cm (6.84 cc) containers which were then measured using the MS2B sensor at 0.465 kHz frequency. The mass correction (MSmass) associated with the magnetic susceptibility measurement was done with the following equation (Bartington Instruments, 1995):

$$corr\ factor = \frac{10}{6.8} \quad (1)$$

$$MS_{mass} = \frac{k \cdot corr\ factor}{\frac{m}{V}} = \frac{k \cdot corr\ factor}{1} \cdot \frac{m}{V} = k * \frac{10(cm^3)}{m(g)} \quad (2)$$

Results obtained with these two instruments are shown in Figure 3.3A. The absolute magnetic susceptibility values measured with the MS2B sensor are systematically lower than those of the MS2K. However, the overall data trend is statistically comparable as demonstrated by their high correlation coefficient ( $R^2 = 0.96$ ) and low  $p$  ( $<.005$ ) values (Fig.3.3B). Despite the significant differences of the MS absolute values, the MS2B results further confirms the validity of the MS variation recorded in the Hedmark samples with the MS2K sensor.

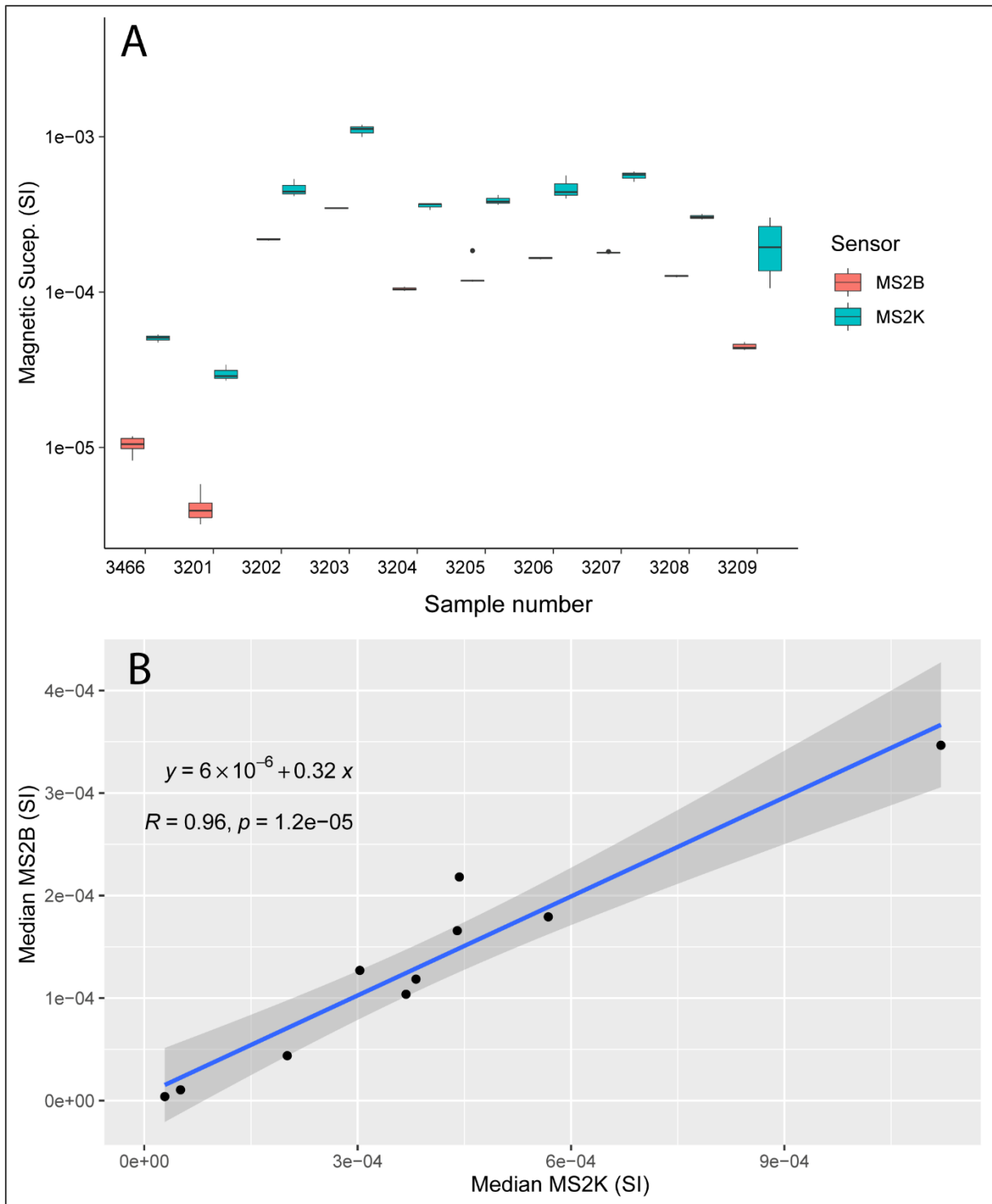


Figure 3.3. Magnetic susceptibility (MS) measured with the MS2B and MS2K sensors. For each sample, MS was measured 3 times with each sensor. A) Absolute MS values measured in SI units are significantly different between the two sensors. B) The high linear correlation between MS values (median value for each sample) obtained with the MS2B and MS2K indicates that the overall MS variability in the Hedmark area is equally registered by both sensors.

## 4 RESULTS

### 4.1 Method detection limits

Practical detection limits, PDL, can be calculated based on analytical duplicates (Flem et al., 2020; Demetriades 2011). A graphical exploratory data analysis (EDA) should always follow a statistical analysis as it might reveal patterns that otherwise is not exposed. Boron (B) and sulphur (S) are examples of elements that have a major part of the analytical data below the labs MDL (Table 3.1). The detection limit, DL, was calculated for S to 5 mg/kg based on 40 field duplicates and their analytical split pairs, two randomly selected MINS-project standards, two randomly selected MINN-project standards, analytical pairs of the laboratory standards OREAS262 and DS11, and 28 randomly selected analytical duplicates selected by the laboratory.

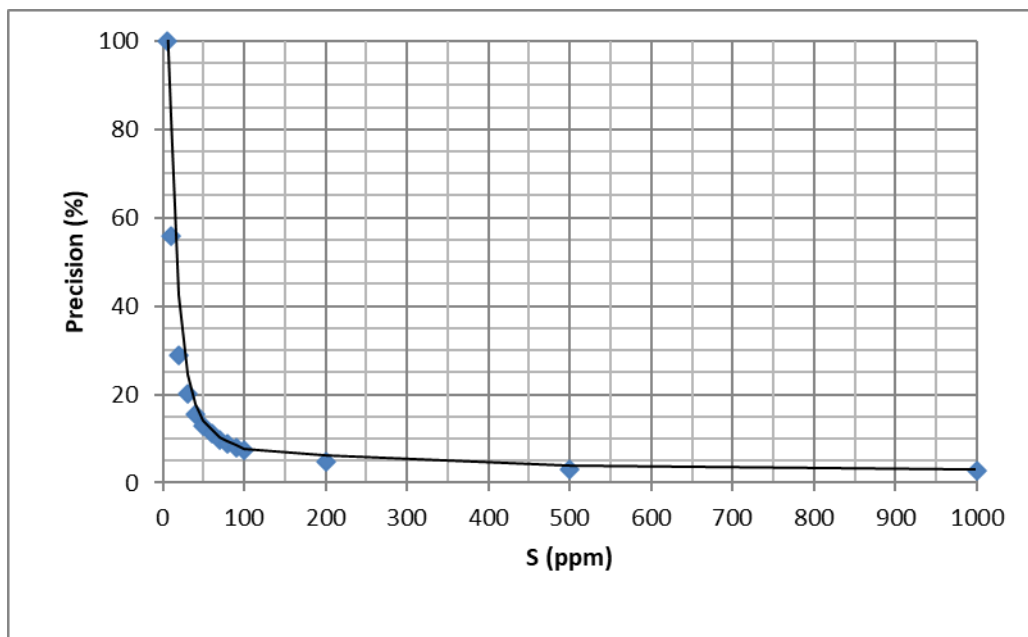


Figure 4.1 Scatter diagram showing the variation of precision (%) with concentration for sulphur (S)

The detection limit, DL, was then defined as the concentration that give rise to a signal equal to twice the standard deviation of blank fluctuations i.e., at a value with a precision,  $P_c = 100\%$  (Equation 3). The PDL for S is set to 15 mg/kg, three times the DL. The variation of the standard deviation of the determination,  $\sigma_c$ , can be expressed as a function of the concentration, C, and the standard deviation at zero concentration,  $\sigma_0$  ( $\sigma_c = \sigma_0 + kC$ ). At concentrations higher than



the detection limit, precision falls asymptotically towards the value of  $1.96k$ . The percentage precision Pc% is calculated as (95% confident level):

$$\text{Pc\%} = \frac{196\sigma}{X_{ci}} + 196k \quad (3)$$

where  $X_{ci}$  is the element concentration determined on individual samples. Figure 4.1 shows the variation of precision (%) in relation to concentration. For further information, and the implications involved in the estimation of these quality control parameters, Thompson and Howarth (1976), Van Loon and Barefoot (1989), or Demetriades (2011) should be consulted.

Random plots for all elements are given in Appendix 1. The laboratory provides data on instrumental rack number for each sample. Figure 4.2 shows random plots displaying the analytical sequences with different colours. Sulphur do not show any analytical trends, the random plot shows random values as it is supposed to. However, the random plot for B, shows a rather clear trend of instrumental drift from high to lower values for most of the analytical sequences. The MDL for B should thus probably be increased. In this QC-report it is chosen to only change the MDL to a PDL for S. All other are unchanged, however, for scientific purposes analytical values below Bureau Veritas official MDL can be obtain by request to NGU.

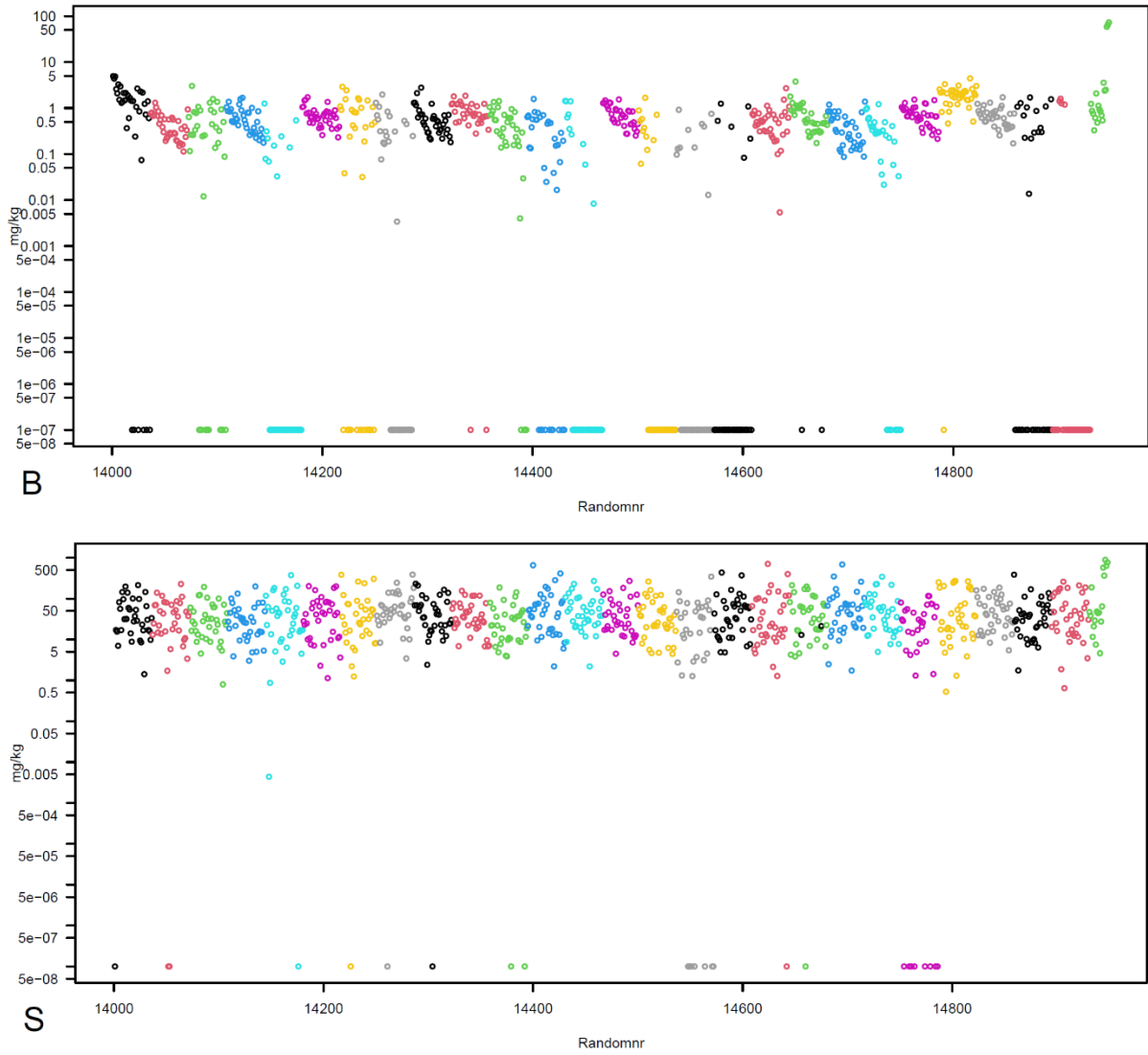


Figure 4.2 *Random plots for boron (B) and sulphur (S) displaying instrumental racks in different colours. Negative laboratory concentration values are set to a low positive value to fit the log scale.*

## 4.2 Analytical quality control, QC

### 4.2.1 NGU project standard, MINS

The in-house NGU project standard, hereafter referred to as MINS standard, has previously been used during the Oppdal survey (Eggen et al. 2017) and later for external QC control for the south Trøndelag survey (Flem et al., 2020). The MINS standard as QC- control for this survey is suitable for most elements except Ag, Ge, Hg, S, and Se (too low), Appendix 1. Thirty-nine splits of the MINS standard were analysed along with the samples, one split after approximately every 20th sample. X-charts for all elements of the MINS standard is given in Appendix 2 along with X-charts of the MINS standard analysis from the Trøndelag survey for comparison. The analytical results are plotted in the same order as they were analysed. For all elements, the median is indicated by a solid line, dashed lines are drawn at median  $\pm$  1 standard deviation (SD) and dotted lines are drawn at median  $\pm$  2 standard deviations (2SD). The analytical repeatability expressed by the robust coefficient of variation (CVR; Reimann et al., 2008), estimated in Table A1, is also reflected in the X-charts. However, no significant analytical trends can be seen.

Statistical summary for the MINS standard is given in Table A1. This includes the minimum, median, and maximum concentration values for all elements. The elements: Ag, B, Ge, Hg, In, Pd, Pt, Re, S, Se, Ta, Te, and W show many measurements below MDL/PDL, which constrain the possibility to calculate the analytical repeatability. Most of the other elements show acceptable analytical repeatability with CVR<15%. The elements Hf, Cd, Th, and Au show a precision (CVR) in growing order from 18.2 to 57.6, mainly due to proximity to MDL and/or sample inhomogeneity (e.g., Au). However, in the case of Hf and Th there is one split of the in-house standard (not the same one) that stands out as an outlier (Appendix 2). For comparison, the summary statistics for the ACME standards DS11 and OREAS262 is given in Table A2 and Table A3 respectively. These standards have been milled and have thus a more homogenic grain size distribution than the MINS standard that is a <2 mm fraction. In addition, the concentration level of most trace elements is higher in the ACME standards than in the MINS standard. Less variation in the analytical results is therefore expected, and, as shown in Tables A2 and A3, the analytical repeatability (CRV) for all elements is 15% or better. The only exception is Hf in DS11 with CVR=23.1 and B in OREAS262 with a CVR= 21.6 which is probably due to proximity to the MDL.

#### 4.2.2 NGU standard, MINN

The NGU standard MINN, hereafter referred as to MINN standard, was used as external quality control of the laboratory analysis for the three first data sets comprising the national geochemical mapping program of Norway in the scale of 1 sample per 36 km<sup>2</sup> (Table 1.1). Nineteen splits of the MINN standard were included in the randomised sample batch sent to Bureau Veritas to give the possibility to align analytical results between analysis collections. Table A4 gives a statistical summary for the MINN standard. This includes the minimum, median, and maximum concentration values for all elements.

#### 4.2.2 Samples re-analysed from previous surveys

In addition to in-house reference material mentioned above quality control was facilitated by including soil samples from previous surveys. Nineteen soil samples from the Nordland/Troms sample collection (Reimann et al. 2011) no:2, 4, 7, 10, 15, 40, 45, 47, 48, 49, 50, 62, 63, 66, 68, 73, 76, 77, and 81 were analysed along with the ordinary sample batch. The results from the laboratory analyses for all 54 elements are shown in Appendix 3 for all mineral soil surveys conducted in the national geochemical mapping program (Table 1.1). The elements Au, B, Be, Bi, Ca, Ge, Hf, Hg, In, Nd, Pd, Pt, Re, S, Sb, Se, Sn, Ta, Te, and W show a generally low precision probably due to nugget effects, grain size distribution, low concentrations, and laboratory batch effects. The elements, Ag, Al, As, Ba, Cd, Ce, Co, Cr, Cs, Cu, Fe, Ga, K, La, Li, Mg, Mn, Mo, Na, Ni, P, Pb, Rb, Sc, Th, Ti, Tl, U, V, Y, Zn, and Zr, show a generally high repeatability. However, one must nevertheless be careful when combining the data sets from the various surveys also for these elements.

Repeatability of the ACME in-house standard DS11 between the 2019 survey (Flem et al., 2020) and this survey is estimated in Table A2.

### 4.3 Precision and Analysis of variance (ANOVA)

A field duplicate was collected at approximately every twentieth sample location. The field duplicates are used to estimate the variation introduced by sampling and to answer the question of whether a comparable result would be obtained if the survey was undertaken a second time at approximately the same sampling sites. Analytical precision is estimated via splits of samples. In this survey splits of the field duplicates are used (an analytical duplicate of the field duplicate). Table A5 gives a precision estimate for all elements with concentrations above MDL for the field and analytical duplicate pairs. In addition, the number of pairs above PDL of the total of 40 pairs analysed are given. The estimated precision, given by the coefficient of variation (CV), for the field duplicates (ordinary sample compared with the field duplicate) ranges from 16% (Ba) to 139% (Cd). The analytical duplicate pairs (the duplicate field sample and the analytical duplicate) show a much smaller range and better precision: 2.5% for Al showing the best precision and 219% for Th showing the lowest precision. The precision for analytical duplicates is improved to 6.3%, 10.8%, 5.4%, 4.5%, and 3.2% for Nb, Se, Th, U, and Y respectively if the analytical duplicate pair 3860D and 3860DD is removed from the analysis.

The correlation between ordinary sample and duplicate sample and the correlation between duplicate sample and analytical duplicate are shown in Appendix 4. Poor correlation is usually due to the influence from a few samples (e.g., Th), low concentrations (e.g., Hf) or due to natural variation.

The field and analytical duplicates can be used to carry out an unbalanced analysis of variance (ANOVA) for those elements with more than five duplicate pairs above MDL. By unbalanced it is meant that unequal numbers of analysis occur at each level of design. In Table A6 the analysis of variance (ANOVA) is given for the 40 sites with a duplicate sample giving the distributed percentage variabilities for all elements. The *p*-value given in Table A6 is for the F-test to determine if the variance at the “between” level are equal for the field and analytical duplicates. The field duplicate ANOVA indicate that the combined sampling and analytical variability is smaller than the between sites regional variability. Silver, Ag, for instance, has an estimated regional variability of 83.2%, 12.5% variability at site (local variability) and 4.29% analytical variability. However, elements such as Au, Hf, Hg, P, S, Se and Zr shows higher local variability (>20%), this mainly reflects the difficulties in determining these elements at low levels.

#### 4.4 Survey data and maps

An overview of the data is presented in Table A7, giving the number of samples above DL, minimum and maximum concentration values measured, and the 2, 5, 10, 25, 50, 75, 90, 95 and 90 % quantiles. In addition, the powers (P) are given as a measure of variation. The powers provide a direct impression of the orders of magnitude each element varies. All data are available on NGUs geochemical database ([http://geo.ngu.no/kart/Geokjemi mobil/](http://geo.ngu.no/kart/Geokjemi_mobil/)).

The geochemical distribution of each element is presented in plots of the cumulative distribution function, ECDF (Appendix 5). The concentration is plotted along the X-axis and the cumulative probability is plotted along the Y-axis. These plots allow the direct visual recognition of breaks in the curve which may indicate different geochemical processes. Breaks in the uppermost 5-10 percentiles of the distribution are often used as thresholds for anomaly identification. All laboratory readings are shown including those below detection limit. Negative results are replaced by a low positive value. In some cases, the lowest positive concentration value below DL given by the laboratory have been increased to improve the readability of the ECDF above DL (e.g., Au, Pd, Pt, Re, Sb, Se).

Exploratory data analysis (EDA) maps of all elements (except for Ge, Pd, Pt, Re, S and Ta due to poor data quality), in addition to magnetic susceptibility are given in Appendix 6.

Figure 4.1 shows the EDA symbols used with percentiles for each class.

	EDA symbol set	Percentiles used
Highest concentration values	■	95-100%
Higher concentration values	+	75-95%
Inner concentration values	•	25-75%
Lower concentration values	○	5-25%
Lowest concentration values	○	0-5%

Figure 4.1 *The EDA (exploratory data analysis) map symbol set used in this report (Appendix 6).*



## 5 PRELIMINARY INTERPRETATION OF THE RESULTS

The main aim of this report is to describe the field work and sampling strategy applied, the analyses used, and to assess the quality of the results. Within the scope of geochemical surveys in Norway, magnetic susceptibility is measured for the samples collected by the national geochemical mapping program of mineral soil for the first time. Data treatment and result compilation allow a first insight into data variability and some first considerations are presented here.

The four main bedrock areas of Hedmark are clearly visible in the geochemical maps, Appendix 6, and even more pronounced in the contour/colour maps of As, Cu, Pb, and Zn given as examples in Figure 5.1. In contrast to the four main bedrock areas the magnetic susceptibility results highlight three main lithologic units; the highly susceptible granitoids in the South, the low susceptible sandstones of the central area and the intermediate susceptibility values associated with the mafic units located to the North. Notably, the high magnetic susceptibility of the granitoids is very well depicted throughout the study area with emphasis in the south where these rocks are dominant. Apart from the main lithological units, minor, until today unknown occurrences of granitoids within other bedrock provinces are also indicated by the magnetic susceptibility data. For example, granitic intrusions located in the north and a narrow SSE-NNW trending strip located in central Hedmark (Fig. 5.2). The magnetic susceptibility map also matches the spatial distribution of elements mainly partitioned in minerals found in granitoids such as Sn, Sr, and Nb (Appendix 6). However, the interpretation of magnetic susceptibility and its usefulness to correlate elements with bedrock provinces is not straight forward as can be exemplified by Ti that is better correlated with the magnetic susceptibility map in the south, but less in northern Hedmark. This pattern most likely represents Ti-rich ferromagnetic minerals like pyroxenes, magnetite, amphibole and micas in the granitic and mafic units opposed by depletion of such minerals (less resistant to physical erosion) in the sandstone. Overall, magnetic susceptibility measurements carried out in soil samples appear to depict the underlying bedrock and to match the concentration distributions of other elements. This has significant implications for the development of mineral exploration vectors and for quaternary geology studies.

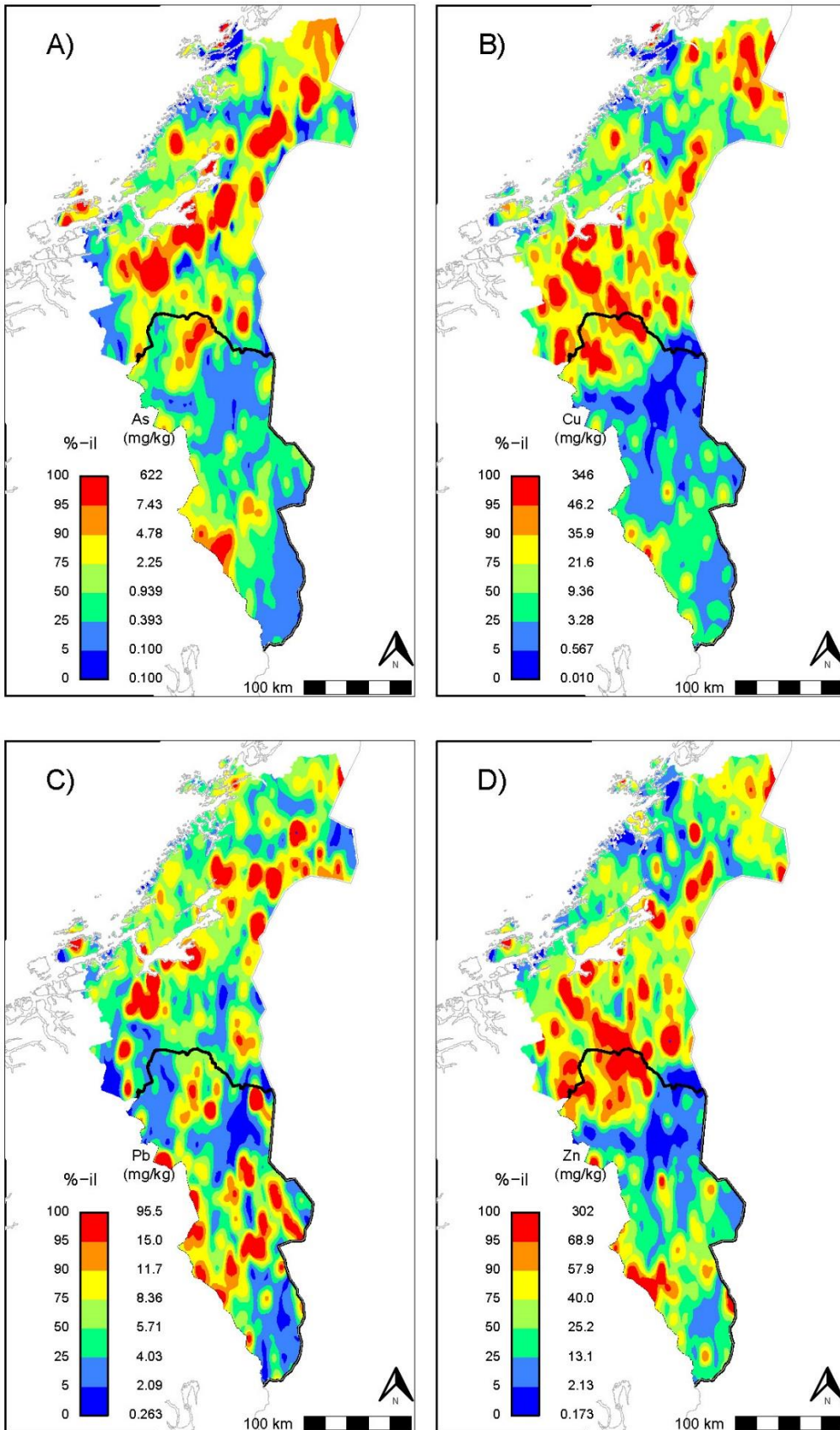


Figure 5.1 Contour/colour maps of As, Cu, Pb, and Zn covering Trøndelag County and Hedmark (Data from this survey; Finne et al., 2014; Flem et al., 2020)

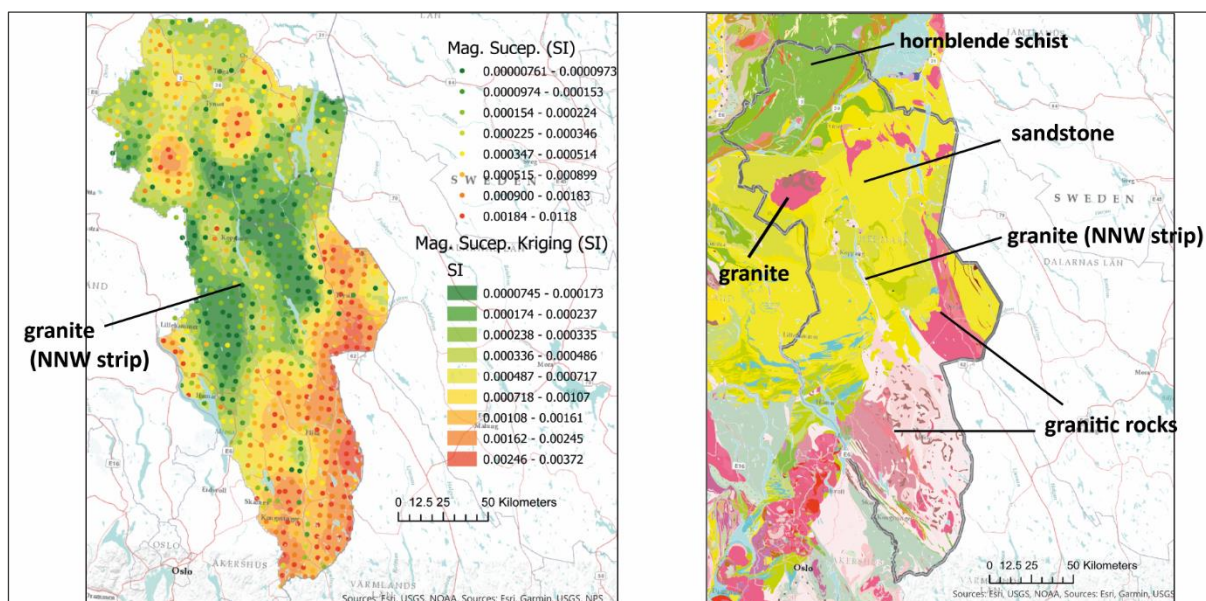


Figure 5.2. A) Distribution of the magnetic susceptibility measurements taken on the soil samples. The points indicate the actual location of each sample analysed. A kriging interpolation (2 km) of these data was carried out to better illustrate the results and compare with the underlying lithologic units. B) Geological map showing different granitic, mafic and sedimentary rocks present in the area of study. (Bedrock units are from NGUs 1:1 350 000 scale bedrock map of Norway (Geological Survey of Norway, 2021)

## 6 SUMMARY

This report gives an evaluation of the quality of the data from the Hedmark geochemical mineral soil survey. Few data are available for B, Ge, In, Pd, Pt, Re, Ta, and Te due to too high detection limits. Re-analysed samples from the Nordland/Troms sample collection (Reimann et al., 2011) as well as re-analysed Trøndelag survey samples (Finne et al., 2014; Flem et al., 2020), show that 32 out of 52 elements have a general good repeatability between batches. However, one must nevertheless be careful when combining the data sets from the various surveys also for these elements. With careful use and working preferentially with quantiles, many elements in the national mapping program datasets, that do not have detection limit issues, can be merged and used as one dataset. However, it is the data user's responsibility to consider if the batch effects are within acceptable limits. Magnetic susceptibility soil sample measurements appear as a suitable and supportive tool to detect even small-scale bedrock variations. This new dataset is now merged into the existing data and is available for further usage. The methodology and data quality are documented in this QC-report for the first time.

## **ACKNOWLEDGMENTS**

We thank the soil sampling team for the fieldwork: Pedro Acosta-Gongora, Malin Andersson, Rut Eikeland, Tor Erik Finne, Belinda Flem, Ivar Haukdal, Iain Henderson, Sverre Iversen, Ane Bang-Kittelsen, Åse Minde, Agnes Raaness, Hild Sissel Thorsnes, and Guri Venvik. In addition, Inga Giese, Amalie Flem Grimstvedt, and Simon Risan, are acknowledged for participating in the pre-analysis/sieving of the samples.

The staff at geomatics are acknowledged for assistance during the preparation of field map and ArcGIS Collector. In addition, gratitude is express to Sverre Iversen for making field photos available.

## REFERENCES

- Acosta-Gongora, P., Flem, B., Finne, T.E., Anderson, M., Heldal, T., 2021: Lime availability in soil, humus, and water. Geological Survey of Norway (NGU). Report no: 2021.034, ISSN 0800-3416, pp. 34.
- Bartington Instruments. 1995. Operation Manual for MS2 Magnetic Susceptibility System. Oxford, UK.
- Dahl, R., Nashoug, O., Nystuen, J.P., 2017. Mjøsområdet – Geologi og landskap. Hedmark geologiforening, Hamar. 276 pp. (in Norwegian).
- Demetriades, A., 2011. Understanding the quality of chemical data from the urban environment - Part 2: Measurement uncertainty in the decision-making process. In: C.C. Johnson, A. Demetriades, R.T. Ottesen & J. Locutura (Editors). Mapping the chemical environment of urban areas. Wiley-Blackwell, Chichester, U.K., pp. 76-98.
- Deng, D.N., 2015. A comparative Study of Handheld Magnetic Suceptibility instruments. Doctoral dissertation, Laurention Uniersity of Sudbury.
- Eggen, O.A., Andersson, M., Gasser, D., 2017. Till geochemistry in Oppdal and Rennebu, Sør-Trøndelag county, Norway. Geological Survey of Norway, NGU Report 2017.023. pp. 111
- Eggen O.A., Reimann C., Flem B., 2019. Reliability of geochemical analyses: Deja vu all over again. *Science of the Total Environment* 670:138-148.  
<https://doi.org/10.1016/j.scitotenv.2019.03.185>.
- Fabian K., Reimann C., de Caritat P., 2017. Quantifying Diffuse Contamination: Method and Application to Pb in Soil. *Environmental Science & Technology* 51:6719-6726.  
<https://doi.org/10.1021/acs.est.7b00741>.
- Finne, T. E., Reimann, C., Eggen, O. A., 2014. Mineral soil geochemistry in Nord-Trøndelag and Fosen. *Norges geologiske undersøkelse, Serie/Kilde: NGU-rapport 2014.047*
- Finne, T. E., Eggen, O. A., 2015. Organic soil geochemistry in Nord-Trøndelag and Fosen. *Norges geologiske undersøkelse, Serie/Kilde: NGU-rapport 2014.057*, pp 82.
- Flem, B., Andersson, M., Finne, T. E., Minde, Å., 2020. Mineral soil geochemistry in southern Trøndelag. Geological Survey of Norway. Report no: 2020.017, ISSN 0800-3416, 127 pp.
- Flem, B., Acosta-Gongora, P., Andersson, M., Minde, Å , Finne, T. E., 2021. Organic soil geochemistry in southern Trøndelag, QC – report. Geological Survey of Norway. Report no: 2021.006, ISSN 0800-3416, 123 pp.
- Flem, B., Reimann, C., Fabian, K., 2022. Excess Cr and Ni in top soil: Comparing the effect of geology, diffuse contamination, and biogenic influence. *Science of The Total Environment*, Vol.843, Pages 138-148.  
<https://doi.org/10.1016/j.scitotenv.2022.157059>
- Geological Survey of Norway, 2021. Bedrock map of Norway 1:1 350 000.  
[https://www.ngu.no/upload/Publikasjoner/Kart/BGNorge\\_1350\\_000.pdf](https://www.ngu.no/upload/Publikasjoner/Kart/BGNorge_1350_000.pdf)
- Van Loon, J.C., Barefoot, R.R., 1989. Analytical methods for geochemical exploration. Academic Press inc. London, pp. 344



- Olsen, L., Bergstrøm, B., Sveian, H., Riiber, K., 2017. Beskrivelse til kvartærgeologisk kart over Hedmark fylke i M 1:300 000. Norges geologiske undersøkelse, Serie/Kilde: NGU-rapport 2017 042
- Ramberg, I.B., Bryhni, I., Nøttvedt, A., Rangnes, K., 2008. The making of a land - Geology of Norway. Norsk Geologisk Forening (Norwegian Geological Association). 624 pp.
- Reimann, C., Fitzmoser, p., Garrett, R., Dutter, R., 2008. Statistical data analysis explained. John Wiley & Sons, Chichester, England, xviii, pp. 343
- Reimann, C., Finne, T. E., Filzmoser, P., 2011. New geochemical data from a collection of till samples from Nordland, Troms and Finnmark. Norges geologiske undersøkelse, Serie/Kilde: NGU-rapport 2011.045
- Reimann, C., Schilling, J., Roberts, D., Fabian, K., 2015. A regional-scale geochemical survey of soil O and C horizon samples in Nord-Trøndelag, Central Norway: Geology and mineral potential. *Applied Geochemistry*, 61: 192-205.  
<https://doi.org/10.1016/j.apgeochem.2015.05.019>
- Reimann, C., Fabian, K., Flem, B., Schilling, J., Roberts, D., Englmaier, P., 2016. Pb concentrations and isotope ratios of soil O and C horizons in Nord-Trøndelag, Central Norway: anthropogenic or natural sources? *Applied Geochemistry* 74, 56-66.  
<https://doi.org/10.1016/j.apgeochem.2016.09.002>.
- Reimann, C., Fabian, K., Flem, B., Englmaier, P., 2019. The large-scale distribution of Cu and Zn in sub and topsoil: Separating topsoil bioaccumulation and natural matrix effects from diffuse and regional contamination. *Science of the Total Environment*, 655, 730-740. <https://doi.org/10.1016/j.scitotenv.2018.11.248>.
- Thompson, M., Howarth, R.J., 1978. A new approach to the estimation of analytical precision. *Journal of Geochemical Exploration*. 9, 23-30





# TABLES

**TABLE A1 The MINS Project standard (Sagelva).**

Summary statistics for the MINS project standard (Sagelva). The minimum (MIN), median, maximum (MAX) is given. In addition, the interquartile range (IQR) and the robust coefficient of variation (CVR) is given as a measure of precision

Element	MINS Project standard (n=39)					Sorted by precision	
	MIN mg/kg	MEDIAN mg/kg	MAX mg/kg	IQR mg/kg	CVR %	Element	CVR %
Ag	<0.002	<0.002	0.00372	-	-	Al	3.2
Al	11 400	12 400	13 800	383	3.2	Fe	3.5
As	2.44	2.77	3.26	0.198	7.7	Mn	3.5
Au	<0.0002	0.000460	0.00181	0.000347	57.6	Co	3.8
B	<1	<1	2.59	0.0851	-	Mg	3.8
Ba	26.7	33.4	37.8	3.53	10.7	Cu	3.8
Be	<0.1	0.251	0.494	0.0313	13.9	Ni	3.8
Bi	0.0257	0.0611	0.0784	0.0157	12.0	Y	4.2
Ca	1 430	1 660	1 860	94.7	5.8	P	4.3
Cd	<0.01	0.0247	0.0368	0.00427	18.2	V	4.4
Ce	27.4	32.8	36.7	2.11	6.5	Rb	4.6
Co	8.78	9.43	10.6	0.343	3.8	Zn	4.8
Cr	43.0	47.8	52.8	2.48	5.5	Cs	5.0
Cs	0.630	0.744	0.797	0.0363	5.0	Cr	5.5
Cu	23.7	25.7	28.4	0.925	3.8	Ca	5.8
Fe	15 300	16 700	18 600	551	3.5	K	5.9
Ga	2.76	3.17	3.63	0.201	7.3	Tl	6.3
Ge	<0.1	<0.1	0.119	-	-	Mo	6.4
Hf	0.0795	0.106	0.249	0.0189	16.2	Ce	6.5
Hg	<0.005	<0.005	0.00814	-	-	Pb	7.2
In	<0.02	<0.02	<0.02	-	-	Ga	7.3
K	997	1 120	1 270	69.8	5.9	As	7.7
La	12.8	15.4	17.1	1.37	10.2	Sr	7.8
Li	10.1	11.3	13.0	1.00	8.4	Li	8.4
Mg	6 750	7 420	7 980	278	3.8	Ti	8.5
Mn	248	271	295	8.49	3.5	Sb	8.9
Mo	0.240	0.270	0.315	0.0160	6.4	Sn	9.5
Na	64.8	77.1	96.8	11.6	13.4	Nb	10.0
Nb	0.292	0.331	0.430	0.0321	10.0	La	10.2
Ni	37.6	40.4	44.6	1.56	3.8	Sc	10.3
P	470	527	583	21.1	4.3	Ba	10.7
Pb	4.33	4.90	5.61	0.384	7.2	Zr	11.4
Pd	<0.01	<0.01	0.0127	-	-	Bi	12.0
Pt	<0.002	<0.002	<0.002	-	-	U	12.8
Rb	7.60	8.23	9.05	0.386	4.6	Na	13.4
Re	<0.001	<0.001	0.00103	-	-	Be	13.9
S	<15	<15	<15	-	-	Hf	16.2
Sb	0.0487	0.0681	0.0814	0.00696	8.9	Cd	18.2

Element	MINS Project standard (n=39)					Sorted by precision	
	MIN mg/kg	MEDIAN mg/kg	MAX mg/kg	IQR mg/kg	CVR %	Element	CVR %
Sc	2.74	3.15	3.87	0.367	10.3	Th	21.1
Se	<0.1	<0.1	0.239	-	-	Au	57.6
Sn	0.188	0.228	0.319	0.0227	9.5	Ag	-
Sr	7.52	8.75	10.0	0.690	7.8	B	-
Ta	<0.05	<0.05	<0.05	-	-	Ge	-
Te	<0.02	<0.02	0.0318	-	-	Hg	-
Th	3.78	4.68	8.89	0.951	21.1	In	-
Ti	585	680	817	70.3	8.5	Pd	-
Tl	0.0687	0.0884	0.0980	0.00544	6.3	Pt	-
U	0.487	0.597	0.719	0.0769	12.8	Re	-
V	21.7	24.1	26.5	1.15	4.4	S	-
W	<0.05	<0.05	0.0802	0.00263	-	Se	-
Y	6.53	7.41	8.16	0.310	4.2	Ta	-
Zn	27.1	29.4	32.2	1.15	4.8	Te	-
Zr	4.52	5.89	8.68	0.635	11.4	W	-

**TABLE A2 BUREAU VERITAS (ACME) standard DS11**

Summary statistics for the ACME in-house standard DS11. The minimum (MIN), median, maximum (MAX) is given. In addition, the interquartile range (IQR) and the robust coefficient of variation (CVR) is given as a measure of precision. Additionally, is the median analysis of DS11 from the 2019 survey (Flem et al., 2020) and the calculated relative difference in analysis value between the present and the 2019 survey given.

Element	DS11 in-house standard (n=28)					MEDIAN	Rel. diff.
	MIN mg/kg	MEDIAN mg/kg	MAX mg/kg	IQR mg/kg	CVR %	2019 mg/kg	2019-2022 %
Ag	1.61	<b>1.72</b>	1.84	0.0833	4.6	<b>1.7</b>	1.16
Al	10 600	<b>11 300</b>	12 700	399	3.6	<b>11 400</b>	-0.88
As	39.7	<b>42.6</b>	46.1	2.29	4.6	<b>42</b>	1.41
Au	0.0548	<b>0.0682</b>	0.0910	0.00704	10.2	<b>0.068</b>	0.29
B	4.51	<b>6.98</b>	9.09	0.885	12.9	<b>6.7</b>	4.01
Ba	319	<b>351</b>	381	26.0	7.3	<b>340</b>	3.13
Be	0.310	<b>0.661</b>	1.05	0.0415	6.3	<b>0.64</b>	3.18
Bi	9.73	<b>10.9</b>	13.0	1.20	9.2	<b>12</b>	-10.09
Ca	9 620	<b>10 400</b>	11 400	226	2.2	<b>10 300</b>	0.96
Cd	2.09	<b>2.28</b>	2.59	0.127	6.2	<b>2.3</b>	-0.88
Ce	30.7	<b>34.9</b>	40.9	3.26	10.2	<b>36</b>	-3.15
Co	12.8	<b>13.9</b>	14.9	0.514	3.6	<b>13</b>	6.47
Cr	55.0	<b>58.5</b>	67.1	2.60	4.6	<b>59</b>	-0.85
Cs	2.49	<b>2.75</b>	3.02	0.121	4.7	<b>2.9</b>	-5.45
Cu	135	<b>144</b>	155	3.29	2.6	<b>150</b>	-4.17
Fe	28 700	<b>30 400</b>	33 000	875	2.8	<b>30 600</b>	-0.66
Ga	4.27	<b>4.74</b>	5.28	0.446	8.8	<b>4.9</b>	-3.38
Ge	<0.1	<b>&lt;0.1</b>	0.130	-	-	<b>&lt;0.1</b>	-
Hf	0.0439	<b>0.0592</b>	0.0821	0.0131	23.1	<b>0.063</b>	-6.42
Hg	0.221	<b>0.250</b>	0.310	0.0131	5.4	<b>0.25</b>	0.00
In	0.210	<b>0.231</b>	0.271	0.0156	7.2	<b>0.24</b>	-3.90
K	3 630	<b>3 900</b>	4 280	121	2.6	<b>3 940</b>	-1.03
La	15.4	<b>17.4</b>	20.5	1.92	11.0	<b>18</b>	-3.45
Li	20.4	<b>22.9</b>	26.2	1.25	5.5	<b>22</b>	3.93
Mg	7 770	<b>8 260</b>	9 000	257	2.7	<b>8 240</b>	0.24
Mn	936	<b>999</b>	1 080	23.0	2.4	<b>1 000</b>	-0.10
Mo	13.5	<b>14.6</b>	16.4	0.865	6.8	<b>14</b>	4.11
Na	664	<b>712</b>	817	29.5	3.6	<b>720</b>	-1.12
Nb	1.24	<b>1.50</b>	1.67	0.134	8.7	<b>1.5</b>	0.00
Ni	75.3	<b>79.1</b>	88.7	3.36	4.5	<b>78</b>	1.39
P	628	<b>681</b>	761	23.1	3.8	<b>710</b>	-4.26
Pb	117	<b>130</b>	148	10.0	8.6	<b>130</b>	0.00
Pd	0.0893	<b>0.0985</b>	0.148	0.0115	8.3	<b>0.11</b>	-11.68
Pt	0.152	<b>0.165</b>	0.189	0.00696	4.8	<b>0.17</b>	-3.03
Rb	30.6	<b>32.7</b>	34.6	1.15	3.8	<b>34</b>	-3.98
Re	0.0398	<b>0.0446</b>	0.0566	0.00368	9.4	<b>0.043</b>	3.59
S	2 460	<b>2 680</b>	2 880	65.3	2.8	<b>2 600</b>	2.99



Element	DS11 in-house standard (n=28)					MEDIAN 2019 mg/kg	Rel. diff. 2019-2022 %
	MIN mg/kg	MEDIAN mg/kg	MAX mg/kg	IQR mg/kg	CVR %		
Sb	6.95	<b>8.39</b>	10.0	0.553	5.3	<b>8.7</b>	-3.69
Sc	2.90	<b>3.14</b>	3.67	0.219	7.2	<b>3.2</b>	-1.91
Se	2.00	<b>2.19</b>	2.54	0.133	5.8	<b>2.2</b>	-0.46
Sn	1.57	<b>1.73</b>	2.11	0.108	7.3	<b>1.8</b>	-4.05
Sr	60.1	<b>65.8</b>	73.8	4.24	6.9	<b>66</b>	-0.30
Ta	<0.05	<b>&lt;0.05</b>	<0.05	-	-	<b>&lt;0.05</b>	-
Te	4.34	<b>4.56</b>	4.81	0.119	3.0	<b>4.5</b>	1.32
Th	6.15	<b>7.17</b>	9.41	1.38	9.2	<b>8.1</b>	-12.97
Ti	800	<b>908</b>	1 140	79.1	8.8	<b>910</b>	-0.22
Tl	4.25	<b>4.67</b>	5.17	0.249	5.2	<b>4.9</b>	-4.93
U	2.15	<b>2.40</b>	2.95	0.309	13.4	<b>2.5</b>	-4.17
V	42.1	<b>47.0</b>	52.0	1.48	3.4	<b>48</b>	-2.13
W	2.56	<b>2.83</b>	3.27	0.144	5.0	<b>3</b>	-6.01
Y	7.38	<b>8.01</b>	8.83	0.407	5.0	<b>7.7</b>	3.87
Zn	309	<b>333</b>	368	10.9	3.3	<b>330</b>	0.90
Zr	2.42	<b>2.79</b>	3.46	0.414	11.7	<b>2.7</b>	3.23

**TABLE A3 BUREAU VERITAS (ACME) standard OREAS262**

Summary statistics for the Bureau Veritas in-house standard OREAS262. The minimum (MIN), median, maximum (MAX) is given. In addition, the interquartile range (IQR) and the robust coefficient of variation (CVR) is given as a measure of precision

Element	In-house standard OREAS262 (n=28)					Sorted by precision	
	MIN mg/kg	MEDIAN mg/kg	MAX mg/kg	IQR mg/kg	CVR %	Element	CVR %
Ag	0.424	0.455	0.493	0.0216	4.5	Mg	1.6
Al	11 100	12 700	13 900	389	3.5	Mn	1.7
As	32.5	35.2	37.6	1.56	4.6	Na	2.1
Au	0.0479	0.0567	0.0728	0.00752	10.0	Cu	2.6
B	<1	3.49	6.36	0.706	21.6	Zn	2.7
Ba	215	236	265	17.7	7.5	P	2.9
Be	0.666	1.06	1.52	0.0806	7.5	S	2.9
Bi	0.859	0.939	1.09	0.0688	8.4	V	3.2
Ca	27 700	29 300	31 200	1 280	4.6	Co	3.3
Cd	0.567	0.616	0.714	0.0337	4.1	Fe	3.3
Ce	26.4	30.6	34.8	2.56	9.2	K	3.4
Co	26.4	27.7	28.9	0.916	3.3	Y	3.5
Cr	39.9	43.1	47.1	2.05	4.3	Al	3.5
Cs	2.26	2.53	2.94	0.254	9.5	Mo	3.6
Cu	107	112	120	3.14	2.6	Rb	3.6
Fe	30 500	32 100	35 500	924	3.3	Ni	3.7
Ga	3.45	3.74	4.27	0.247	7.6	Cd	4.1
Ge	<0.1	<0.1	<0.1	-	-	Cr	4.3
Hf	0.171	0.255	0.333	0.0352	13.5	Hg	4.4
Hg	0.141	0.156	0.186	0.00702	4.4	Ag	4.5
In	0.0261	0.0316	0.0501	0.00454	12.7	As	4.6
K	2 700	2 990	3 220	94.1	3.4	Ca	4.6
La	13.2	15.5	18.2	1.81	11.1	Sn	4.6
Li	15.4	16.9	19.4	0.867	5.7	Sr	4.8
Mg	10 800	11 500	12 100	212	1.6	Tl	4.9
Mn	496	531	568	9.03	1.7	Te	5.5
Mo	0.580	0.669	0.735	0.0309	3.6	Li	5.7
Na	660	676	735	22.4	2.1	Zr	6.0
Nb	<0.02	<0.02	0.0280	-	-	Pb	7.5
Ni	60.6	64.0	67.7	2.38	3.7	Ba	7.5
P	355	386	404	9.14	2.9	Be	7.5
Pb	49.9	55.0	60.0	4.13	7.5	Ga	7.6
Pd	<0.01	<0.01	<0.01	-	-	Bi	8.4
Pt	<0.002	<0.002	0.00213	-	-	Sc	8.5
Rb	17.2	18.1	19.7	0.678	3.6	Ce	9.2
Re	<0.001	<0.001	0.00162	-	-	U	9.4
S	2 310	2 490	2 650	63.1	2.9	Cs	9.5
Sb	3.59	4.66	6.22	0.931	10.7	Au	10.0

Element	In-house standard OREAS262 (n=28)					Sorted by precision	
	MIN mg/kg	MEDIAN mg/kg	MAX mg/kg	IQR mg/kg	CVR %	Element	CVR %
Sc	2.93	3.17	3.64	0.248	8.5	Th	10.3
Se	0.150	0.471	0.680	0.0608	13.9	Sb	10.7
Sn	0.480	0.510	0.679	0.0220	4.6	La	11.1
Sr	32.4	34.4	37.9	1.77	4.8	In	12.7
Ta	<0.05	<0.05	<0.05	-	-	Hf	13.5
Te	0.179	0.226	0.257	0.0144	5.5	W	13.5
Th	7.91	8.82	11.1	1.18	10.3	Se	13.9
Ti	21.4	28.0	35.3	3.72	15.6	Ti	15.6
Tl	0.408	0.443	0.487	0.0188	4.9	B	21.6
U	1.06	1.14	1.37	0.109	9.4	Nb	-
V	19.4	21.0	23.0	0.765	3.2	Ge	-
W	0.142	0.194	0.249	0.0279	13.5	Pd	-
Y	10.0	10.6	11.7	0.363	3.5	Pt	-
Zn	141	149	154	4.23	2.7	Re	-
Zr	7.09	11.9	13.5	0.800	6.0	Ta	-

**TABLE A4 The MINN Project standard.**

Summary statistics for the MINN project standard. The minimum (MIN), median, maximum (MAX) is given. In addition, the interquartile range (IQR) and the robust coefficient of variation (CVR) is given as a measure of precision.

Element	MINN Project standard (n=19)					Sorted by precision	
	MIN mg/kg	MEDIAN mg/kg	MAX mg/kg	IQR mg/kg	CVR %	Element	CVR %
Ag	<0.002	<0.002	0.00372	-	-	Al	3.2
Al	11 400	12 400	13 800	383	3.2	Fe	3.5
As	2.44	2.77	3.26	0.198	7.7	Mn	3.5
Au	<0.0002	0.000460	0.00181	0.000347	57.6	Co	3.8
B	<1	<1	2.59	0.0851	-	Mg	3.8
Ba	26.7	33.4	37.8	3.53	10.7	Cu	3.8
Be	<0.1	0.251	0.494	0.0313	13.9	Ni	3.8
Bi	0.0257	0.0611	0.0784	0.0157	12.0	Y	4.2
Ca	1 430	1 660	1 860	94.7	5.8	P	4.3
Cd	<0.01	0.0247	0.0368	0.00427	18.2	V	4.4
Ce	27.4	32.8	36.7	2.11	6.5	Rb	4.6
Co	8.78	9.43	10.6	0.343	3.8	Zn	4.8
Cr	43.0	47.8	52.8	2.48	5.5	Cs	5.0
Cs	0.630	0.744	0.797	0.0363	5.0	Cr	5.5
Cu	23.7	25.7	28.4	0.925	3.8	Ca	5.8
Fe	15 300	16 700	18 600	551	3.5	K	5.9
Ga	2.76	3.17	3.63	0.201	7.3	Tl	6.3
Ge	<0.1	<0.1	0.119	-	-	Mo	6.4
Hf	0.0795	0.106	0.249	0.0189	16.2	Ce	6.5
Hg	<0.005	<0.005	0.00814	-	-	Pb	7.2
In	<0.02	<0.02	<0.02	-	-	Ga	7.3
K	997	1 120	1 270	69.8	5.9	As	7.7
La	12.8	15.4	17.1	1.37	10.2	Sr	7.8
Li	10.1	11.3	13.0	1.00	8.4	Li	8.4
Mg	6 750	7 420	7 980	278	3.8	Ti	8.5
Mn	248	271	295	8.49	3.5	Sb	8.9
Mo	0.240	0.270	0.315	0.0160	6.4	Sn	9.5
Na	64.8	77.1	96.8	11.6	13.4	Nb	10.0
Nb	0.292	0.331	0.430	0.0321	10.0	La	10.2
Ni	37.6	40.4	44.6	1.56	3.8	Sc	10.3
P	470	527	583	21.1	4.3	Ba	10.7
Pb	4.33	4.90	5.61	0.384	7.2	Zr	11.4
Pd	<0.01	<0.01	0.0127	-	-	Bi	12.0
Pt	<0.002	<0.002	<0.002	-	-	U	12.8
Rb	7.60	8.23	9.05	0.386	4.6	Na	13.4
Re	<0.001	<0.001	0.00103	-	-	Be	13.9
S	<15	<15	<15	-	-	Hf	16.2
Sb	0.0487	0.0681	0.0814	0.00696	8.9	Cd	18.2

Element	MINN Project standard (n=19)					Sorted by precision	
	MIN mg/kg	MEDIAN mg/kg	MAX mg/kg	IQR mg/kg	CVR %	Element	CVR %
Sc	2.74	3.15	3.87	0.367	10.3	Th	21.1
Se	<0.1	<0.1	0.239	-	-	Au	57.6
Sn	0.188	0.228	0.319	0.0227	9.5	Ag	-
Sr	7.52	8.75	10.0	0.690	7.8	B	-
Ta	<0.05	<0.05	<0.05	-	-	Ge	-
Te	<0.02	<0.02	0.0318	-	-	Hg	-
Th	3.78	4.68	8.89	0.951	21.1	In	-
Ti	585	680	817	70.3	8.5	Pd	-
Tl	0.0687	0.0884	0.0980	0.00544	6.3	Pt	-
U	0.487	0.597	0.719	0.0769	12.8	Re	-
V	21.7	24.1	26.5	1.15	4.4	S	-
W	<0.05	<0.05	0.0802	0.00263	-	Se	-
Y	6.53	7.41	8.16	0.310	4.2	Ta	-
Zn	27.1	29.4	32.2	1.15	4.8	Te	-
Zr	4.52	5.89	8.68	0.635	11.4	W	-

**TABLE A5 PRECISION OF DUPLICATES**

The precision for analytical duplicates is improved to 6.3%, 10.8%, 5.4%, 4.5%, and 3.2% for Nb, Se, Th, U, and Y respectively if the analytical duplicate pair 3860D and 3860DD is removed from the analysis.

Field duplicates (40 pairs)						Analytical duplicates (40 pairs)					
Alphabetical			Sorted			Alphabetical			Sorted		
Element	No. pair >MDL	Precision (CV) %	Element	No. pair >MDL	Precision (CV) %	Element	No. pair >MDL	Precision (CV) %	Element	No. pair >MDL	Precision (CV) %
<b>Ag</b>	32	41	<b>Ba</b>	40	16	<b>Ag</b>	33	11.3	<b>Al</b>	40	2.5
<b>Al</b>	40	27	<b>Th</b>	40	17	<b>Al</b>	40	2.5	<b>Fe</b>	40	3.1
<b>As</b>	39	75	<b>B</b>	5	18	<b>As</b>	37	8.4	<b>Ti</b>	39	3.3
<b>Au</b>	18	37	<b>Fe</b>	40	19	<b>Au</b>	18	32.2	<b>V</b>	40	3.3
<b>B</b>	5	18	<b>Sc</b>	39	21	<b>B</b>	4	-	<b>Mg</b>	39	3.5
<b>Ba</b>	40	16	<b>Y</b>	40	21	<b>Ba</b>	40	3.8	<b>Mn</b>	40	3.6
<b>Be</b>	30	30	<b>Sn</b>	34	23	<b>Be</b>	29	15.5	<b>Cs</b>	40	3.7
<b>Bi</b>	33	33	<b>La</b>	40	25	<b>Bi</b>	34	7.5	<b>Ba</b>	40	3.8
<b>Ca</b>	36	36	<b>Ce</b>	40	25	<b>Ca</b>	37	3.8	<b>Ca</b>	37	3.8
<b>Cd</b>	28	139	<b>P</b>	40	26	<b>Cd</b>	29	9.3	<b>Sr</b>	40	3.8
<b>Ce</b>	40	25	<b>Al</b>	40	27	<b>Ce</b>	40	4.9	<b>Zn</b>	40	3.8
<b>Co</b>	39	29	<b>Pb</b>	40	27	<b>Co</b>	39	6.2	<b>Pb</b>	40	3.9
<b>Cr</b>	40	42	<b>Ti</b>	39	28	<b>Cr</b>	40	5.0	<b>Rb</b>	40	3.9
<b>Cs</b>	40	30	<b>W</b>	12	29	<b>Cs</b>	40	3.7	<b>Sc</b>	40	3.9
<b>Cu</b>	40	39	<b>Sr</b>	40	29	<b>Cu</b>	40	4.5	<b>K</b>	40	4.0
<b>Fe</b>	40	19	<b>V</b>	40	29	<b>Fe</b>	40	3.1	<b>Li</b>	40	4.4
<b>Ga</b>	40	31	<b>Co</b>	39	29	<b>Ga</b>	40	5.0	<b>Cu</b>	40	4.5
<b>Ge</b>	0	-	<b>Na</b>	33	29	<b>Ge</b>	0	-	<b>P</b>	40	4.5
<b>Hf</b>	33	44	<b>Be</b>	30	30	<b>Hf</b>	33	13.3	<b>Ce</b>	40	4.9
<b>Hg</b>	21	50	<b>Cs</b>	40	30	<b>Hg</b>	19	19.9	<b>Tl</b>	34	4.9
<b>In</b>	4	-	<b>Ga</b>	40	31	<b>In</b>	2	-	<b>Cr</b>	40	5.0
<b>K</b>	40	52	<b>Se</b>	16	32	<b>K</b>	40	4.0	<b>Ga</b>	40	5.0
<b>La</b>	40	25	<b>U</b>	40	33	<b>La</b>	40	5.8	<b>Ni</b>	40	5.6
<b>Li</b>	39	58	<b>Bi</b>	33	33	<b>Li</b>	40	4.4	<b>La</b>	40	5.8
<b>Mg</b>	37	41	<b>Ni</b>	40	35	<b>Mg</b>	39	3.5	<b>Co</b>	39	6.2
<b>Mn</b>	40	43	<b>Ca</b>	36	36	<b>Mn</b>	40	3.6	<b>Zr</b>	39	6.4
<b>Mo</b>	38	130	<b>Nb</b>	40	36	<b>Mo</b>	37	7.3	<b>Na</b>	34	7.0
<b>Na</b>	33	29	<b>Au</b>	18	37	<b>Na</b>	34	7.0	<b>Mo</b>	37	7.3
<b>Nb</b>	40	36	<b>Rb</b>	40	37	<b>Nb</b>	40	11.5	<b>Bi</b>	34	7.5
<b>Ni</b>	40	35	<b>Cu</b>	40	39	<b>Ni</b>	40	5.6	<b>As</b>	37	8.4
<b>P</b>	40	26	<b>Tl</b>	33	39	<b>P</b>	40	4.5	<b>Cd</b>	29	9.3
<b>Pb</b>	40	27	<b>Mg</b>	37	41	<b>Pb</b>	40	3.9	<b>Sn</b>	35	9.7
<b>Pd</b>	0	-	<b>Ag</b>	32	41	<b>Pd</b>	0	-	<b>Te</b>	7	9.9
<b>Pt</b>	0	-	<b>Zn</b>	40	41	<b>Pt</b>	0	-	<b>W</b>	13	10.3
<b>Rb</b>	40	37	<b>Cr</b>	40	42	<b>Rb</b>	40	3.9	<b>Y</b>	40	10.9
<b>Re</b>	0	-	<b>Mn</b>	40	43	<b>Re</b>	0	-	<b>Ag</b>	33	11.3



Field duplicates (40 pairs)						Analytical duplicates (40 pairs)					
Alphabetical			Sorted			Alphabetical			Sorted		
Element	No. pair >MDL	Precision (CV) %	Element	No. pair >MDL	Precision (CV) %	Element	No. pair >MDL	Precision (CV) %	Element	No. pair >MDL	Precision (CV) %
<b>S</b>	26	102	<b>Hf</b>	33	44	<b>S</b>	31	46.8	<b>Nb</b>	40	11.5
<b>Sb</b>	24	80	<b>Zr</b>	40	44	<b>Sb</b>	24	27.4	<b>Hf</b>	33	13.3
<b>Sc</b>	39	21	<b>Hg</b>	21	50	<b>Sc</b>	40	3.9	<b>Be</b>	29	15.5
<b>Se</b>	16	32	<b>K</b>	40	52	<b>Se</b>	14	22.0	<b>Hg</b>	19	19.9
<b>Sn</b>	34	23	<b>Li</b>	39	58	<b>Sn</b>	35	9.7	<b>Se</b>	14	22.0
<b>Sr</b>	40	29	<b>Te</b>	7	66	<b>Sr</b>	40	3.8	<b>Sb</b>	24	27.4
<b>Ta</b>	0	-	<b>As</b>	39	75	<b>Ta</b>	1	-	<b>U</b>	40	29.4
<b>Te</b>	7	66	<b>Sb</b>	24	80	<b>Te</b>	7	9.9	<b>Au</b>	18	32.2
<b>Th</b>	40	17	<b>S</b>	26	102	<b>Th</b>	40	219.0	<b>S</b>	31	46.8
<b>Ti</b>	39	28	<b>Mo</b>	38	130	<b>Ti</b>	39	3.3	<b>Th</b>	40	219.0
<b>Tl</b>	33	39	<b>Cd</b>	28	139	<b>Tl</b>	34	4.9	<b>B</b>	4	-
<b>U</b>	40	33	<b>Ta</b>	0	-	<b>U</b>	40	29.4	<b>Ge</b>	0	-
<b>V</b>	40	29	<b>Ge</b>	0	-	<b>V</b>	40	3.3	<b>In</b>	2	-
<b>W</b>	12	29	<b>In</b>	4	-	<b>W</b>	13	10.3	<b>Pd</b>	0	-
<b>Y</b>	40	21	<b>Pd</b>	0	-	<b>Y</b>	40	10.9	<b>Pt</b>	0	-
<b>Zn</b>	40	41	<b>Pt</b>	0	-	<b>Zn</b>	40	3.8	<b>Re</b>	0	-
<b>Zr</b>	40	44	<b>Re</b>	0	-	<b>Zr</b>	39	6.4	<b>Ta</b>	1	-

**TABLE A6 ANOVA**

Analysis of variance table (ANOVA) for the 40 duplicate sites giving the distributed percentage variabilities for all elements with < 4 pairs above DL. The p-value is for the F-test. All variables were log-transformed prior to the calculation

Element	Regional %	Site %	Analytical %	p- value	Element	Regional %	Site %	Analytical %	p- value
Ag	83.2	12.5	4.29	0.33	Mo	93.5	5.5	0.93	0.30
Al	85.9	14.0	0.10	0.46	Na	96.5	1.9	1.62	0.52
As	86.0	10.6	3.40	0.26	Nb	81.3	18.4	0.38	0.23
Au	52.8	23.5	23.71	0.39	Ni	88.8	11.1	0.10	0.43
Ba	95.1	4.7	0.21	0.43	P	72.6	26.4	1.09	0.16
Be	83.6	9.1	7.30	0.37	Pb	86.3	13.5	0.18	0.27
Bi	82.9	12.3	4.79	0.35	Rb	91.2	8.7	0.15	0.41
Ca	93.6	5.9	0.57	0.39	S	60.8	28.9	10.28	0.07
Cd	82.1	12.7	5.16	0.14	Sb	91.8	7.7	0.53	0.32
Ce	85.7	13.6	0.74	0.25	Sc	93.3	6.2	0.55	0.42
Co	87.9	12.0	0.18	0.34	Se	67.1	25.1	7.80	0.08
Cr	94.1	5.8	0.07	0.49	Sn	85.3	12.1	2.62	0.46
Cs	93.8	6.1	0.12	0.44	Sr	91.4	8.4	0.22	0.31
Cu	91.3	8.6	0.06	0.35	Te	81.2	12.0	6.78	0.27
Fe	94.4	5.5	0.10	0.42	Th	87.8	11.2	1.03	0.36
Ga	92.4	7.4	0.30	0.37	Ti	94.0	5.9	0.06	0.48
Hf	71.4	24.3	4.30	0.19	Tl	91.9	7.8	0.37	0.41
Hg	52.6	33.2	14.17	0.06	U	89.3	9.9	0.82	0.25
K	91.1	8.7	0.13	0.53	V	96.2	3.7	0.15	0.49
La	87.8	10.8	1.39	0.23	W	82.1	15.6	2.30	0.44
Li	85.3	14.5	0.19	0.36	Y	88.5	11.2	0.30	0.33
Mg	91.1	8.8	0.09	0.46	Zn	88.6	11.2	0.11	0.33
Mn	82.1	17.8	0.12	0.14	Zr	73.6	25.7	0.70	0.23

## TABLE A7 SURVEY DATA

Summary statistics for the survey data (n=787) giving the number of samples above the methodical detection limit (MDL), minimum (Min), maximum (Max) concentration values, and the measured concentration at the 2, 5, 10, 25, 50, 75, 90, 95 and 90 % quantiles. In addition, the powers (P) are given as a measure on variation. Summary of the magnetic susceptibility (MS) measurement is given at the end of the Table.

	N>DL		Min	Q2	Q5	Q10	Q25	Q50	Q75	Q90	Q95	Q98	Max	P
Ag	686	mg/kg	<0.002	<0.002	<0.002	<0.002	0.00437	0.01	0.0266	0.0584	0.0873	0.143	0.491	2.4
Al	787	mg/kg	258	660	1575	2476	4072	6376	10370	15878	19848	25000	40963	2.2
As	753	mg/kg	<0.1	<0.1	0.116	0.204	0.372	0.694	1.38	3.07	5.44	7.77	20.1	2.3
Au	413	mg/kg	<0.0002	<0.0002	<0.0002	<0.0002	<0.0002	0.000217	0.000448	0.000784	0.0012	0.00183	0.0172	1.9
B	141	mg/kg	<1	<1	<1	<1	<1	<1	<1	1.37	1.72	2.43	4.94	0.7
Ba	787	mg/kg	3.15	7.53	9.18	11.9	17.1	25.9	41	72.2	99.5	157	1228	2.6
Be	642	mg/kg	<0.1	<0.1	<0.1	<0.1	0.134	0.224	0.35	0.505	0.61	0.85	3.9	1.6
Bi	687	mg/kg	<0.02	<0.02	<0.02	<0.02	0.0319	0.052	0.0806	0.129	0.158	0.204	0.506	1.4
Ca	730	mg/kg	<100	<100	<100	128	403	859	1394	1959	2385	2986	9540	2
Cd	603	mg/kg	<0.01	<0.01	<0.01	<0.01	0.0113	0.0236	0.0434	0.0716	0.101	0.161	0.374	1.6
Ce	787	mg/kg	1.32	9.9	13.1	16.7	22.4	30.2	42.1	57.8	68.8	92.8	269	2.3
Co	768	mg/kg	<0.1	<0.1	0.361	0.844	1.77	3.17	5.99	12.4	16.1	20	38.9	2.6
Cr	781	mg/kg	<0.5	0.815	1.68	2.54	4.13	6.71	12.2	49.5	70.9	101	464	3
Cs	787	mg/kg	0.0643	0.119	0.16	0.218	0.353	0.57	0.993	1.66	2.4	3.43	5.66	1.9
Cu	786	mg/kg	<0.01	0.154	0.443	0.975	2.31	4.63	10.6	22.4	31.5	45.3	78.2	3.9
Fe	787	mg/kg	167	1336	2456	3883	5959	9356	16370	25543	31024	36168	86015	2.7
Ga	785	mg/kg	<0.1	0.273	0.425	0.593	1.04	1.7	2.92	4.41	5.4	6.7	17	2.2
Ge	39	mg/kg	<0.1	<0.1	<0.1	<0.1	<0.1	<0.1	<0.1	<0.1	<0.1	0.135	0.642	0.8
Hf	652	mg/kg	<0.02	<0.02	<0.02	<0.02	0.0264	0.0517	0.0825	0.128	0.171	0.225	0.56	1.4
Hg	469	mg/kg	<0.005	<0.005	<0.005	<0.005	<0.005	0.00706	0.0141	0.0255	0.0359	0.0527	0.11	1.3
In	67	mg/kg	<0.02	<0.02	<0.02	<0.02	<0.02	<0.02	<0.02	<0.02	0.0245	0.0307	0.176	0.9
K	786	mg/kg	<100	160	204	240	360	552	920	1583	2606	4918	13891	2.1
La	787	mg/kg	0.677	4.88	6.52	7.86	10.3	13.5	18.3	24.5	29.5	35.5	184	2.4

	N>DL		Min	Q2	Q5	Q10	Q25	Q50	Q75	Q90	Q95	Q98	Max	P
Li	769	mg/kg	<0.1	<0.1	0.516	1.33	3.12	5.4	9.94	18.3	23.9	32.7	84	2.9
Mg	757	mg/kg	<100	<100	231	530	1008	1828	3384	8228	11337	13492	25878	2.4
Mn	785	mg/kg	<1	6.14	18	35.6	75.4	129	224	357	457	636	4733	3.7
Mo	752	mg/kg	<0.01	<0.01	0.0117	0.0231	0.0646	0.16	0.329	0.742	1.37	3.23	16.7	3.2
Na	692	mg/kg	<10	<10	<10	<10	14.8	26.1	48.5	78.9	102	149	496	1.7
Nb	785	mg/kg	<0.02	0.0609	0.124	0.183	0.315	0.531	0.889	1.37	1.76	2.19	18.9	3
Ni	781	mg/kg	<0.1	0.174	0.764	1.56	3.11	5.44	10.6	32	49.7	74.8	196	3.3
P	786	mg/kg	<10	41.1	66.7	116	196	307	446	584	707	892	2765	2.4
Pb	787	mg/kg	0.342	1.69	2.22	2.68	3.52	5.13	8.14	11.9	15.9	20.8	95.5	2.4
Pd	1	mg/kg	<0.01	<0.01	<0.01	<0.01	<0.01	<0.01	<0.01	<0.01	<0.01	<0.01	0.0117	0.1
Pt	6	mg/kg	<0.002	<0.002	<0.002	<0.002	<0.002	<0.002	<0.002	<0.002	<0.002	<0.002	0.0031	0.2
Rb	787	mg/kg	0.847	1.79	2.34	2.9	4.3	6.72	11	18.5	25.9	38	86.6	2
Re	14	mg/kg	<0.001	<0.001	<0.001	<0.001	<0.001	<0.001	<0.001	<0.001	<0.001	<0.001	0.00274	0.4
S	598	mg/kg	<15	<15	<15	<15	15.8	36.2	73.1	142	198	270	710	1.7
Sb	483	mg/kg	<0.02	<0.02	<0.02	<0.02	<0.02	0.0262	0.0531	0.0912	0.138	0.226	0.7	1.5
Sc	769	mg/kg	<0.1	<0.1	0.192	0.377	0.729	1.17	1.85	2.93	3.65	4.57	10.9	2
Se	397	mg/kg	<0.1	<0.1	<0.1	<0.1	<0.1	0.101	0.188	0.304	0.399	0.571	0.919	1
Sn	714	mg/kg	<0.1	<0.1	<0.1	0.102	0.154	0.253	0.38	0.534	0.634	0.882	4.15	1.6
Sr	783	mg/kg	<0.5	1.21	1.67	2.33	3.94	6.54	9.9	14.6	19.3	25.6	46.9	2
Ta	3	mg/kg	<0.05	<0.05	<0.05	<0.05	<0.05	<0.05	<0.05	<0.05	<0.05	<0.05	0.119	0.4
Te	138	mg/kg	<0.02	<0.02	<0.02	<0.02	<0.02	<0.02	<0.02	0.029	0.0387	0.0518	0.214	1
Th	786	mg/kg	<0.1	0.729	1.18	1.77	2.68	3.72	5.33	6.84	8.06	9.71	23.9	2.4
Ti	785	mg/kg	<10	41	61.5	94.1	193	368	608	978	1177	1625	2934	2.5
Tl	715	mg/kg	<0.02	<0.02	<0.02	0.0206	0.0316	0.0536	0.0974	0.17	0.254	0.366	0.616	1.5
U	787	mg/kg	0.07	0.207	0.285	0.354	0.494	0.681	1.01	1.42	1.77	2.56	32.5	2.7
V	775	mg/kg	<1	1.55	2.59	3.37	6.25	11.1	20.3	35.5	43.5	58.8	201	2.3
W	303	mg/kg	<0.05	<0.05	<0.05	<0.05	<0.05	<0.05	0.0754	0.117	0.144	0.194	0.543	1
Y	787	mg/kg	0.456	0.937	1.52	2.42	3.57	5.3	7.31	9.96	12.6	17.4	46.3	2

	<b>N&gt;DL</b>		<b>Min</b>	<b>Q2</b>	<b>Q5</b>	<b>Q10</b>	<b>Q25</b>	<b>Q50</b>	<b>Q75</b>	<b>Q90</b>	<b>Q95</b>	<b>Q98</b>	<b>Max</b>	<b>P</b>
Zn	787	mg/kg	0.288	0.748	2.68	5.27	11.6	20.5	34.6	55.4	67.5	80	150	2.7
Zr	784	mg/kg	<0.1	0.23	0.46	0.765	1.4	2.45	4.02	5.79	7.53	10.4	20.4	2.3
MS	775		7.60E-06	3.31E-05	5.66E-05	8.22E-05	1.50E-04	3.50E-04	8.94E-04	0.00211	0.00273	0.0038	0.0118	3.2





# **APPENDIXES**

**Appendix 1: Random plots**

**Appendix 2: X-charts including analysis of splits with the MINN in-house  
standard from 2019 and 2022**

**Appendix 3: Samples re-analysed from previous surveys**

**Appendix 4: Correlation plots field duplicates and analytical duplicates**

**Appendix 5: ECDF-PLOTS**

**Appendix 6: Geochemical maps**

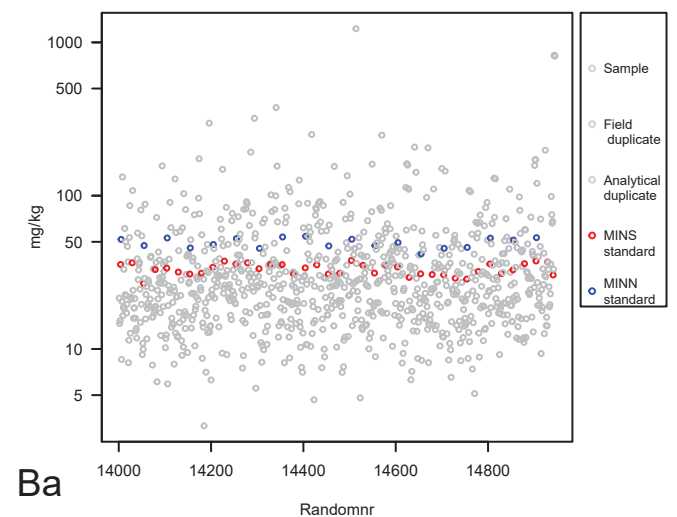
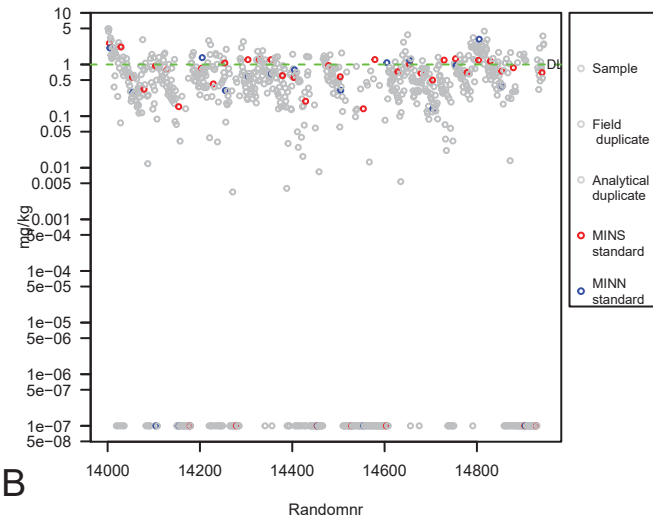
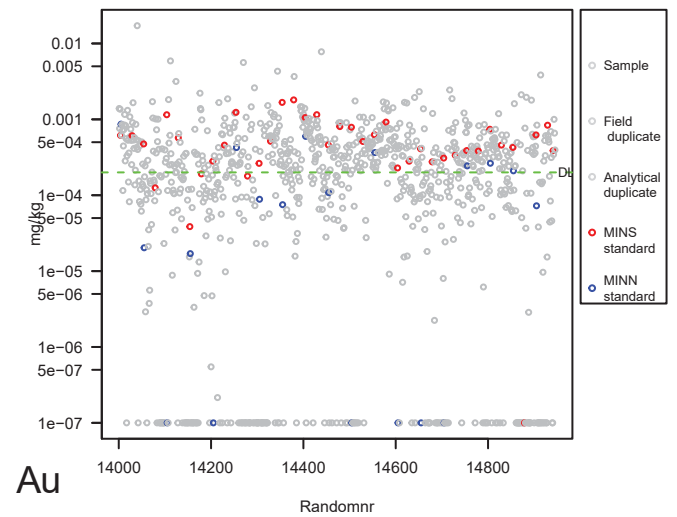
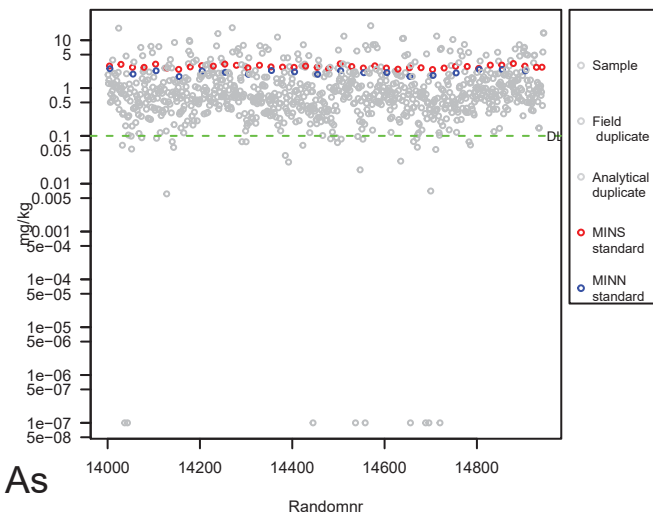
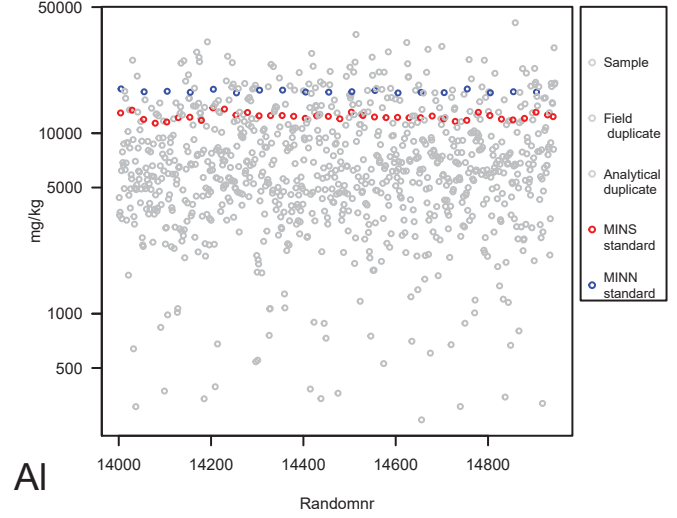
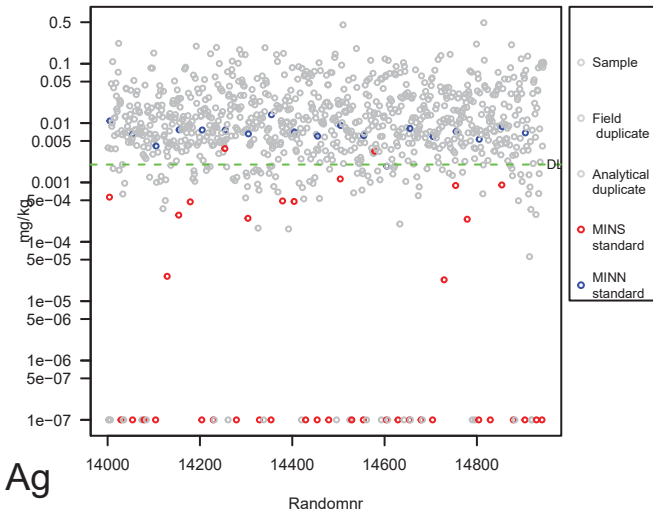


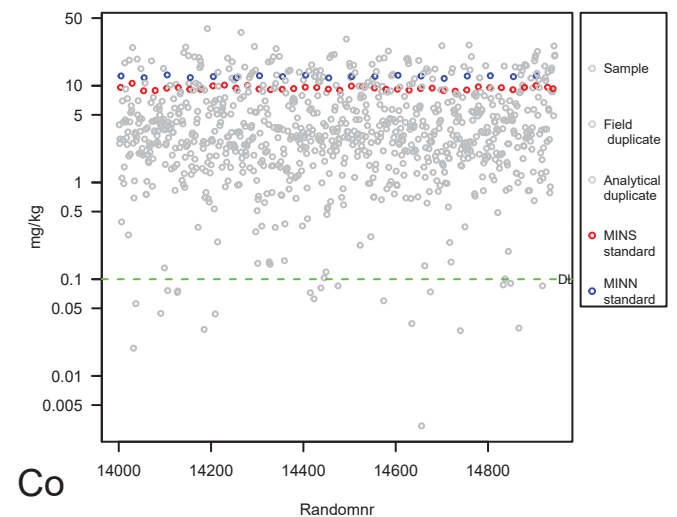
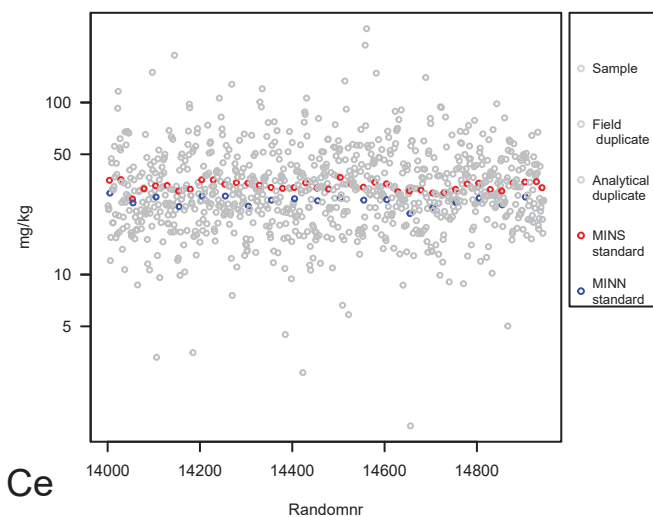
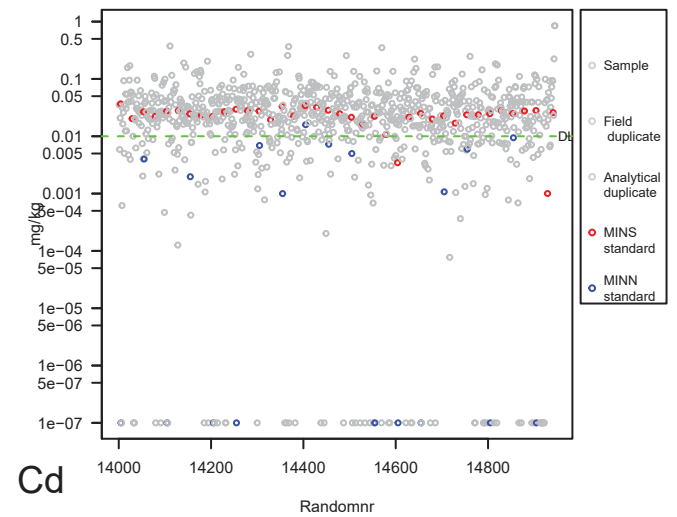
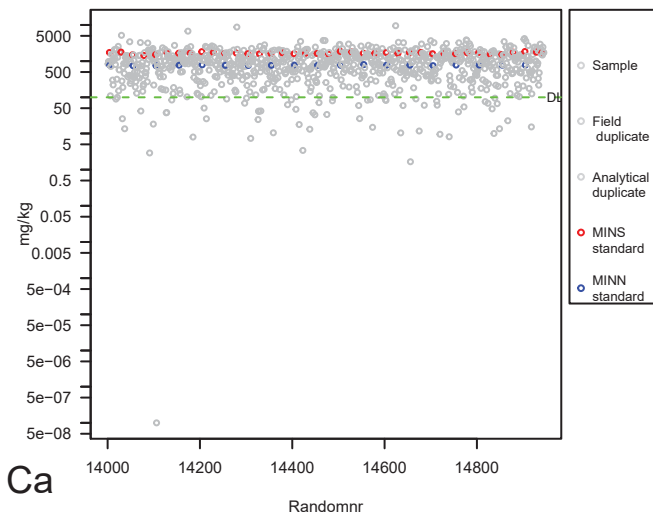
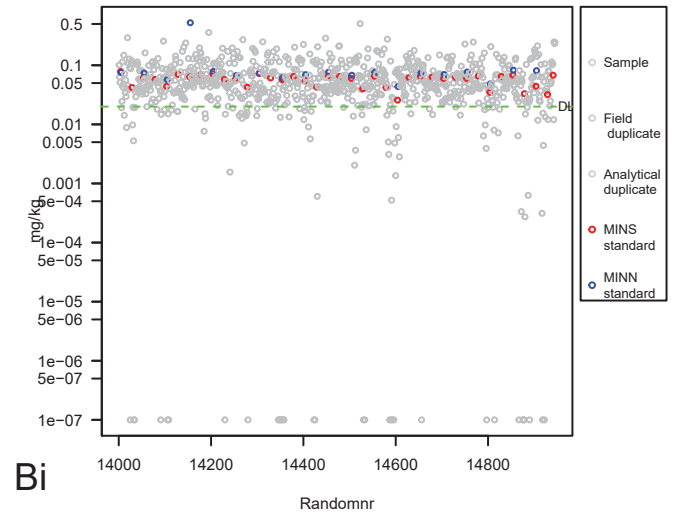
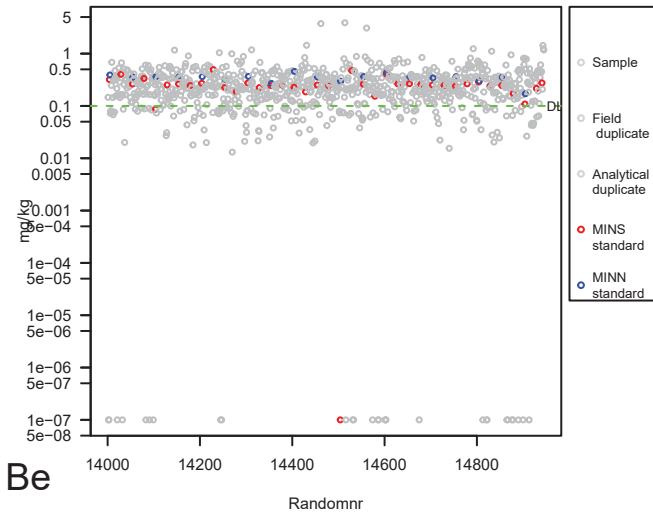
## APPENDIX 1: RANDOM PLOTS

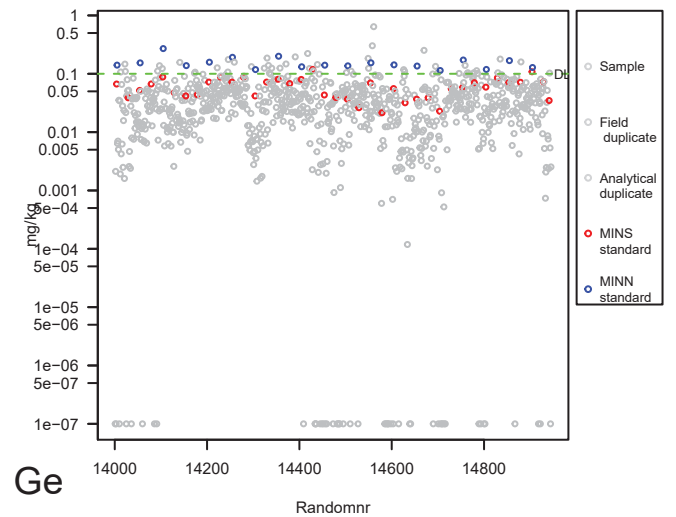
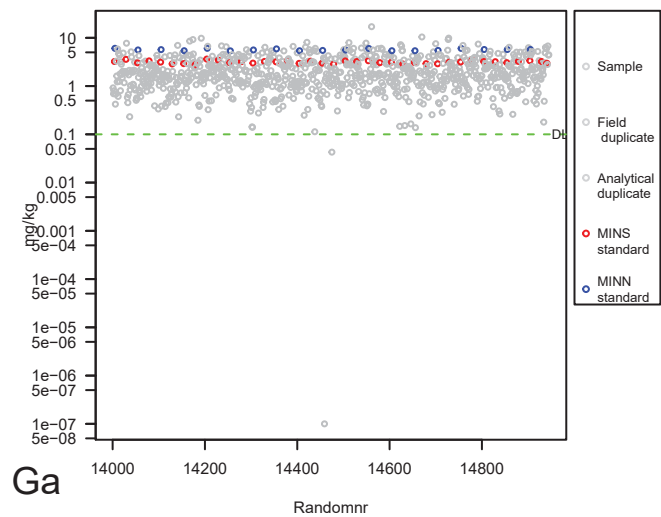
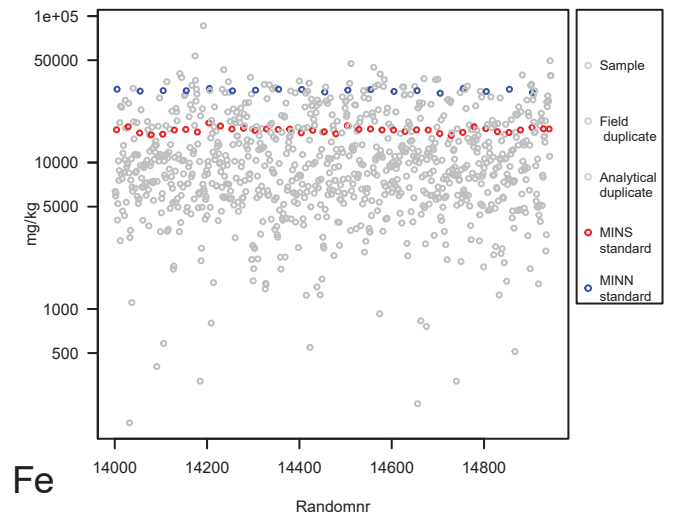
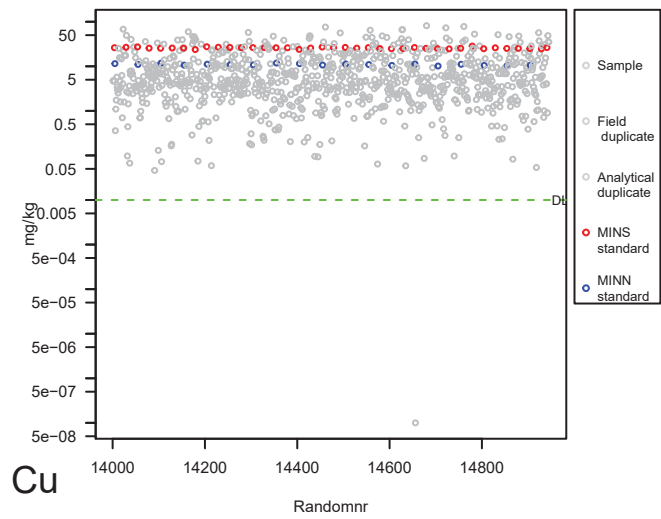
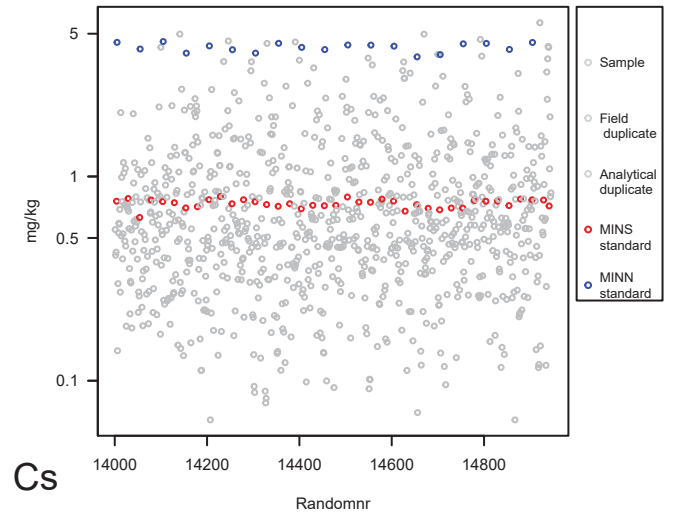
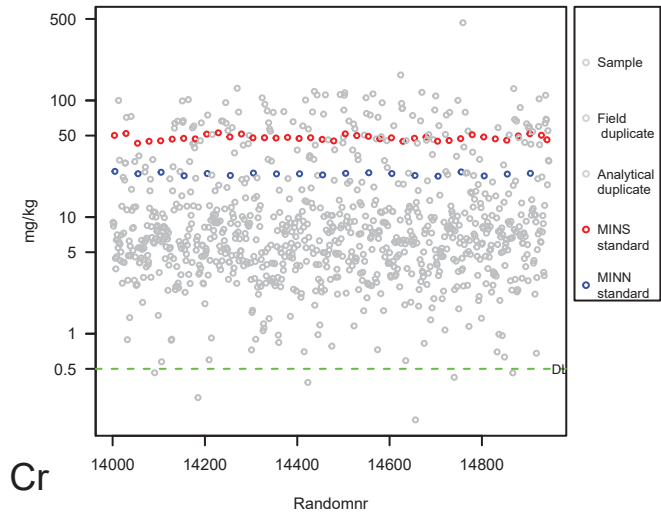
Random plots of all samples with field and analytical duplicates in addition to the in-house standards MINS and MINN.

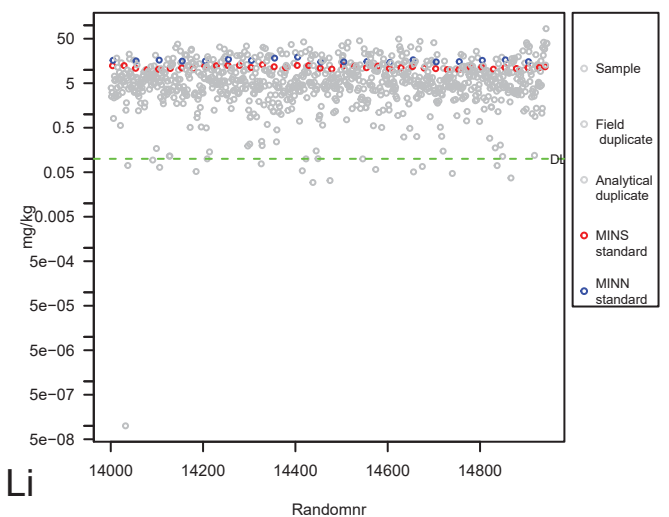
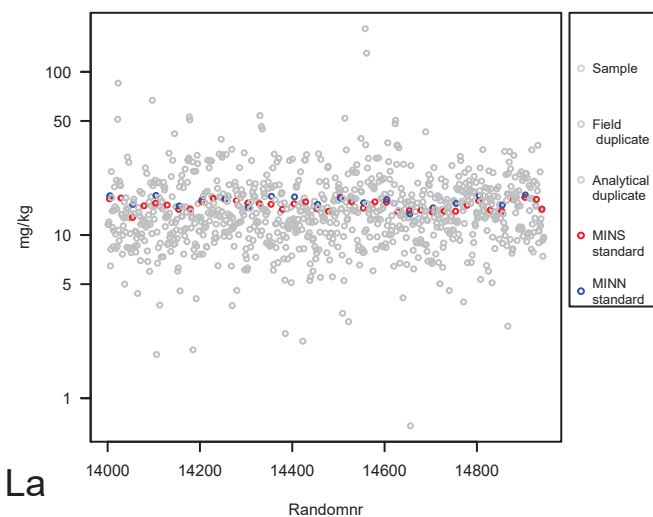
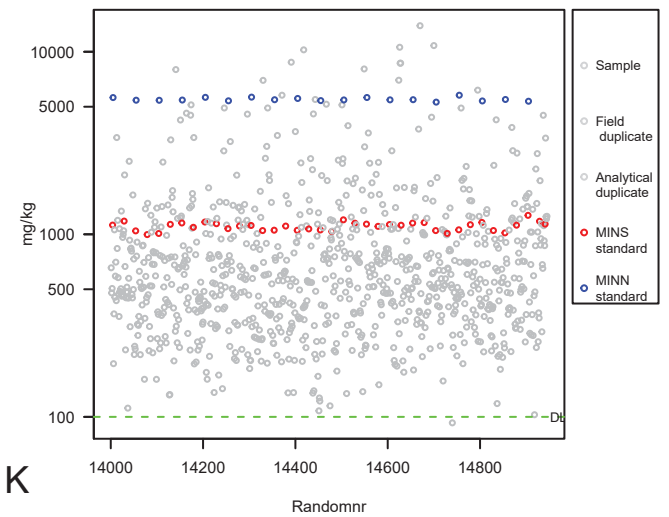
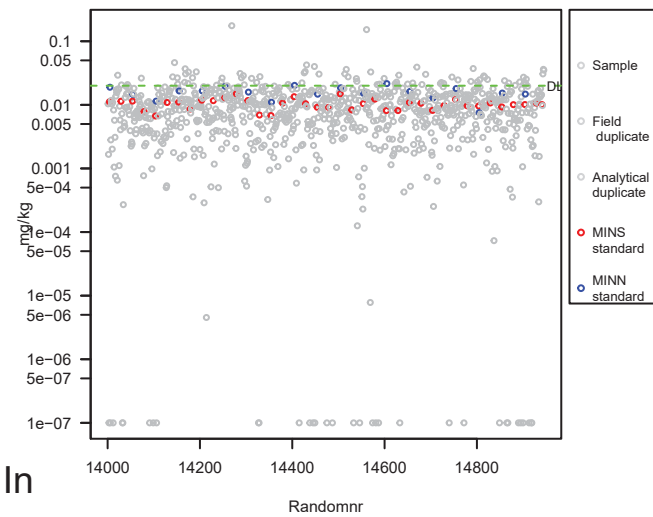
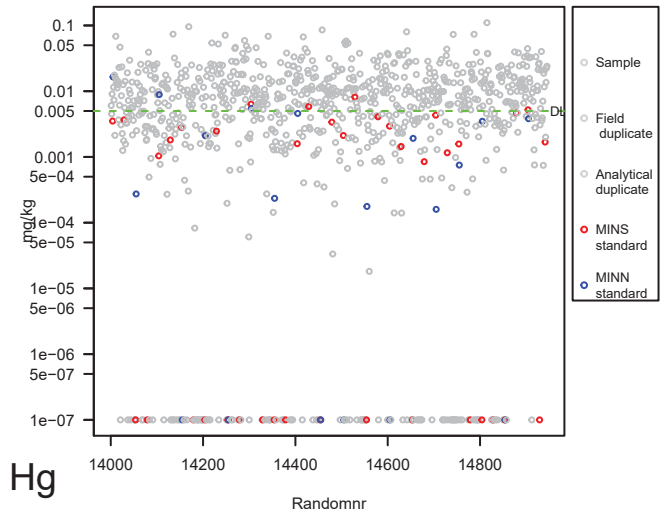
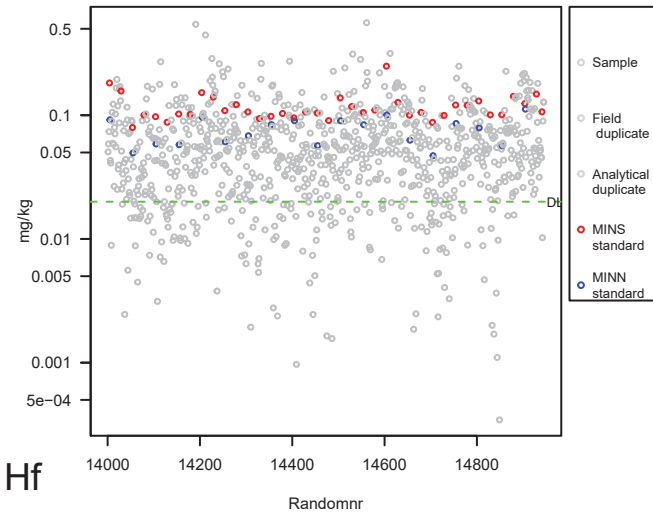
The laboratory method detection limit (MDL) is indicated by a green dotted line for elements with concentrations close to MDL. The green dotted line is indicating a PDL for S.

Negative laboratory concentration values set to a low positive value to fit the log scale.

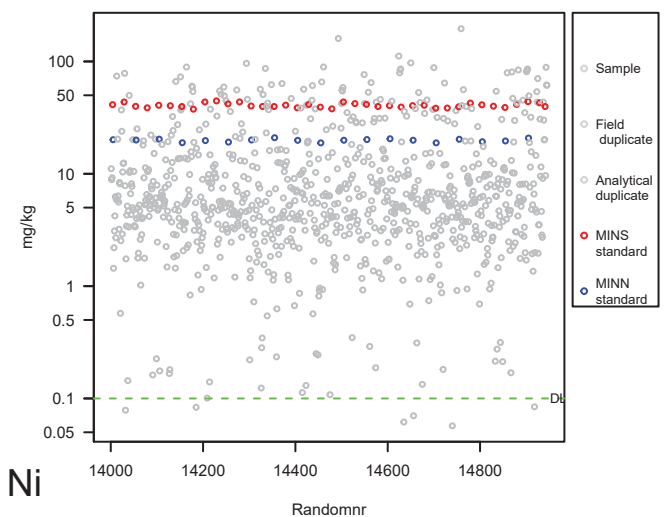
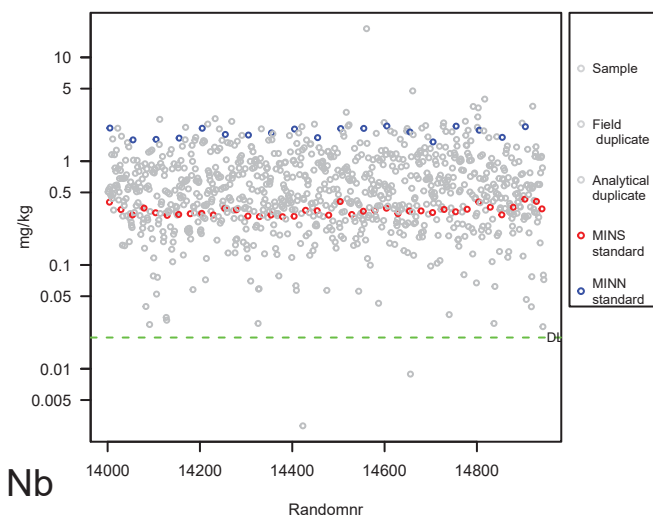
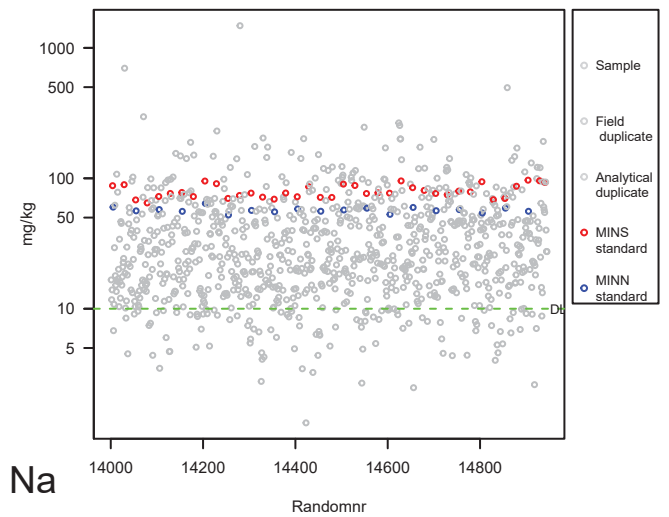
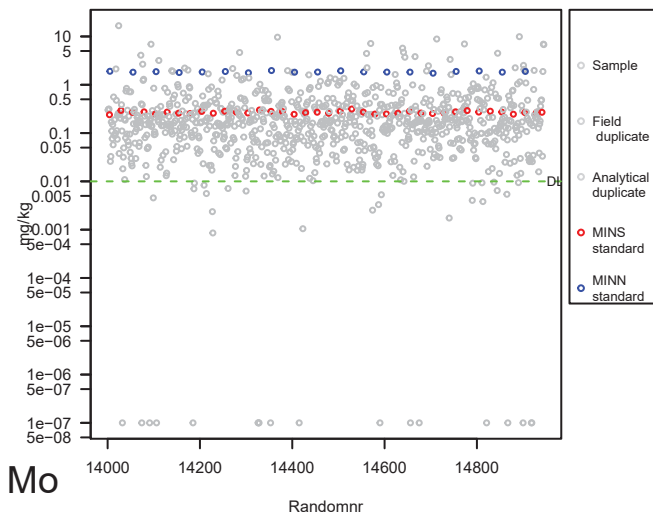
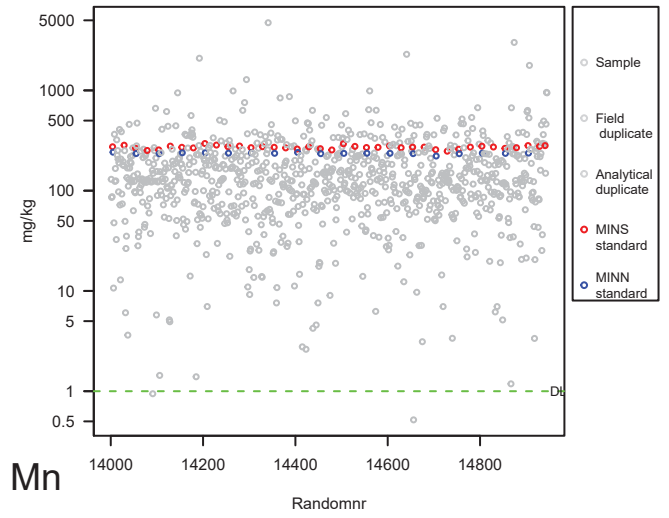
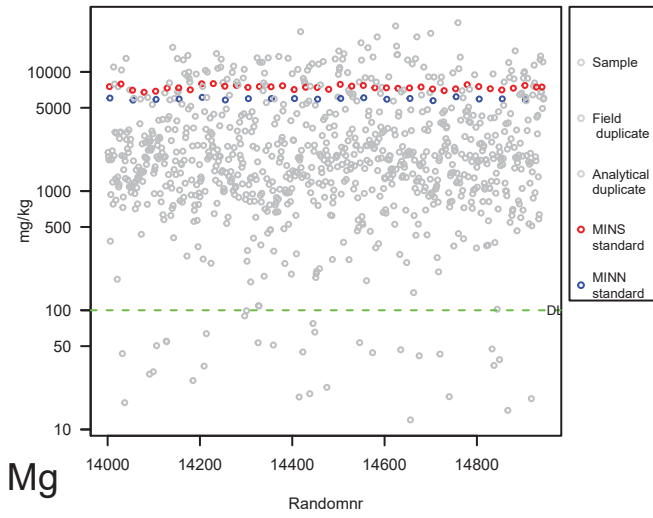


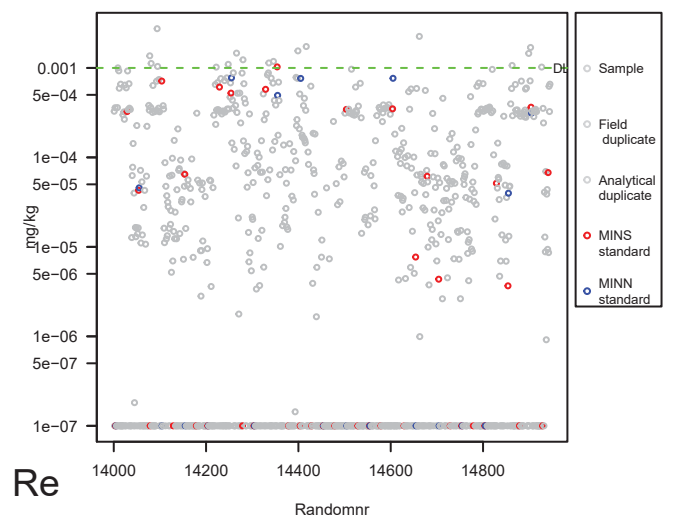
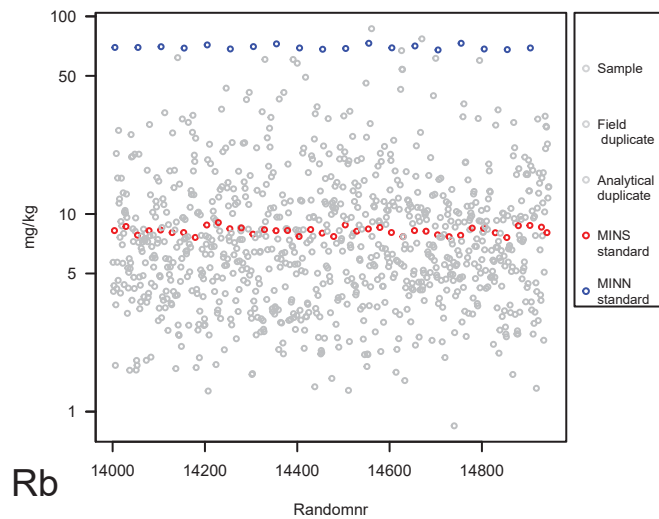
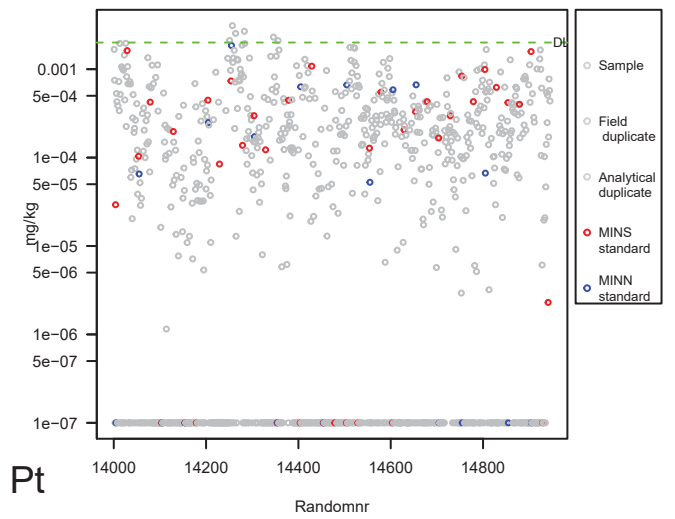
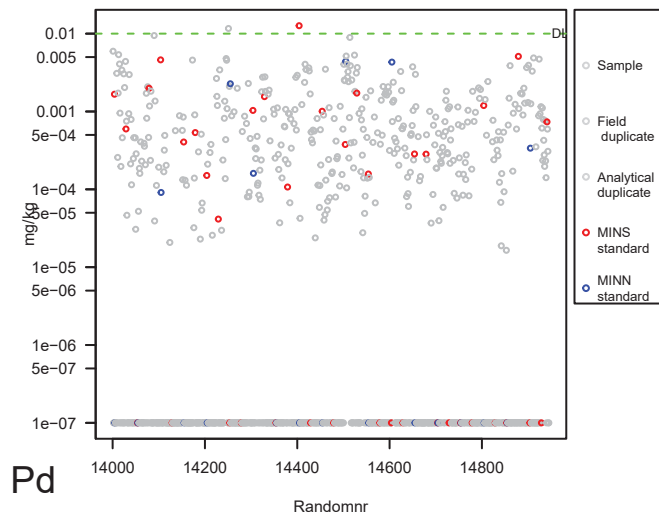
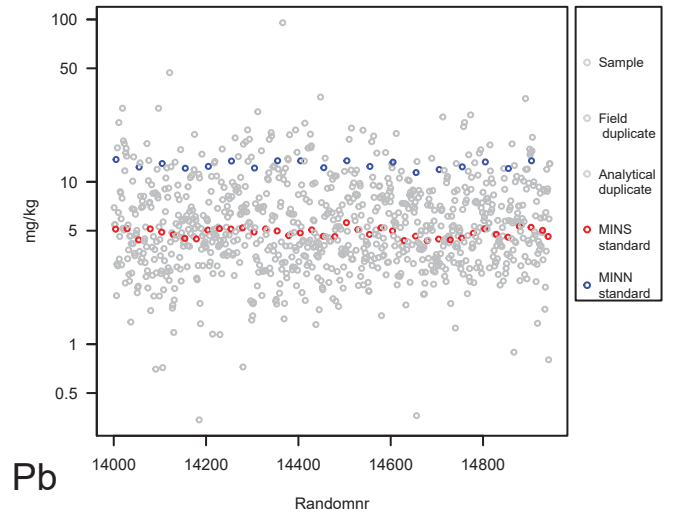
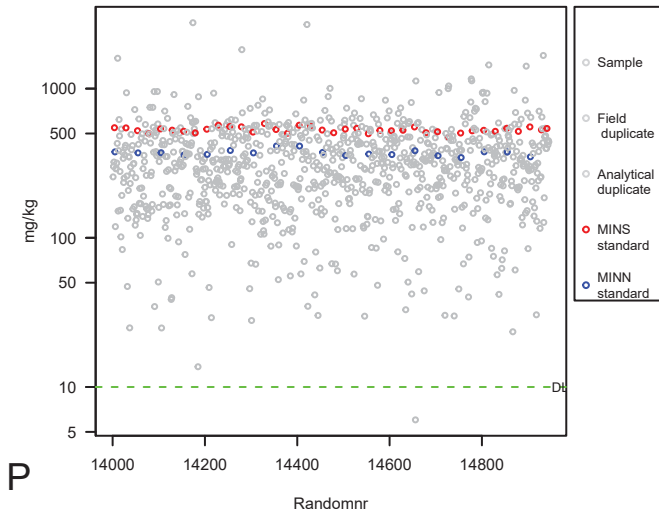


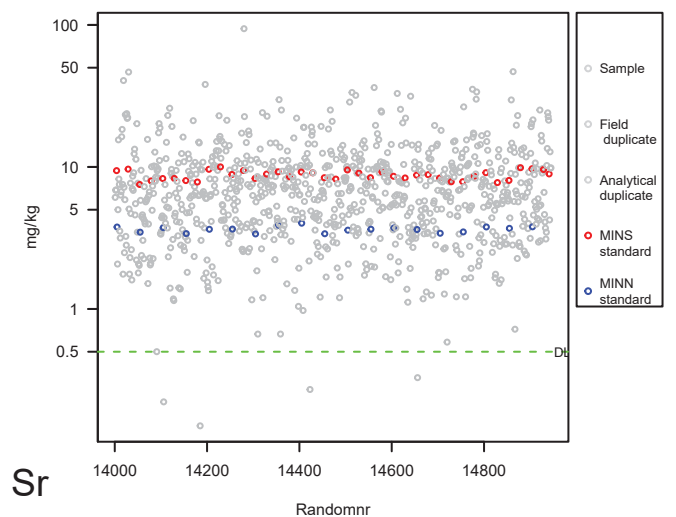
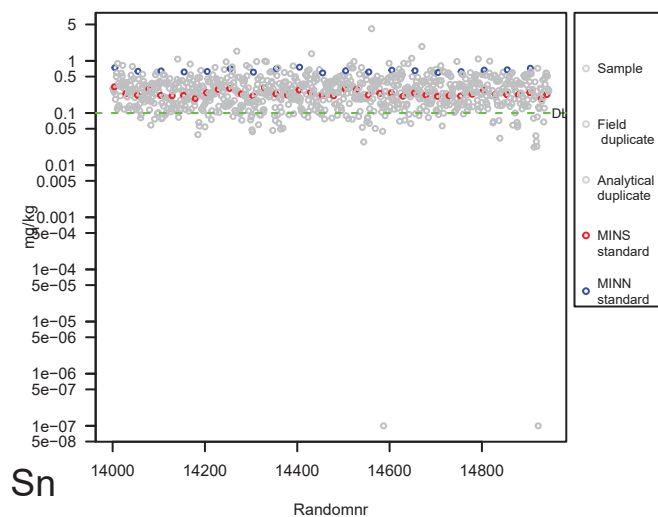
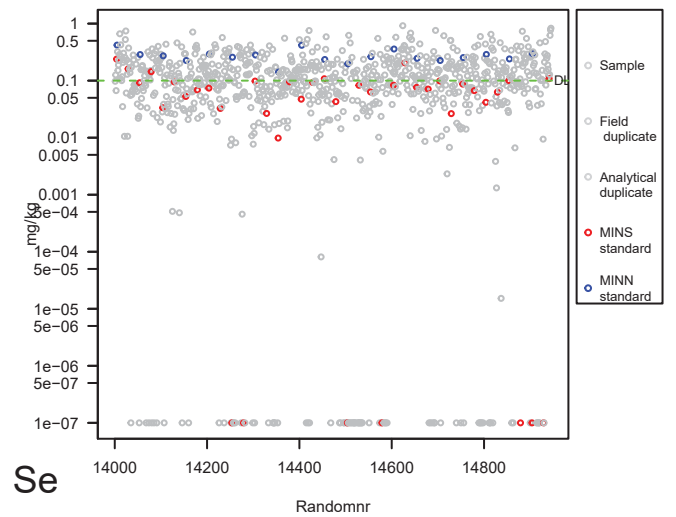
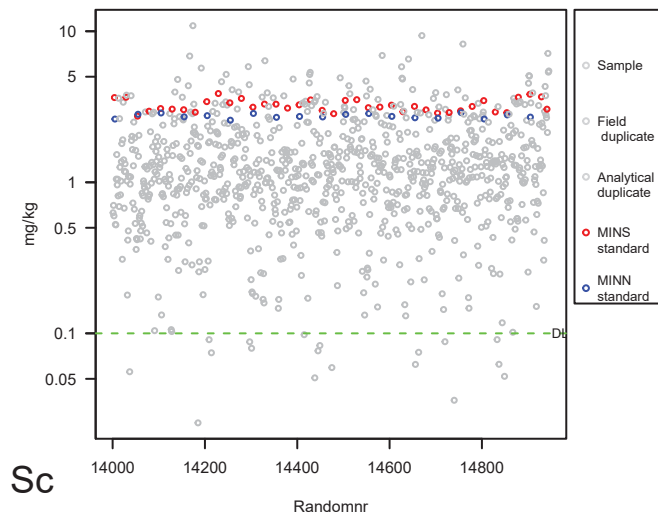
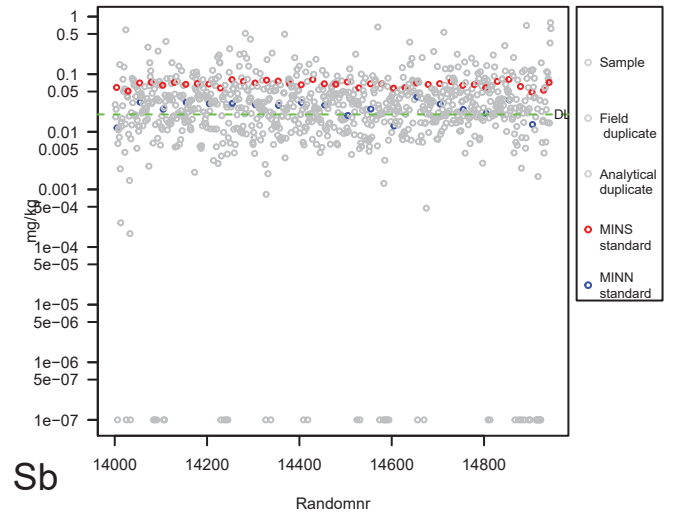
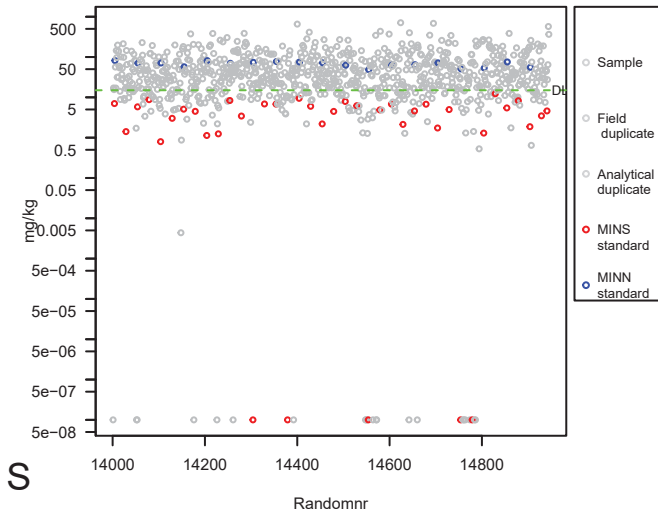


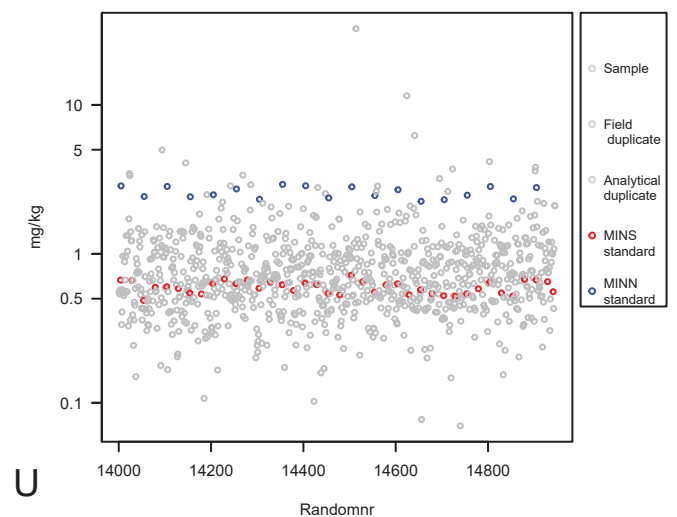
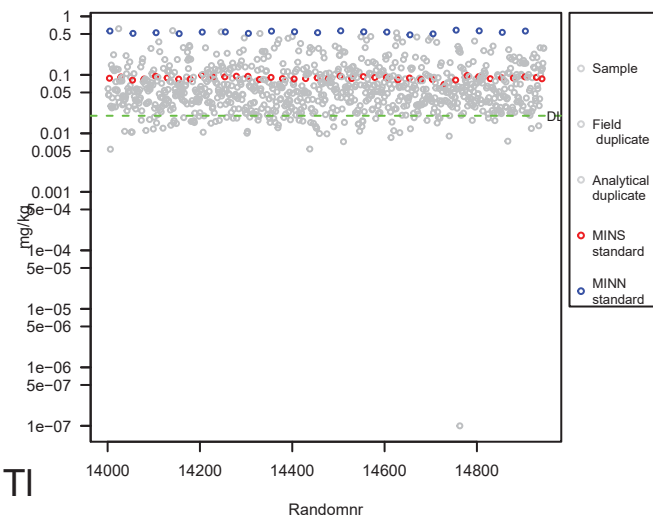
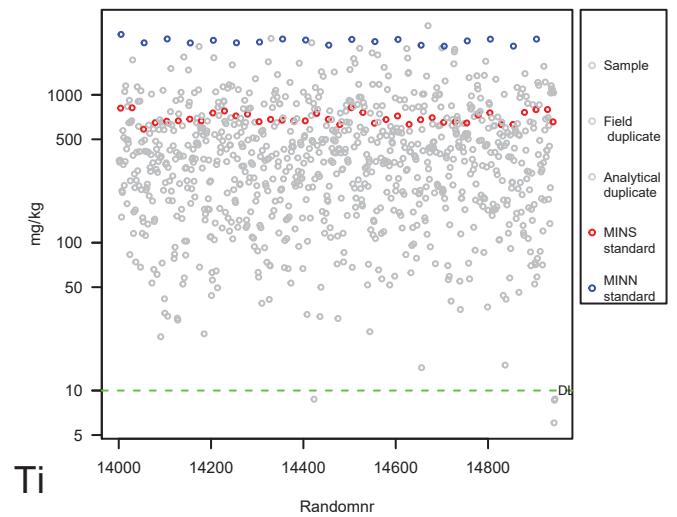
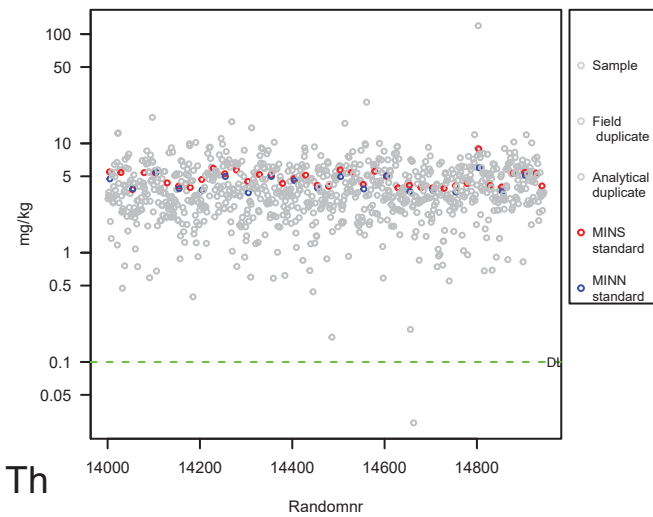
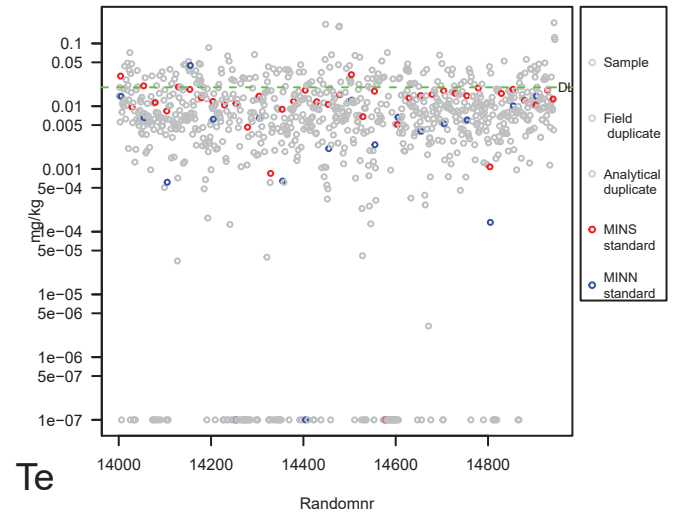
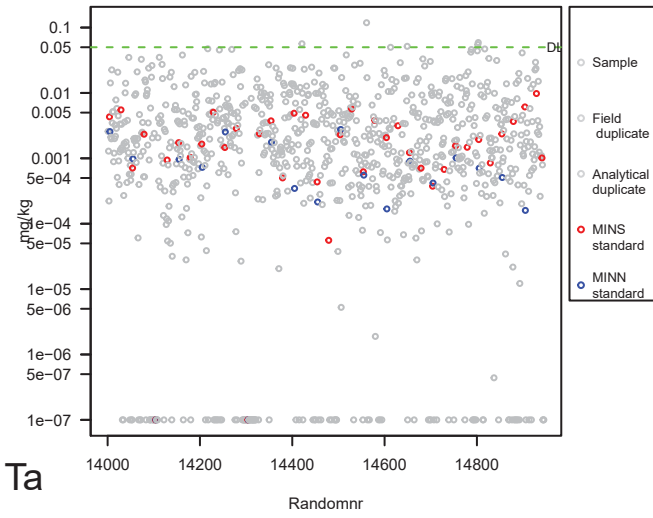


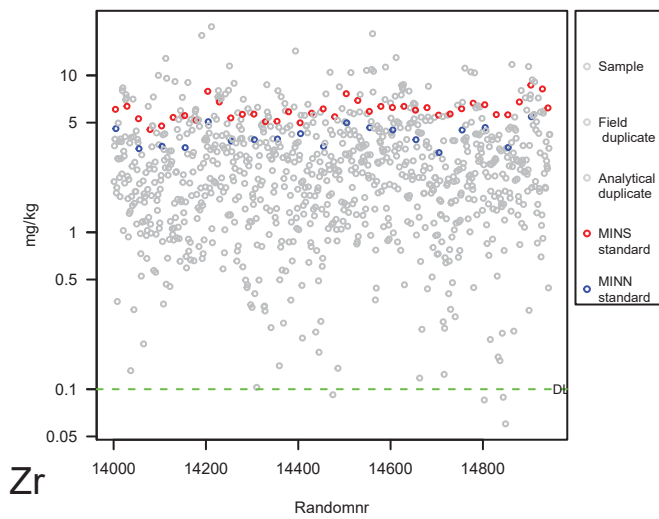
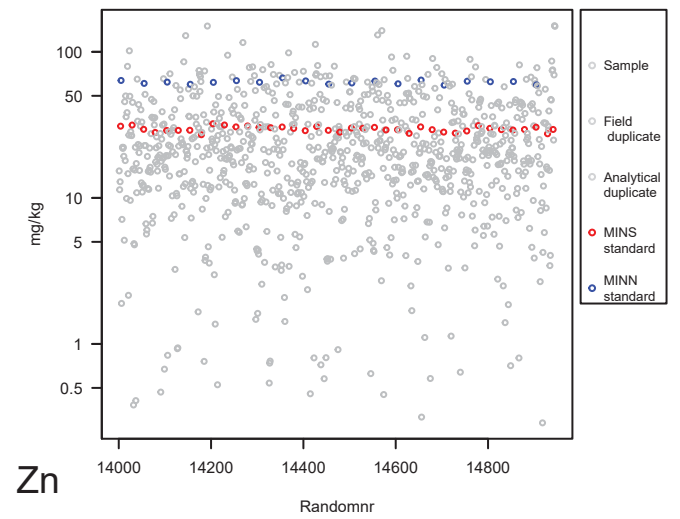
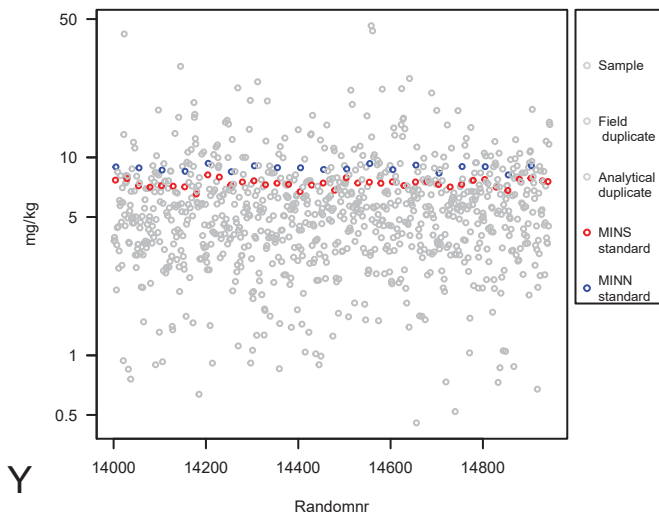
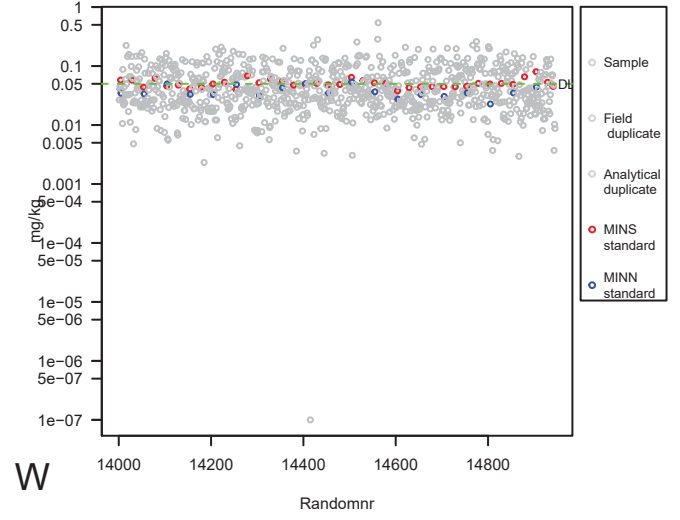
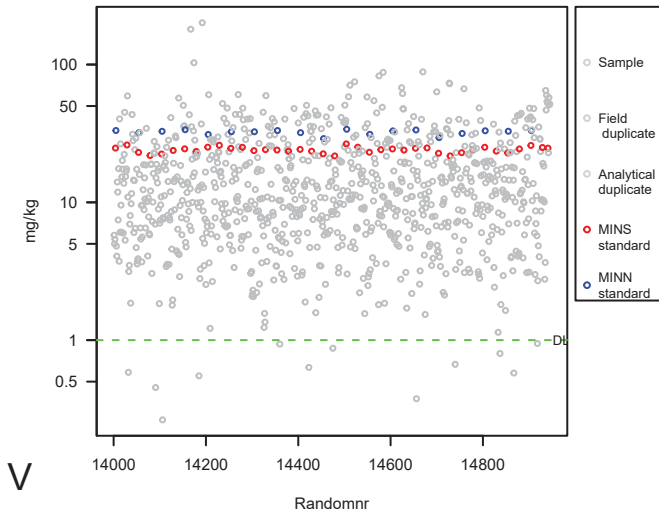












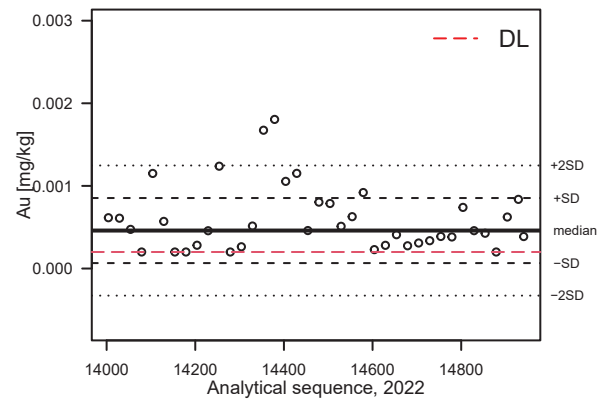
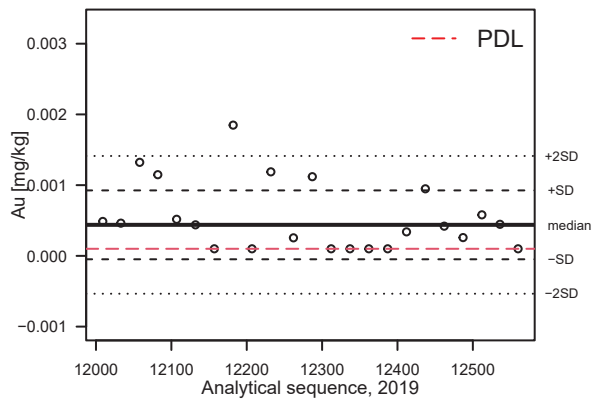
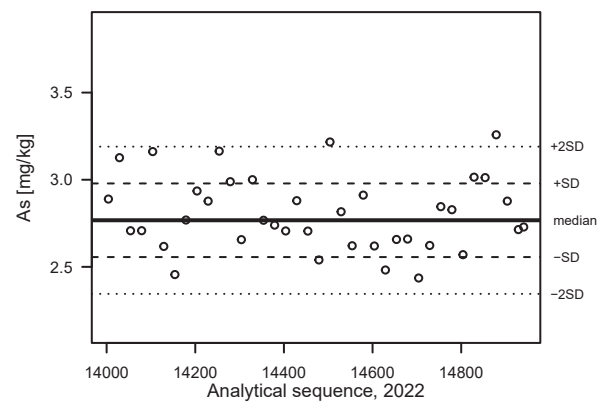
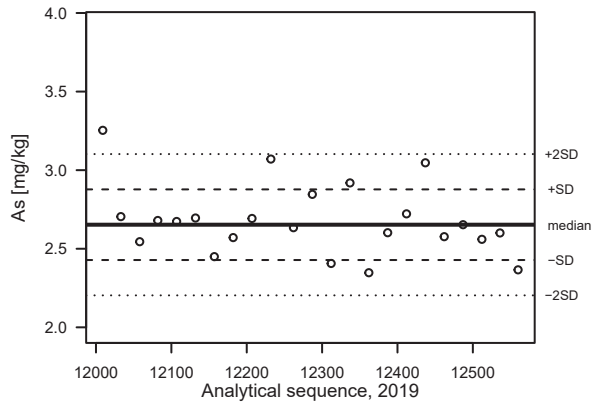
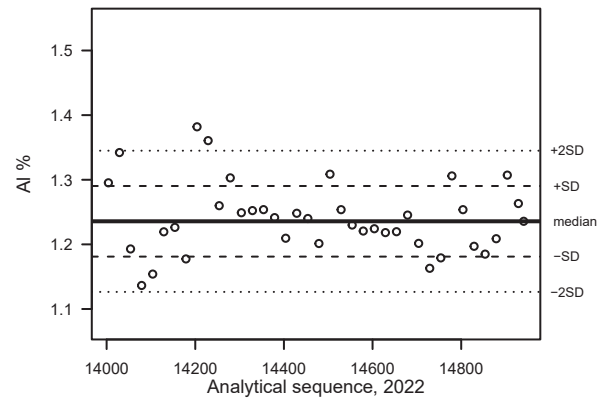
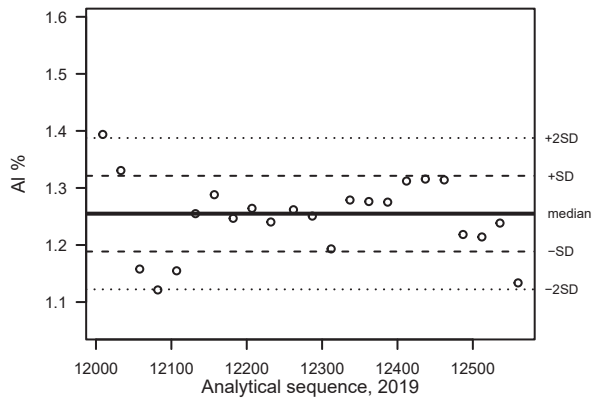
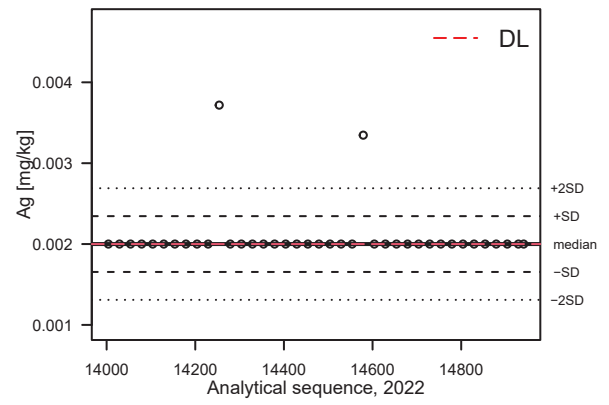
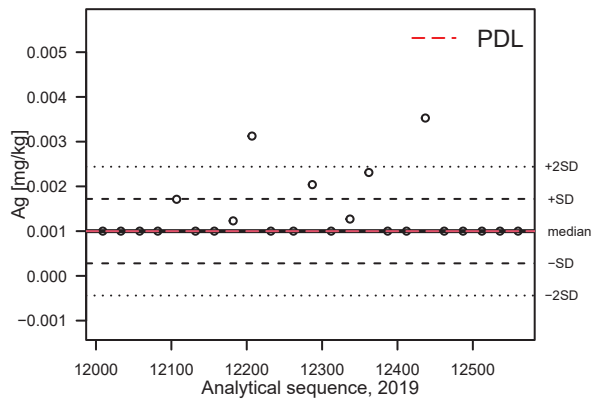
## APPENDIX 2: X-CHARTS

X-charts including analysis of splits with the MINN in-house standard from 2019 and 2022.

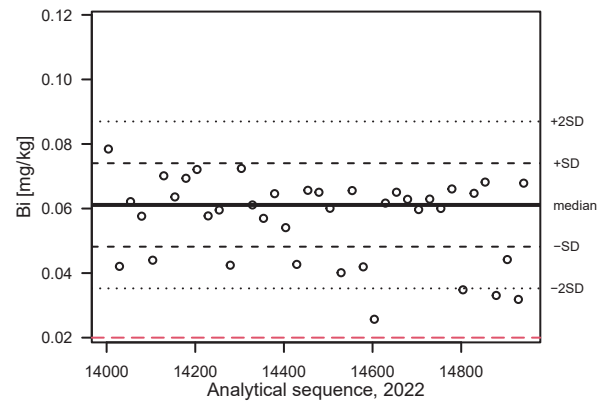
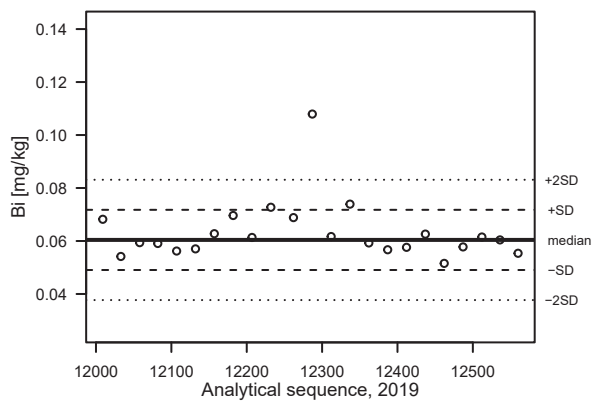
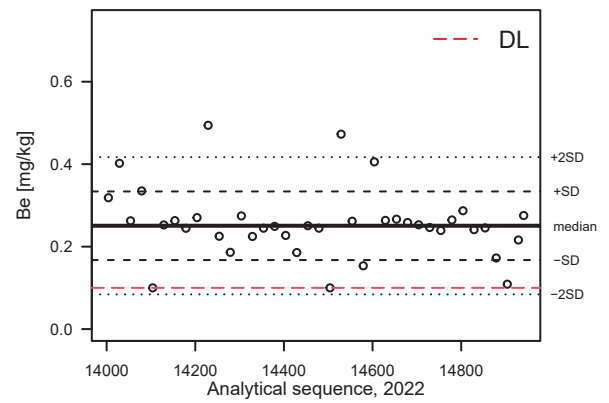
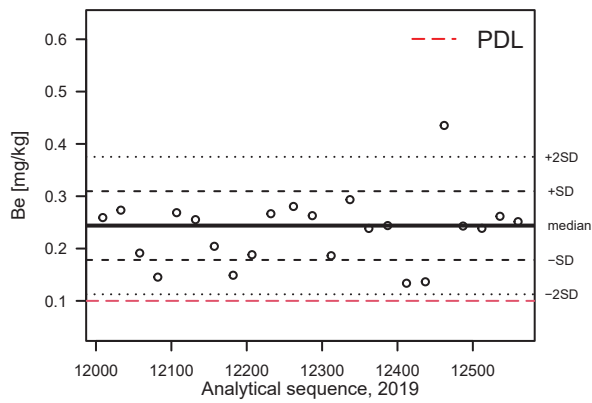
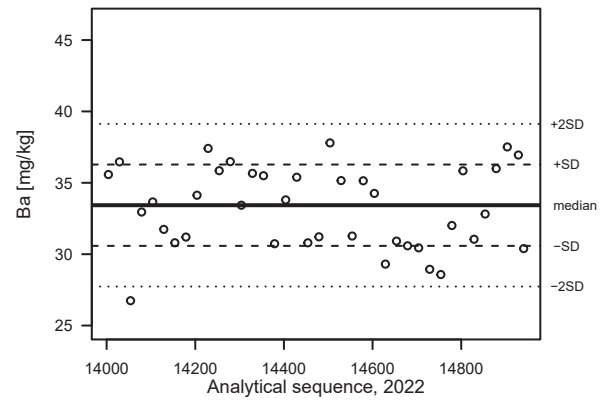
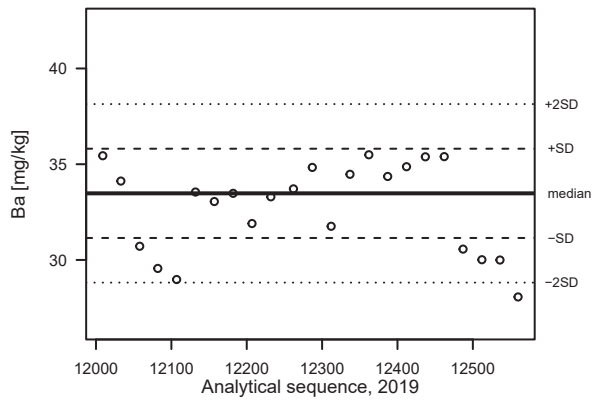
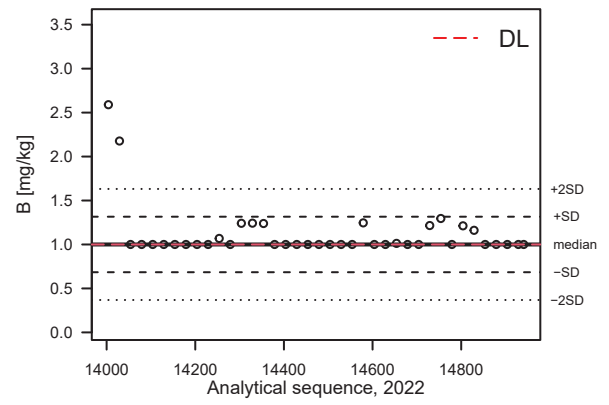
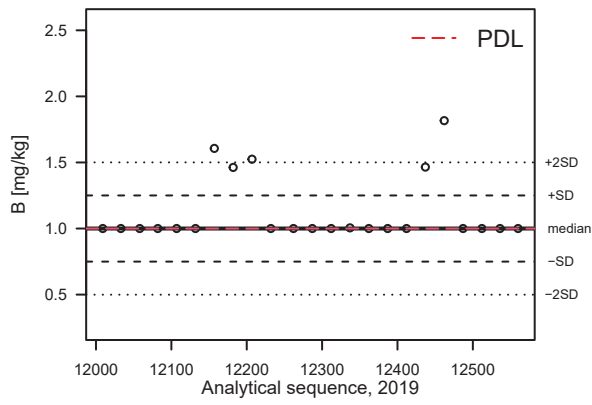
Twenty-three analyses from 2019 (Flem et al., 2020) and 39 analyses from this survey plotted in the same order as the analytical sequence in the lab.

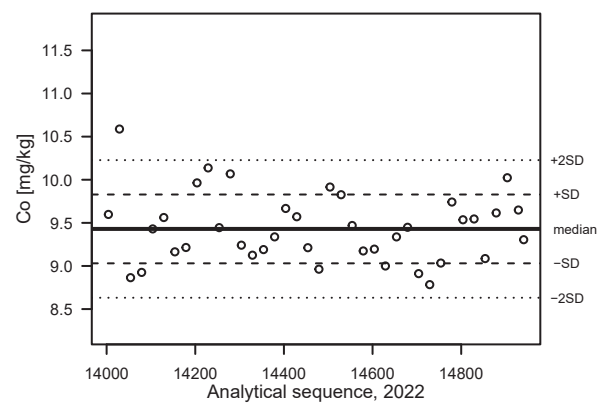
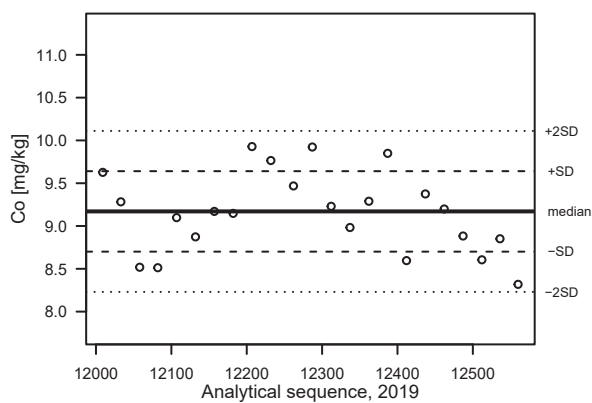
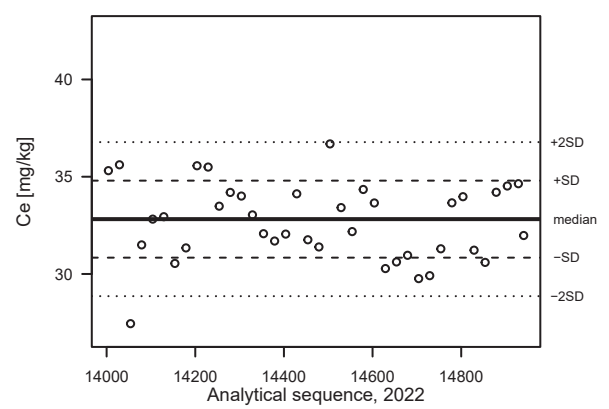
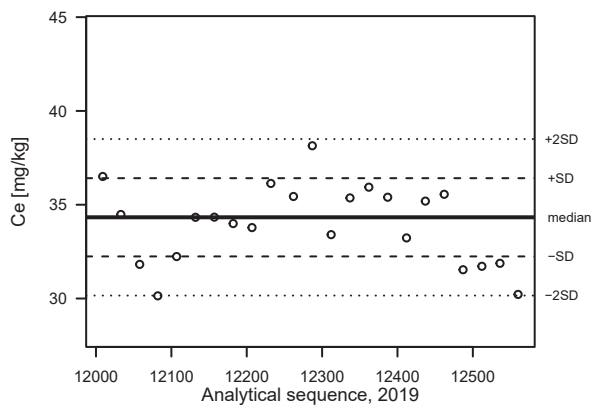
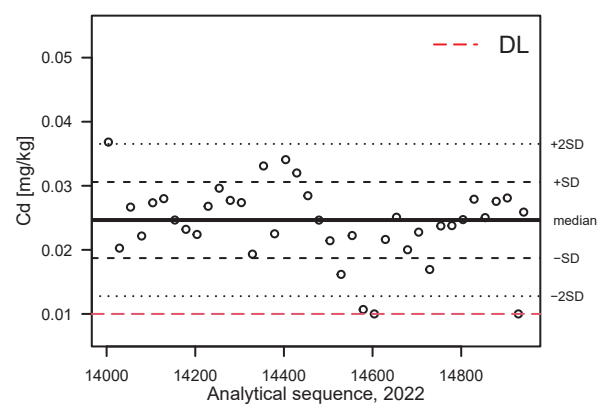
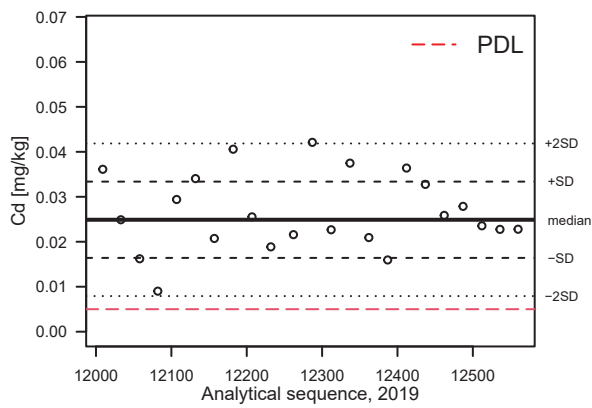
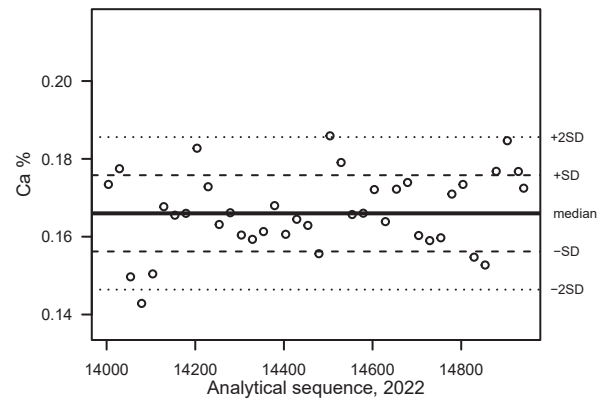
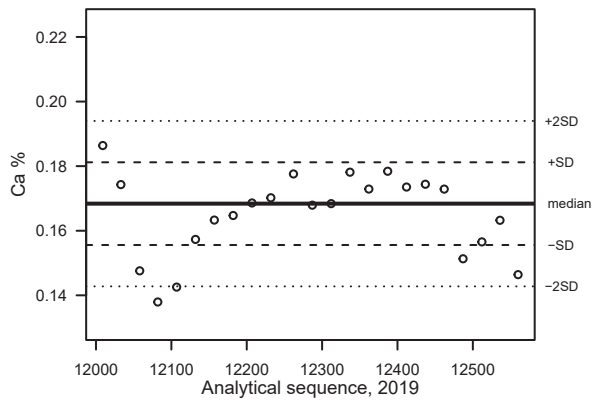
The median is indicated by a solid line, dashed lines are drawn at median  $\pm$  1 standard deviation (SD) and dotted lines are drawn at median  $\pm$  2 standard deviations (2SD).

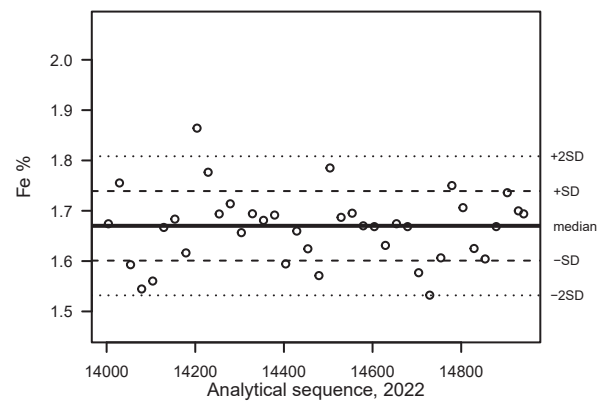
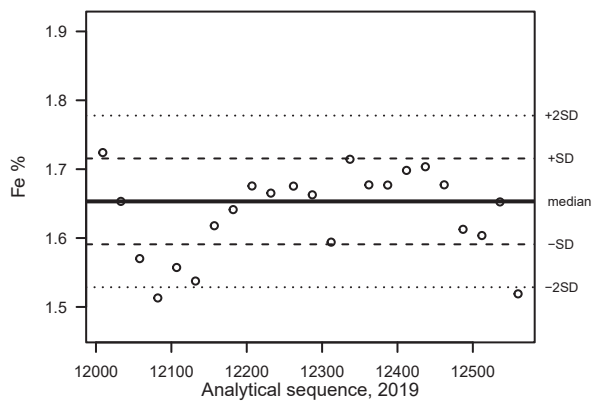
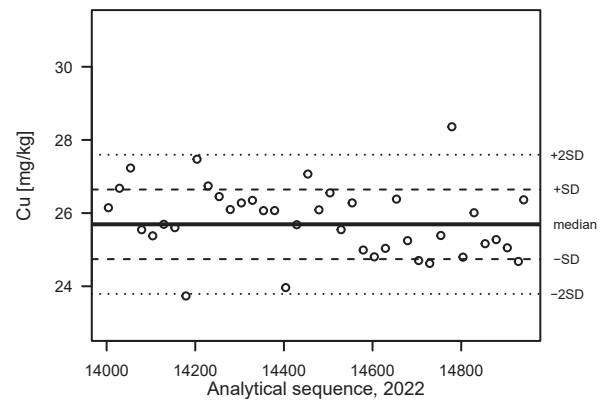
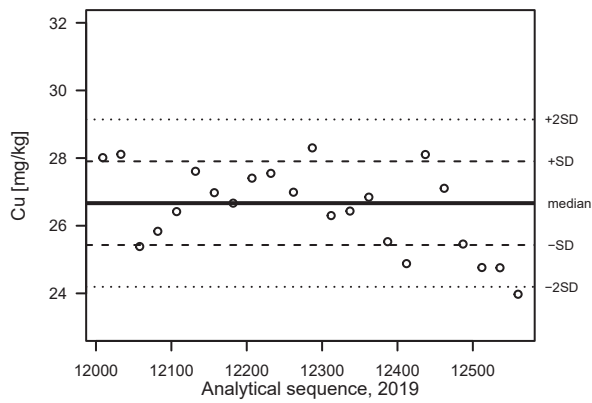
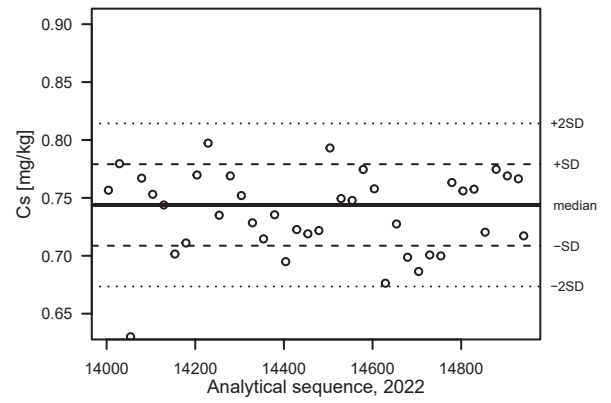
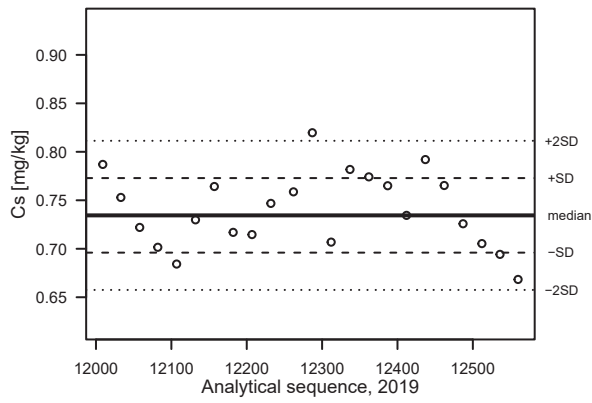
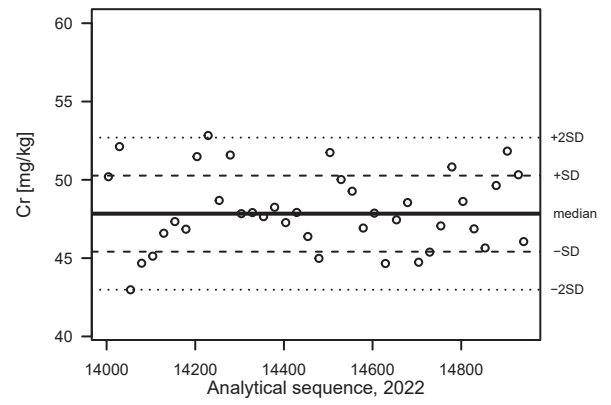
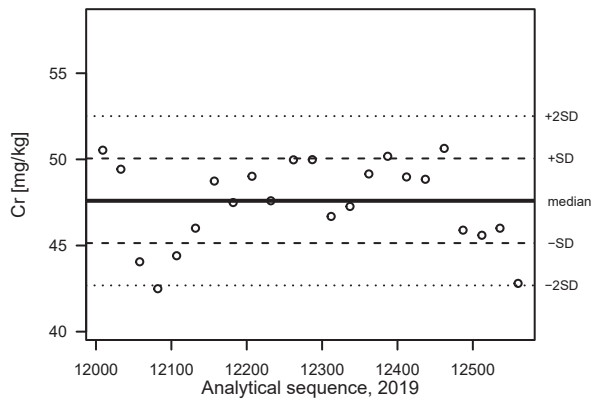
A red dash dotted line is draw at the practical detection limit (PDL) or method detection limit (DL).

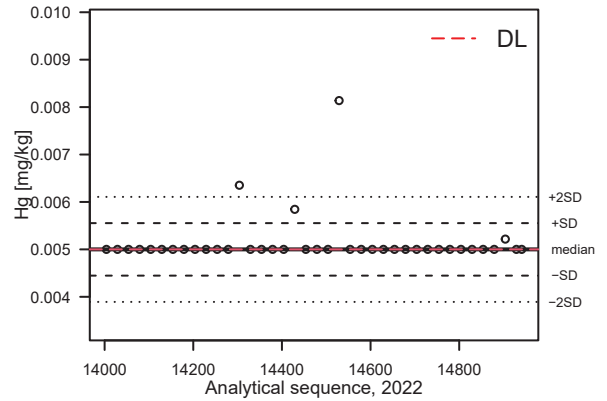
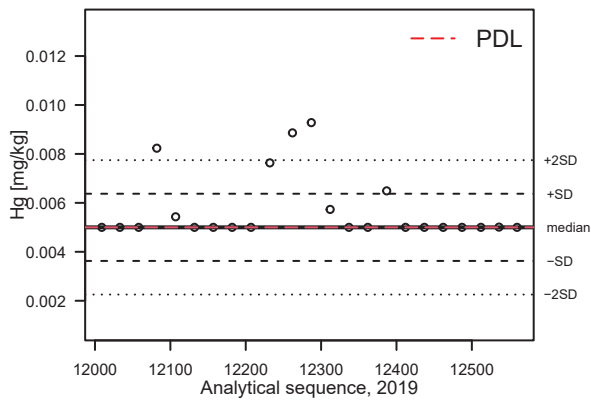
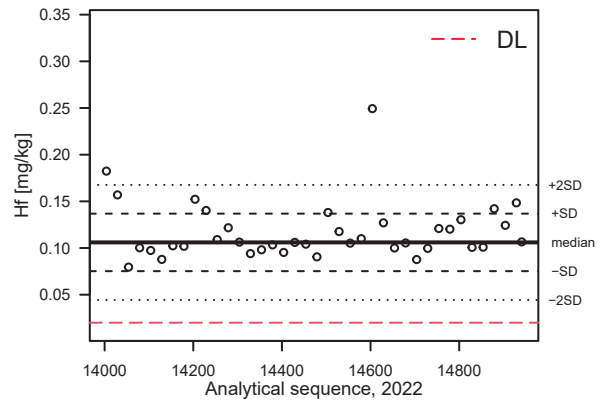
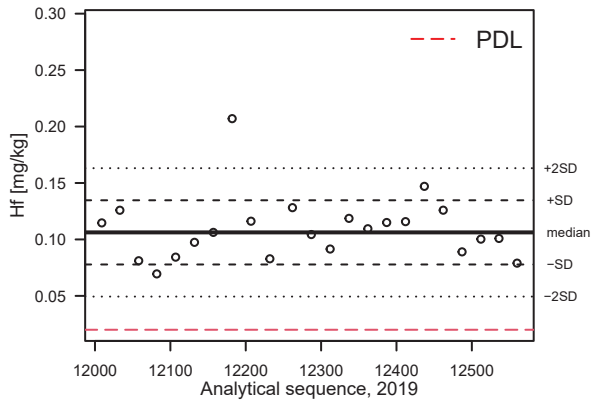
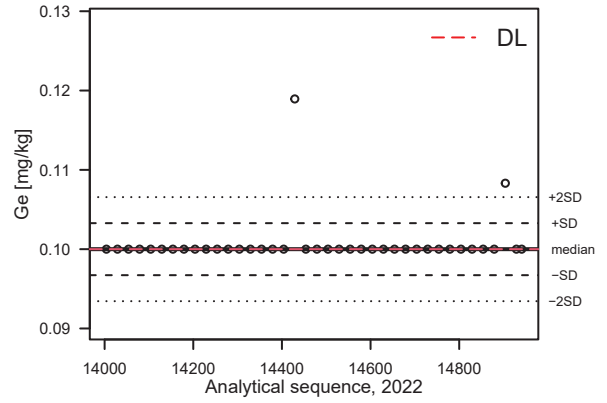
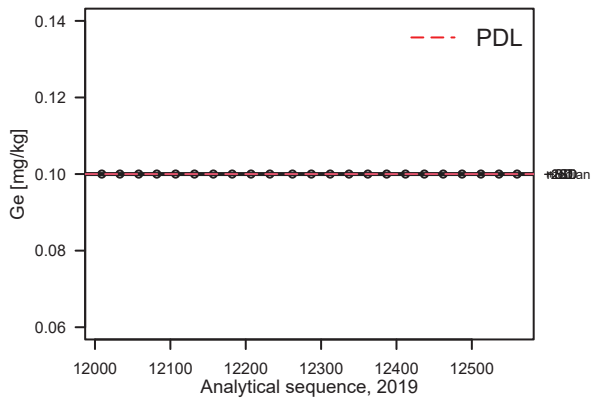
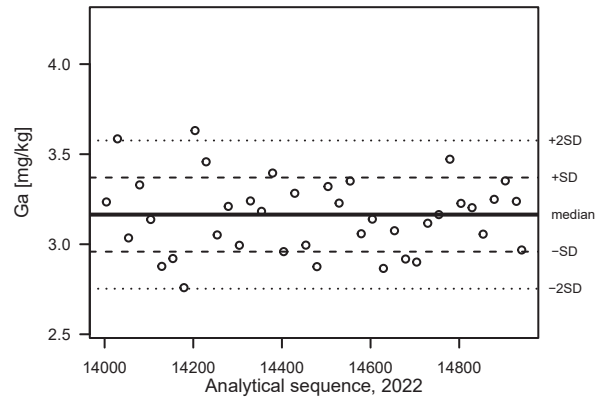
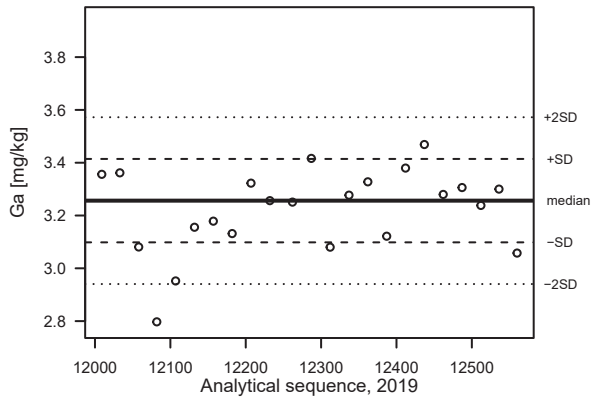


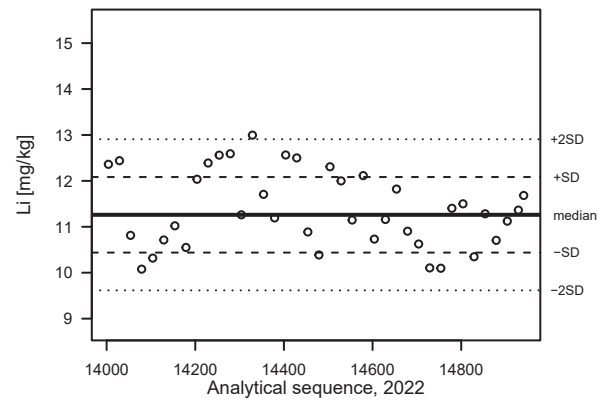
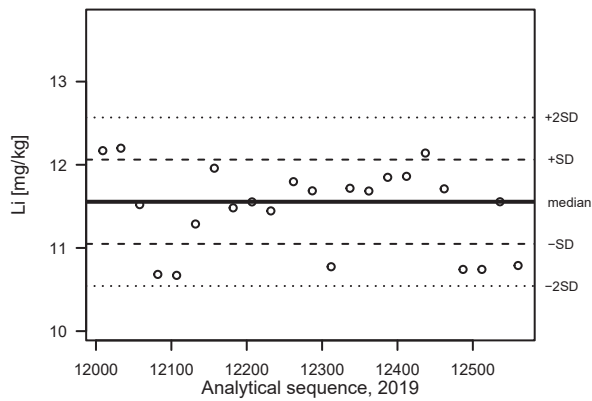
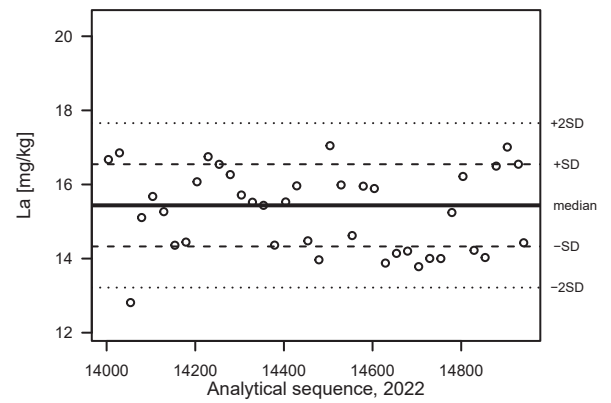
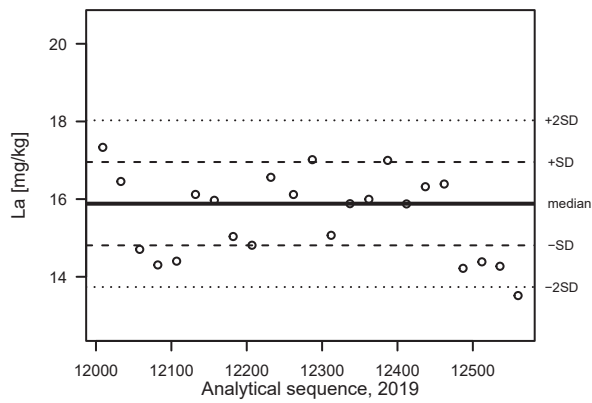
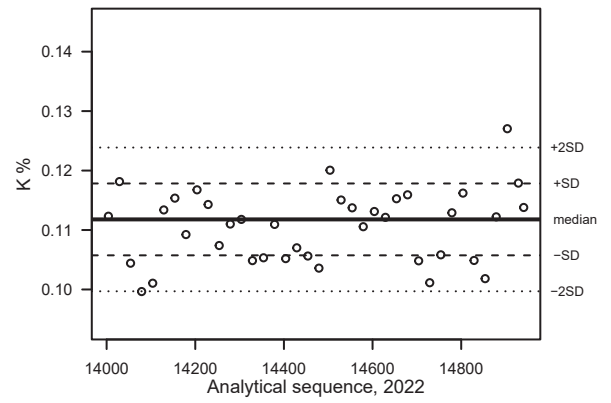
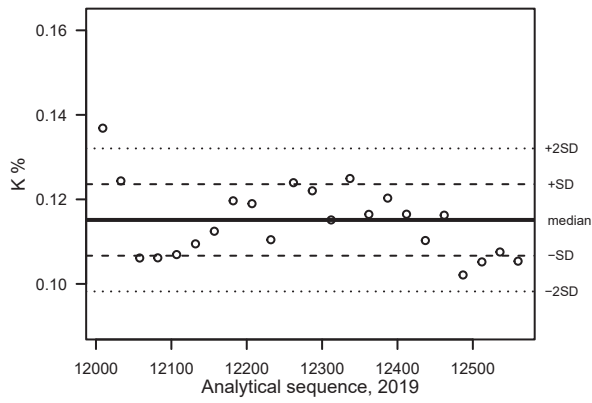
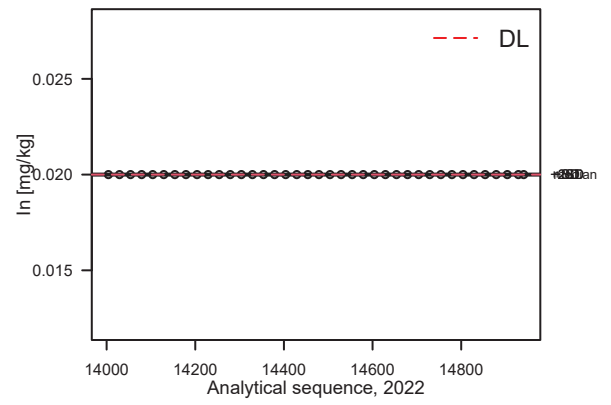
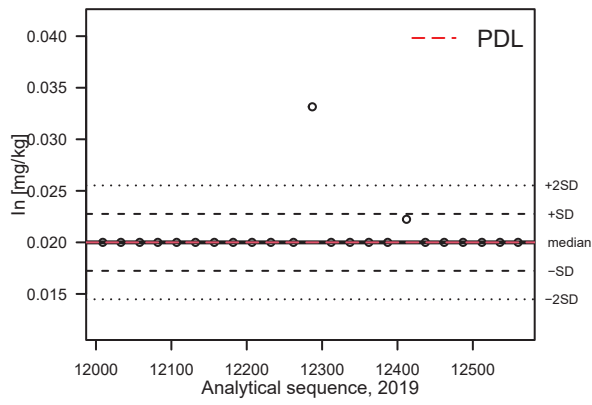


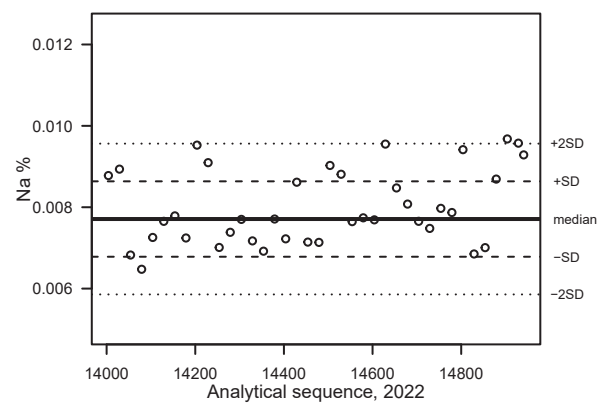
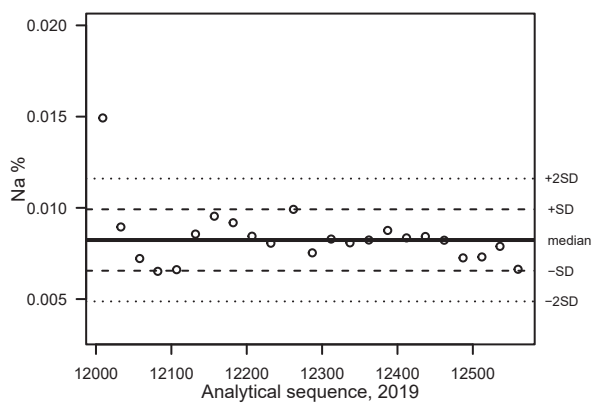
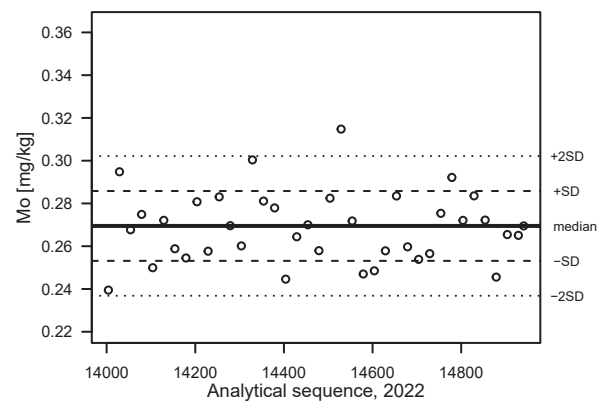
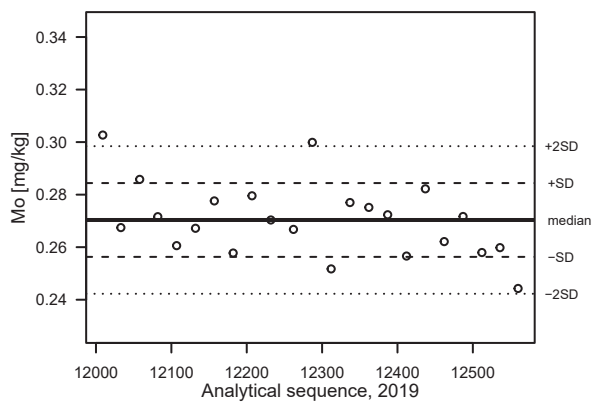
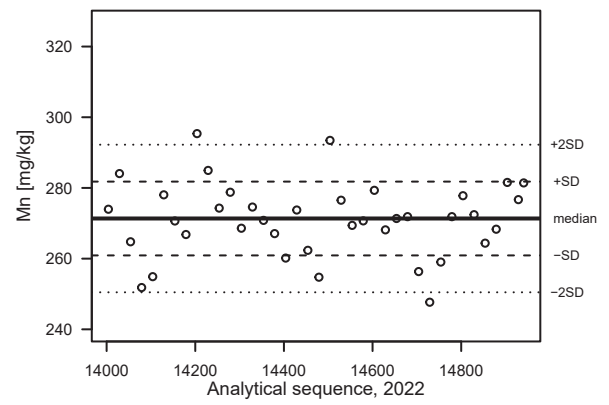
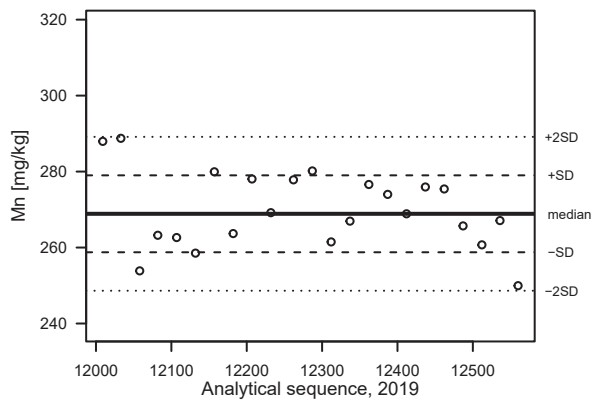
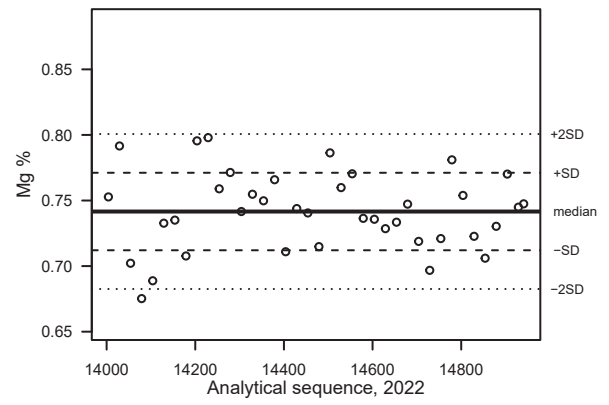
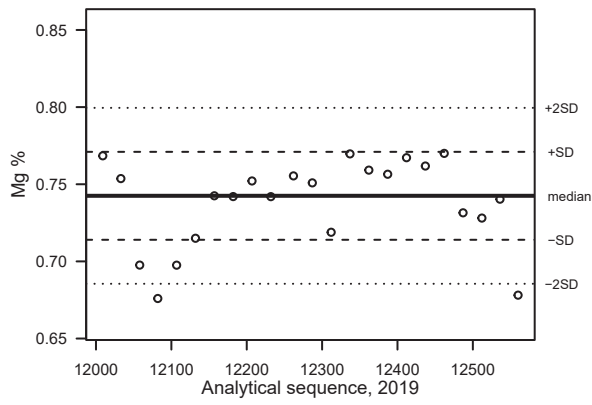


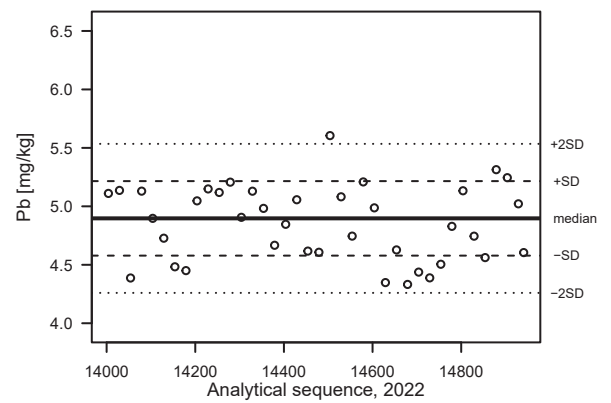
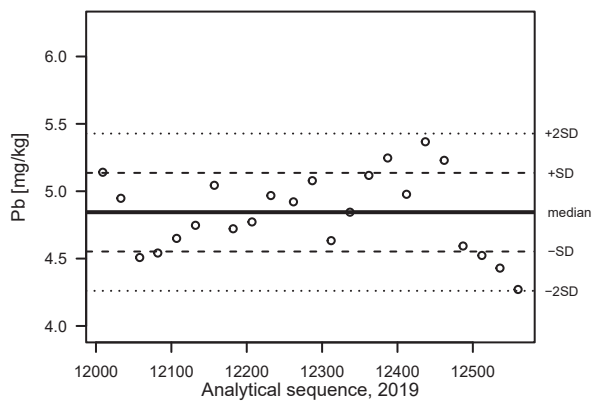
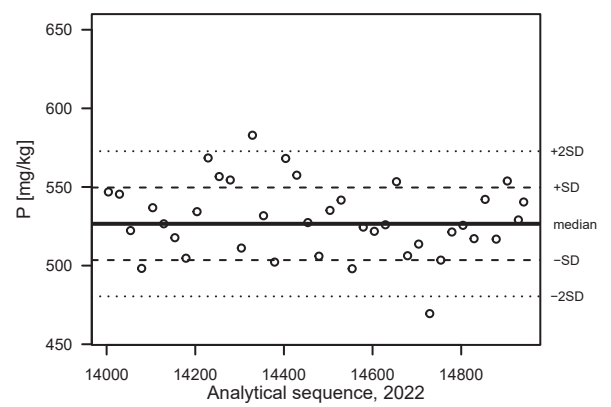
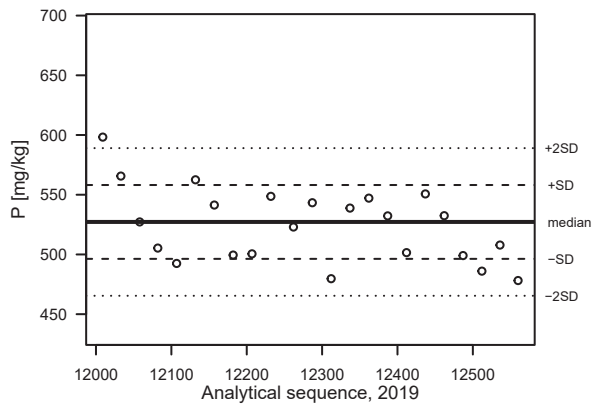
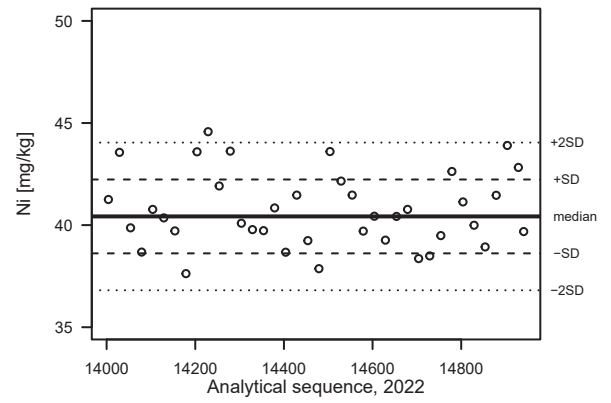
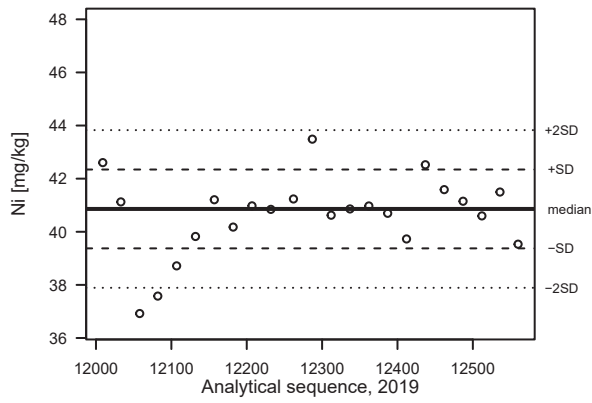
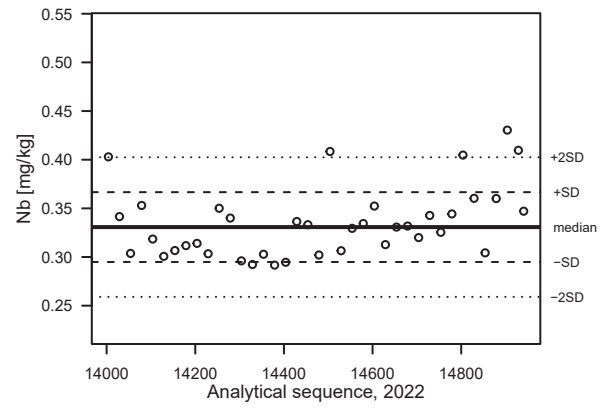
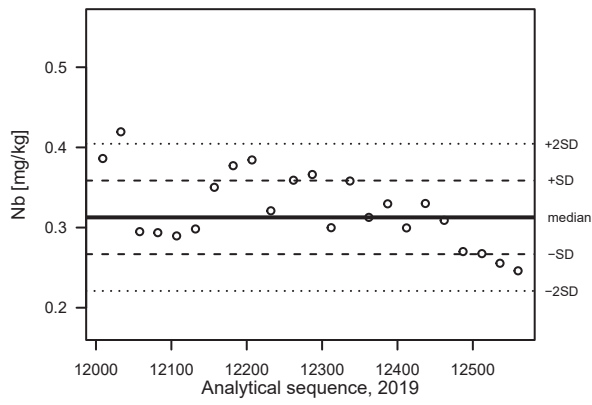


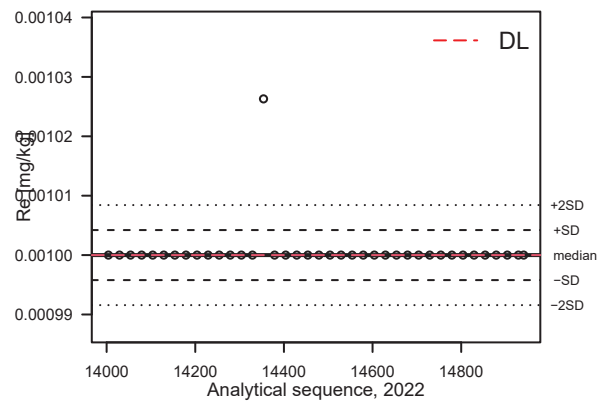
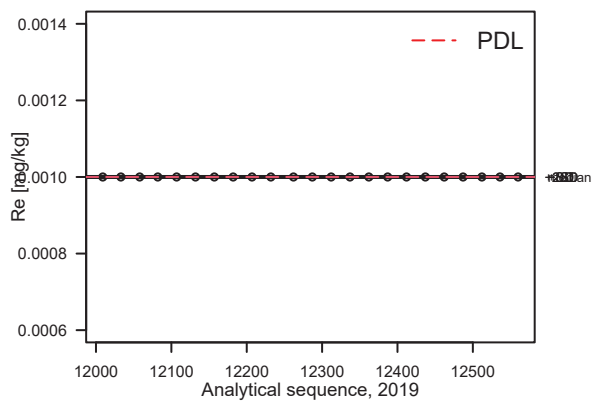
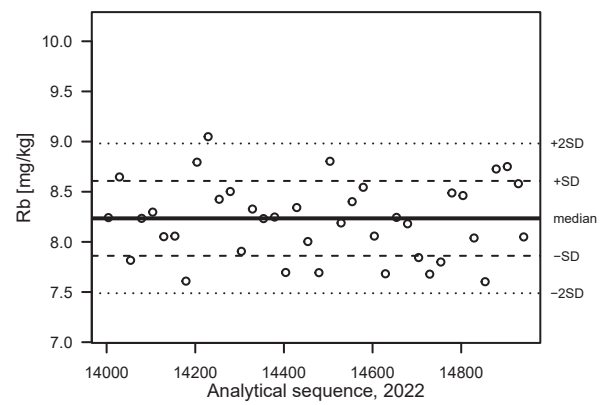
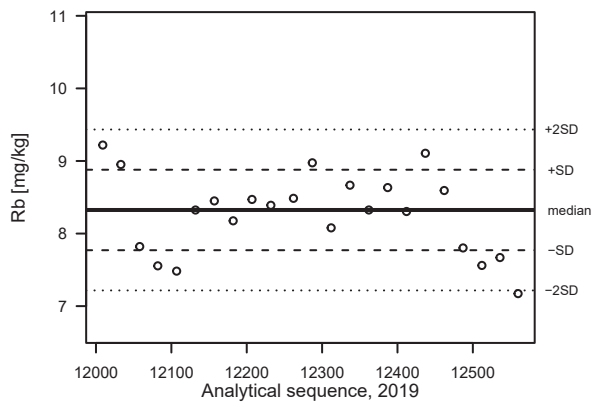
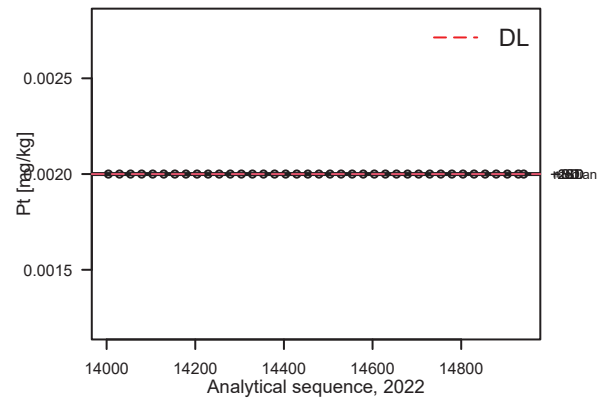
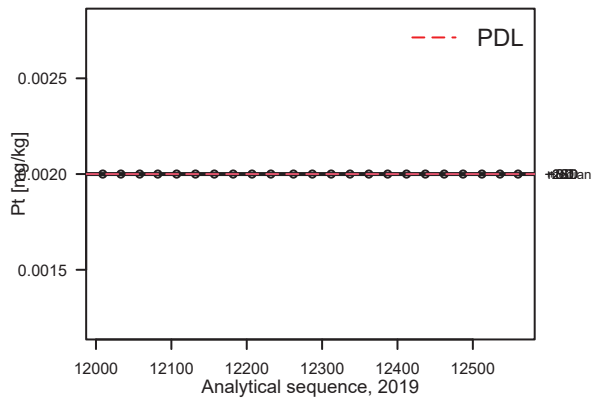
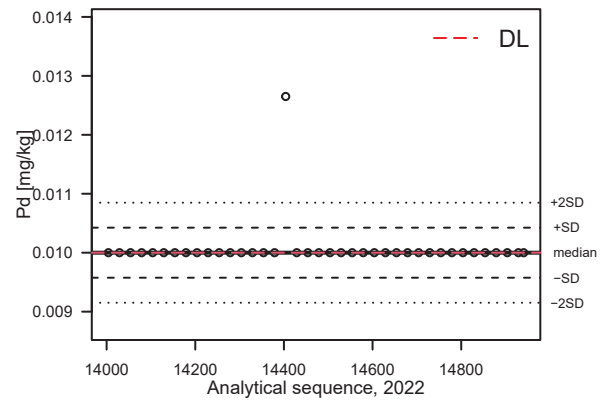
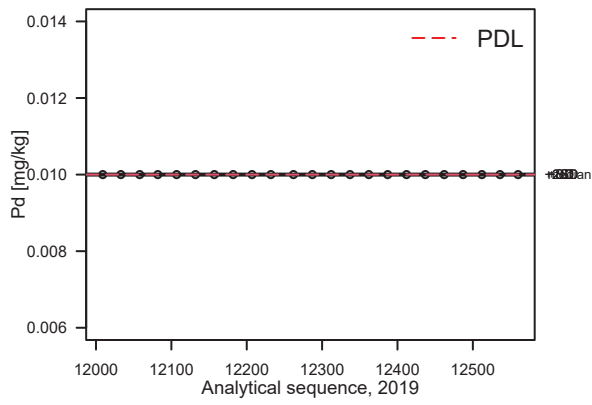




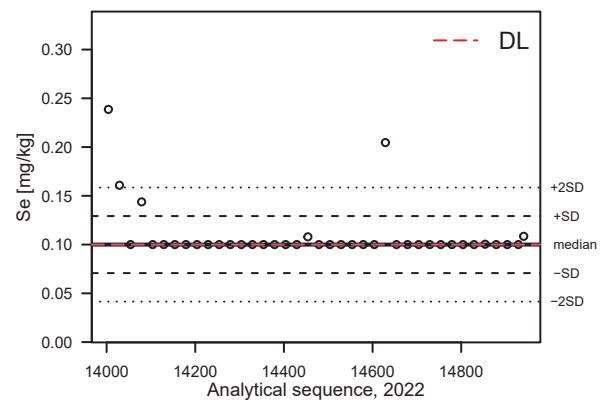
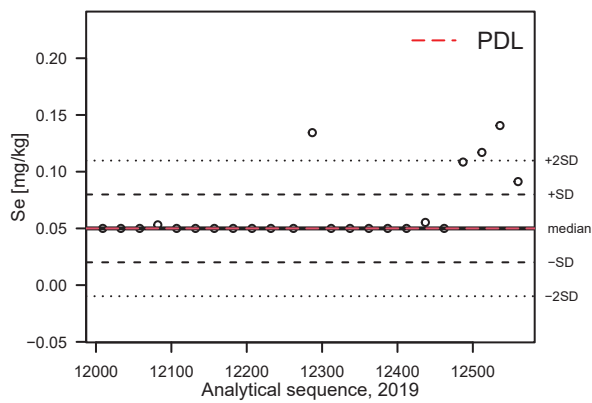
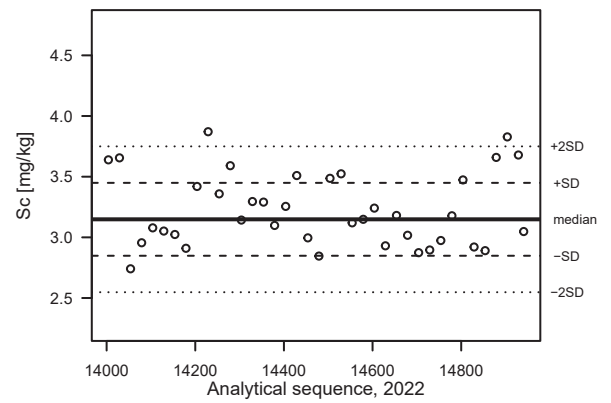
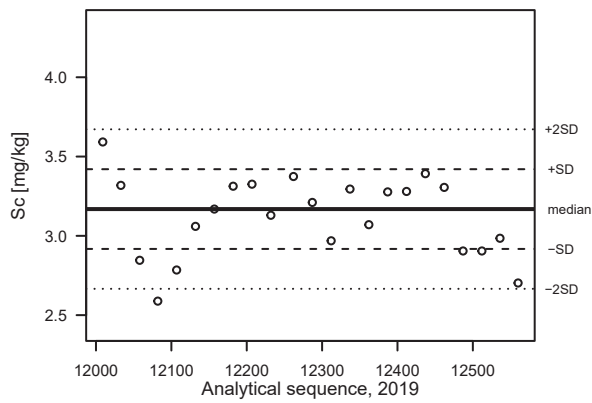
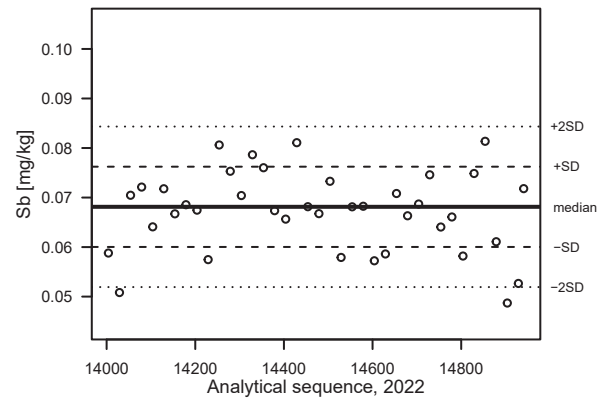
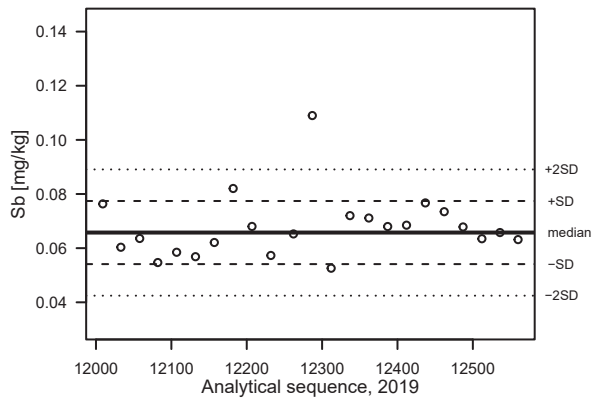
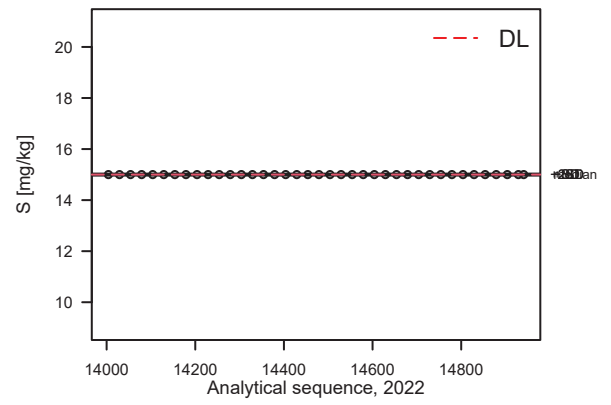
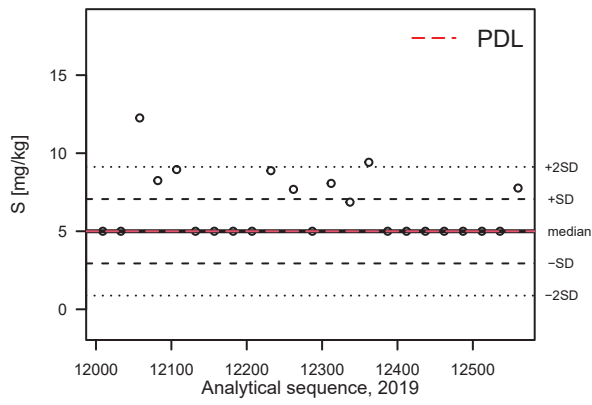


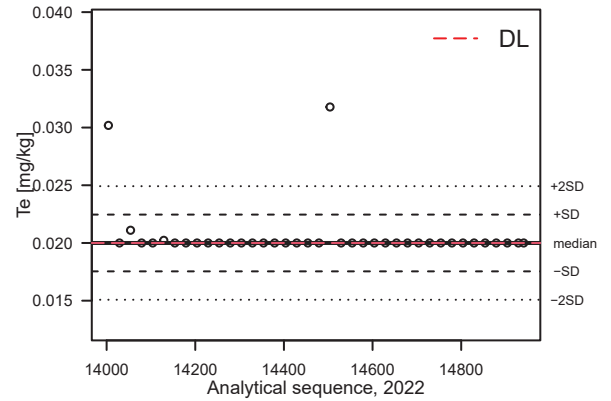
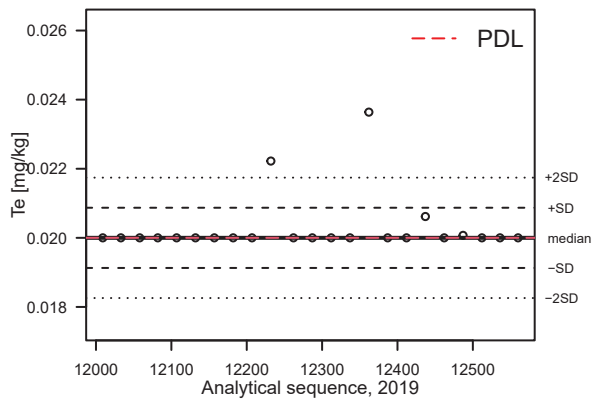
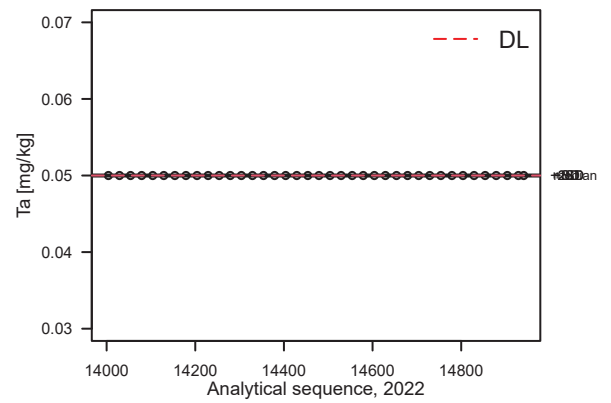
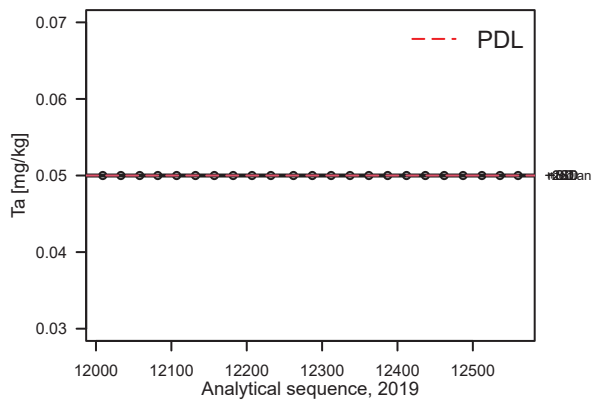
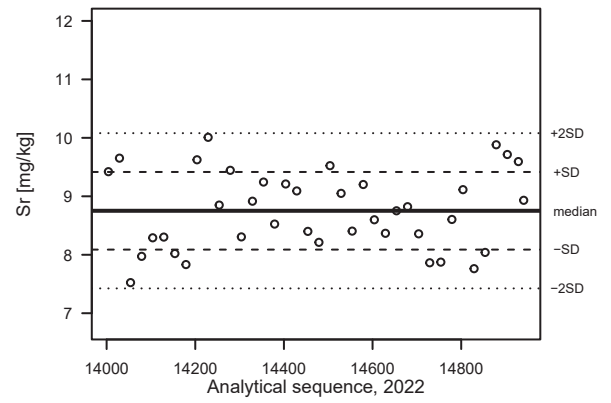
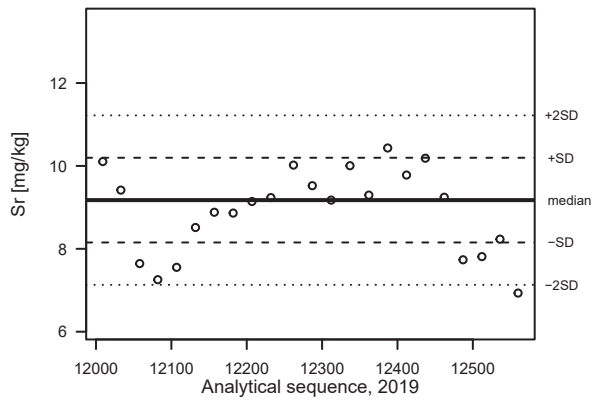
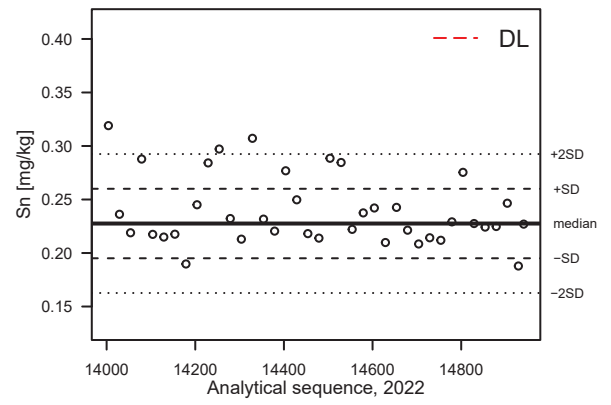
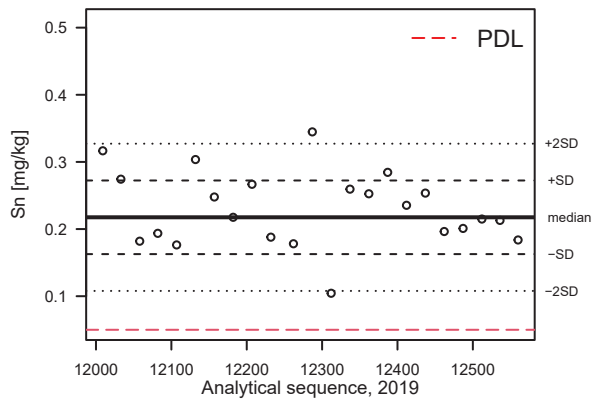


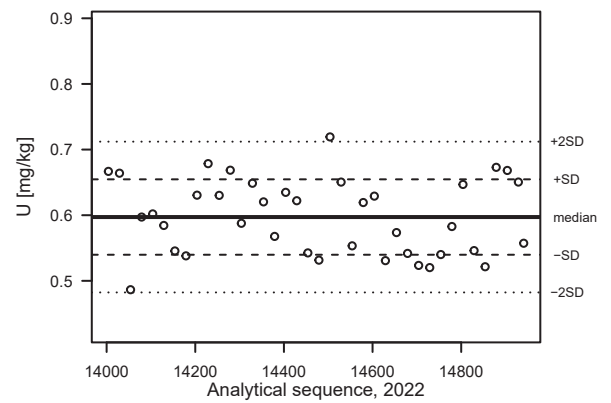
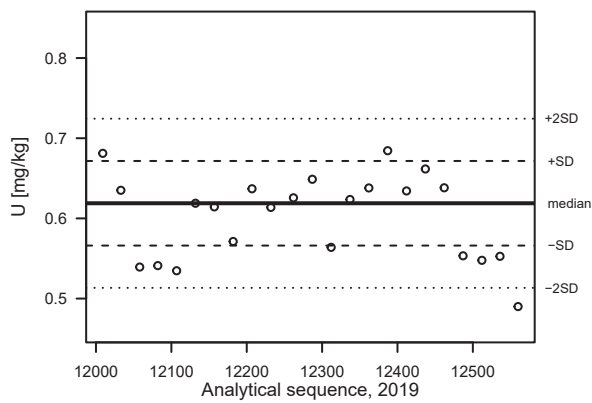
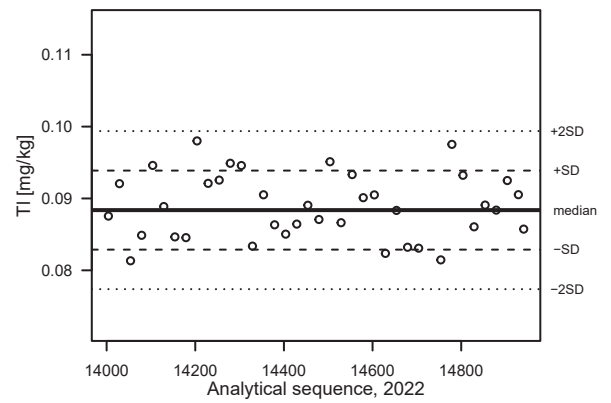
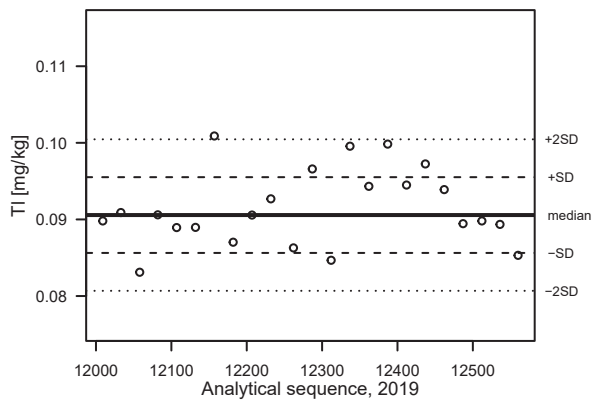
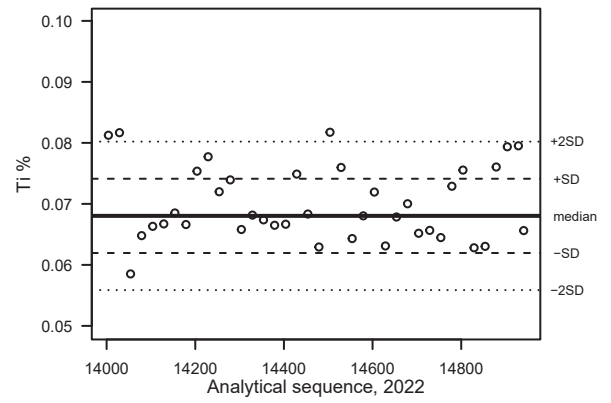
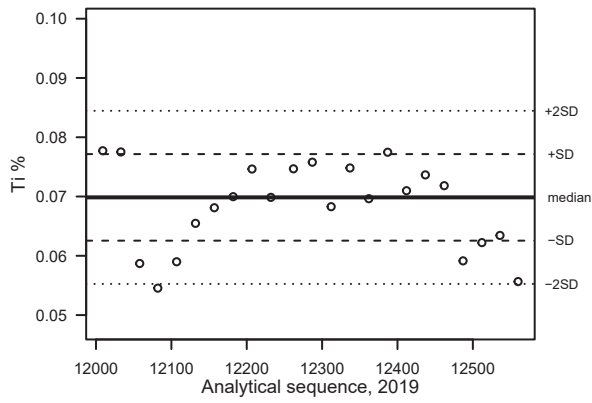
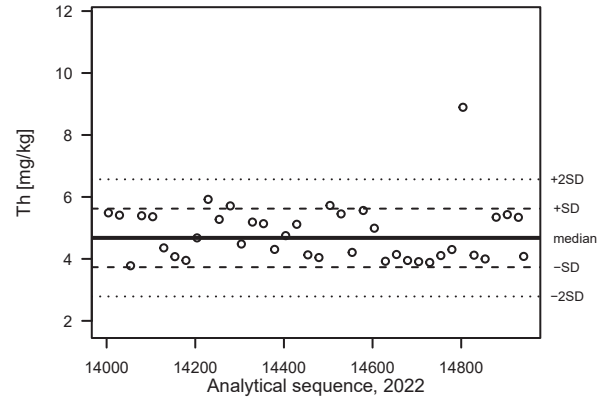
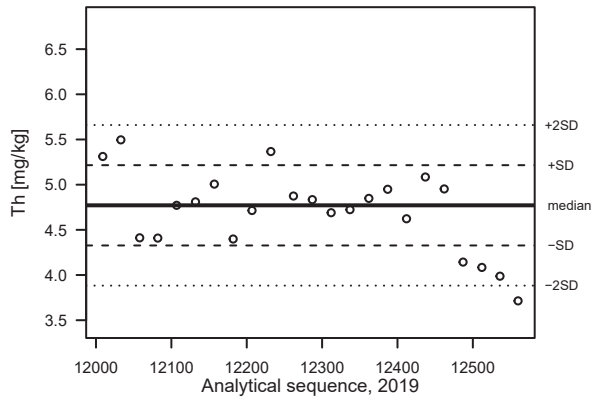


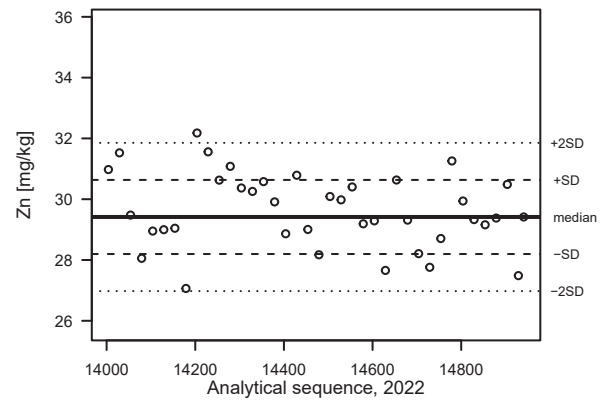
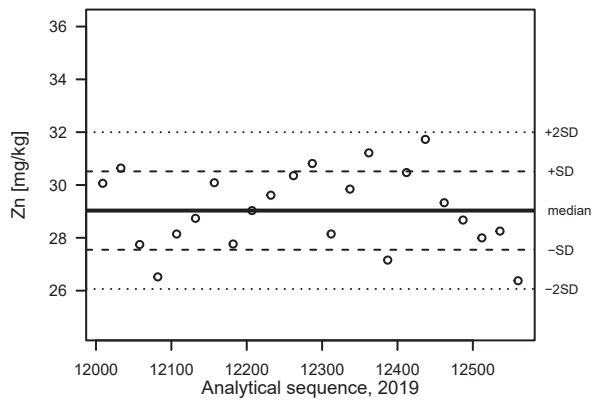
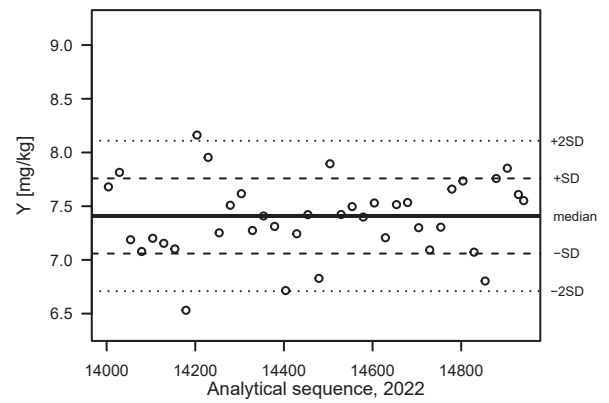
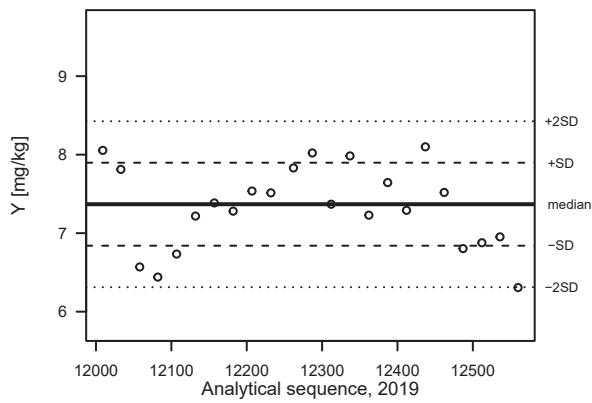
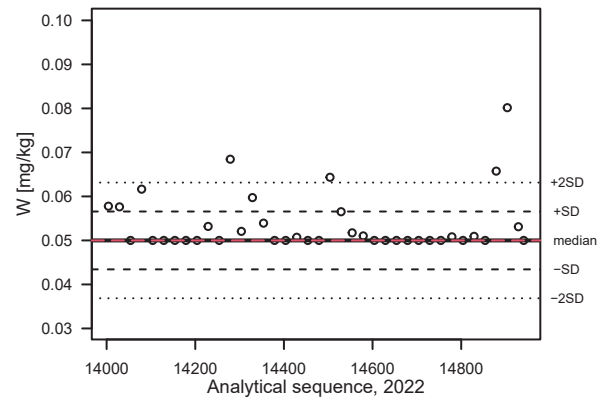
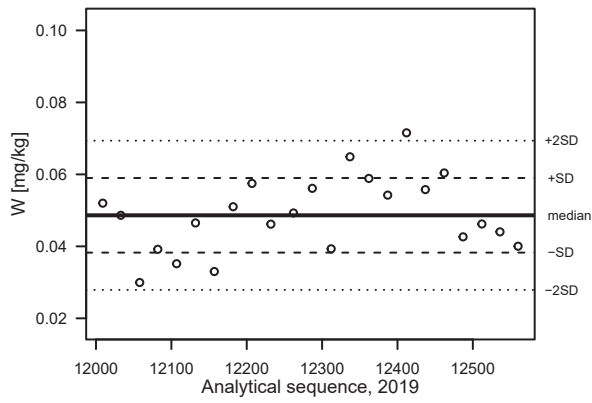
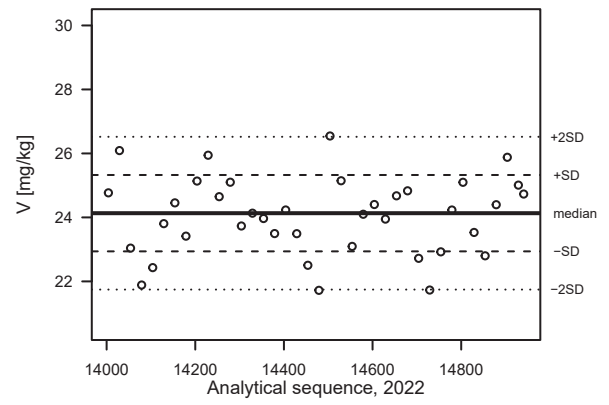
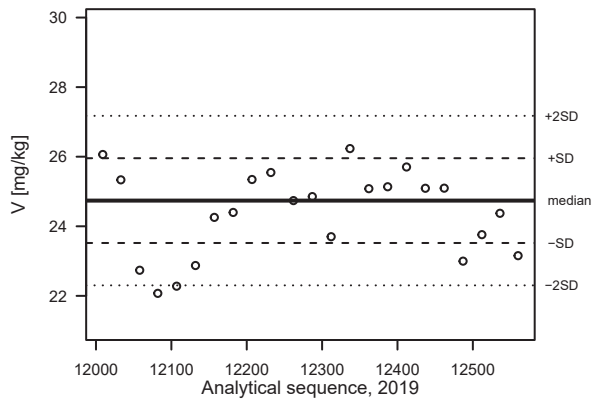


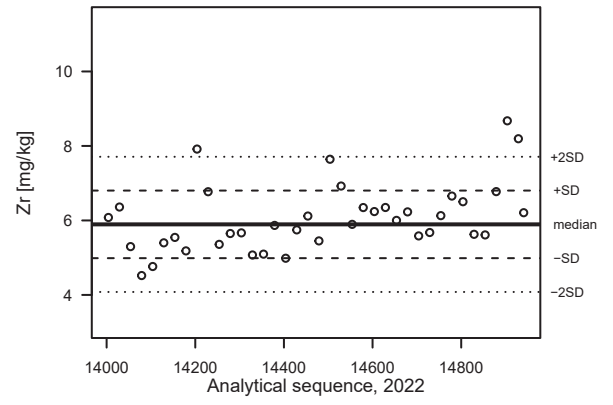
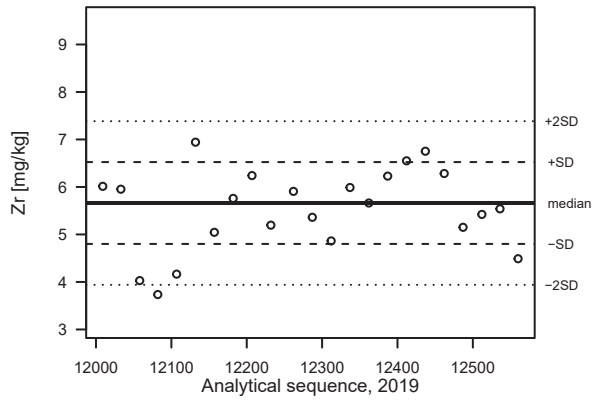










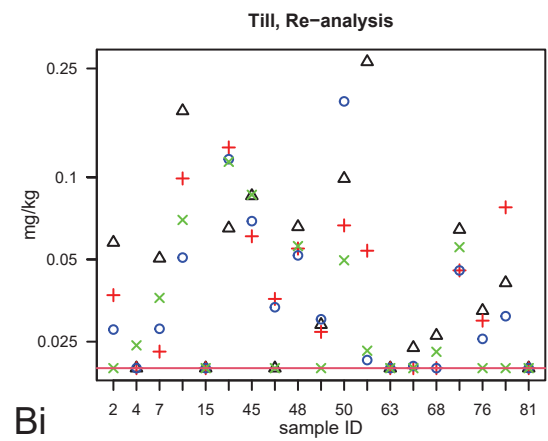
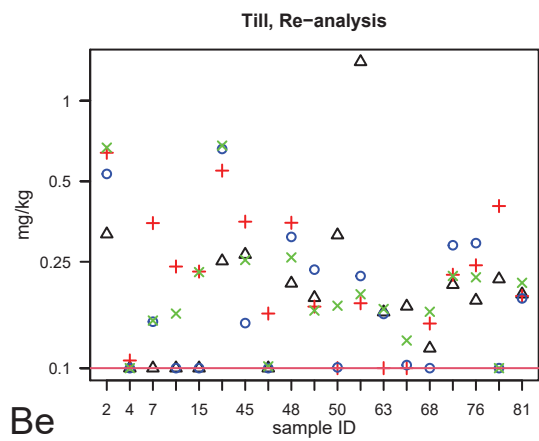
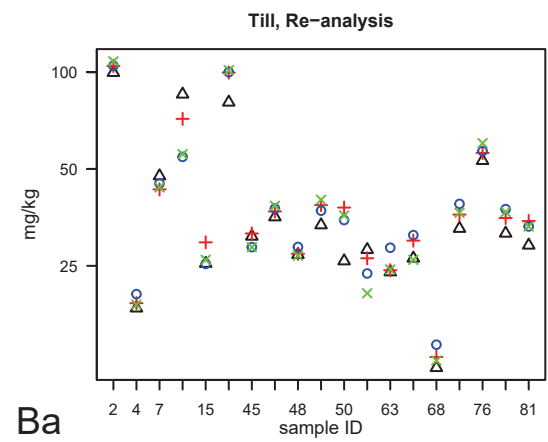
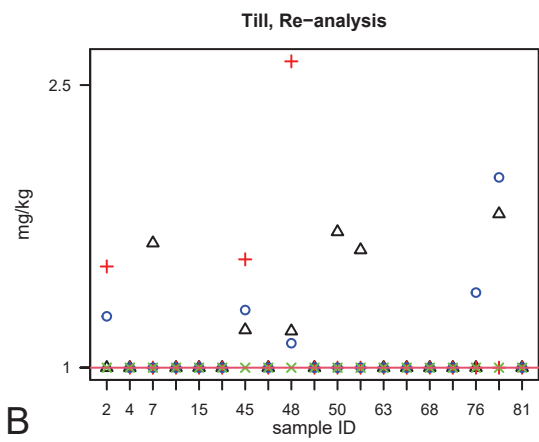
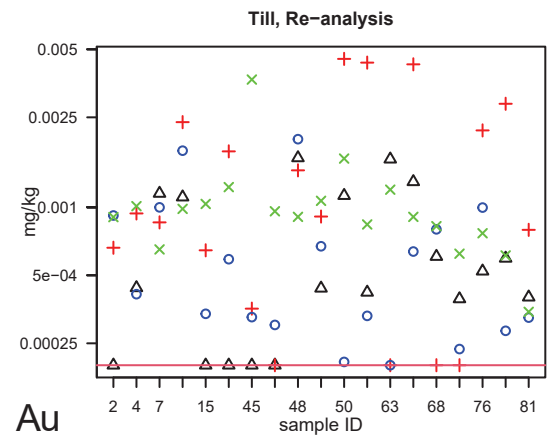
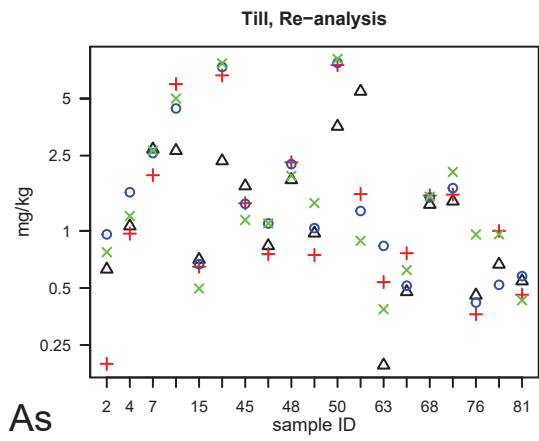
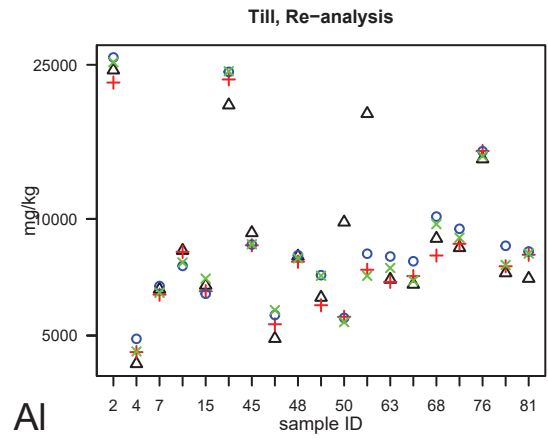
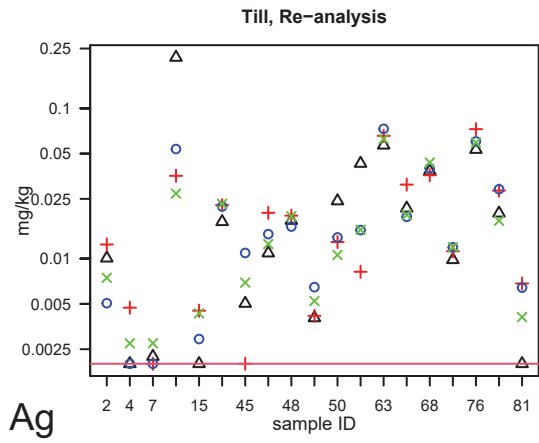




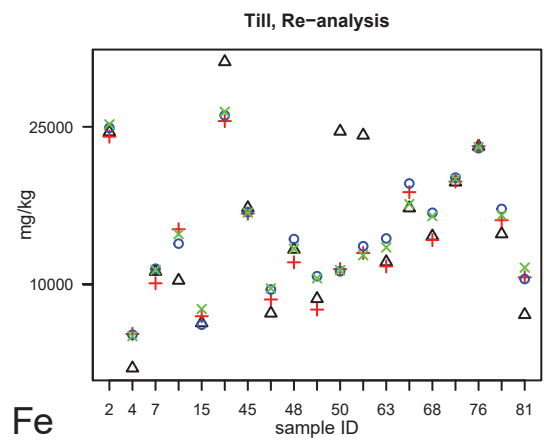
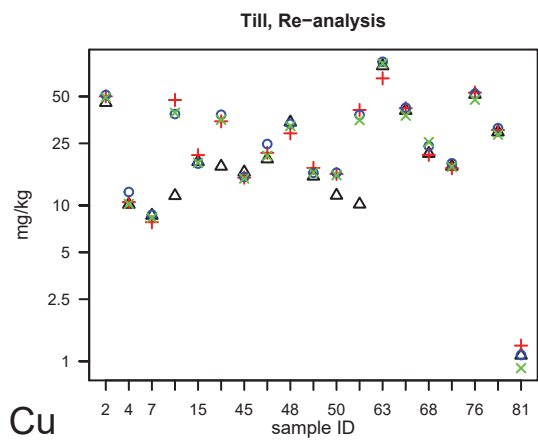
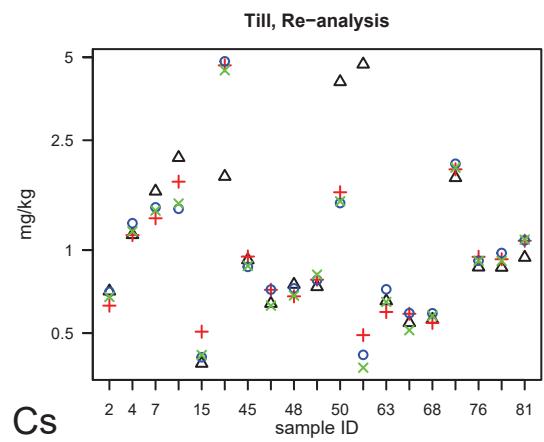
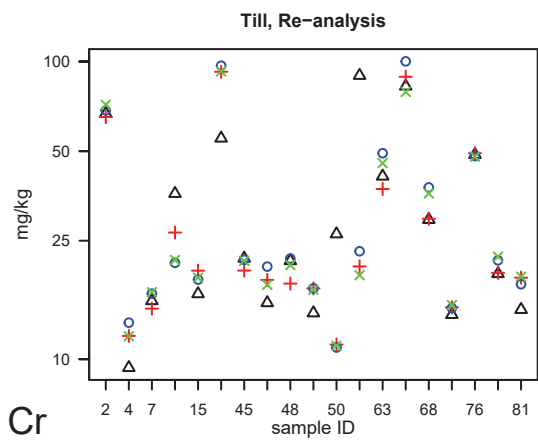
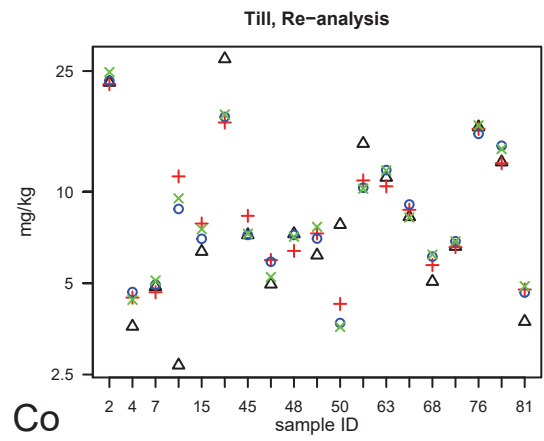
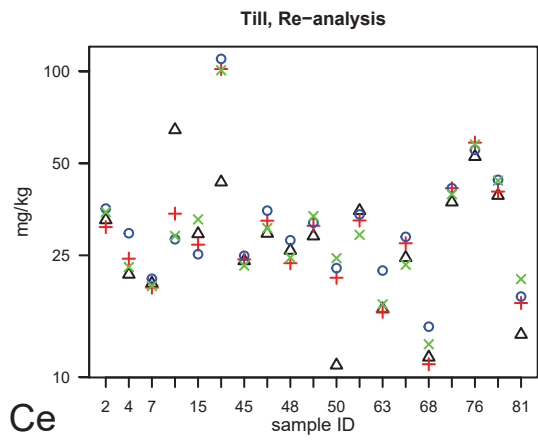
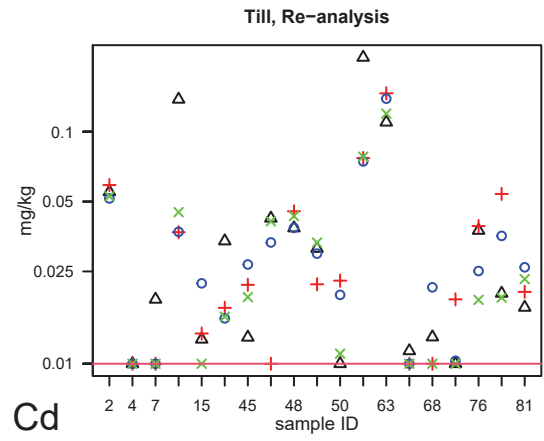
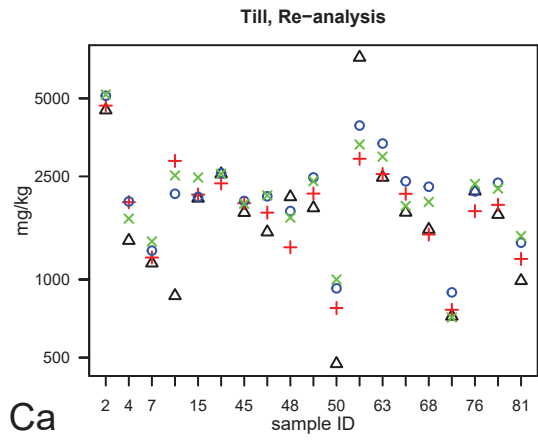
### Appendix 3: Samples re-analysed from previous surveys

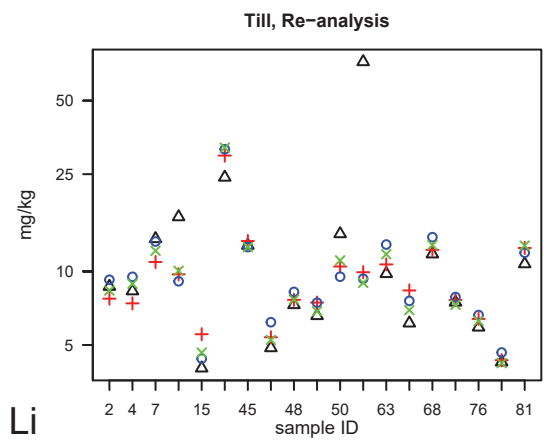
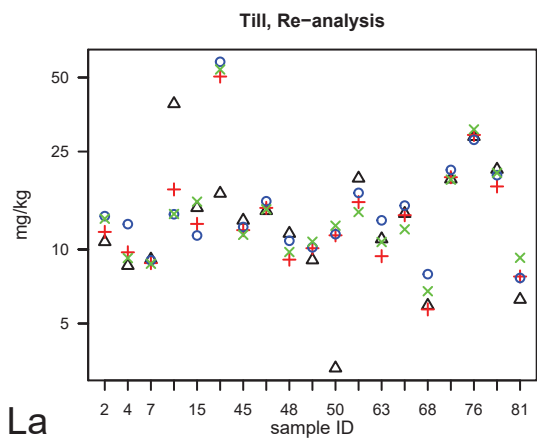
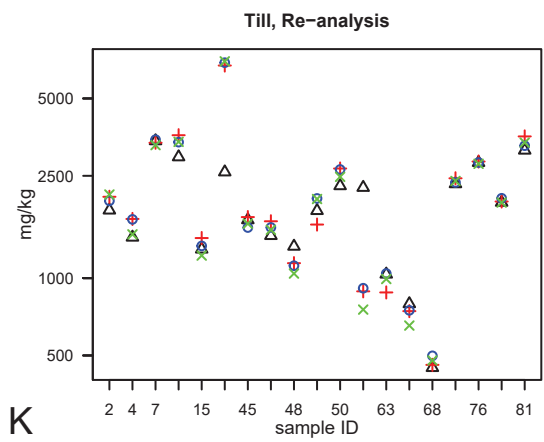
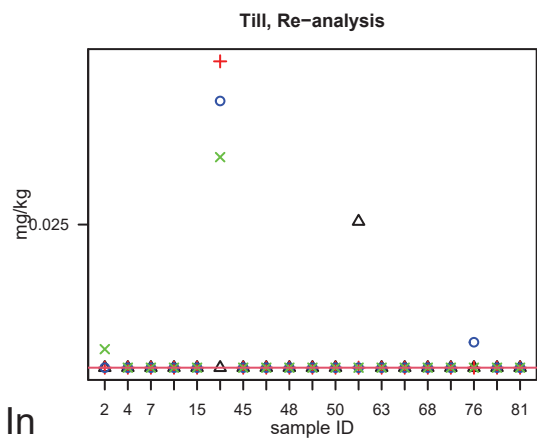
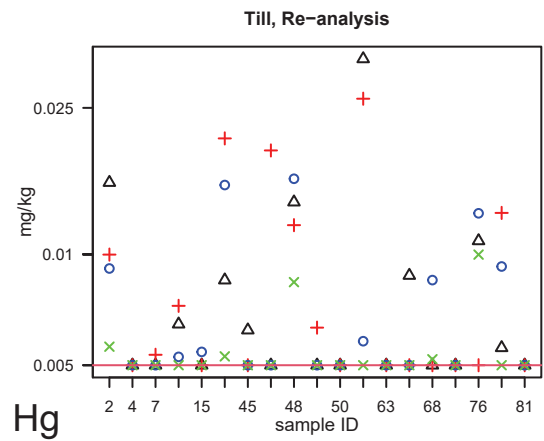
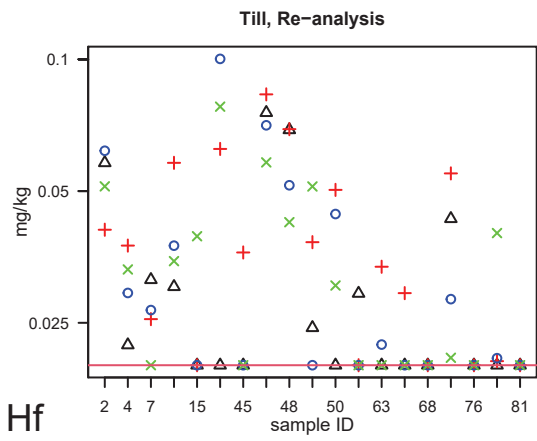
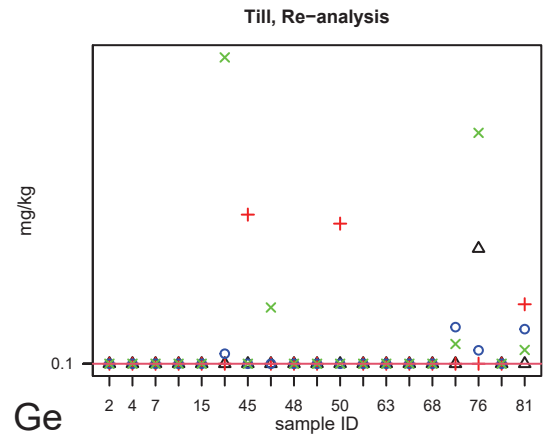
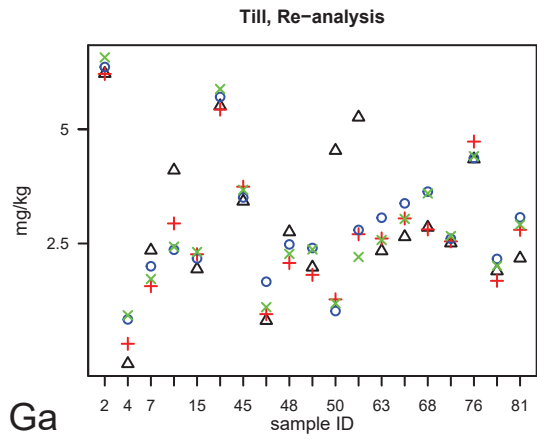
Analytical results for 19 samples (no:2, 4, 7, 10, 15, 17, 40, 45, 47, 48, 49, 50, 62, 63, 66, 68, 73, 76, 77, and 81) from the Nordland/Troms collection (Reimann et al., 2011) which were re-analysed along with the North-Trøndelag and Fosen samples in 2013-2014 (Finne et al., 2014), with the South-Trøndelag survey (Flem et al., 2020) and now for the fourth time with the present survey. The same lab, Bureau Veritas Minerals, Vancouver, Canada, have been used for all four sample collections.

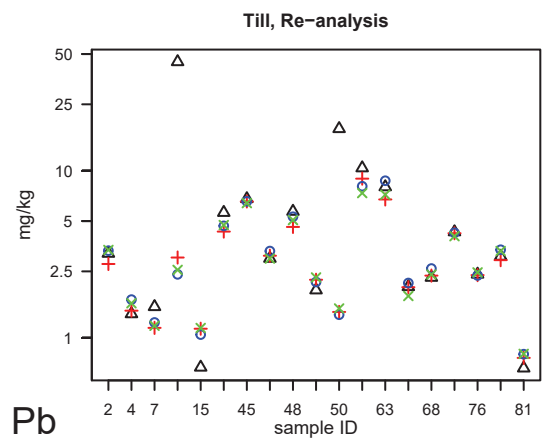
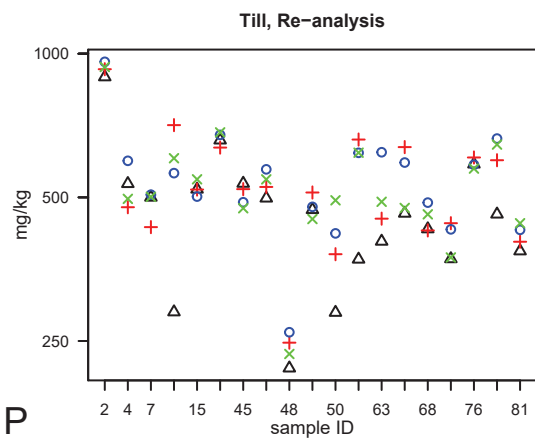
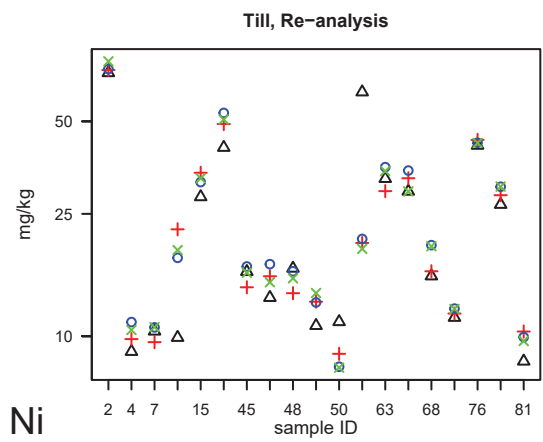
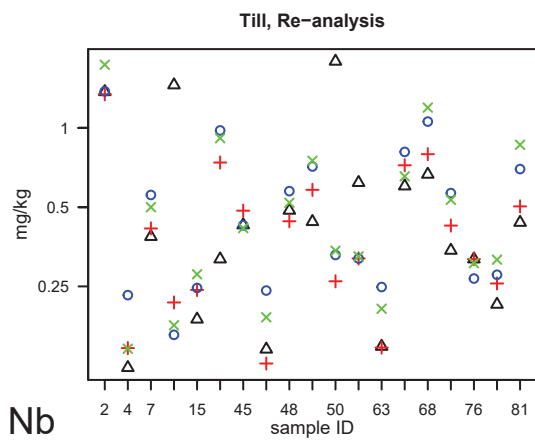
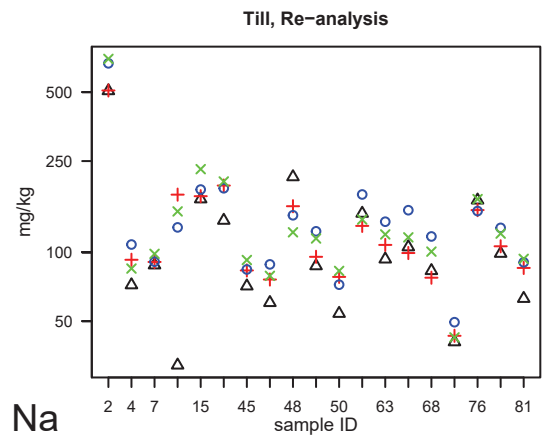
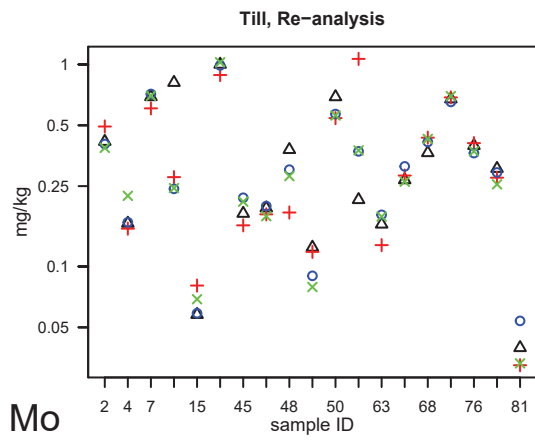
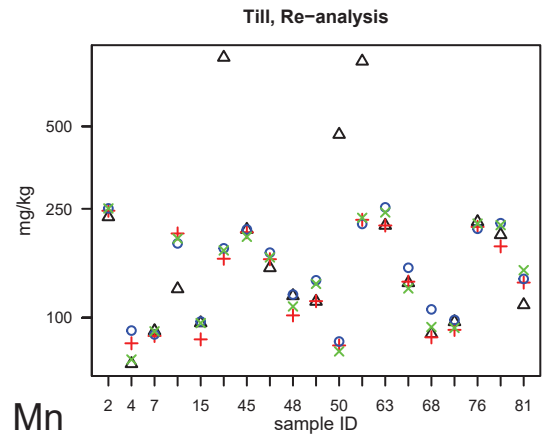
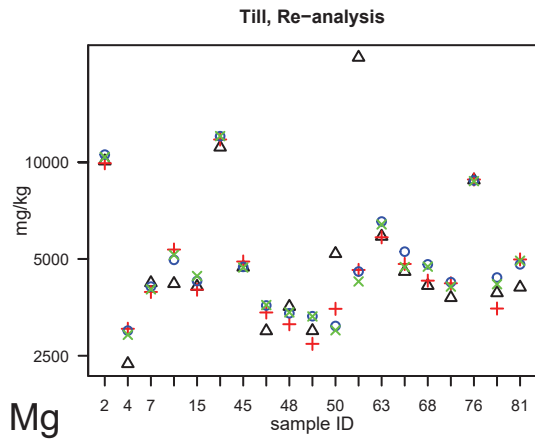
Sample collection	Symbology
Nordland/Troms	Δ
North-Trøndelag and Fosen	+
South-Trøndelag	○
Hedmark	X
Laboratory detection limit	—

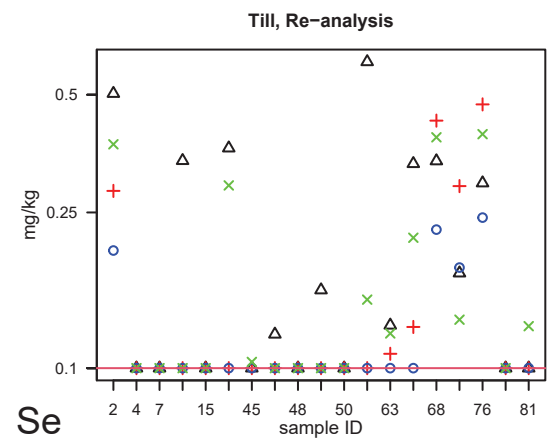
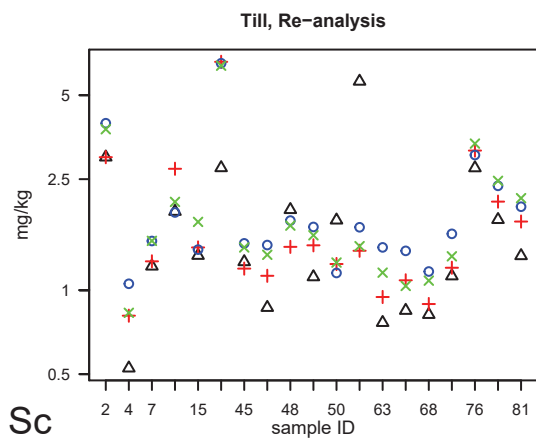
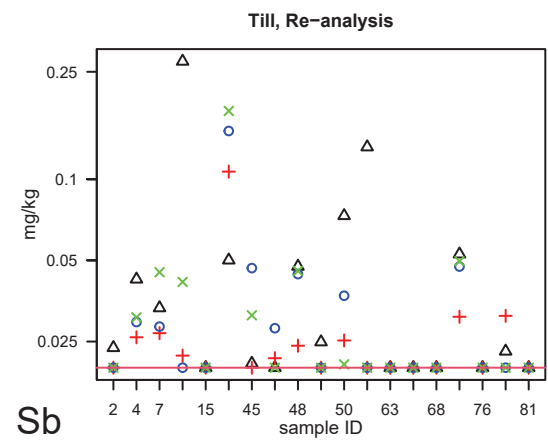
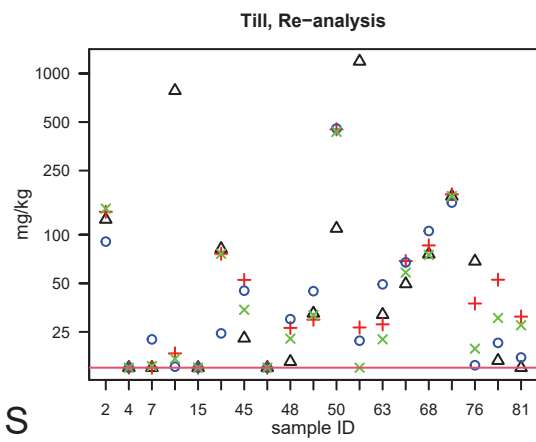
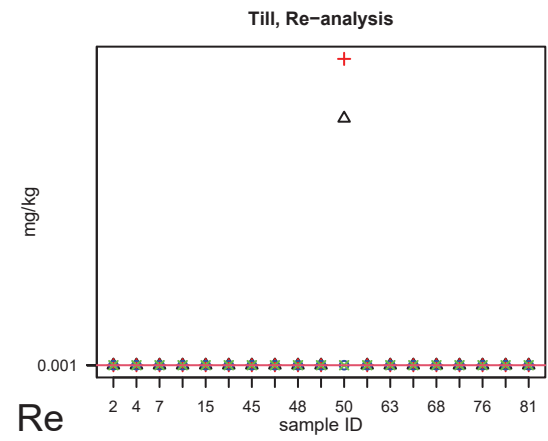
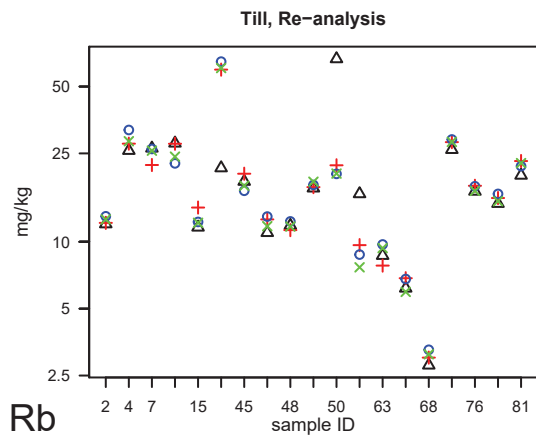
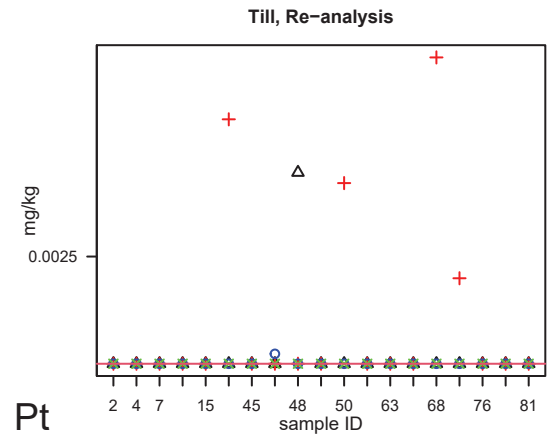
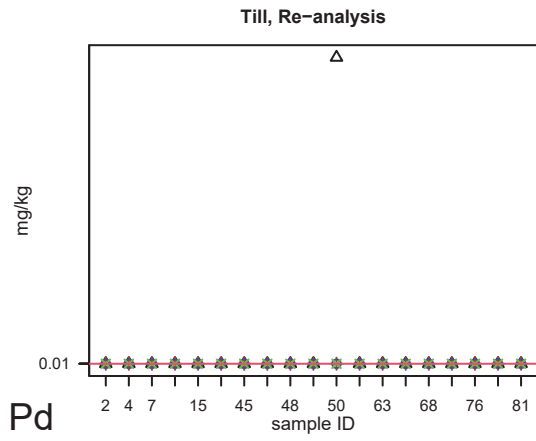


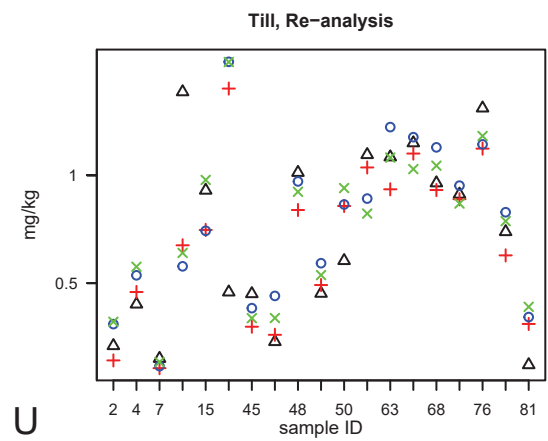
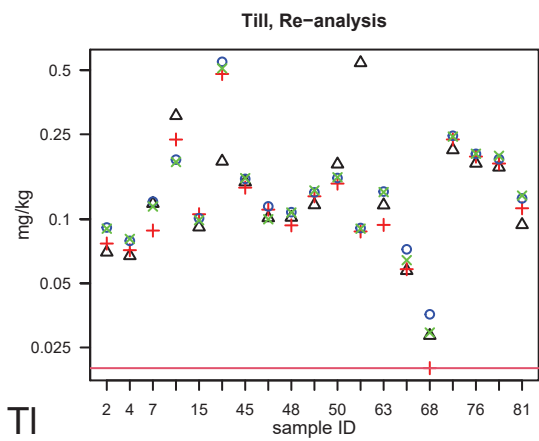
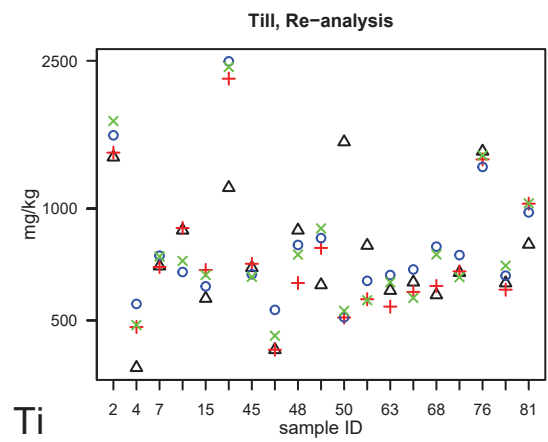
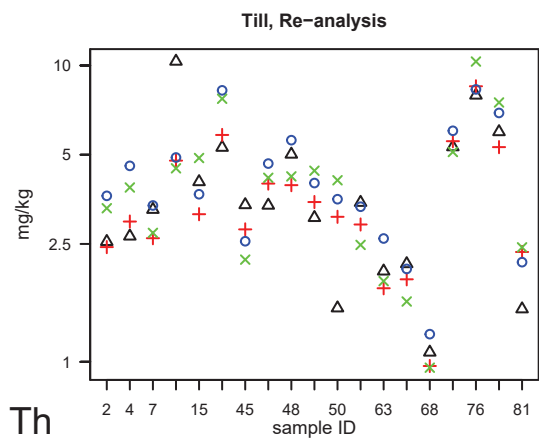
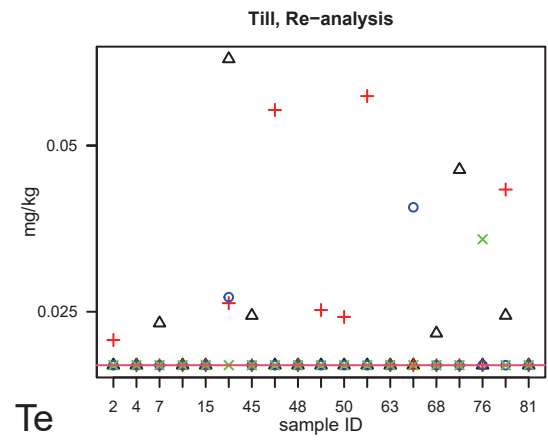
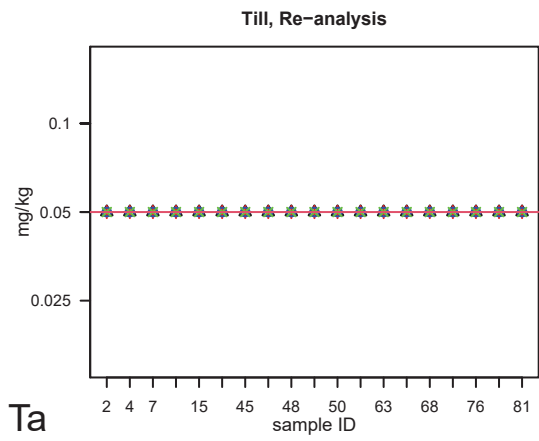
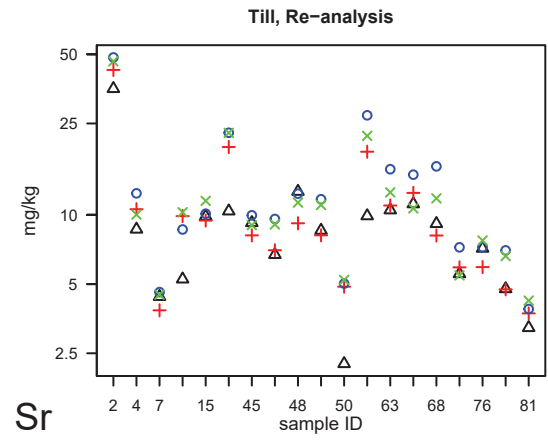
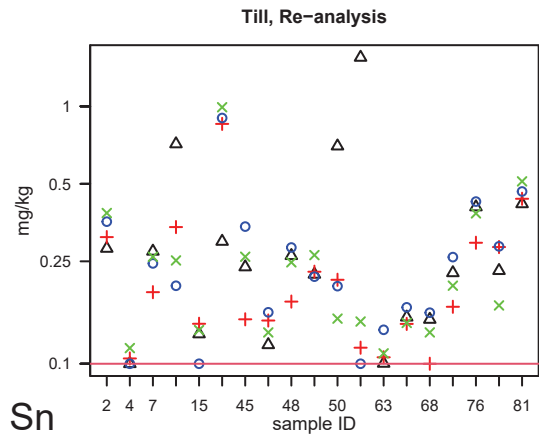


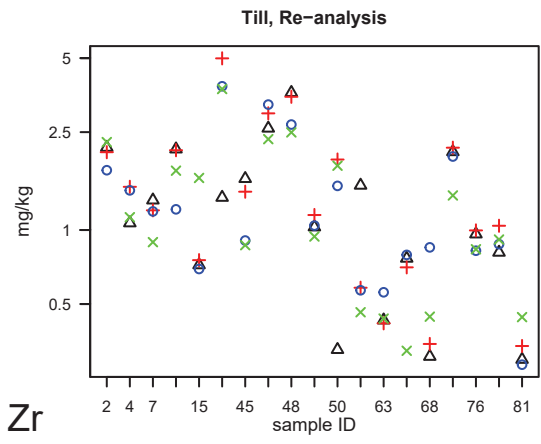
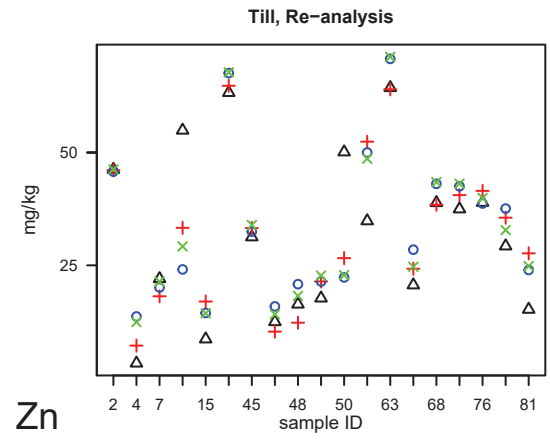
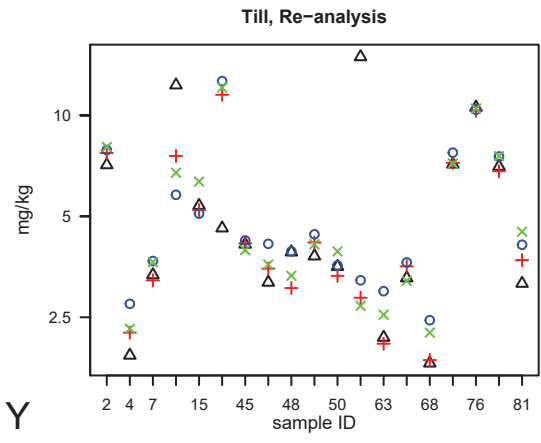
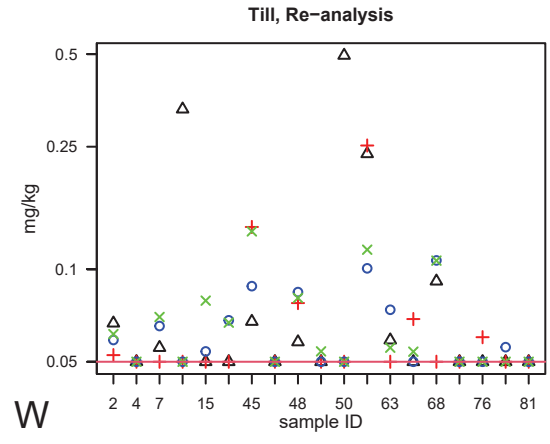
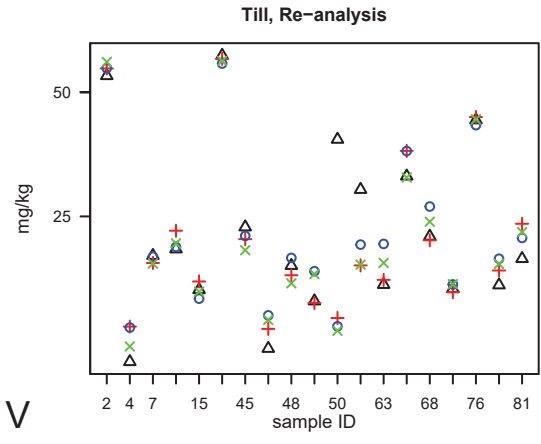






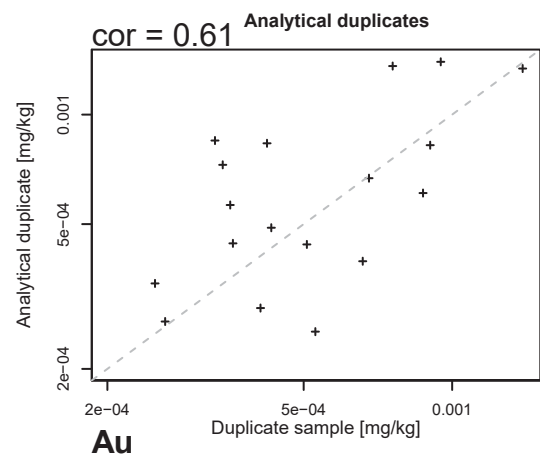
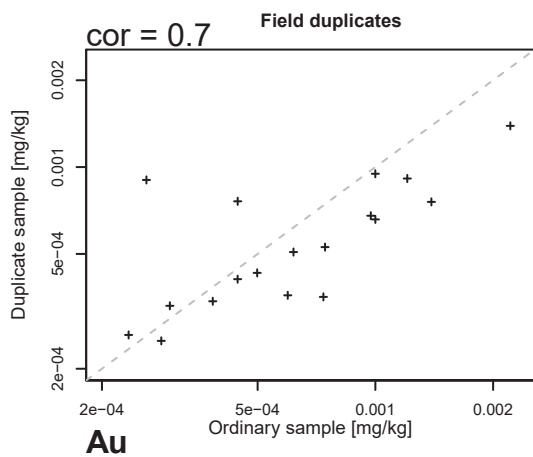
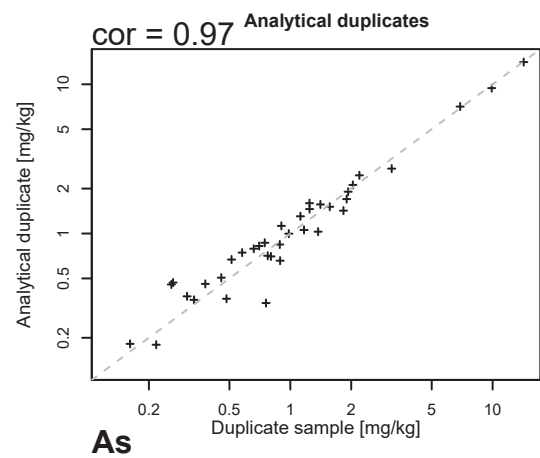
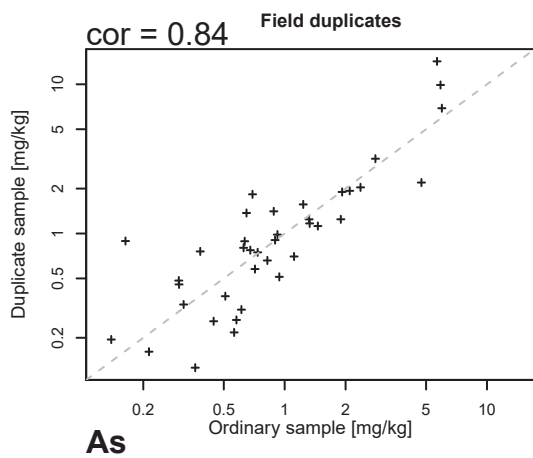
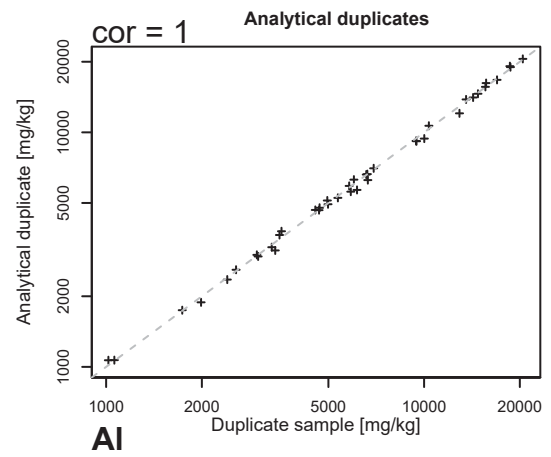
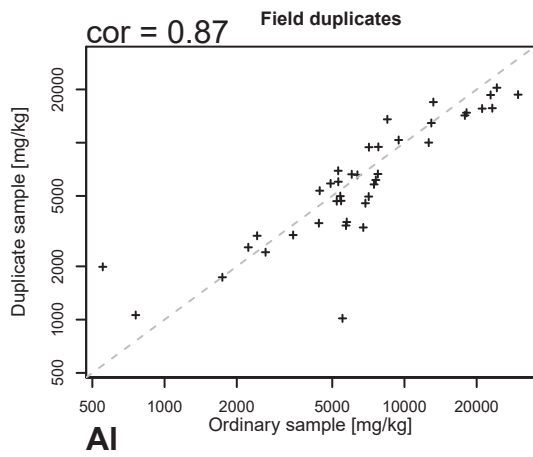
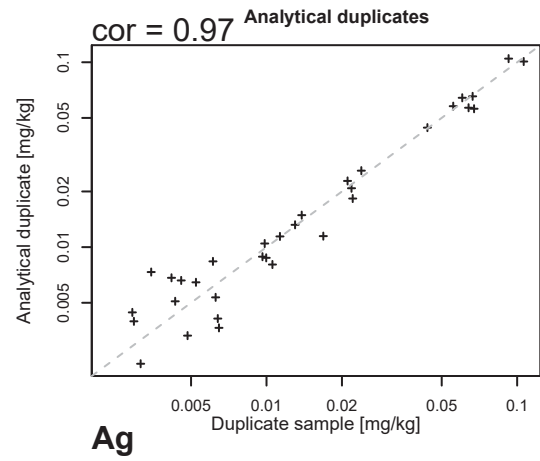
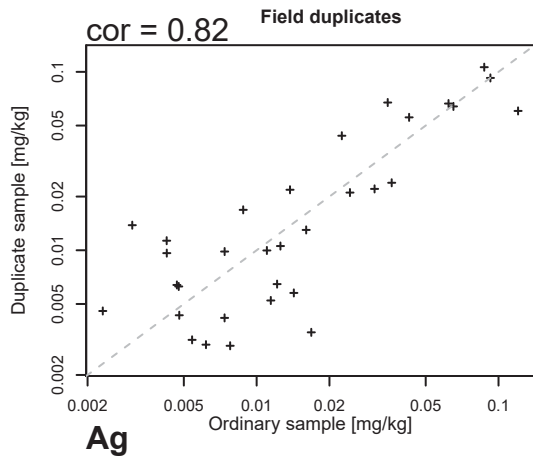




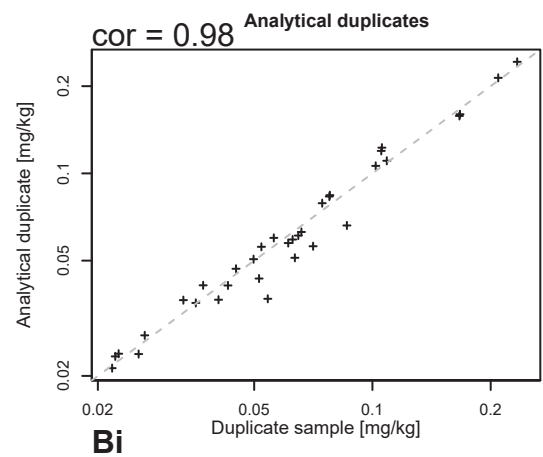
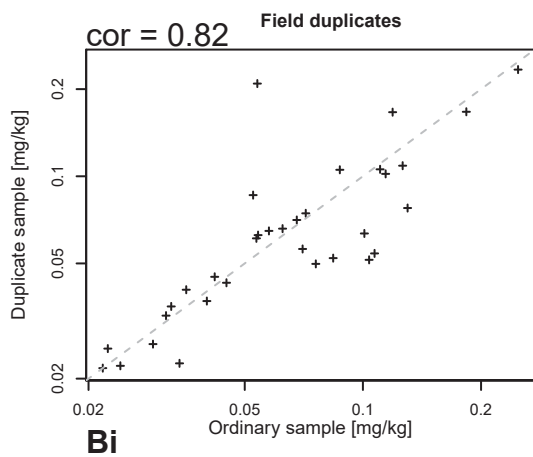
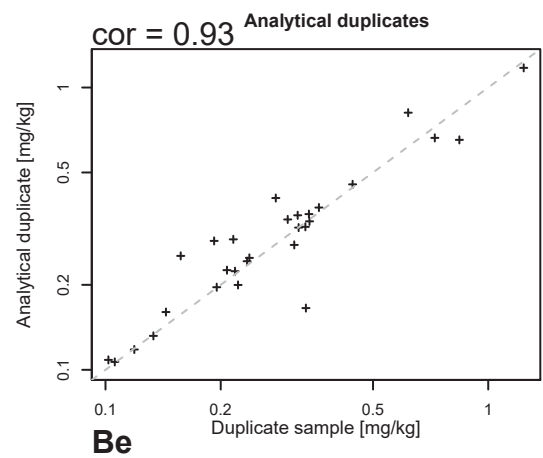
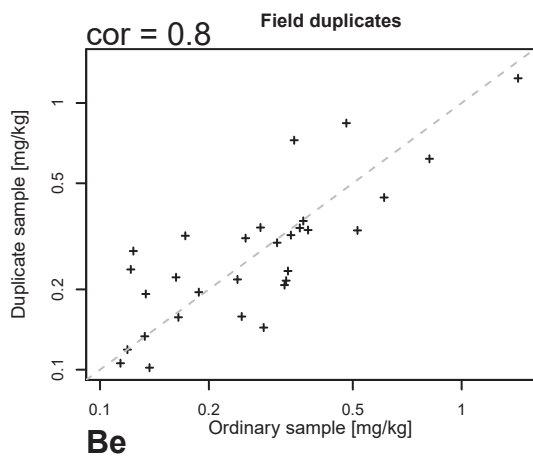
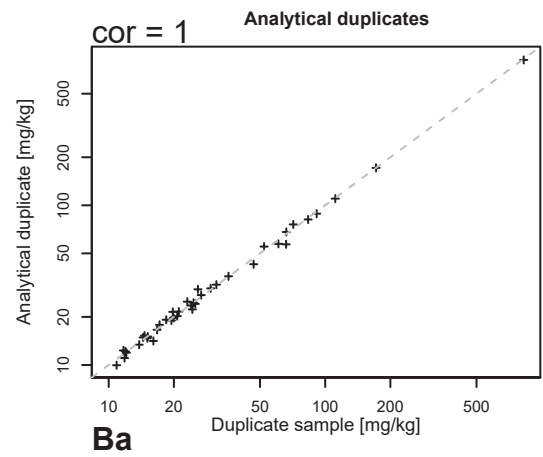
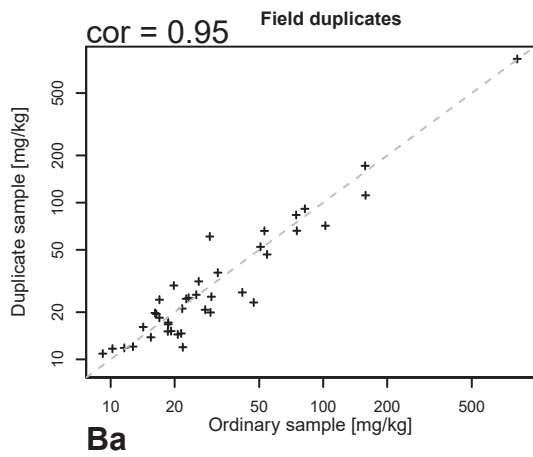
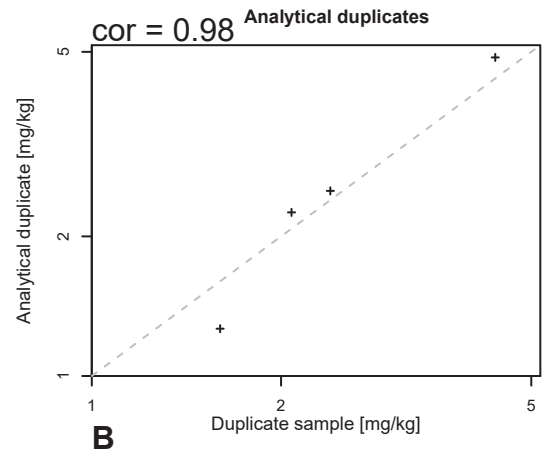
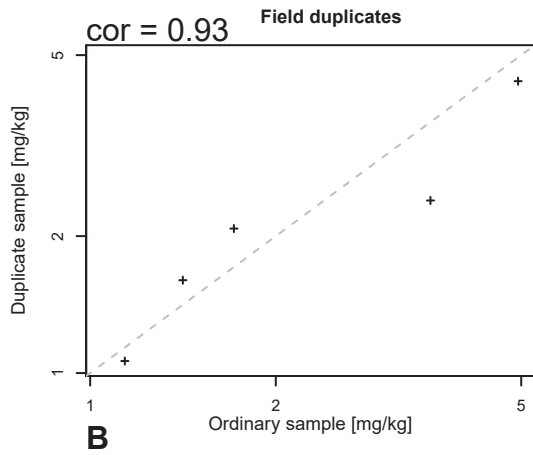


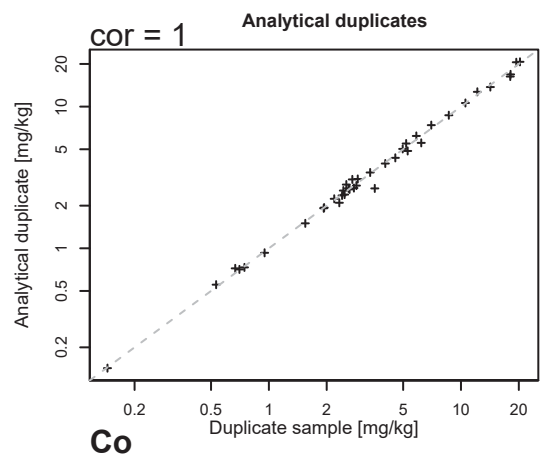
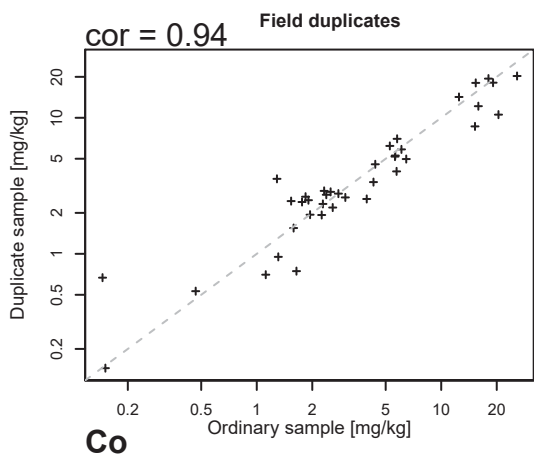
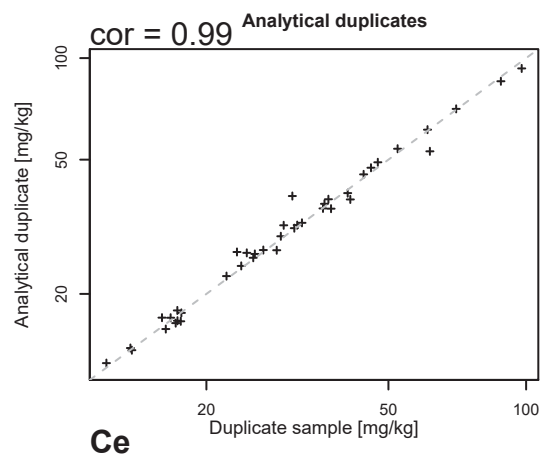
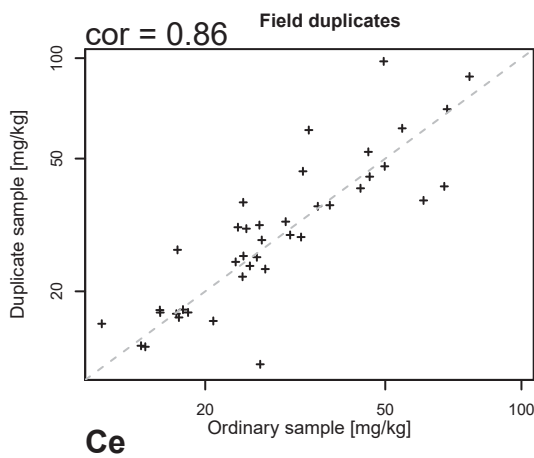
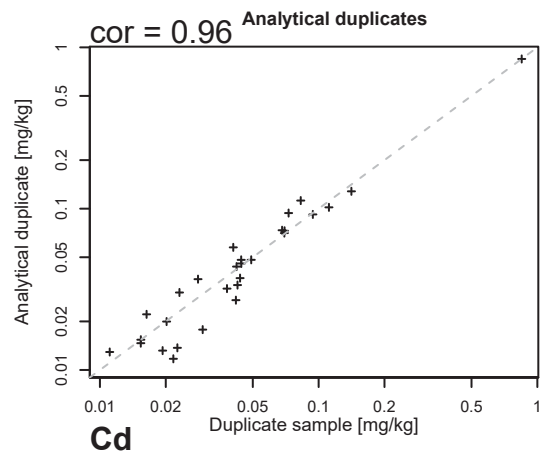
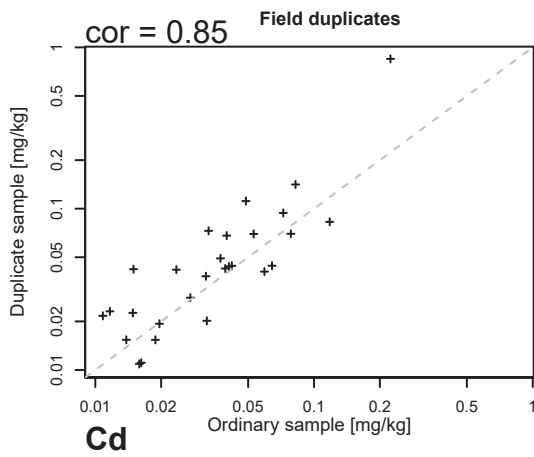
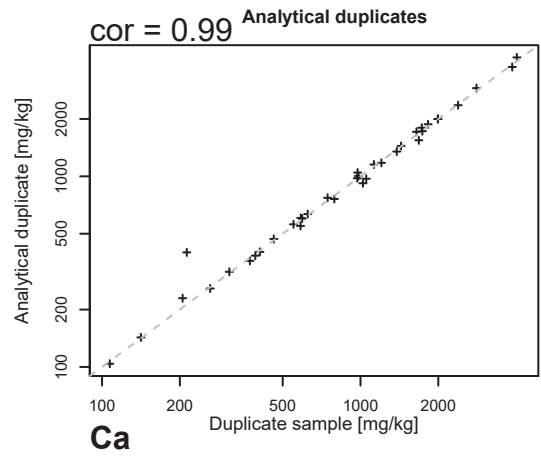
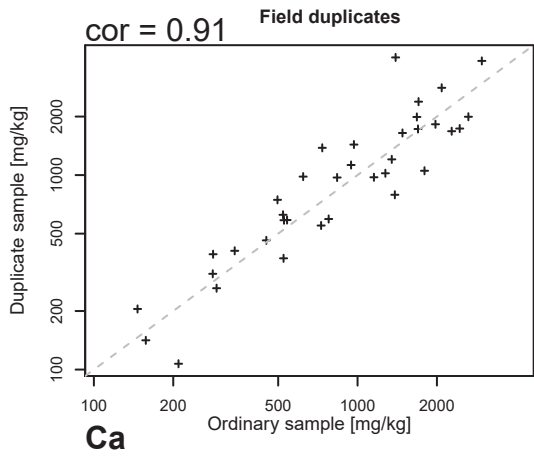
## Appendix 4: Correlation plots, field- and analytical duplicates

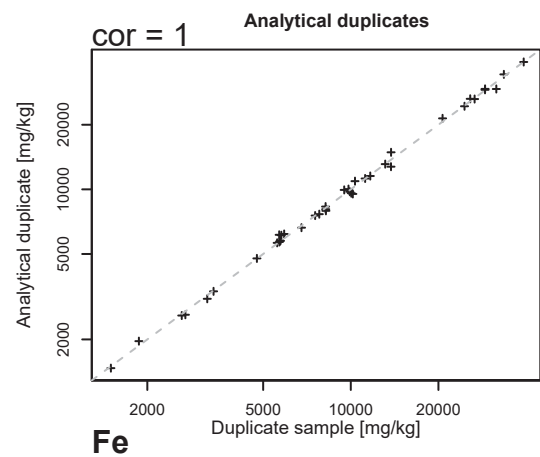
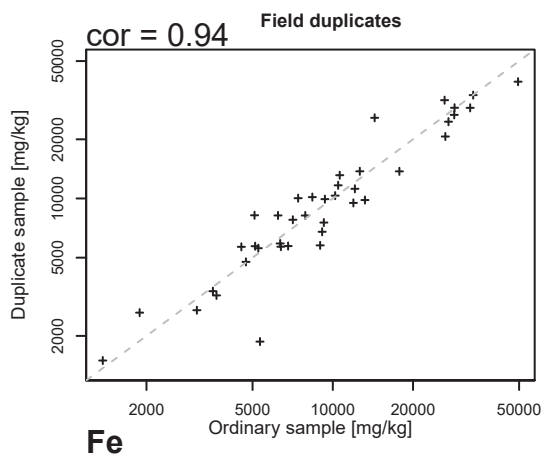
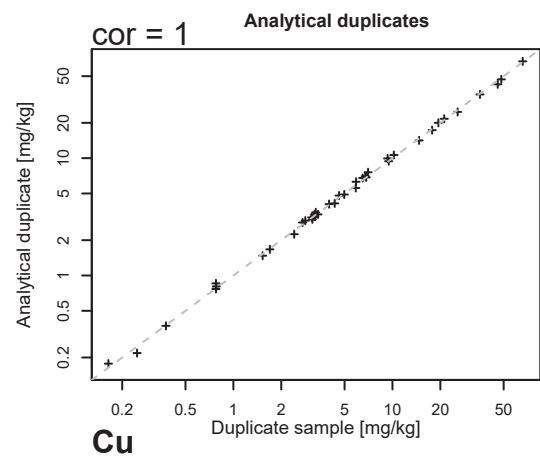
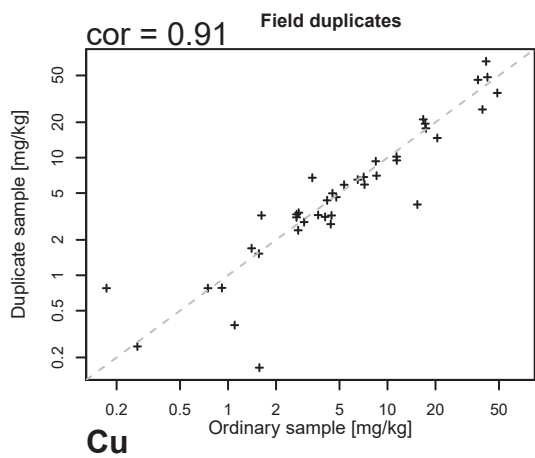
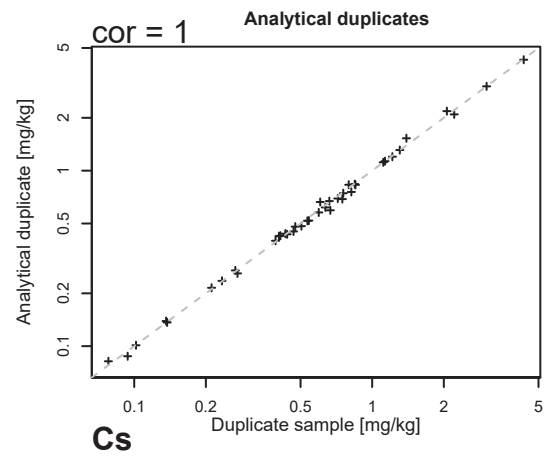
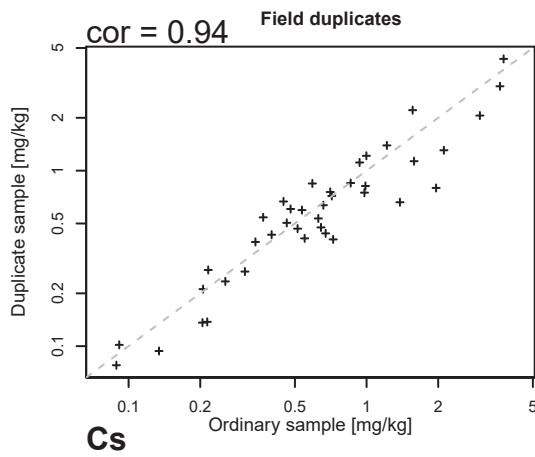
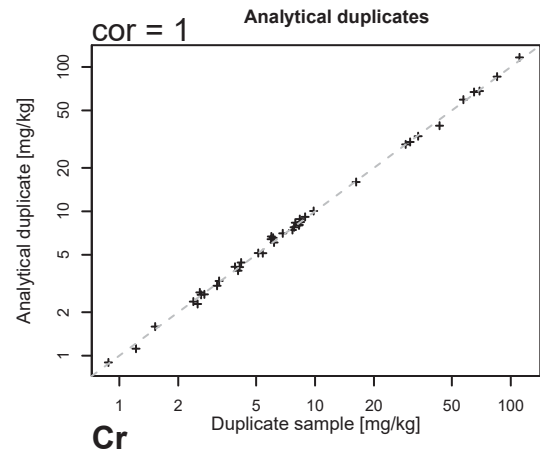
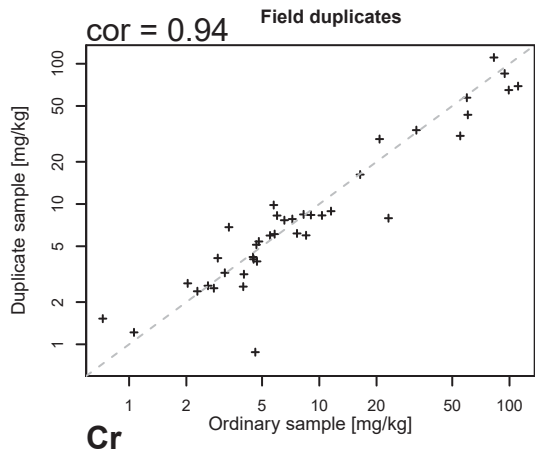
The correlation between ordinary sample and duplicate sample (left hand figure) and the correlation between duplicate sample and analytical duplicate (right hand figure) shown for all elements that have at least five duplicate pairs above MDL. Above each plot is the covariance or correlation (cor) given.

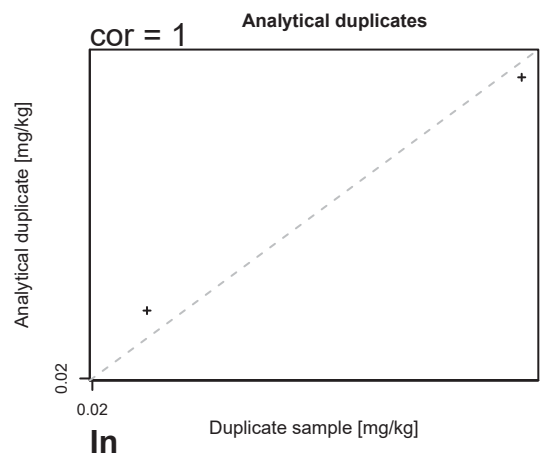
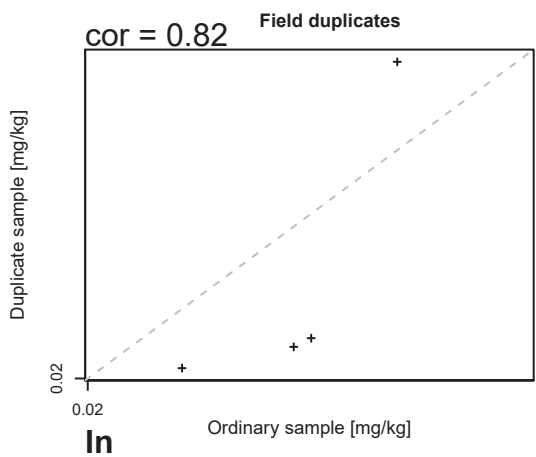
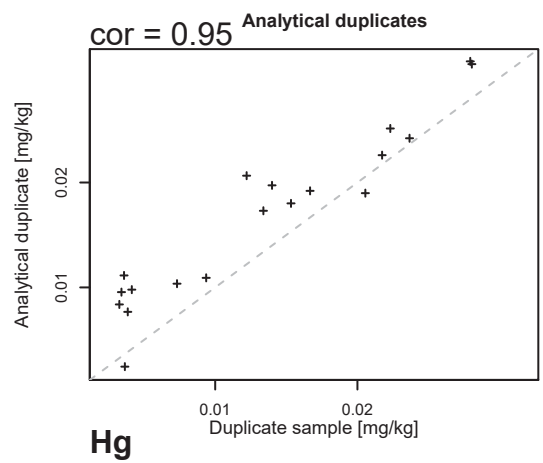
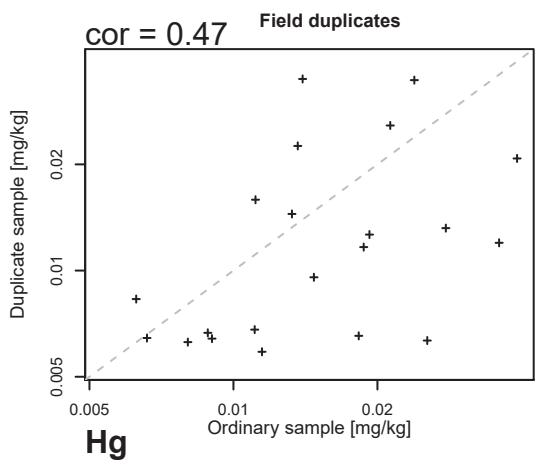
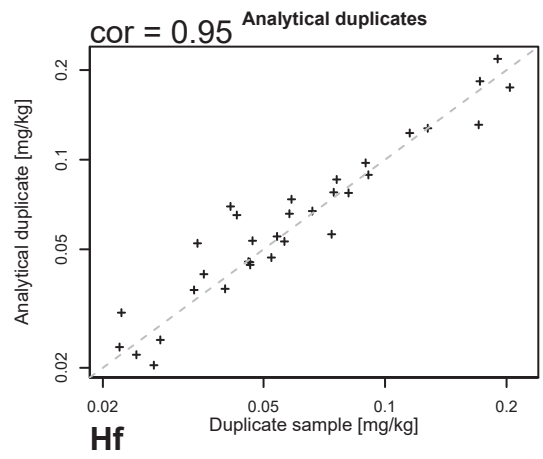
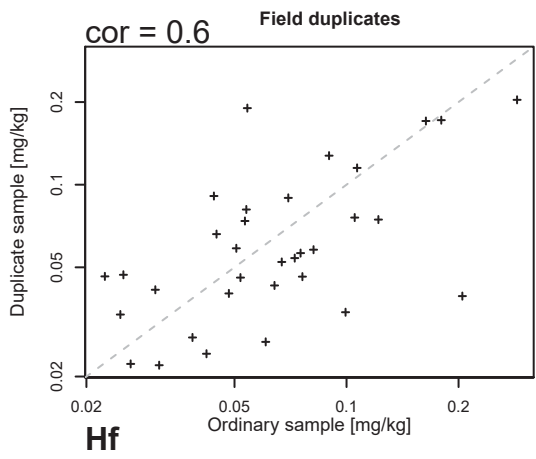
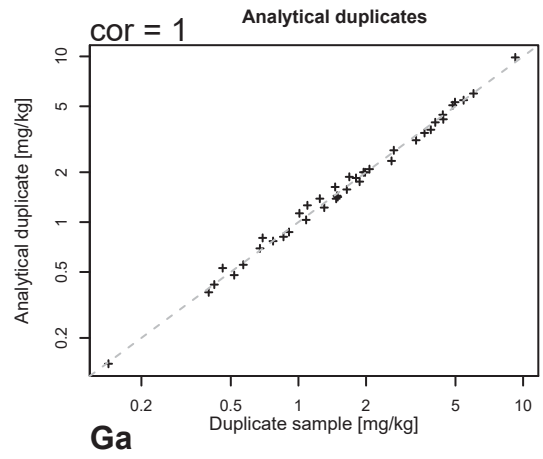
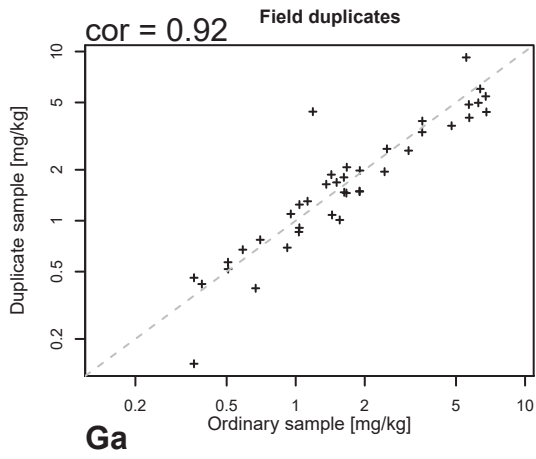


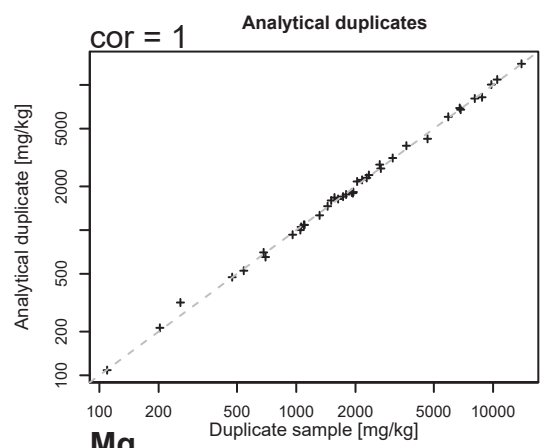
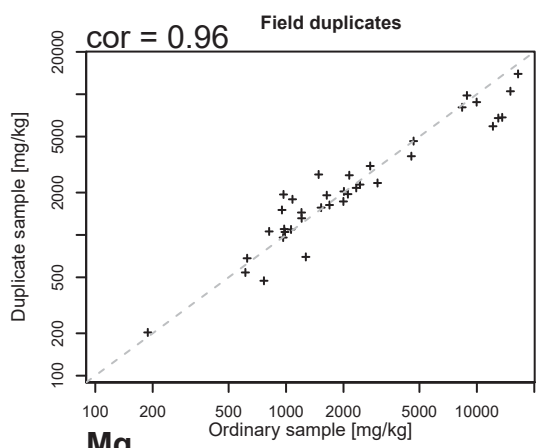
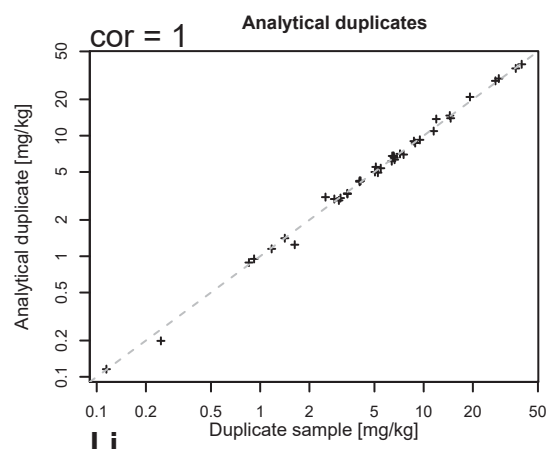
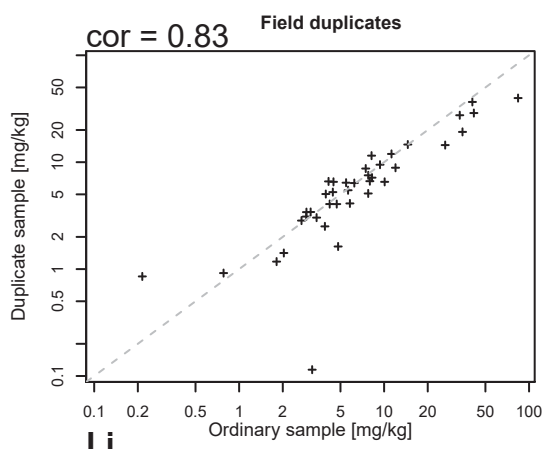
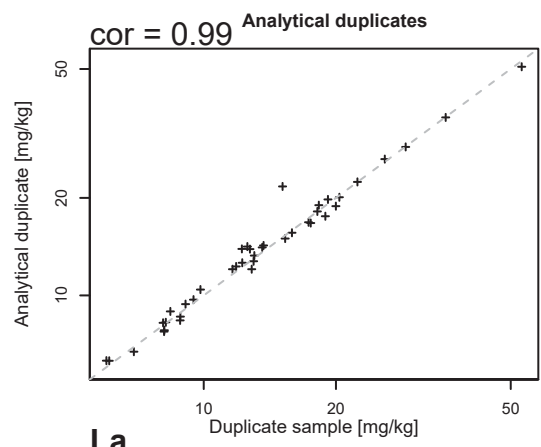
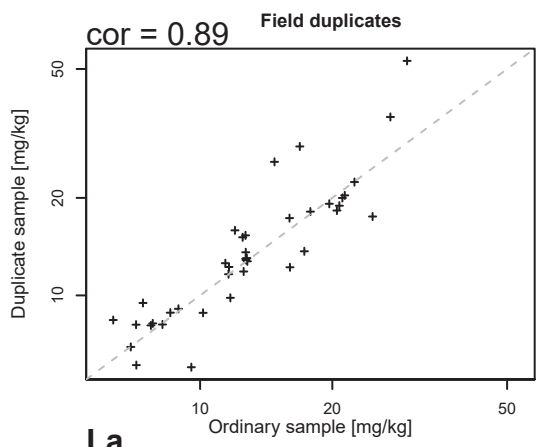
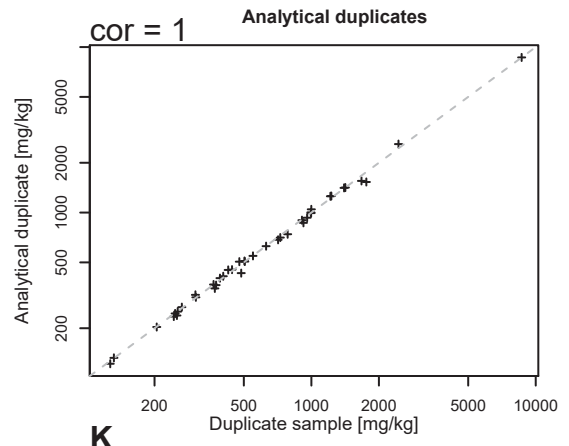
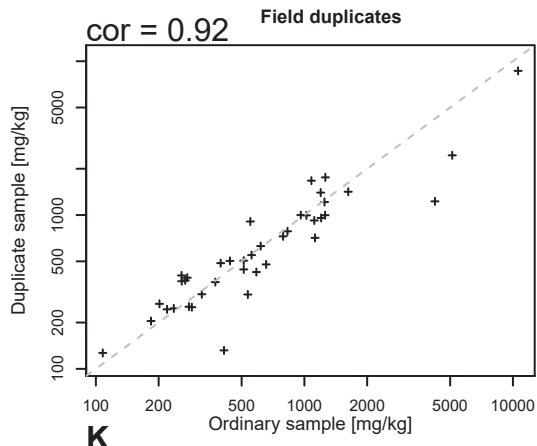


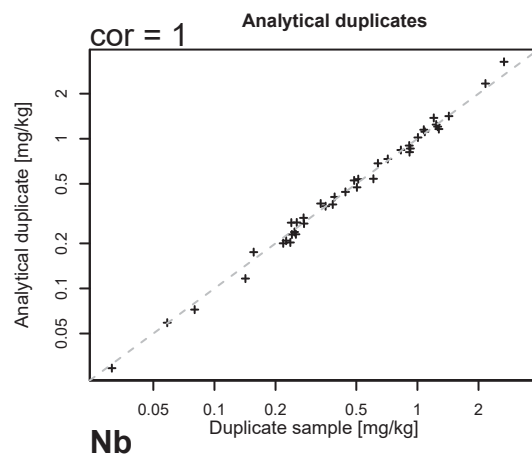
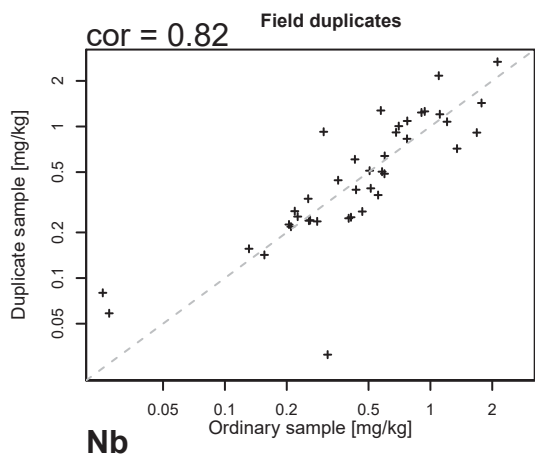
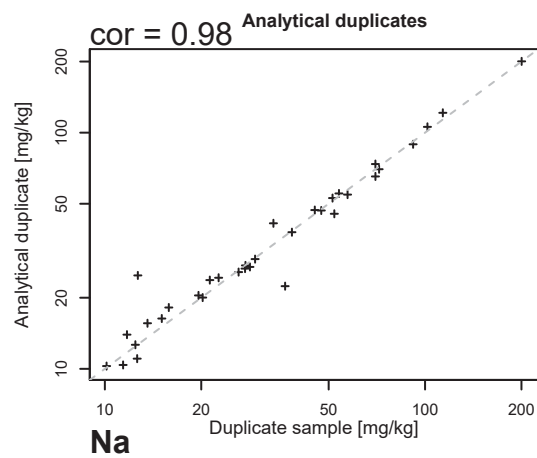
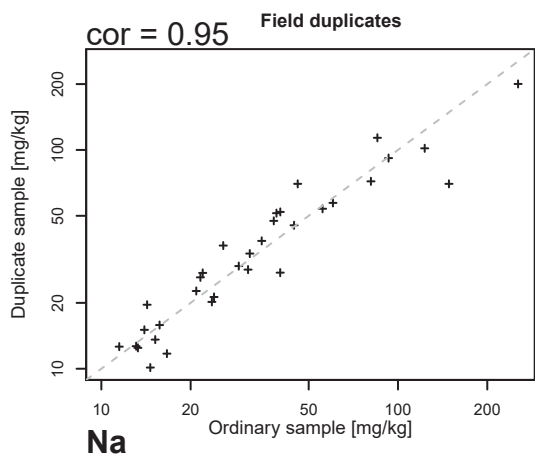
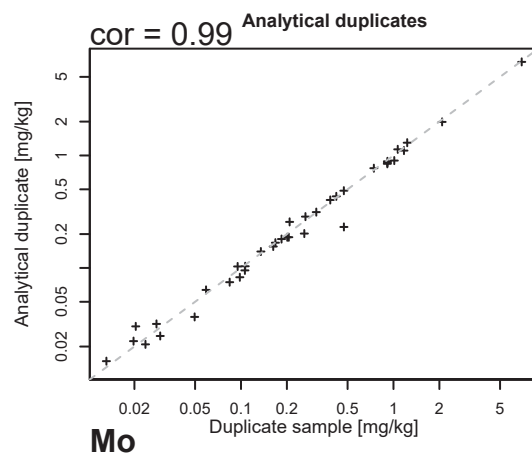
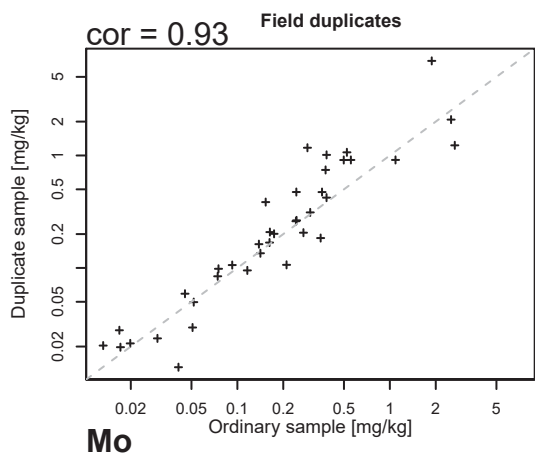
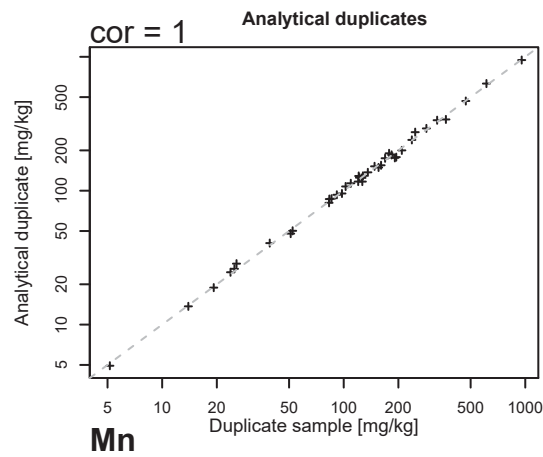
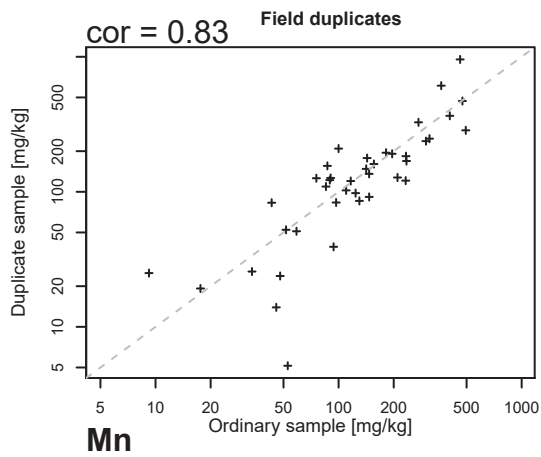


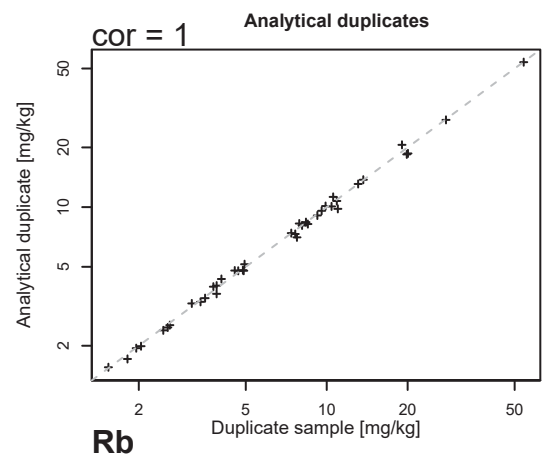
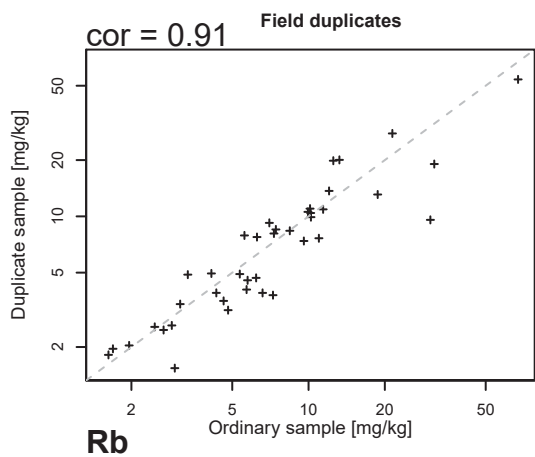
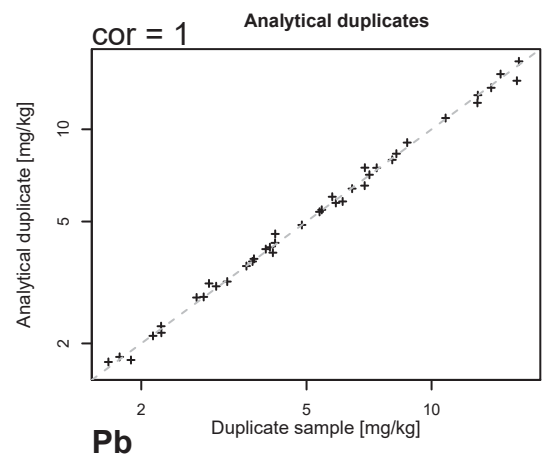
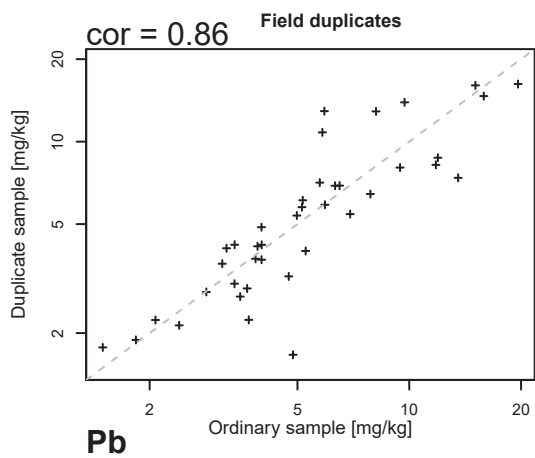
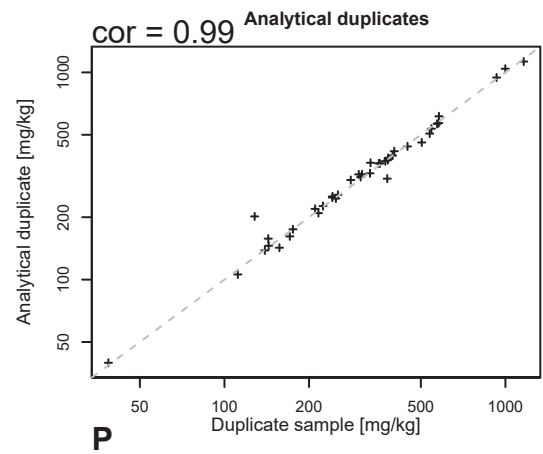
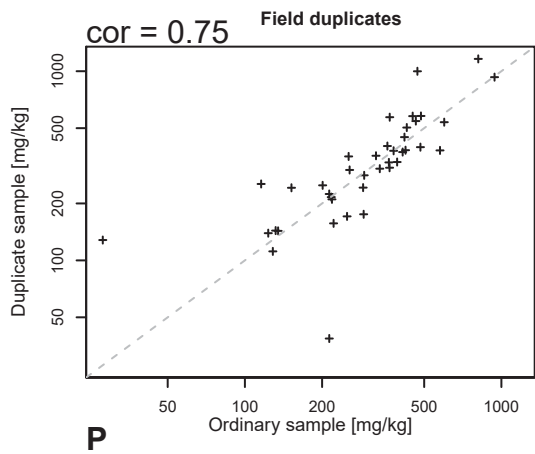
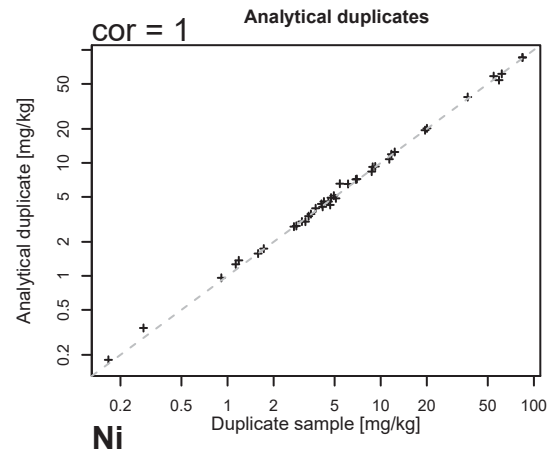
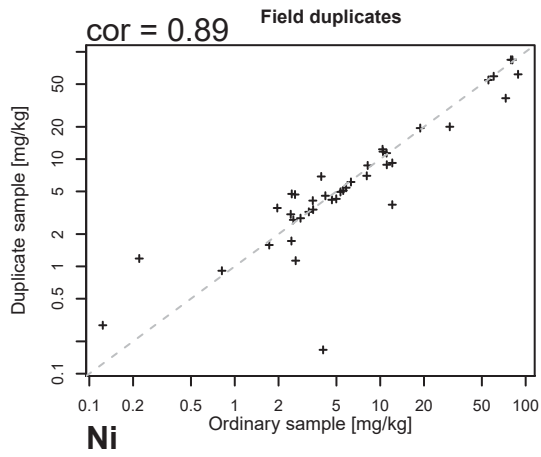


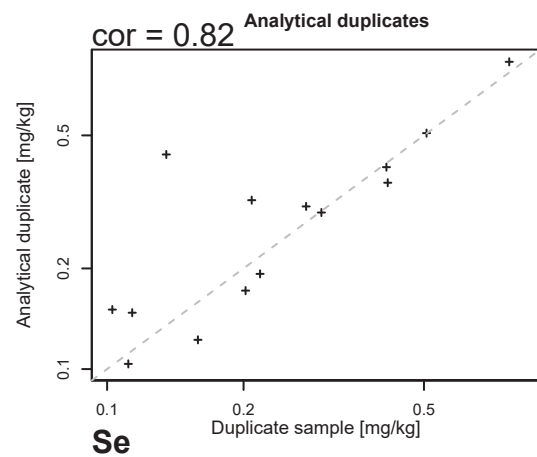
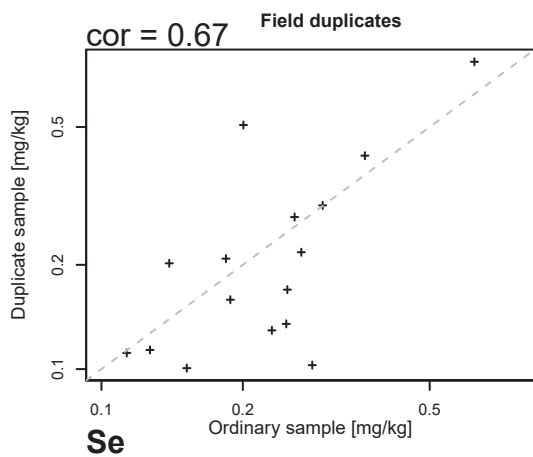
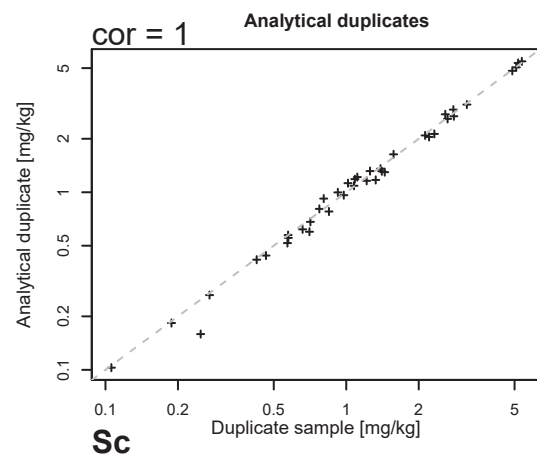
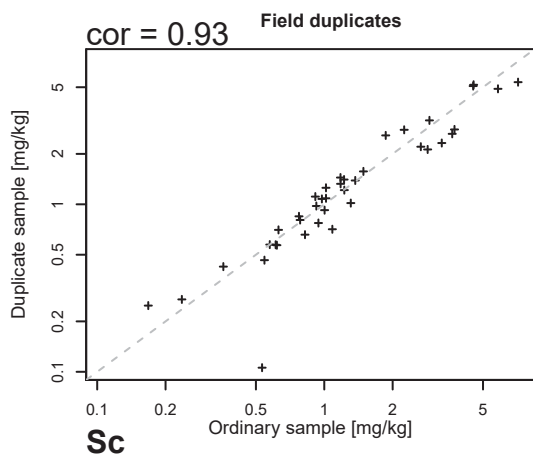
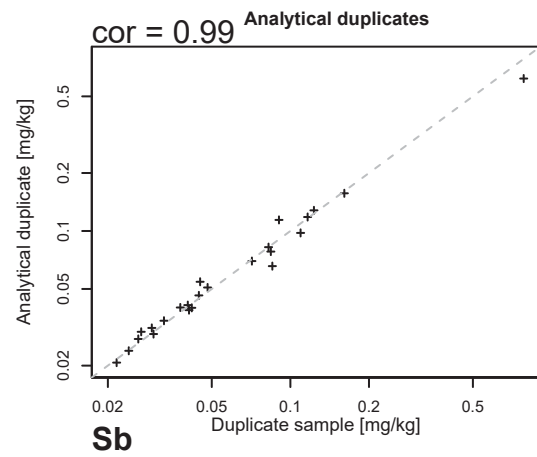
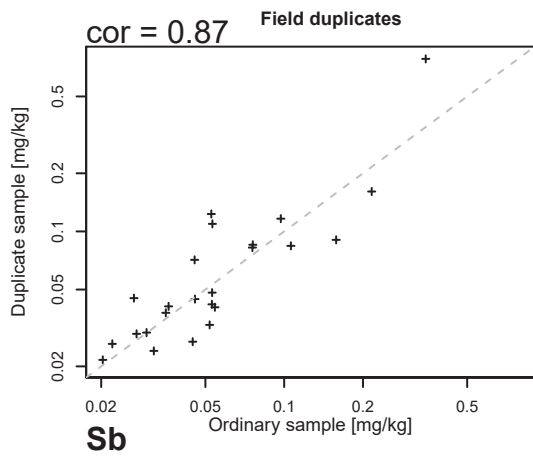
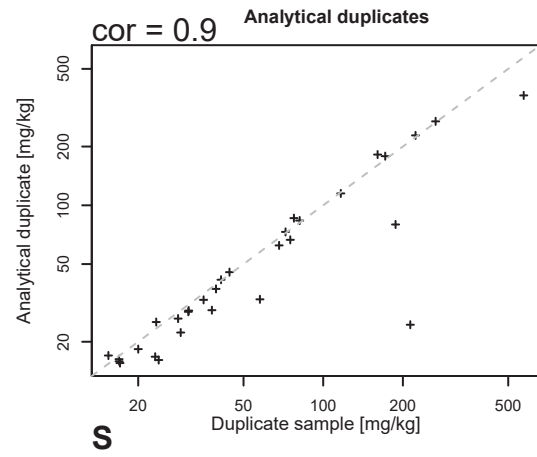
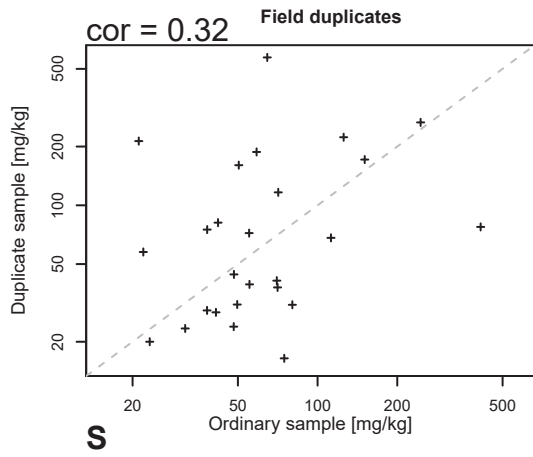




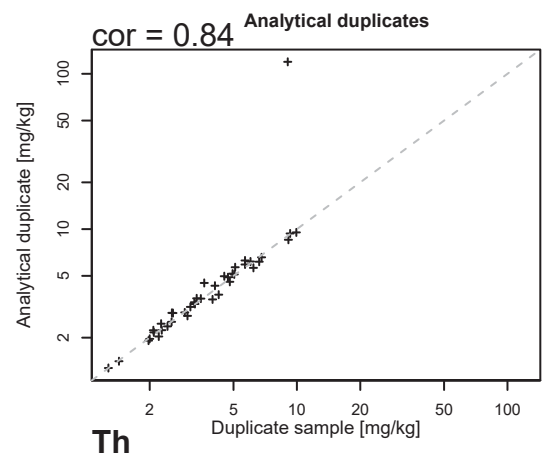
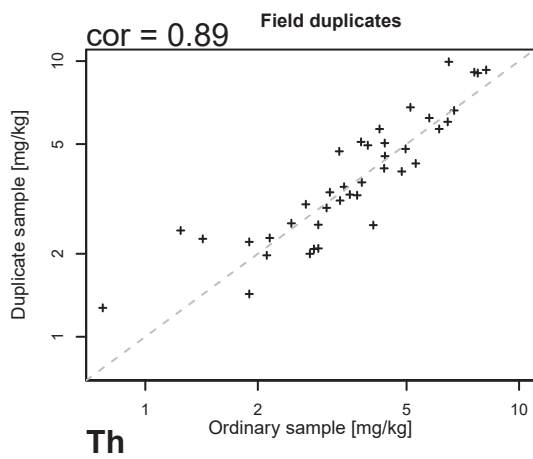
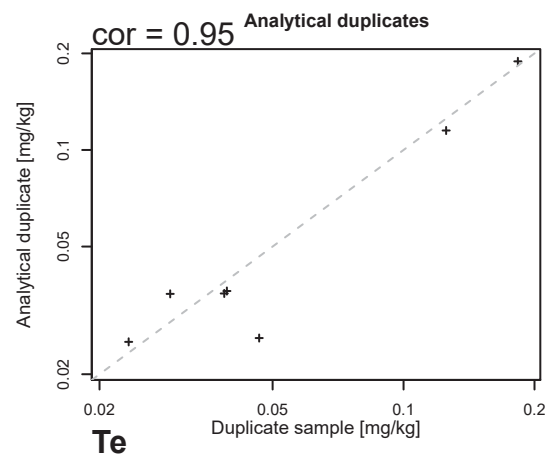
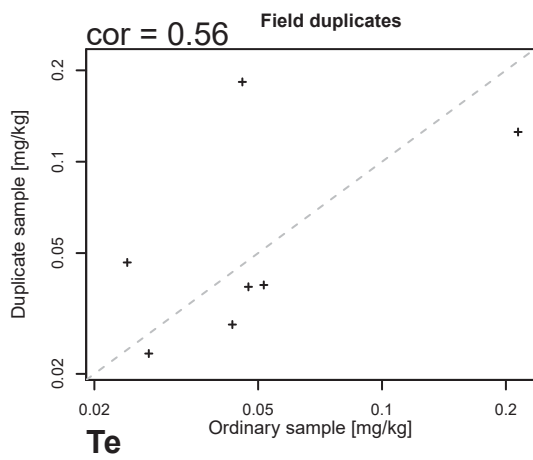
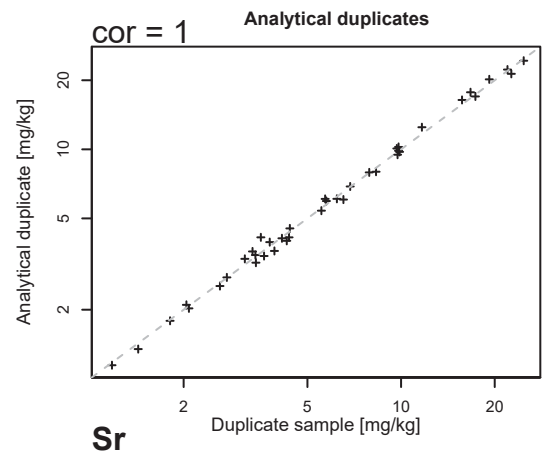
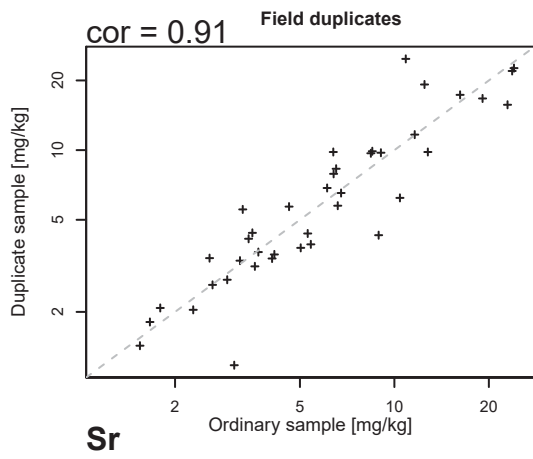
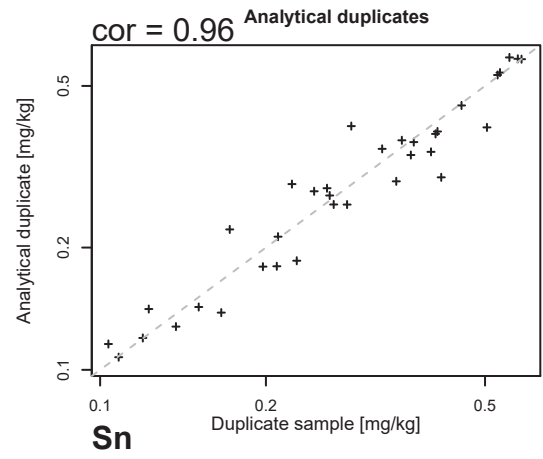
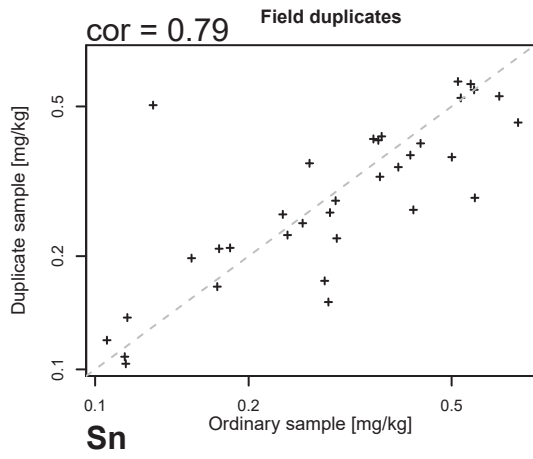


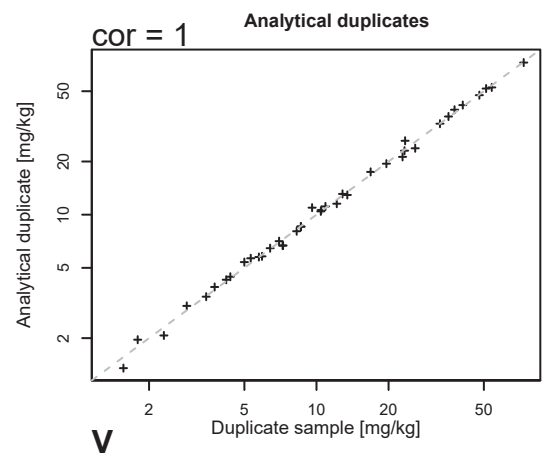
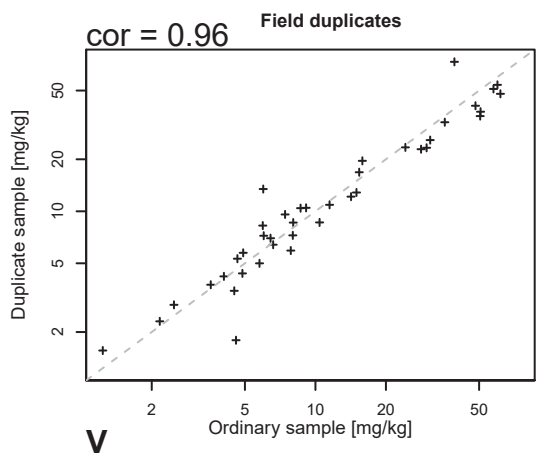
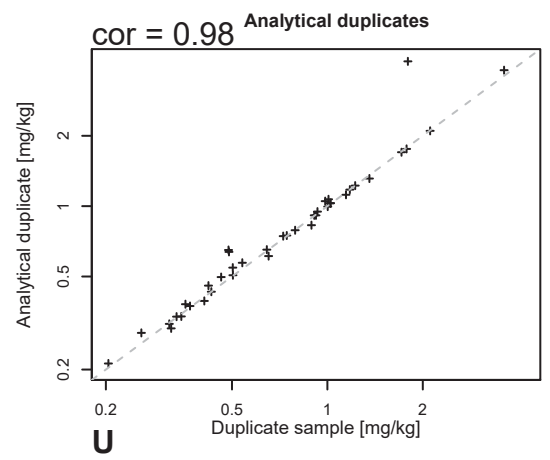
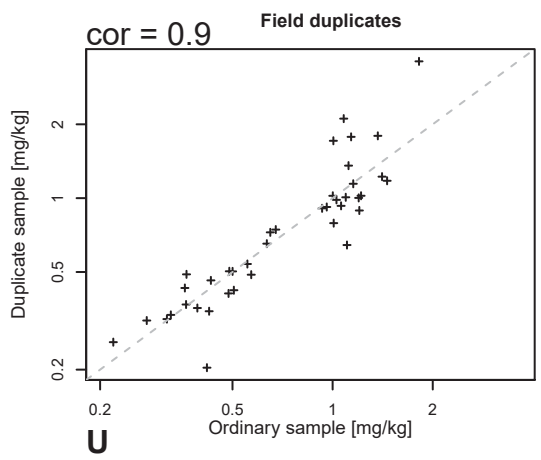
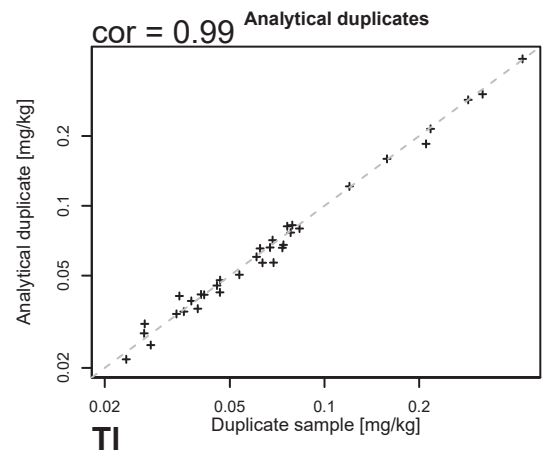
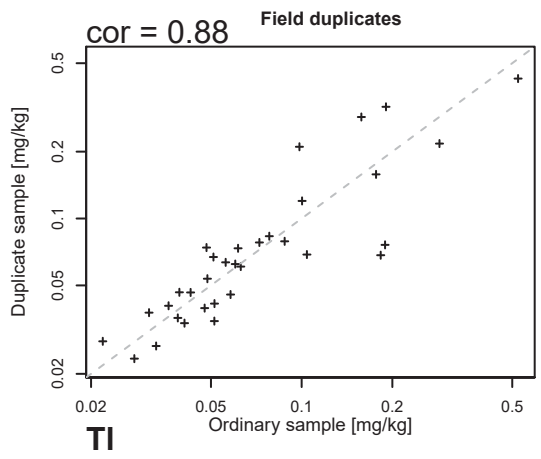
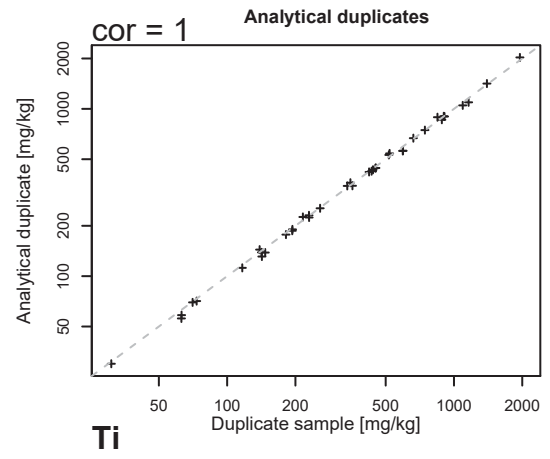
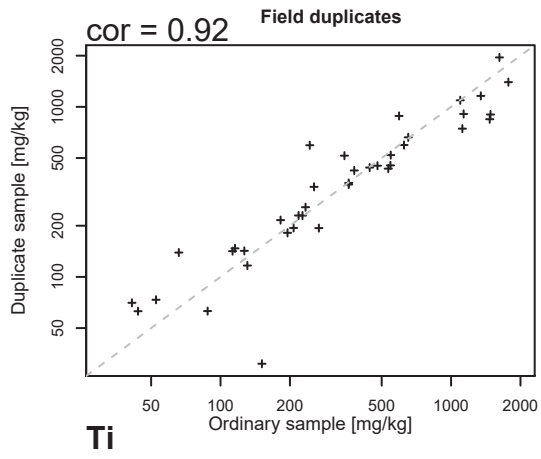


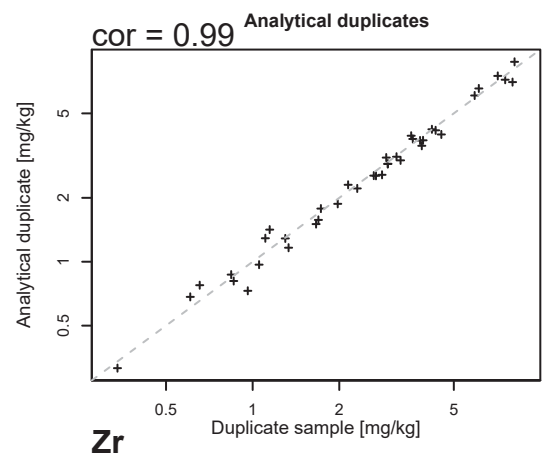
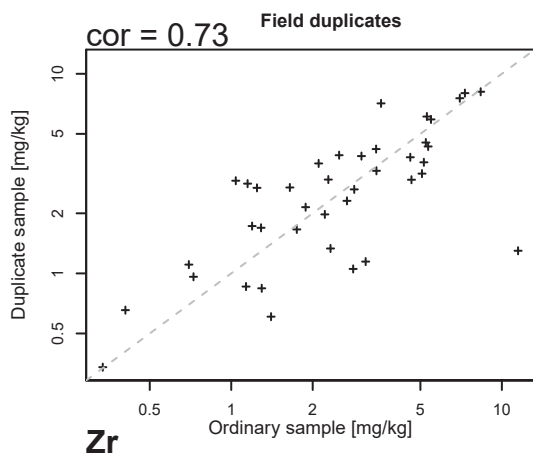
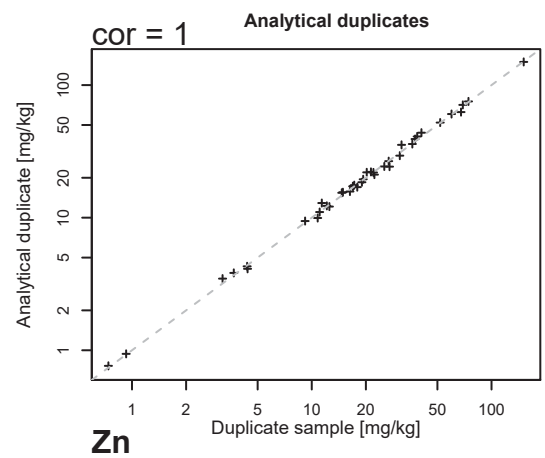
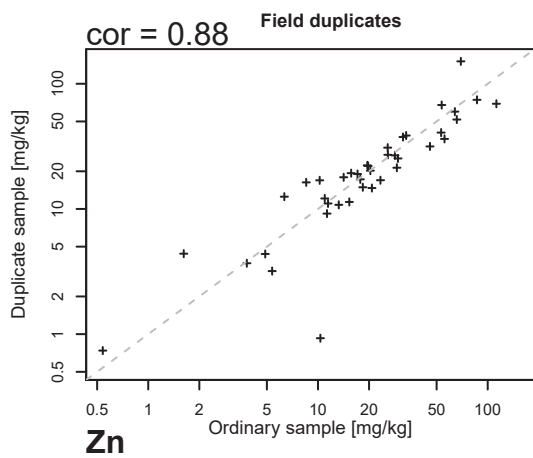
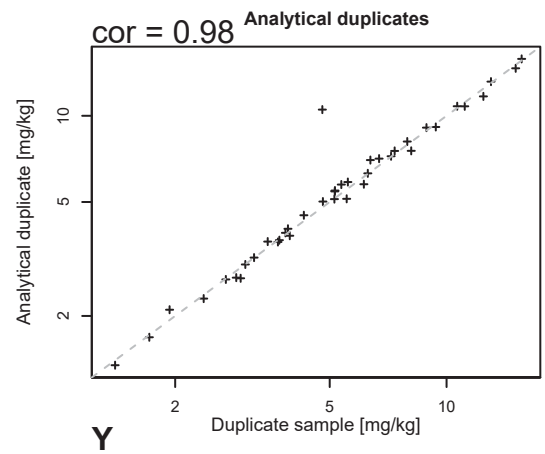
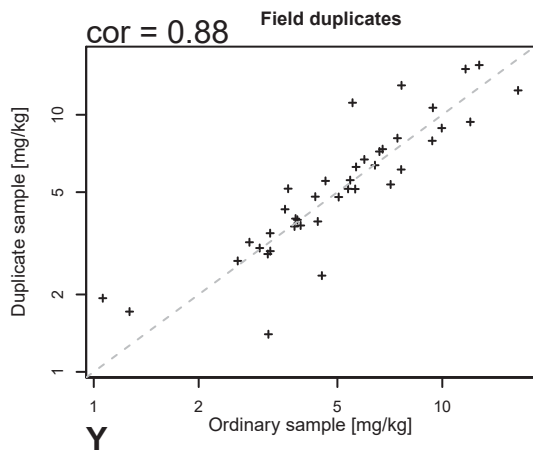
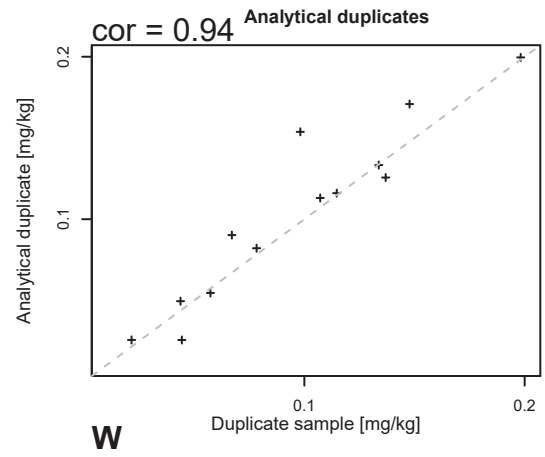
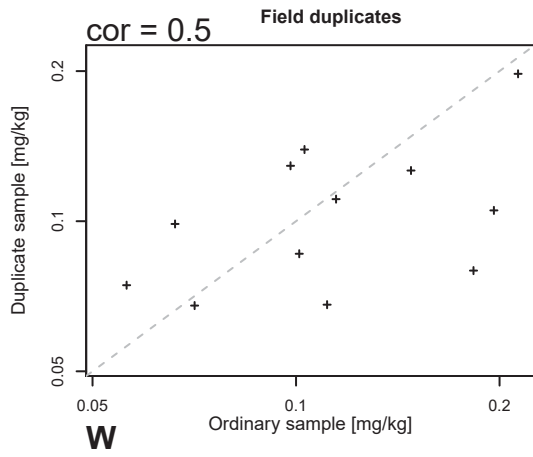










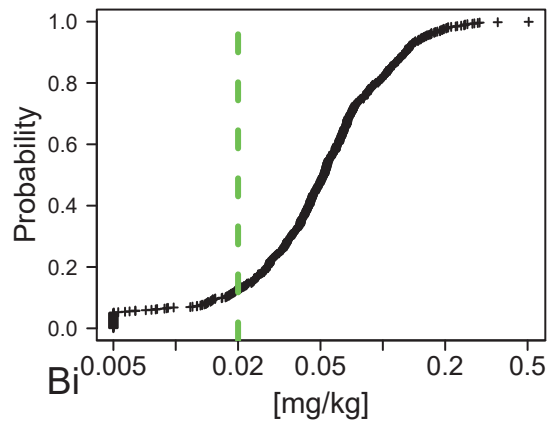
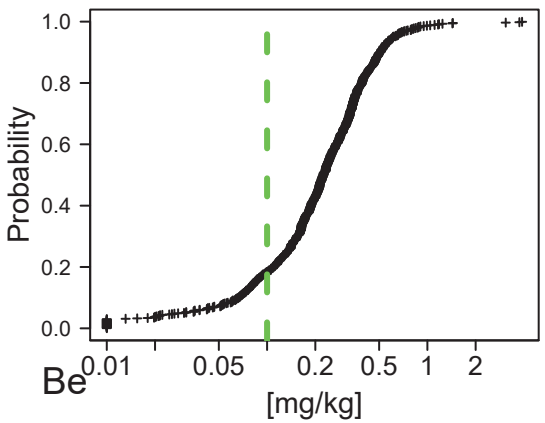
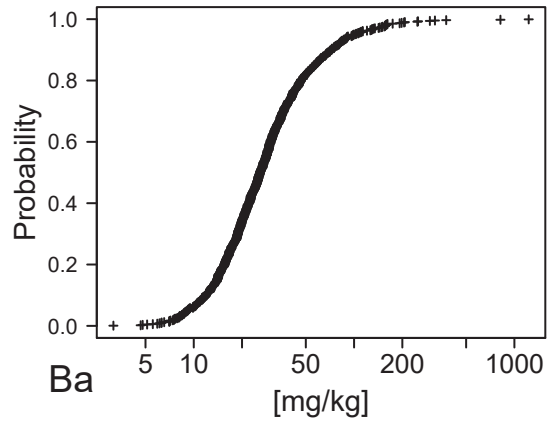
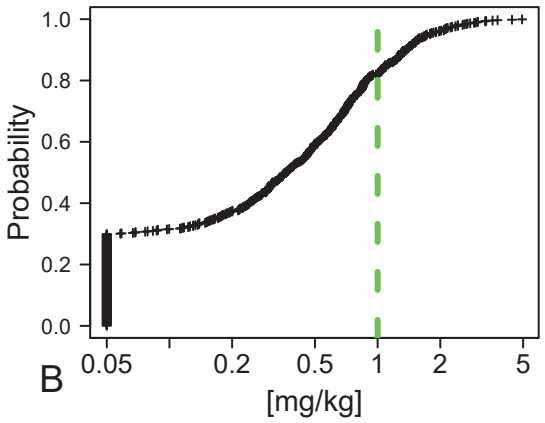
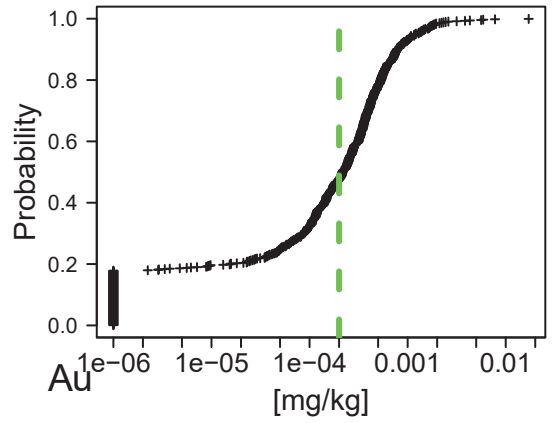
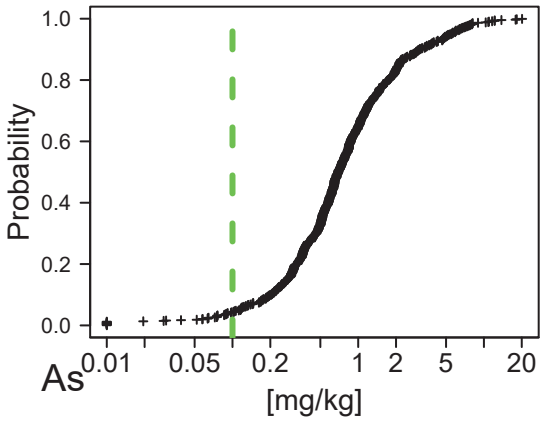
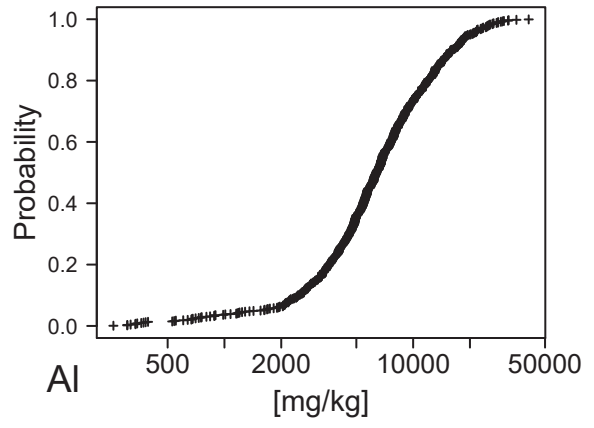
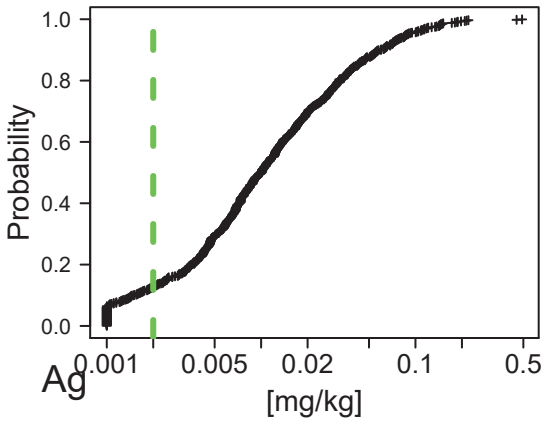


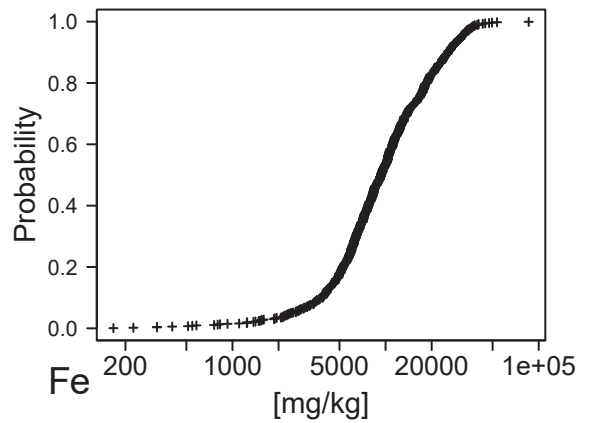
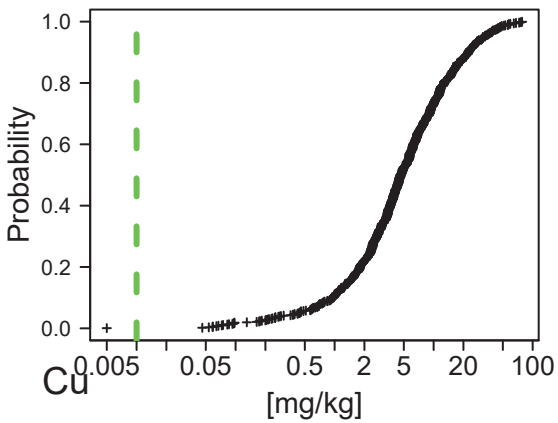
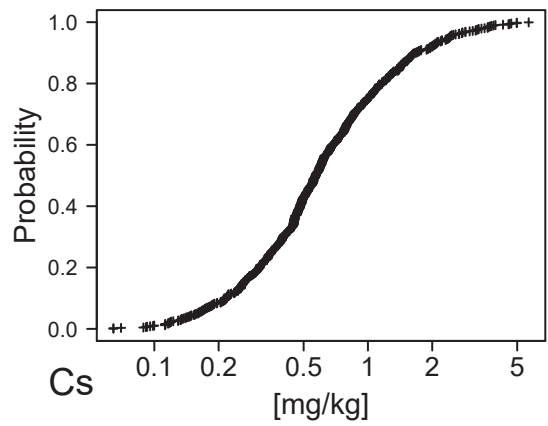
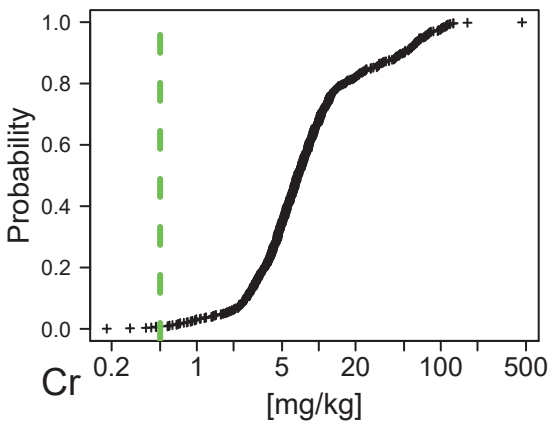
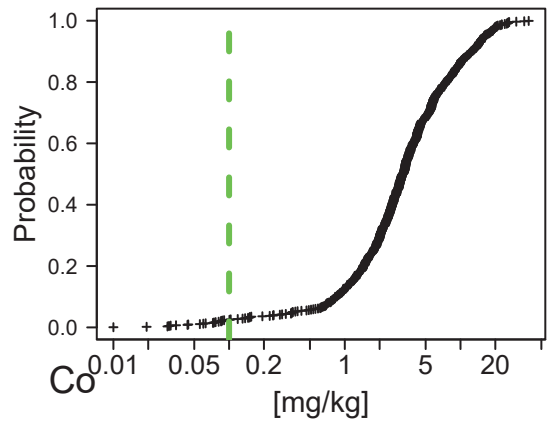
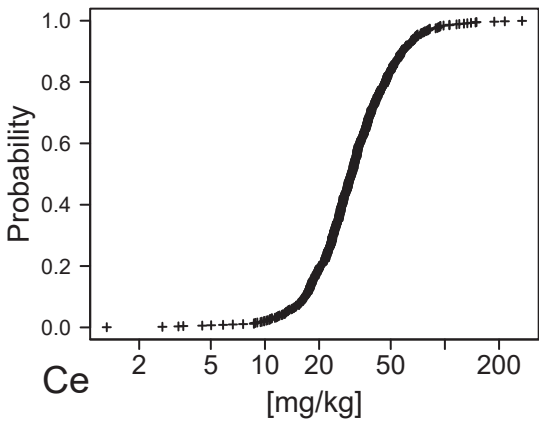
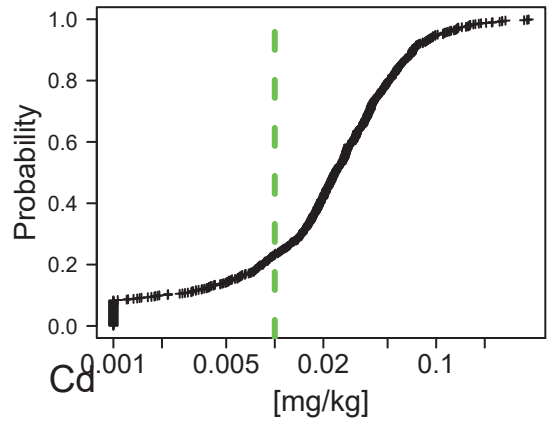
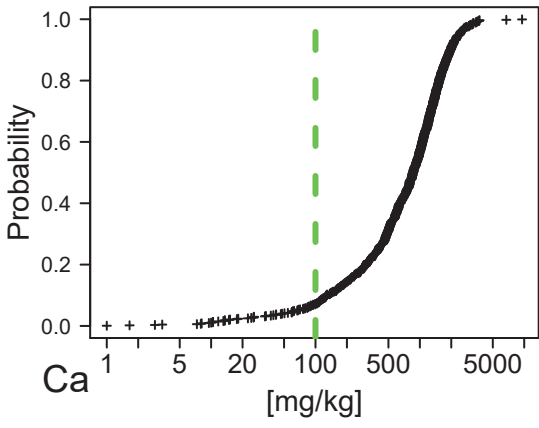


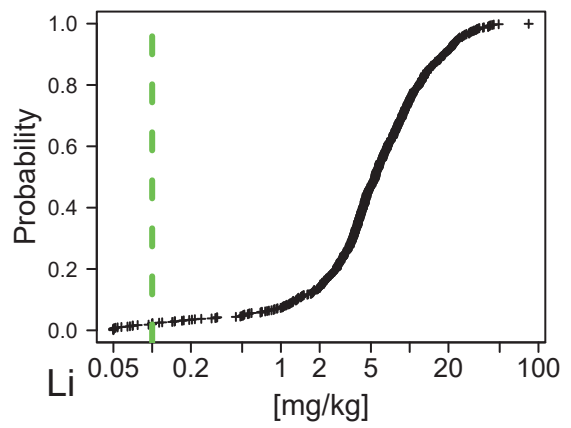
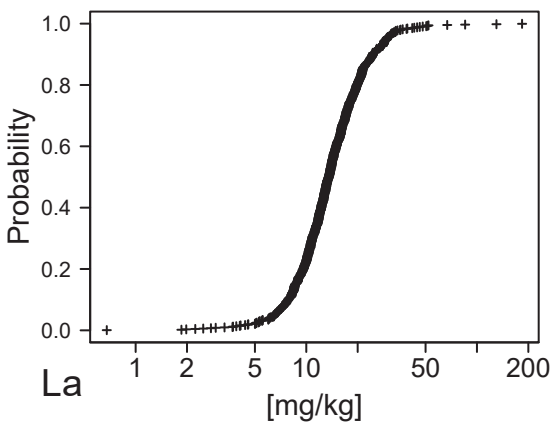
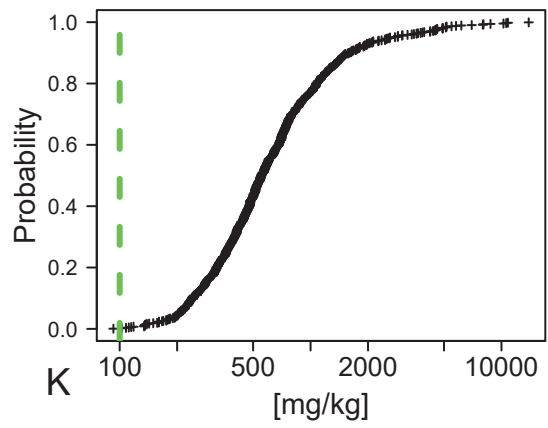
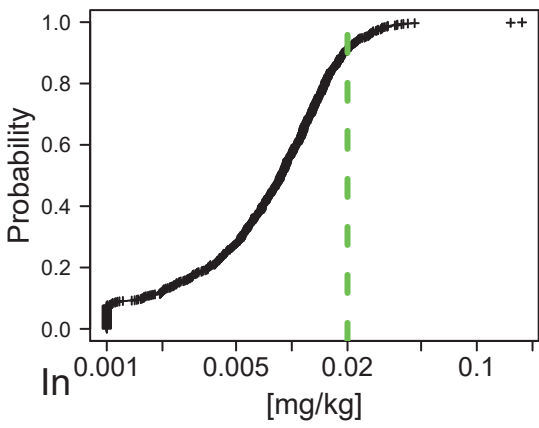
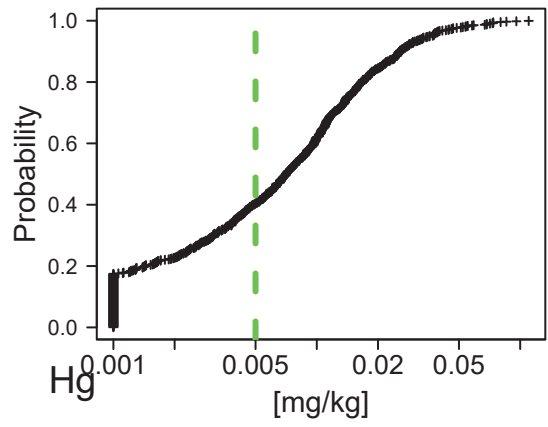
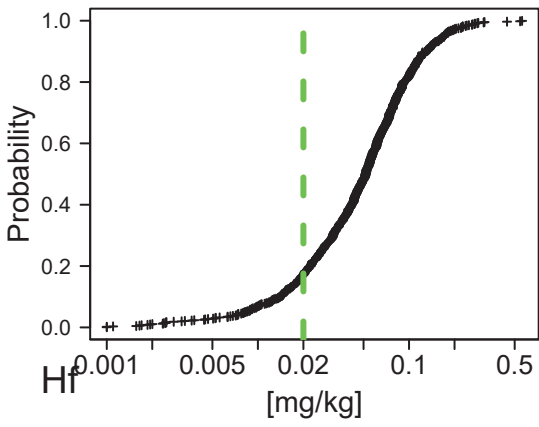
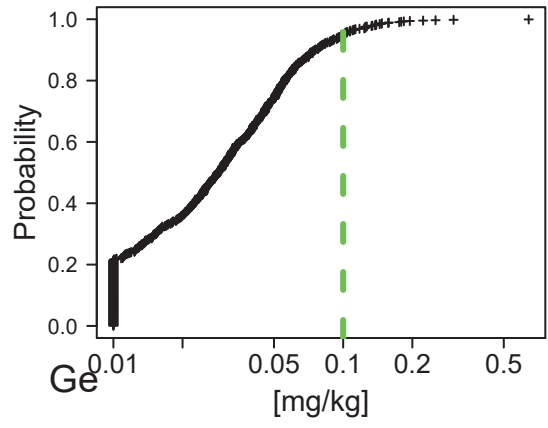
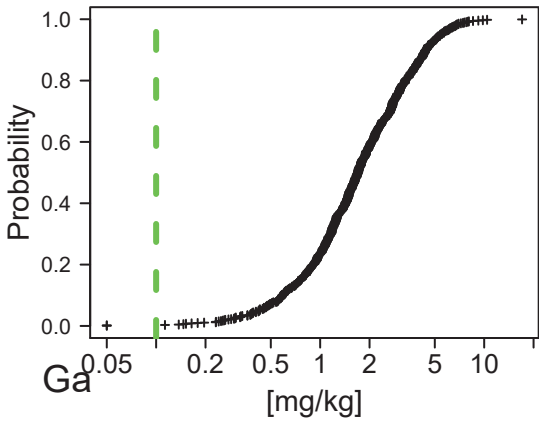
## APPENDIX 5: ECDF-PLOT

Plots of the empirical cumulative distribution function (ECDF-plots) for all 53 elements analysed and magnetic susceptibility. All laboratory readings are shown also those below detection limit, negative reading is however replaced by a low positive value. In some cases, the lowest positive value below DL given by the laboratory have been increased to improve the readability of the ECDF above DL.

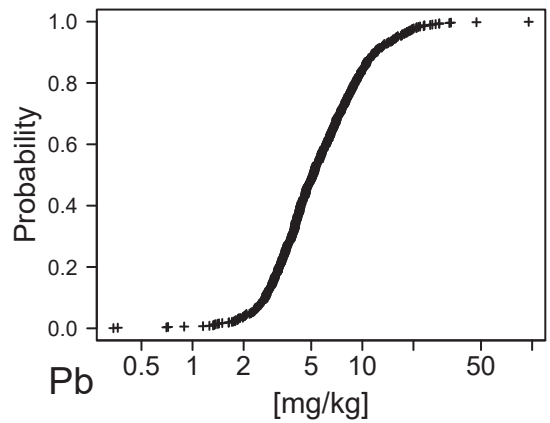
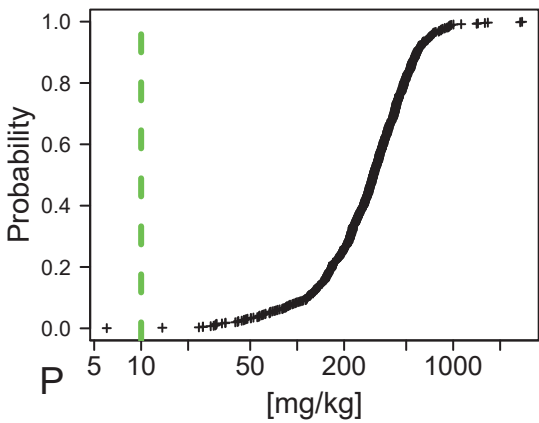
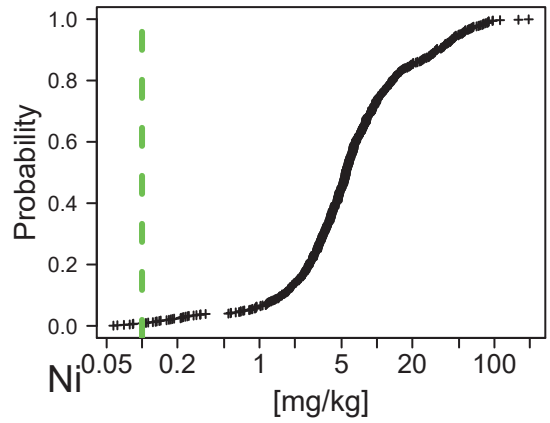
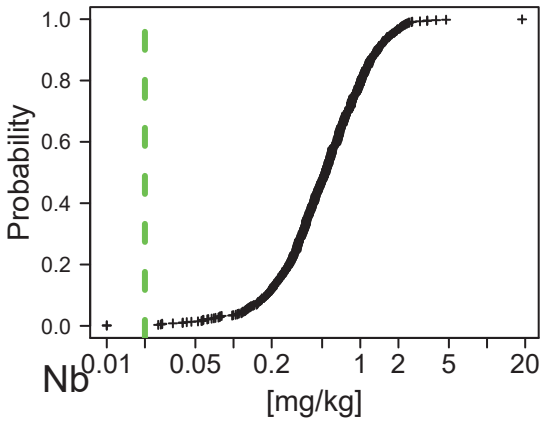
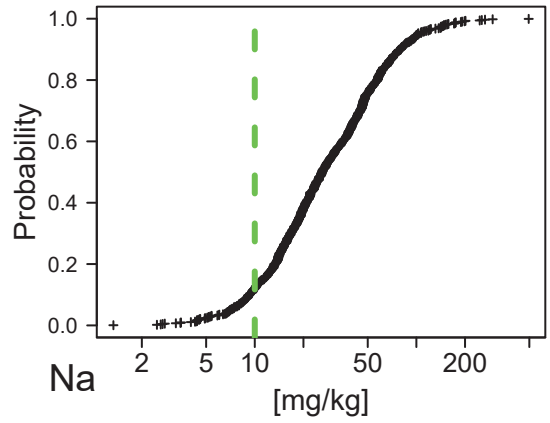
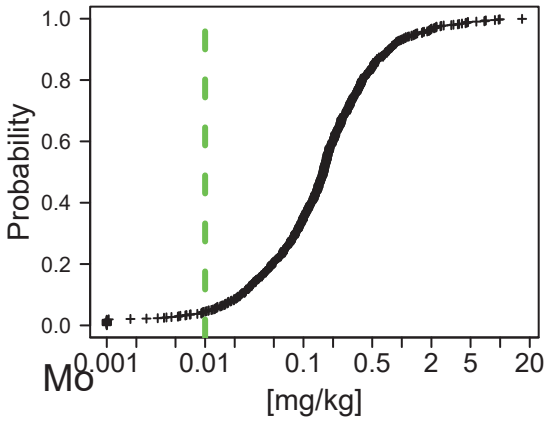
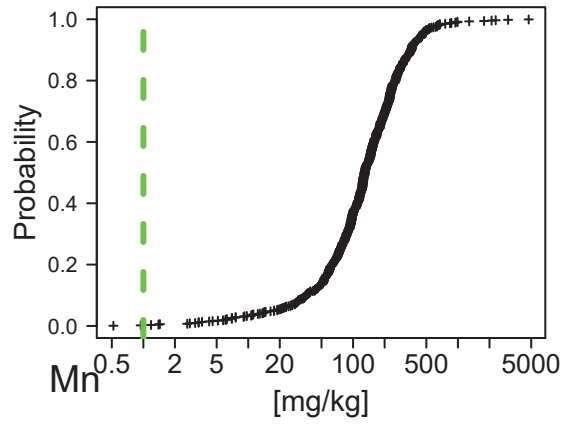
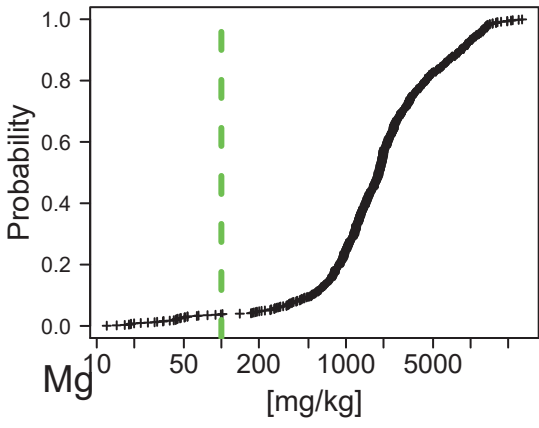
The laboratory detection limit (DL) is indicated by a green dotted line for elements showing concentrations values close to and/or below DL.

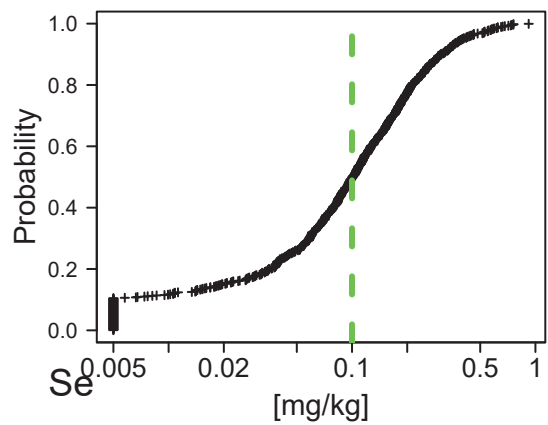
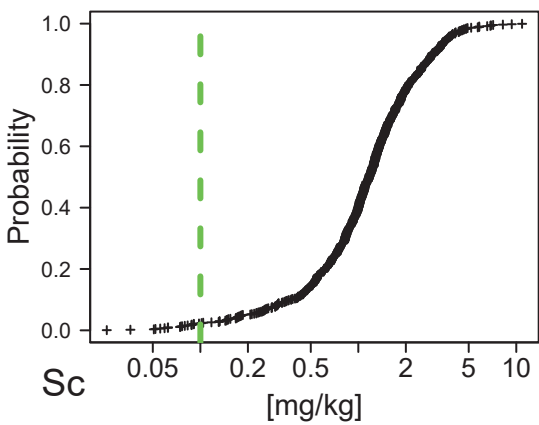
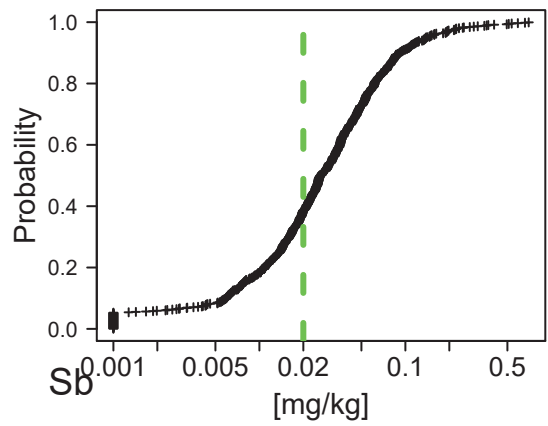
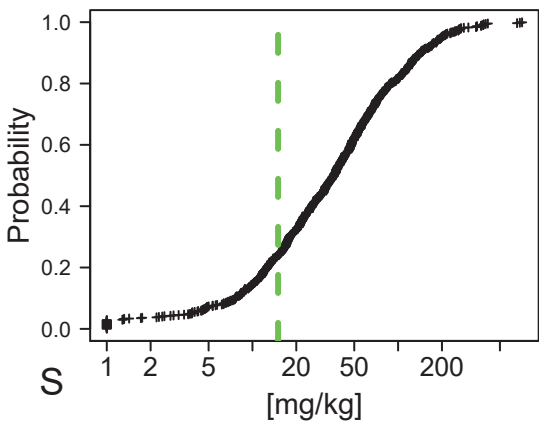
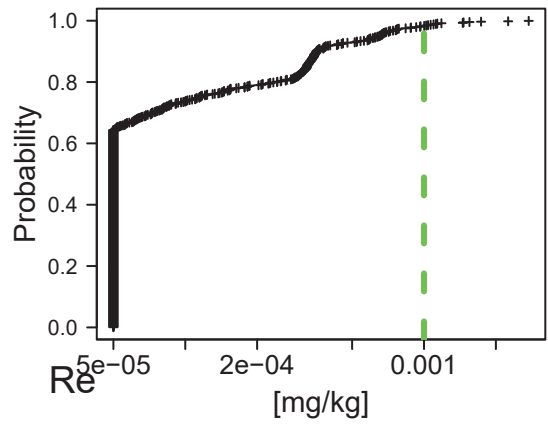
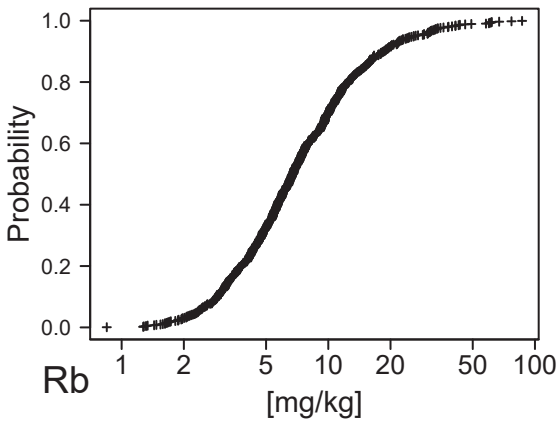
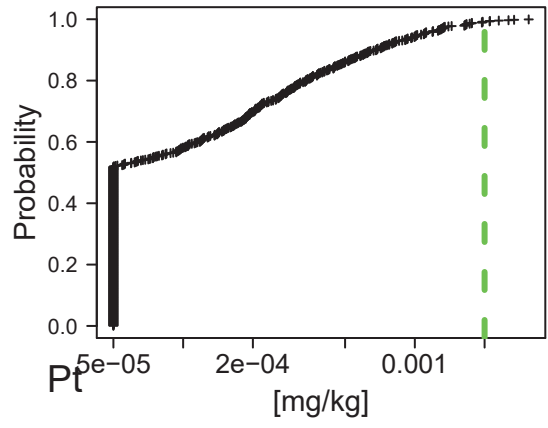
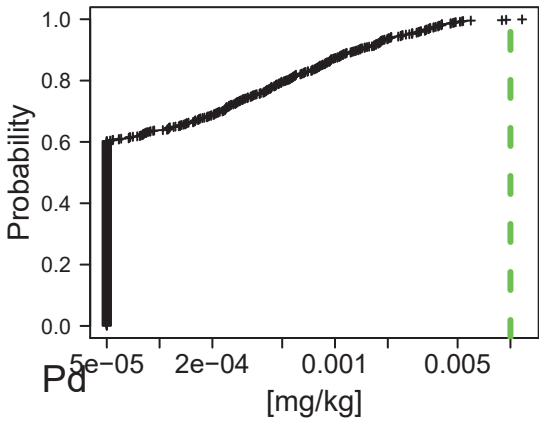


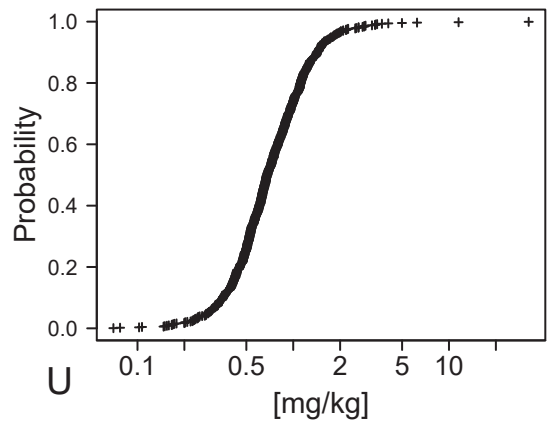
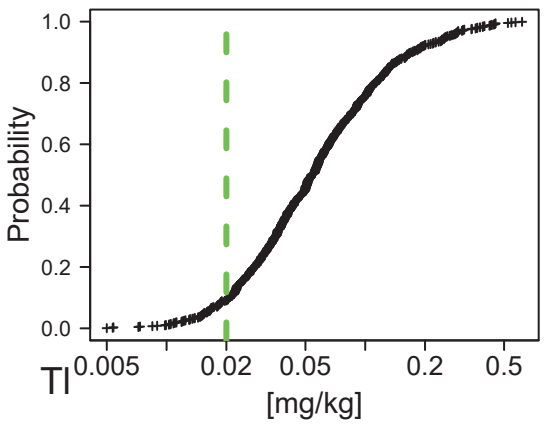
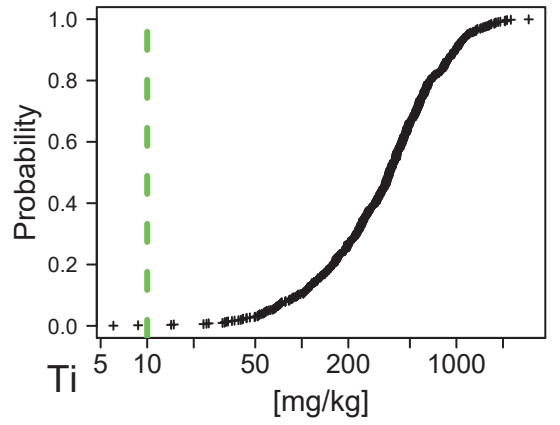
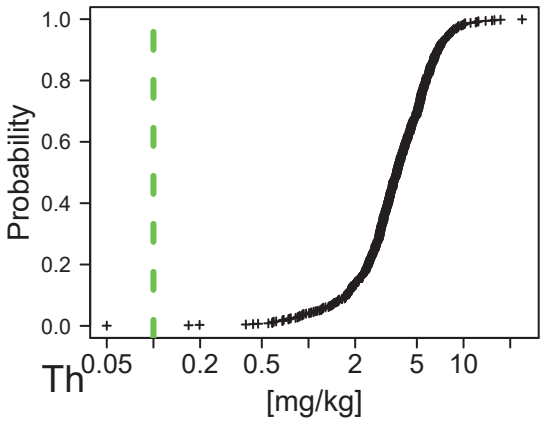
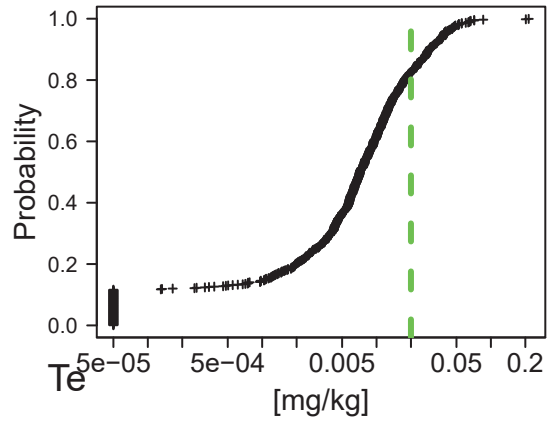
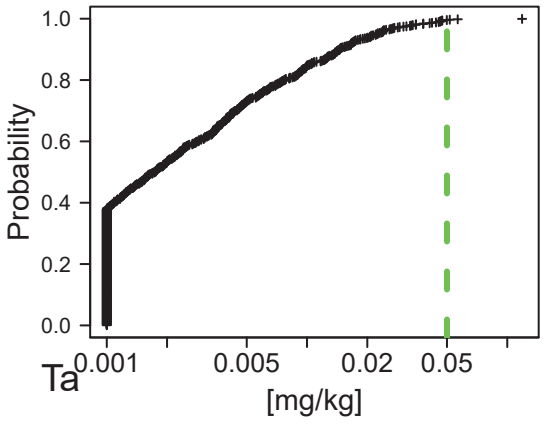
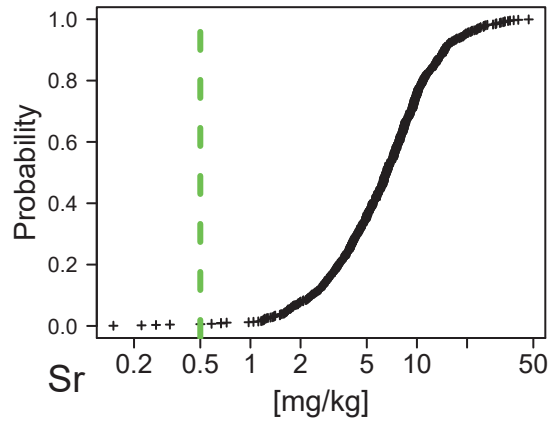
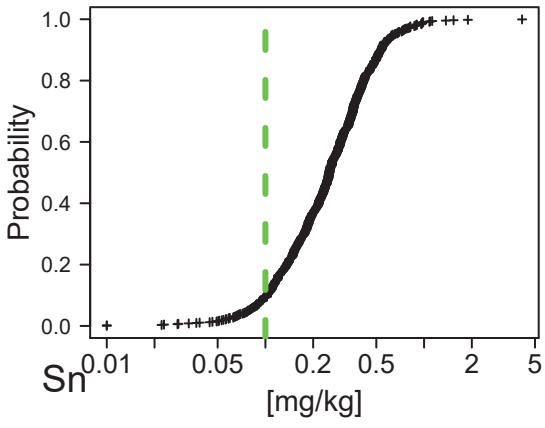


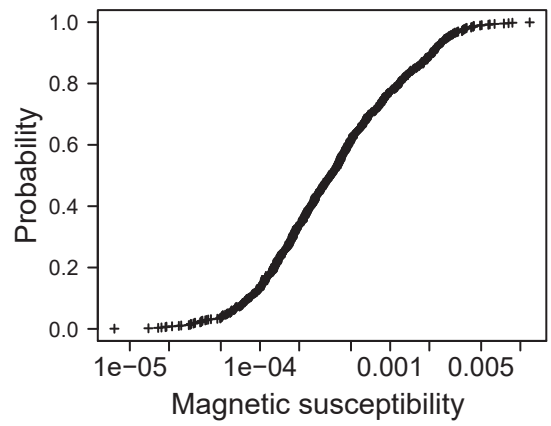
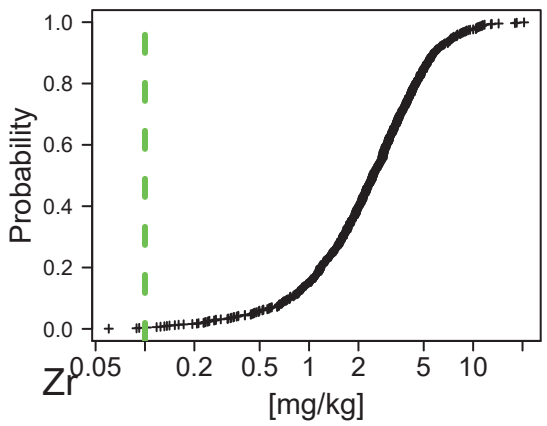
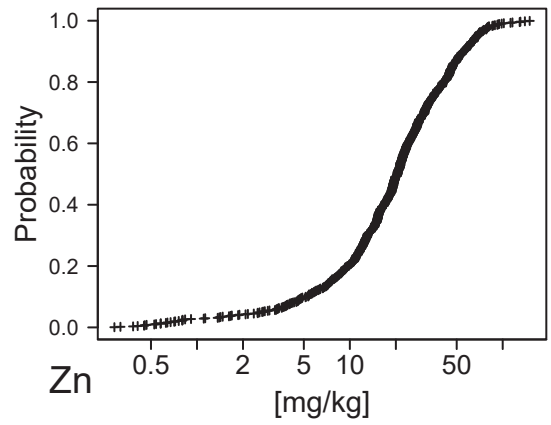
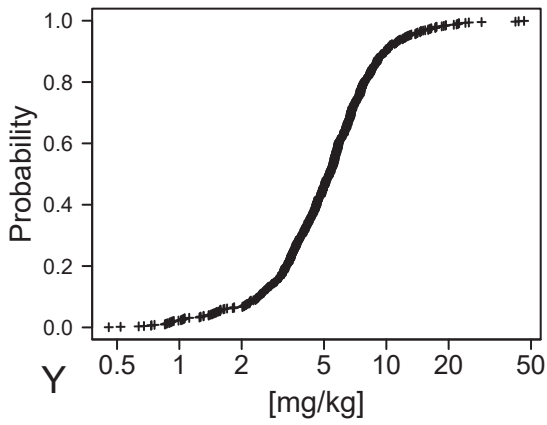
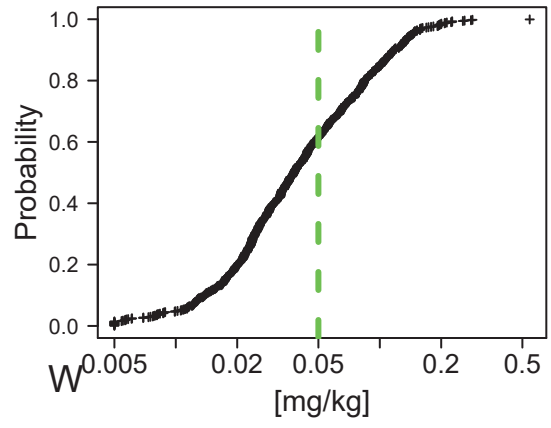
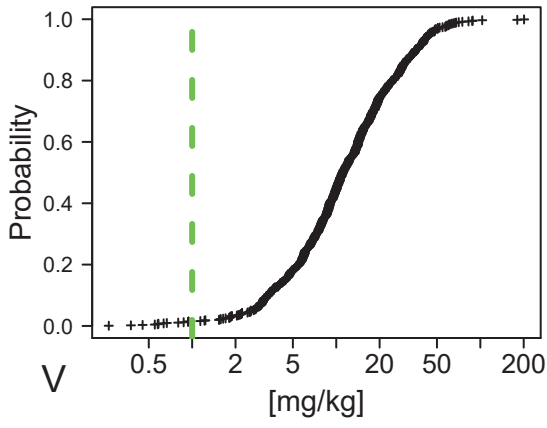












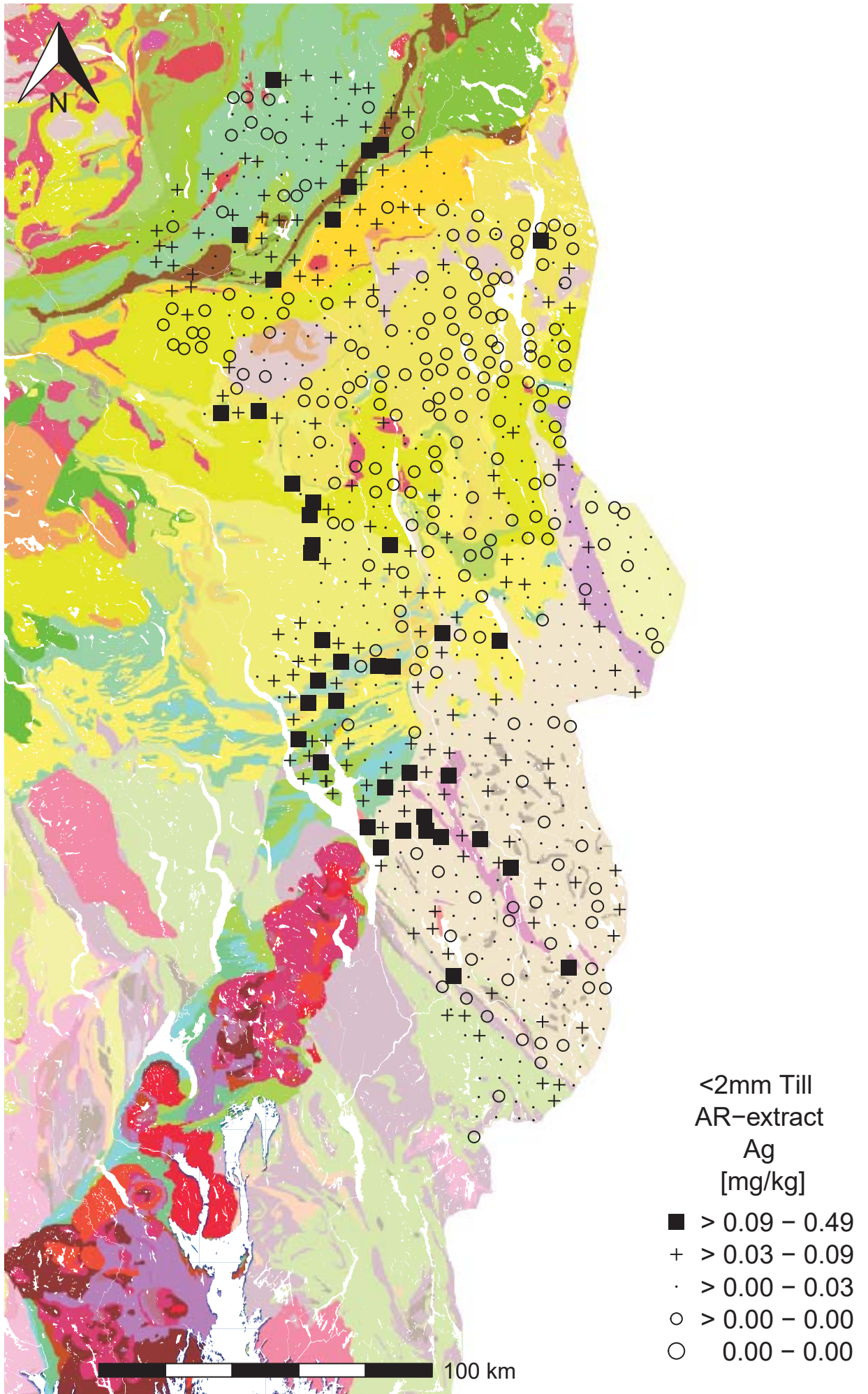
## APPENDIX 6: GEOCHEMICAL MAPS

Geochemical maps of the survey area for all elements, except Ge, Pd, Pt, Re, S and Ta due to poor data quality, and magnetic susceptibility plotted on top of bedrock map.

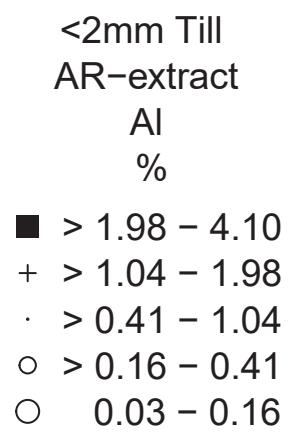
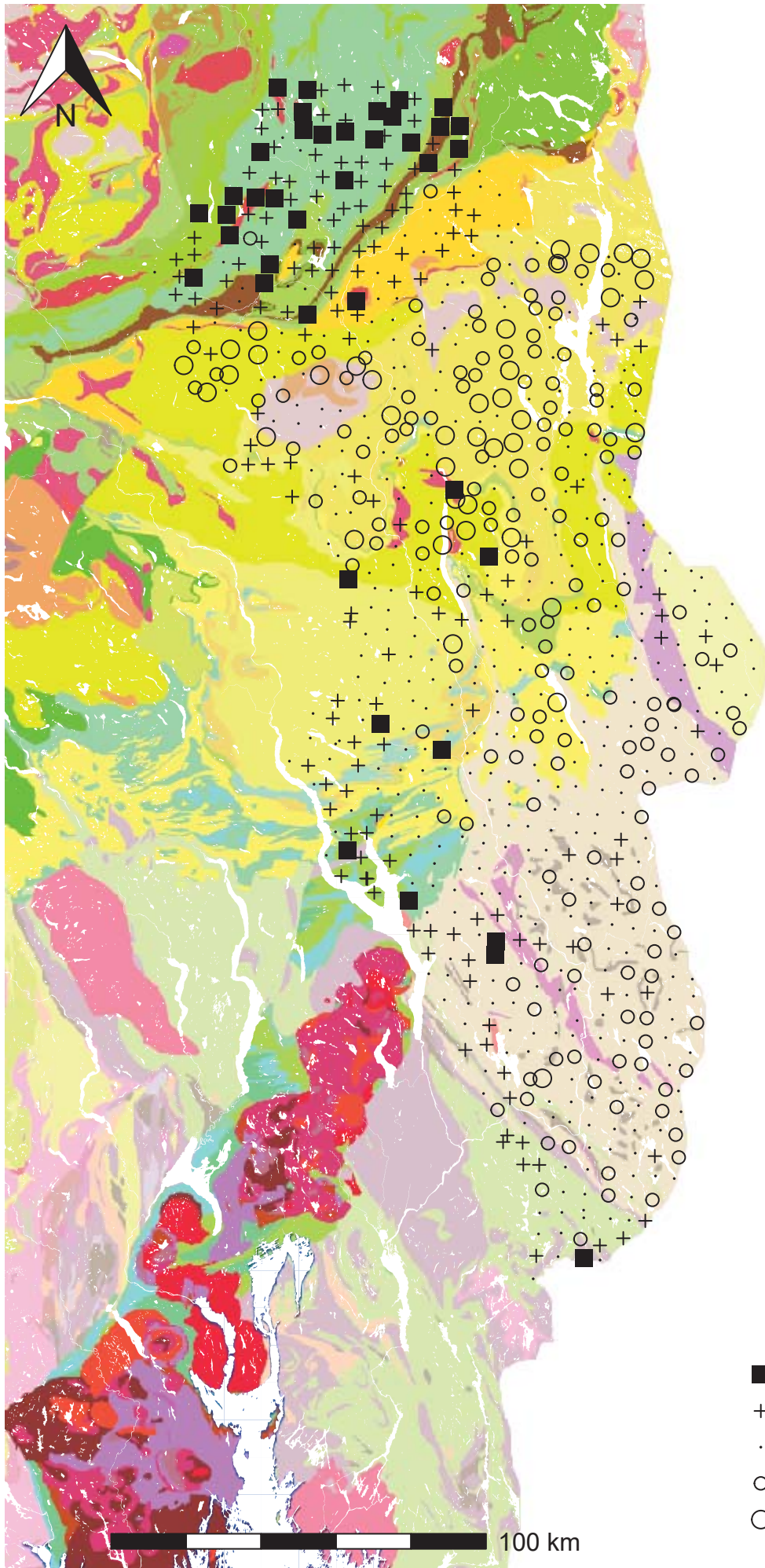
EDA map intervals: 0-5%, 5-25%, 25-75%, 75-95%, 95-100%.

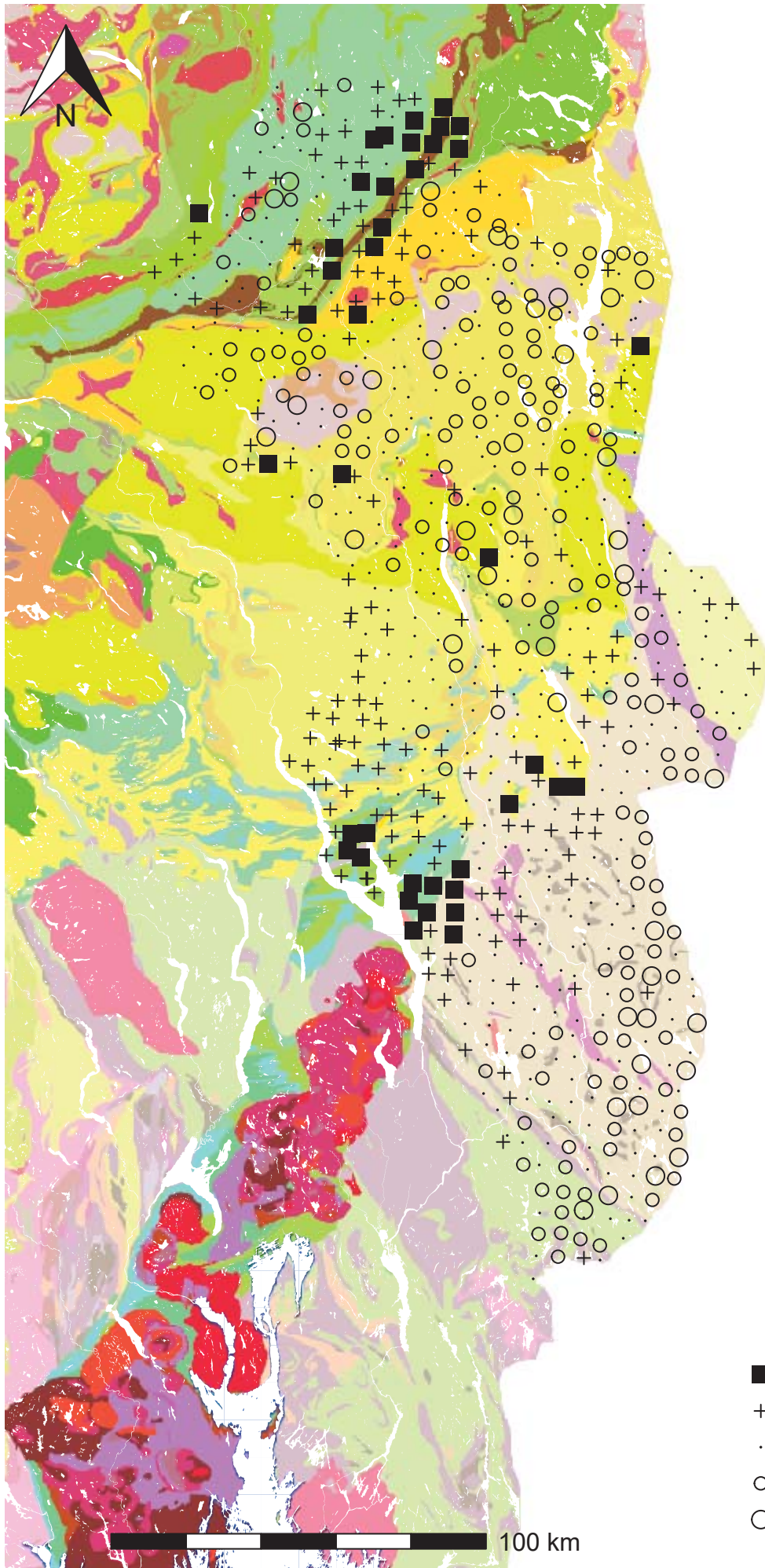
Bedrock map legend:

	Quartz alkali-feldspar syenite to nepheline syenite, in places porphyritic; 295–255 Ma
	Monzonite (larvikite), monzodiorite (kjelsåsite), in places syenite; 300–265 Ma
	Rhyolite and trachyte, in places ignimbrite, subordinate latite and basalt; 280–270 Ma
	Latite, porphyritic (rhomb porphyry), subordinate sedimentary rocks; 300–280 Ma
	Basalt; 300–295 Ma, and underlying sedimentary rocks; 320–295 Ma
	Gabbro, diorite, tonalite, ultramafic rocks and granite; 440–430 Ma
	Metabasalt, subordinate felsic volcanic rocks, conglomerate and breccia; 475–460 Ma
	Metabasalt and metagabbro, subordinate ultramafic rocks, in places felsic rocks; 500–475 Ma
	Metabasalt, subordinate intermediate and felsic volcanic rocks; antatt 1000–420 Ma
	Calcareous mica schist, calc-silicate schist and amphibole schist, subordinate marble; antatt 1000–420 Ma
	Metagabbro and metamonzonite, orthopyroxene-bearing; 1660–1230 Ma
	Mica schist and phyllite, subordinate peridotite and serpentinite; 500–470 Ma
	Metabasalt, subordinate serpentinite and soapstone; 500–470 Ma
	Mica gneiss and mica schist, subordinate marble and amphibolite; 1000–900 Ma or younger
	Amphibolite and gabbro, in places anorthosite and ultramafic rocks; 1670–420 Ma
	Granitic to tonalitic gneiss, in places mylonitic; north: 2850–1600 Ma, south: 1660–940 Ma
	Limestone and slate (lower part), sandstone and conglomerate (upper part); 440–420 Ma
	Sandstone, subordinate conglomerate and phyllite; 470–440 Ma
	Limestone, slate, alum shale and sandstone, in places conglomerate; 540–470 Ma
	Tillite and slate; 630–580 Ma
	Limestone and slate; 650–600 Ma
	Sandstone alternating with shale, in places conglomerate; 750–600 Ma
	Metarhyolite and metadacite; 1680–1600 Ma
	Granitic to dioritic gneiss, in places augen gneiss, in places migmatitic; 1680–1600 Ma
	Quartzite, metasandstone and mica gneiss, subordinate amphibolite; 1520–1350 Ma
	Granitic to tonalitic gneiss, augen gneiss, in places migmatitic; 1520–1480 Ma
	Granitic to dioritic gneiss and mica gneiss, mainly banded; 1560–1000 Ma
	Mica gneiss, metagreywacke and amphibolite, in places migmatitic; 1740–1520 Ma
	Tonalitic to granitic and quartz-dioritic gneiss, in places migmatitic; 1660–1520 Ma
	Metarhyolite and metatuff; 1740–1660 Ma
	Granitic to monzonitic and granodioritic gneiss, subordinate augen gneiss; 1740–1660 Ma
	Sandstone, subordinate basalt and dolerite; 1580–1260 Ma

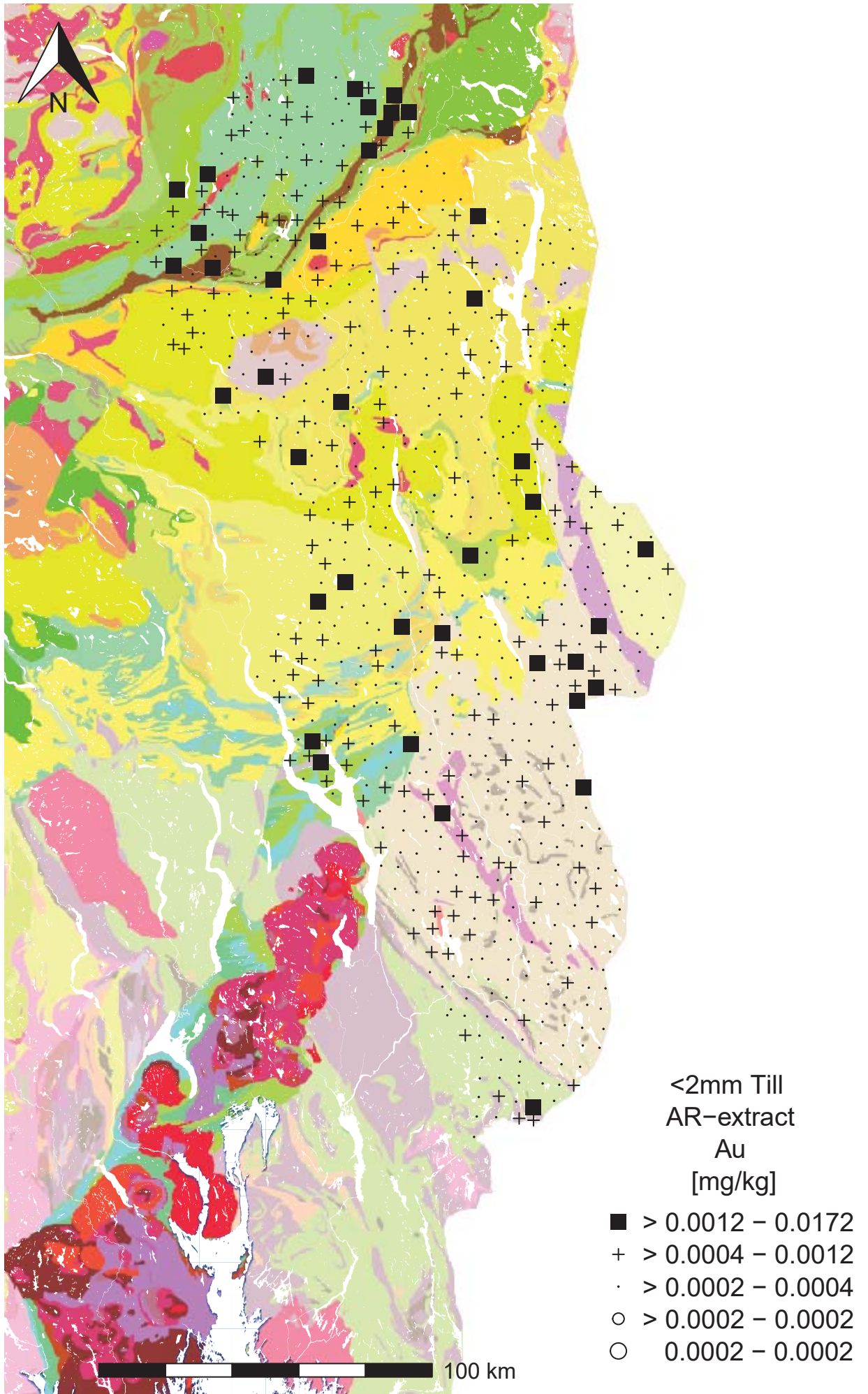


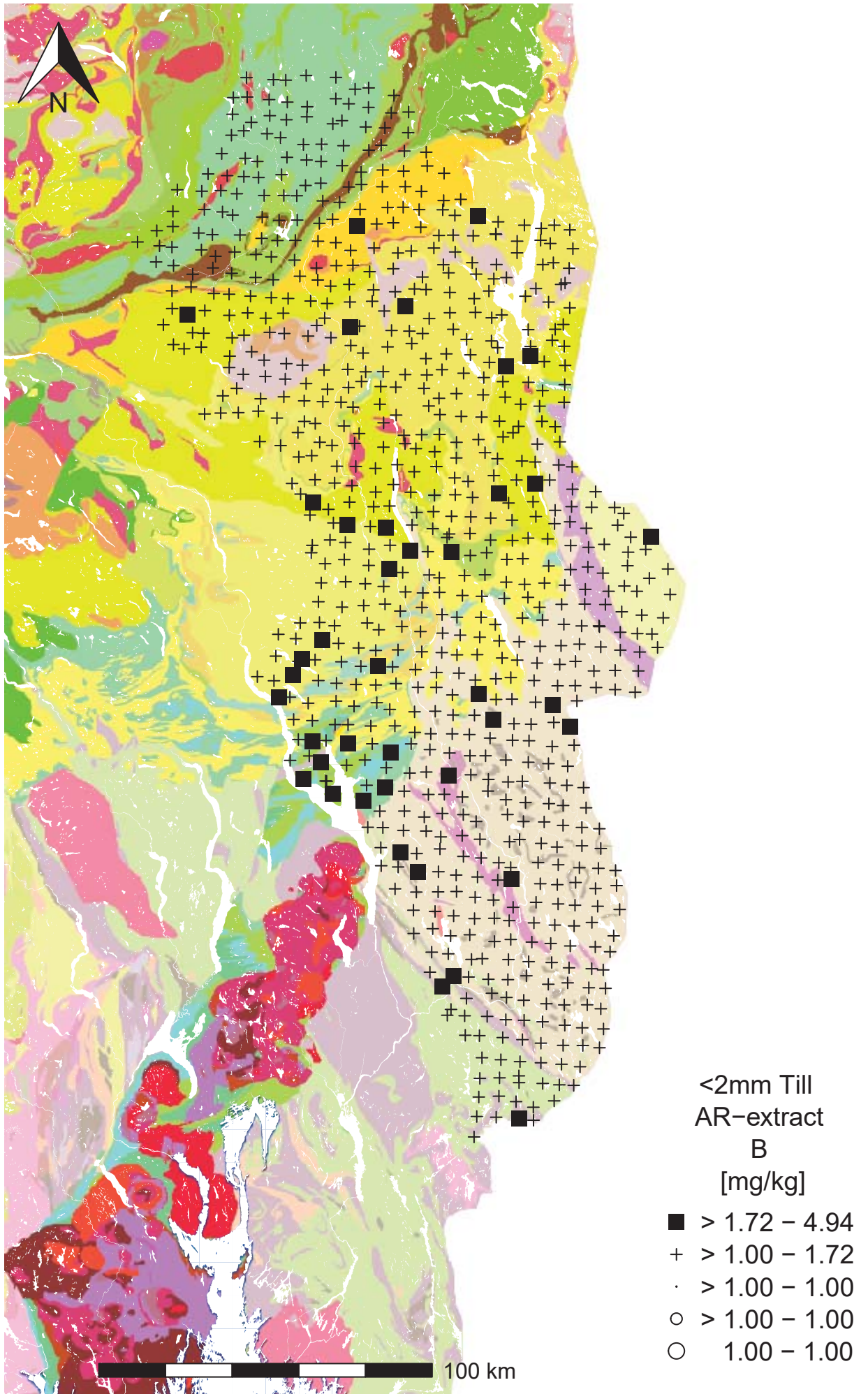




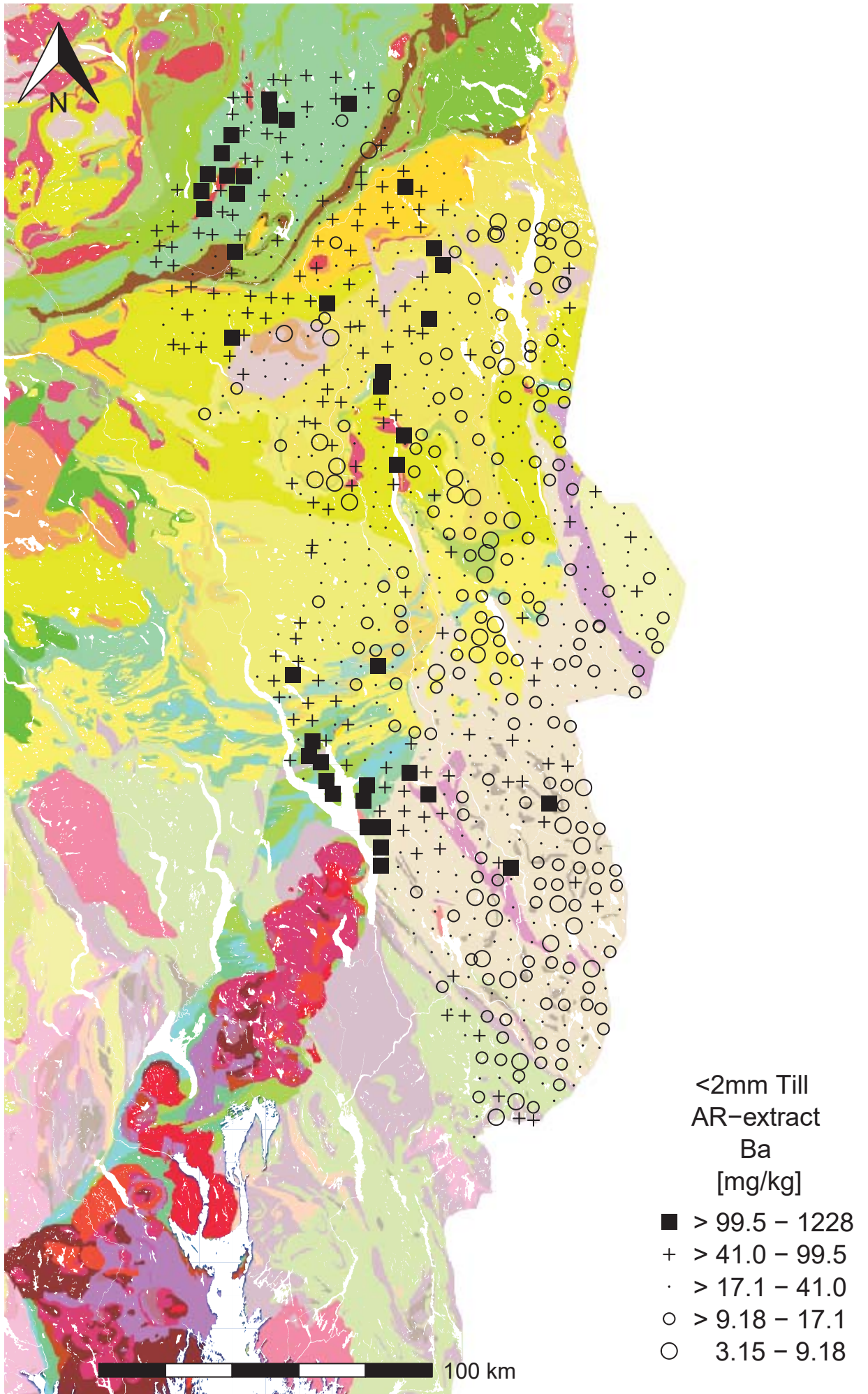


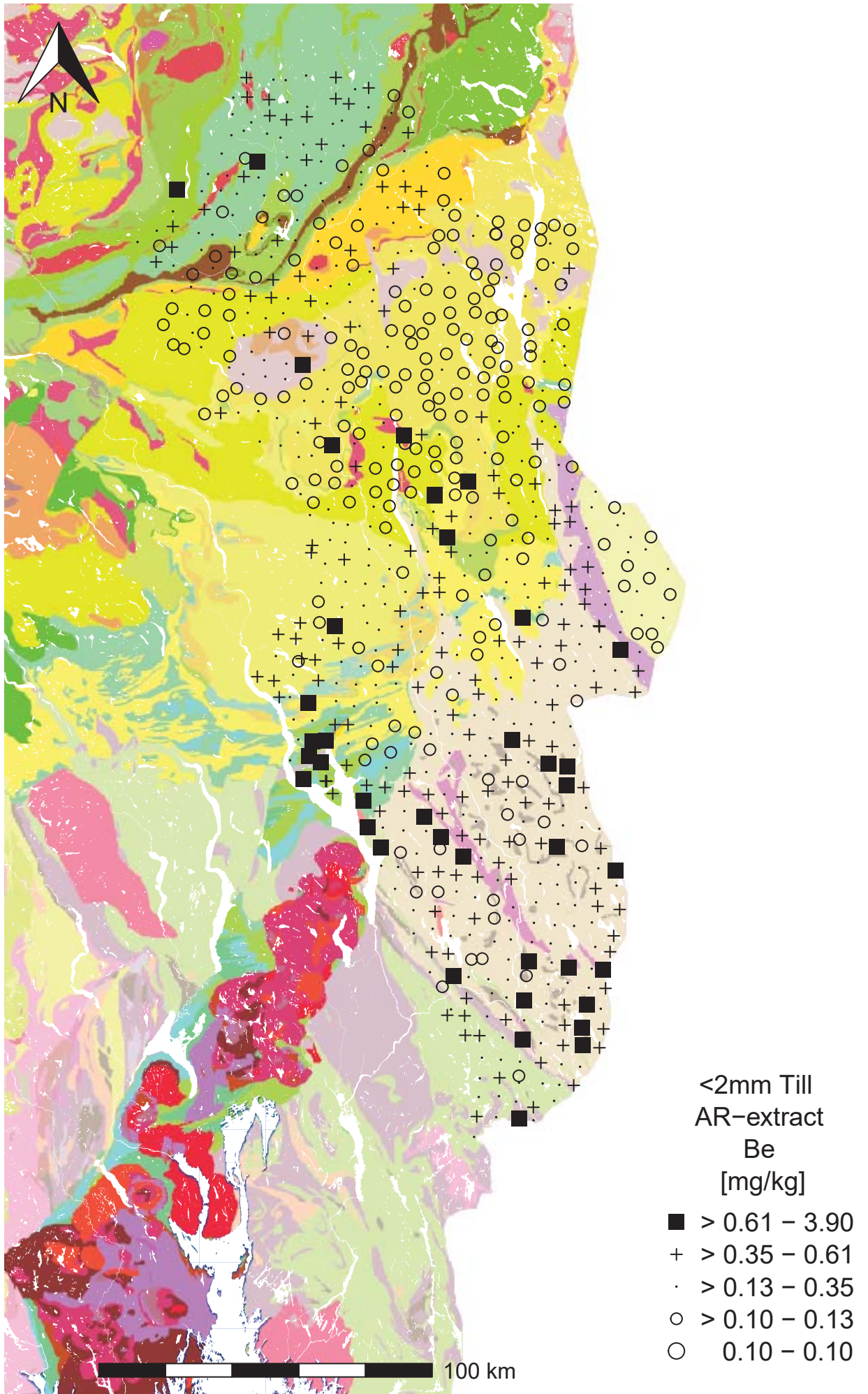




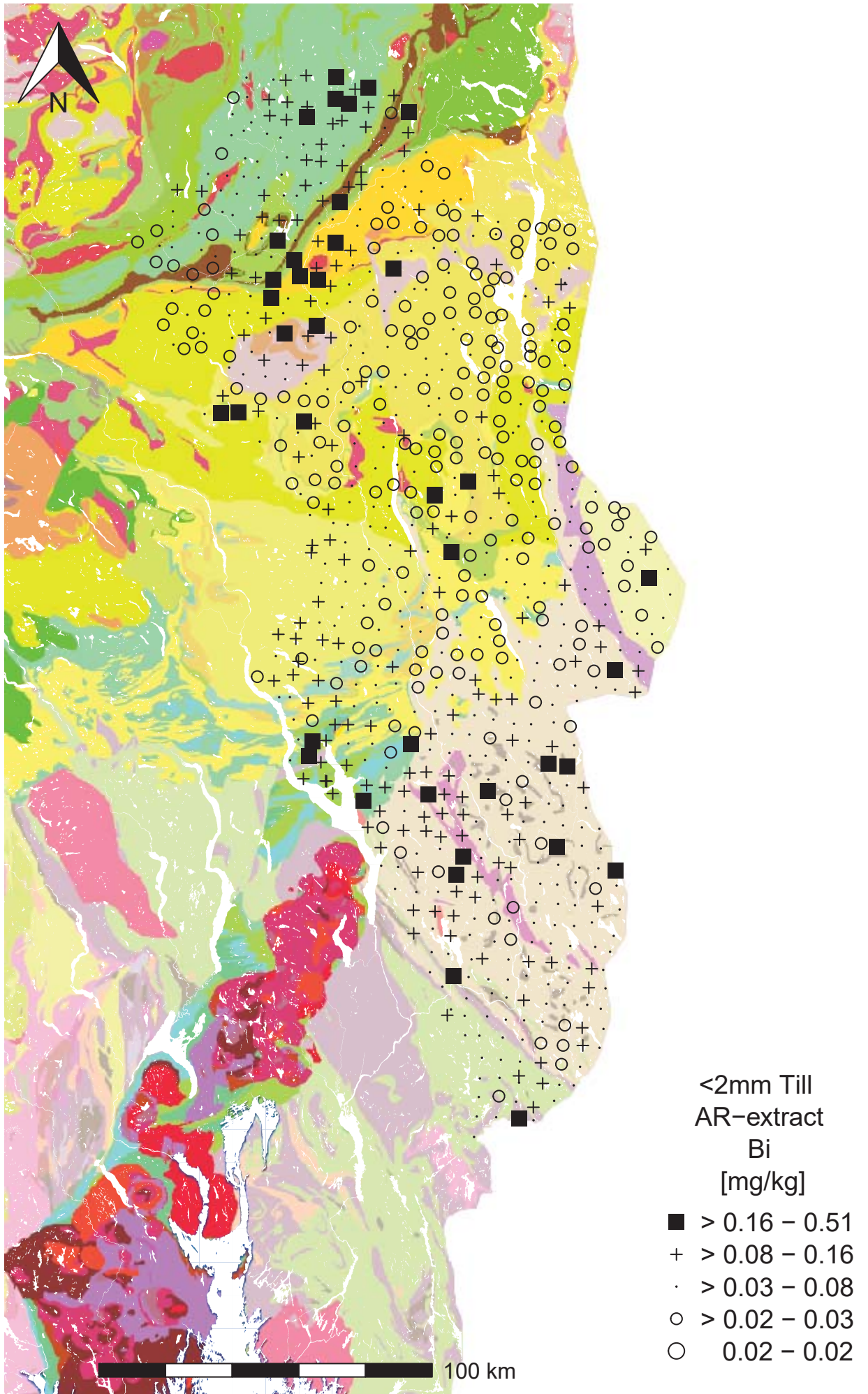


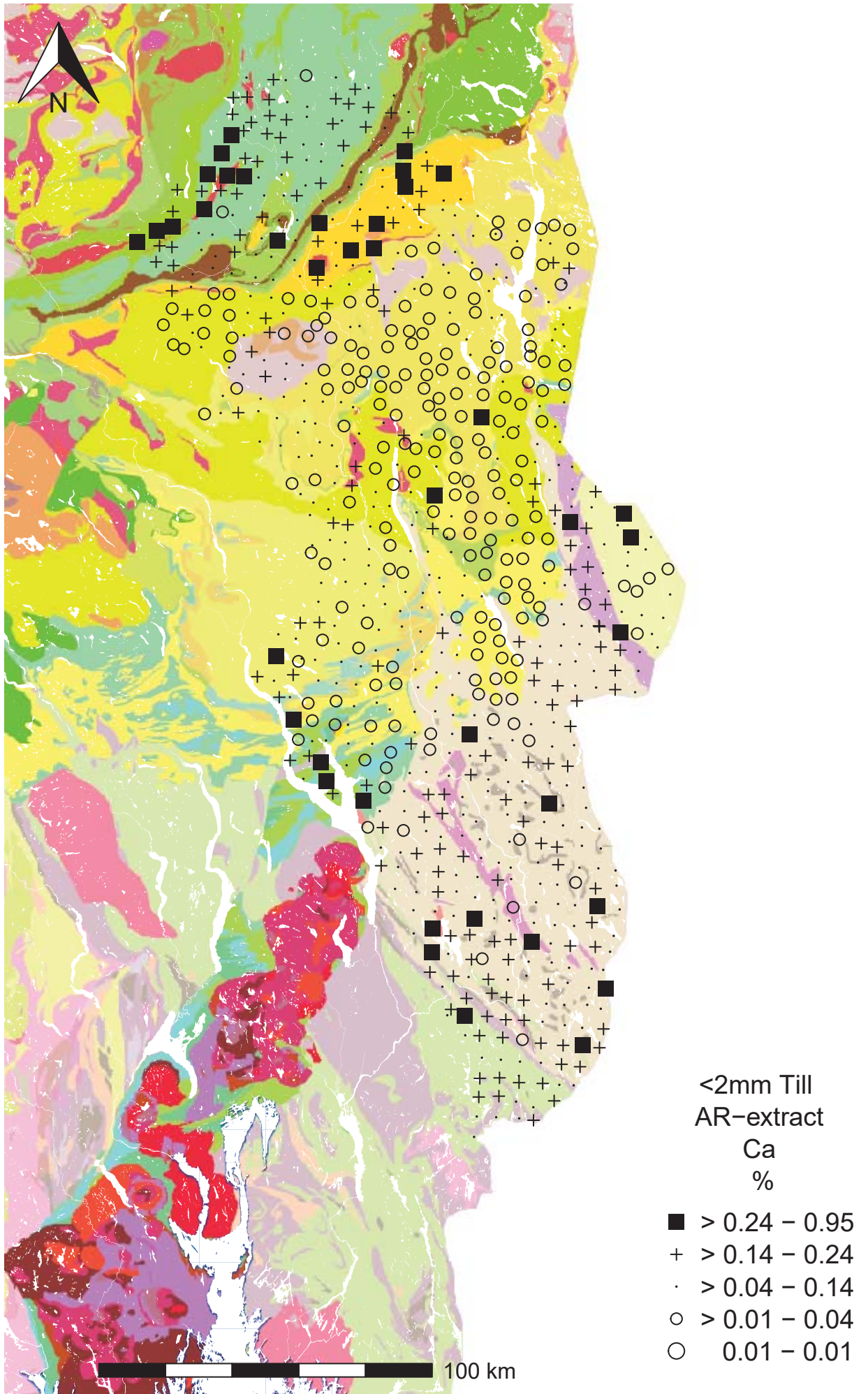




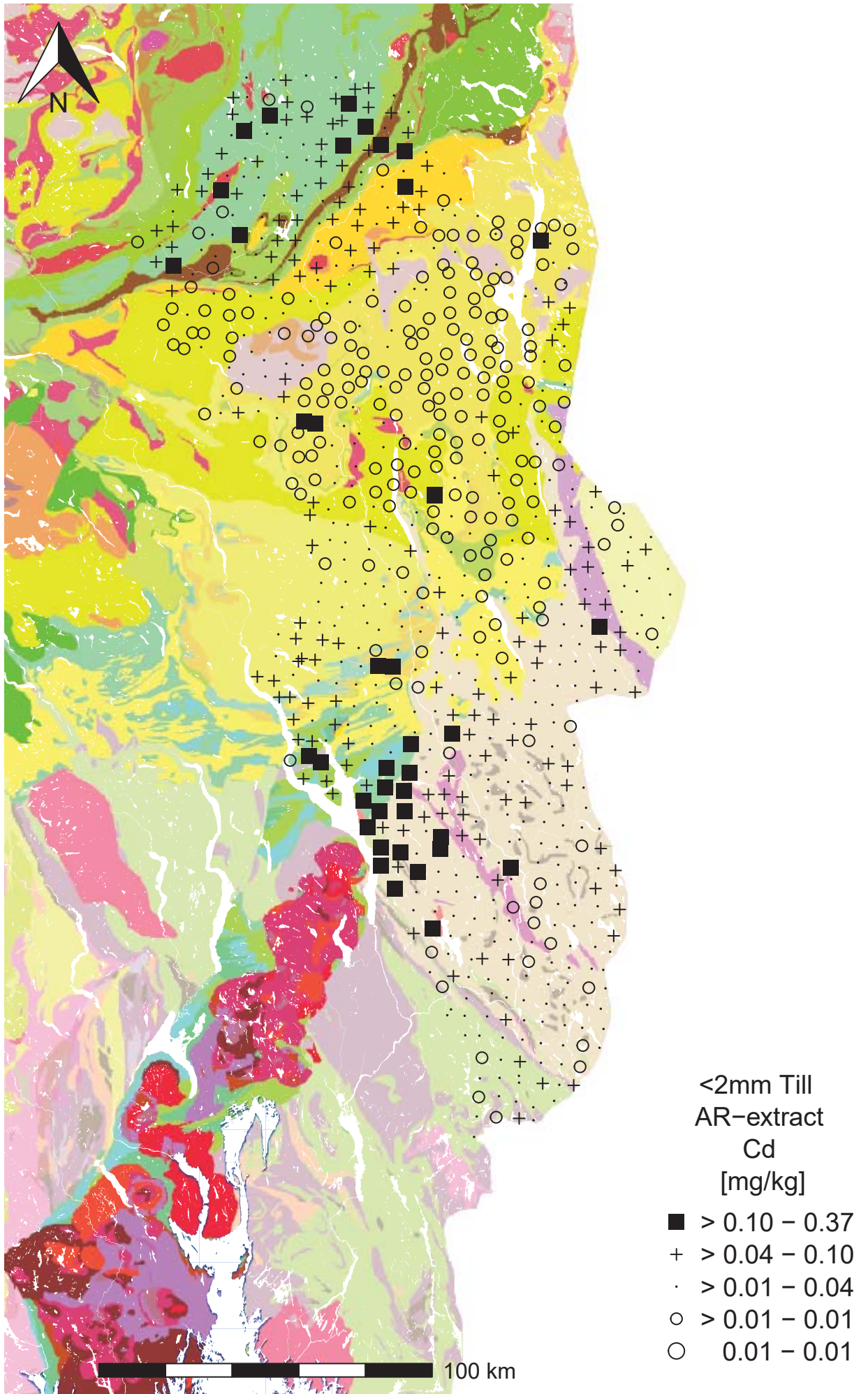


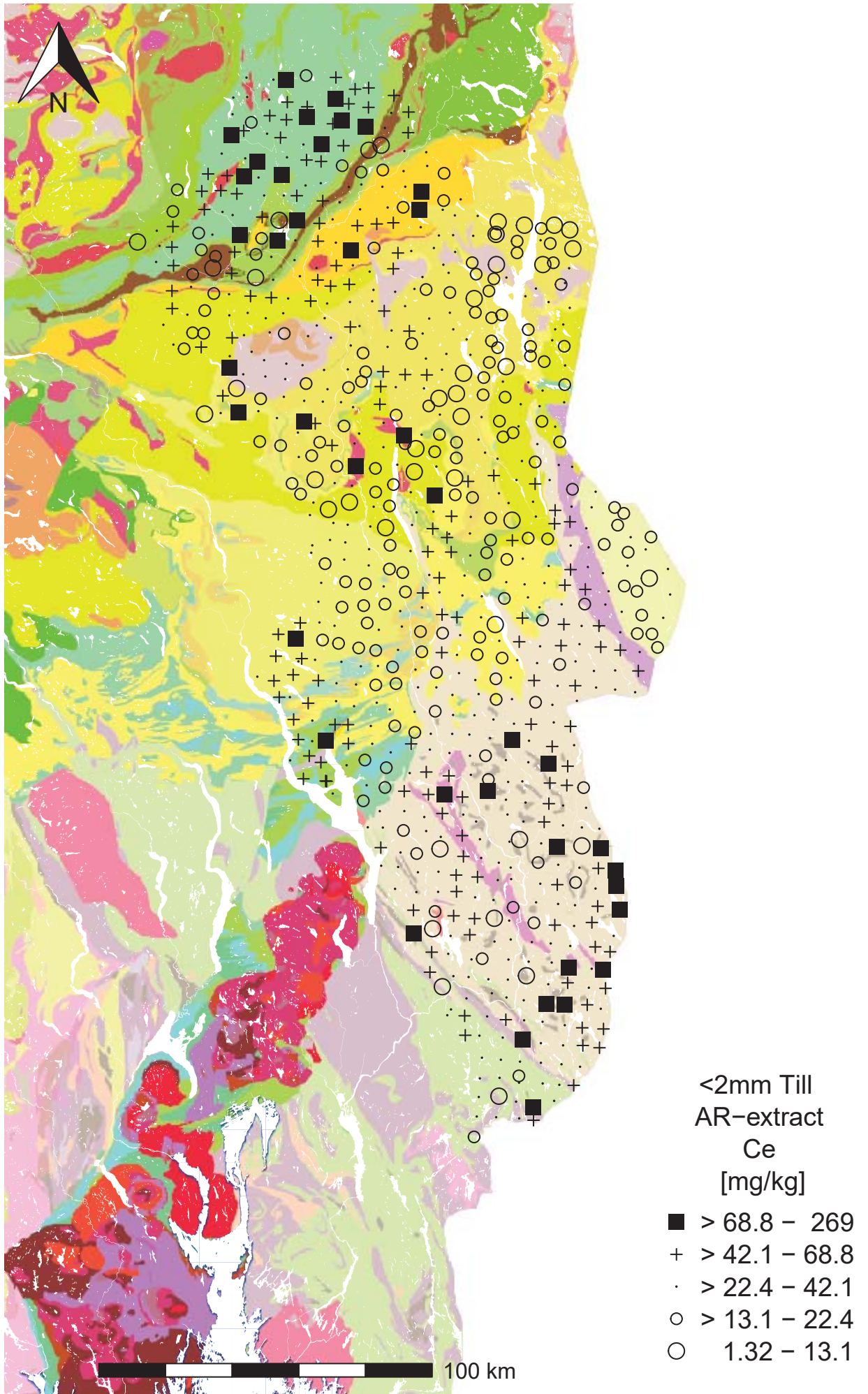




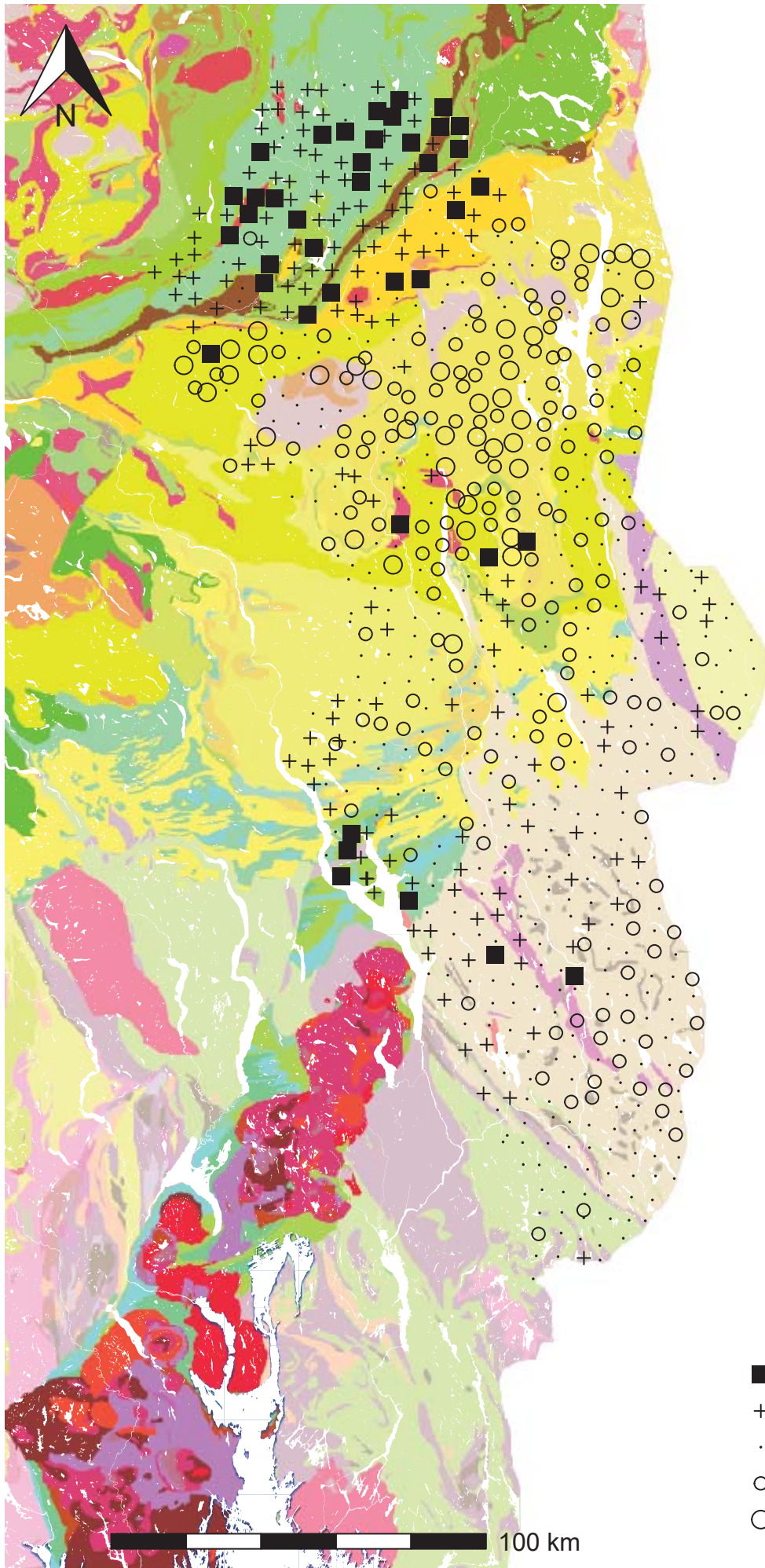


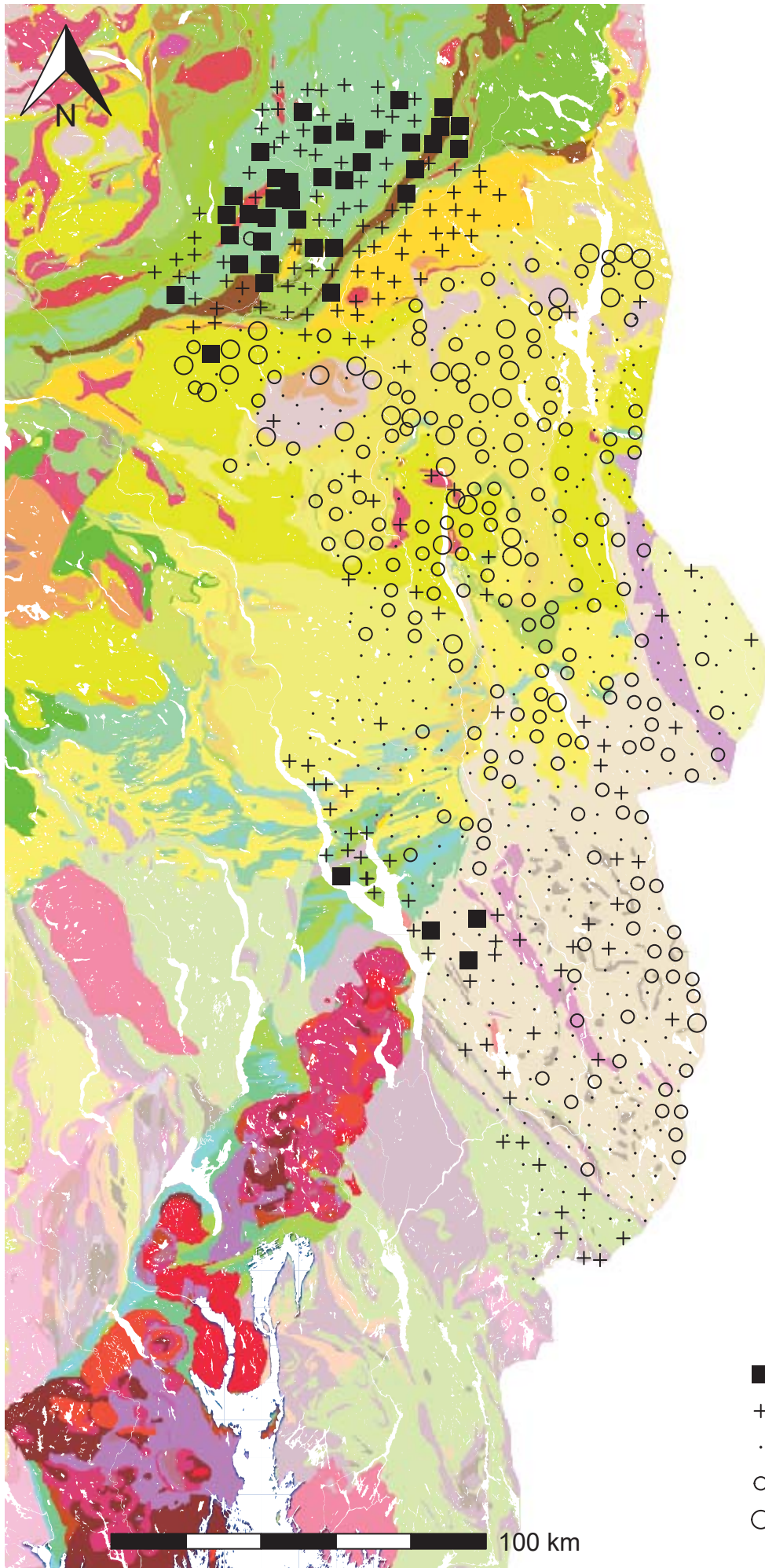




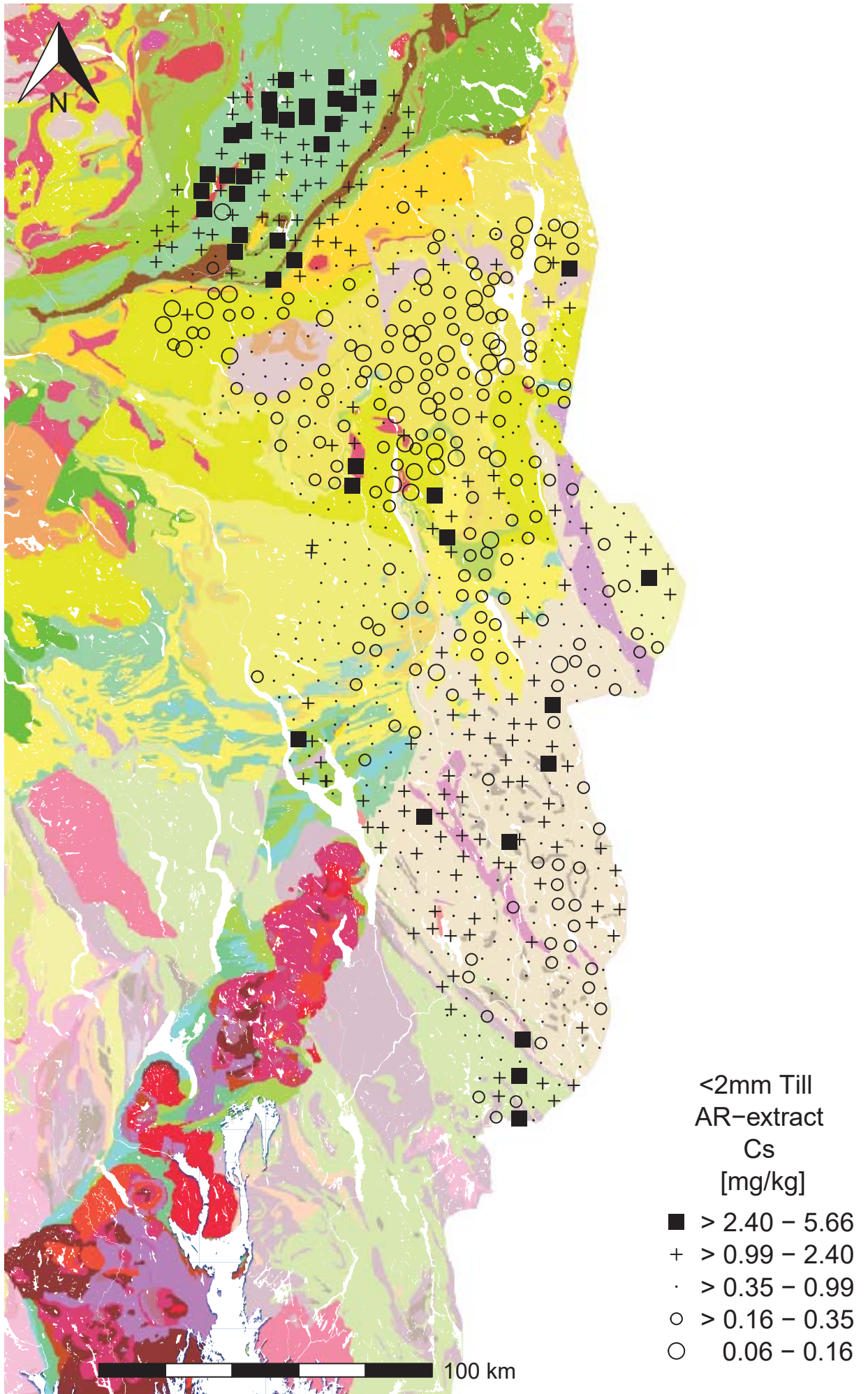


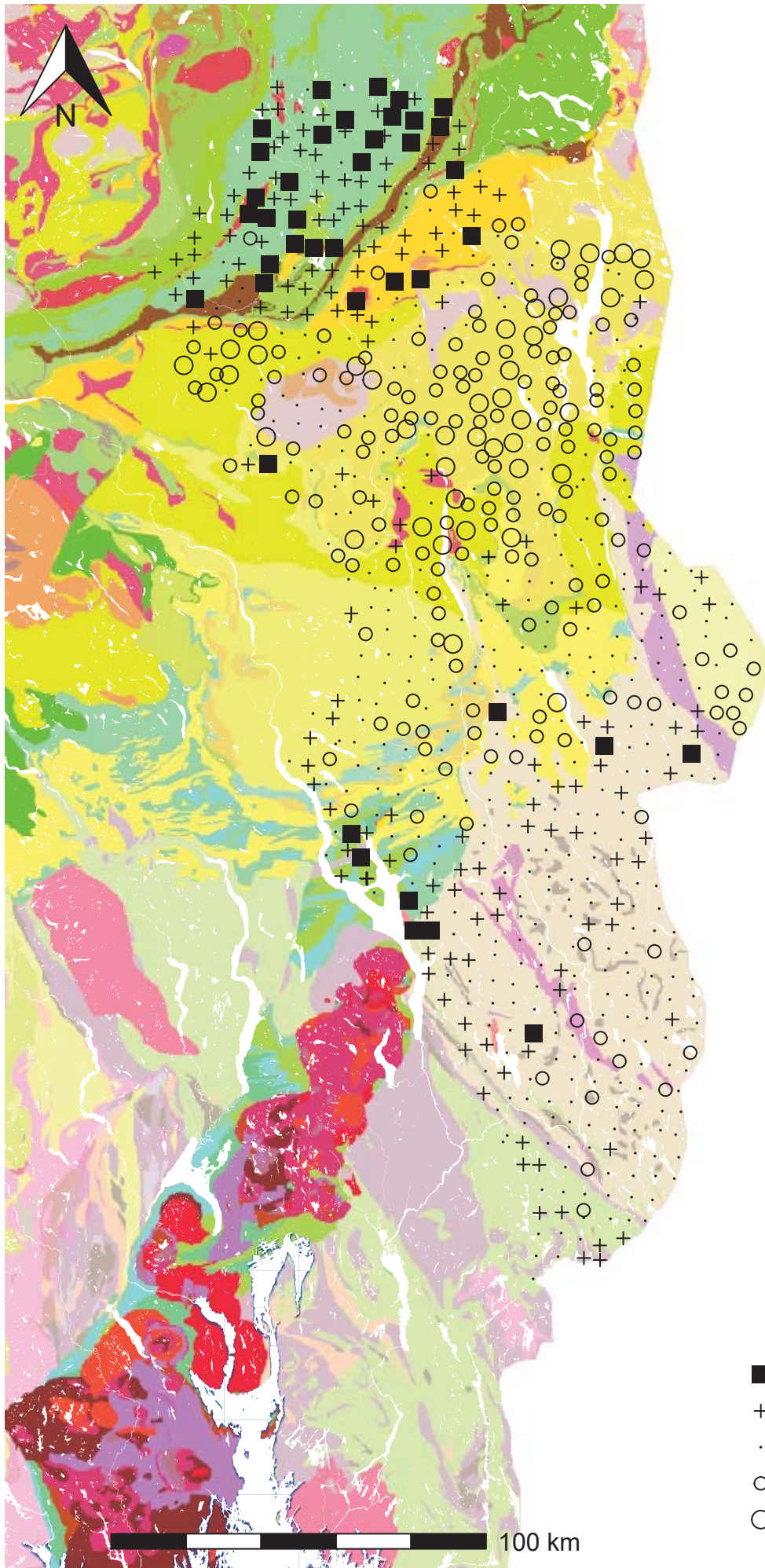




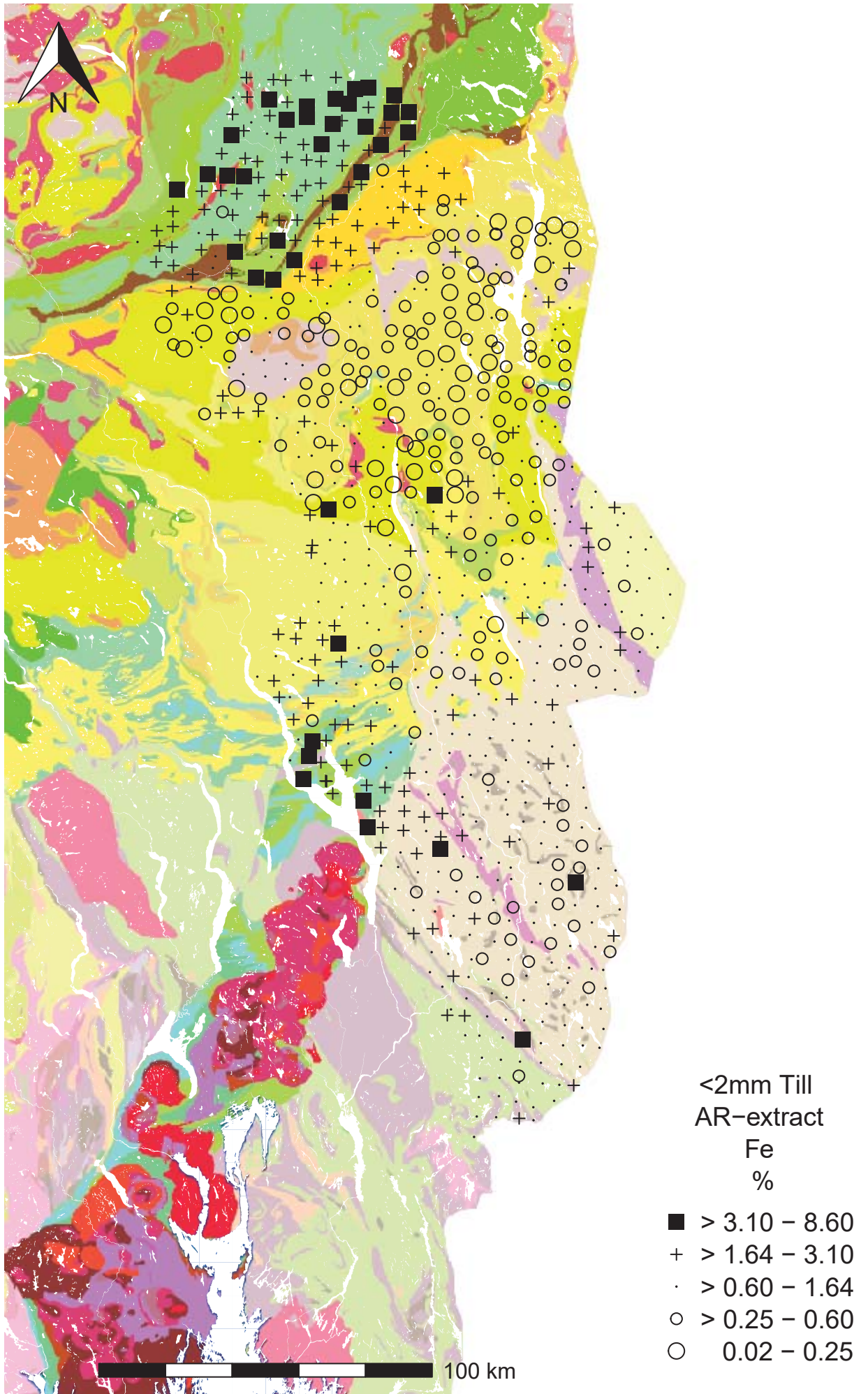


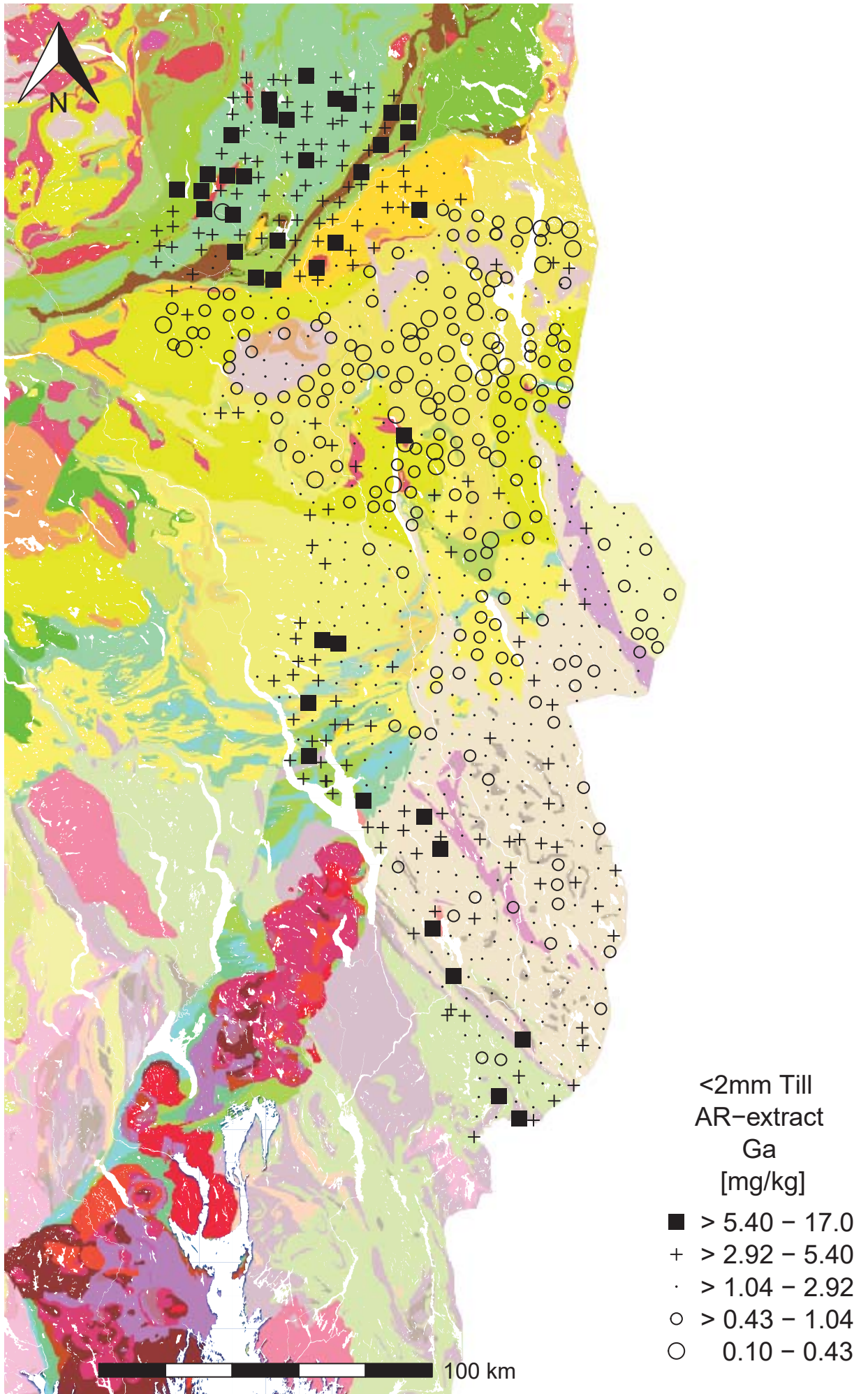




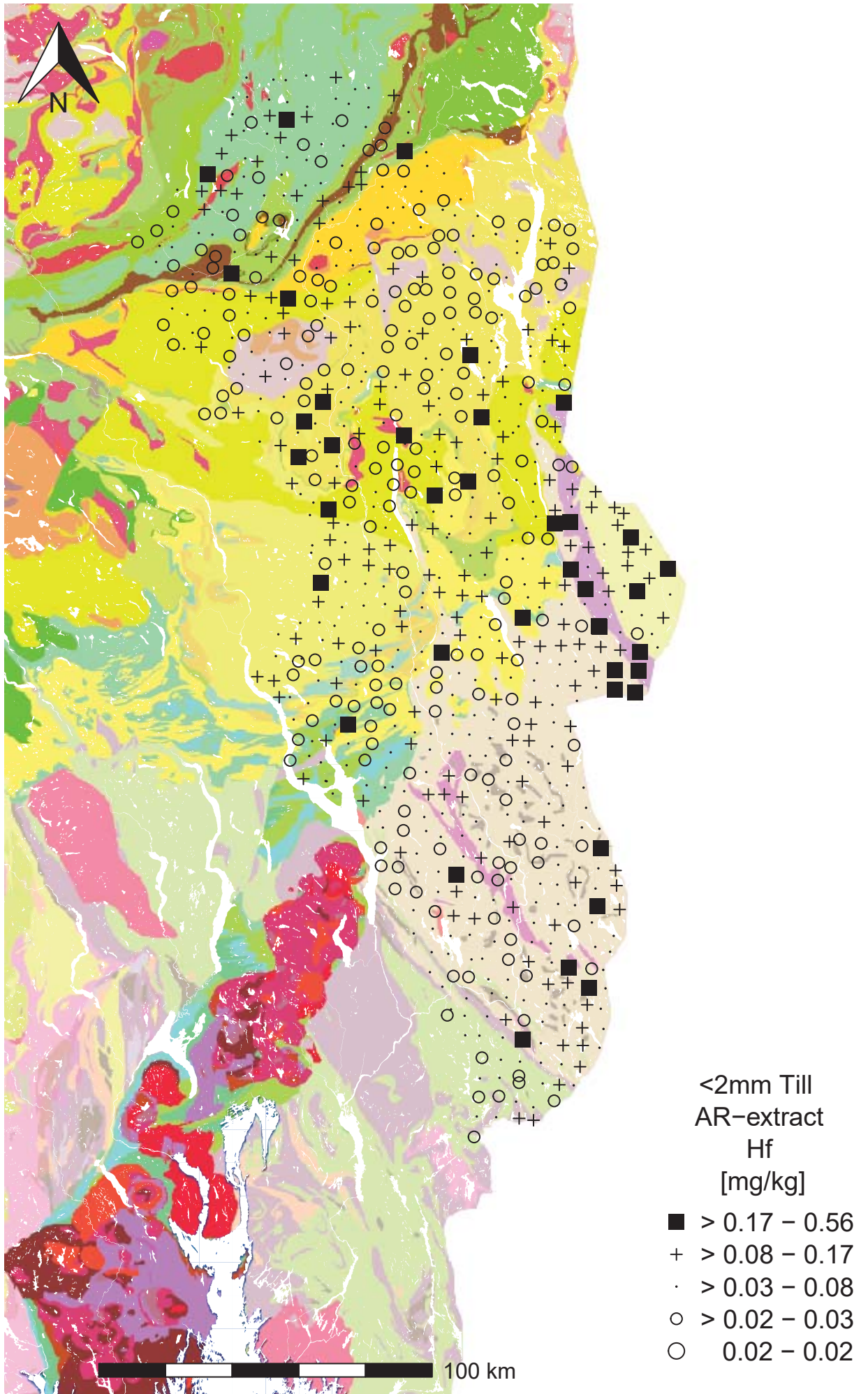


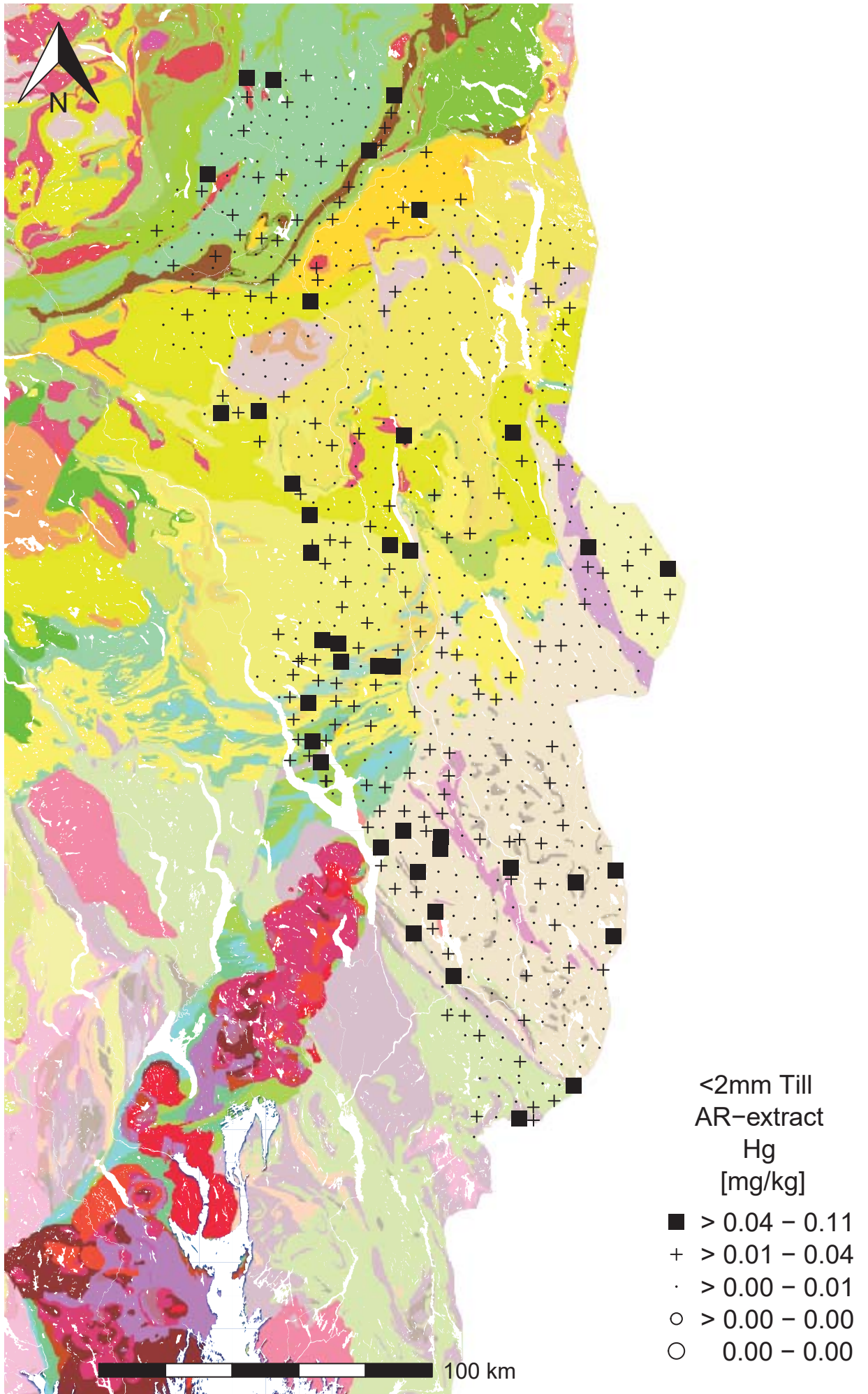




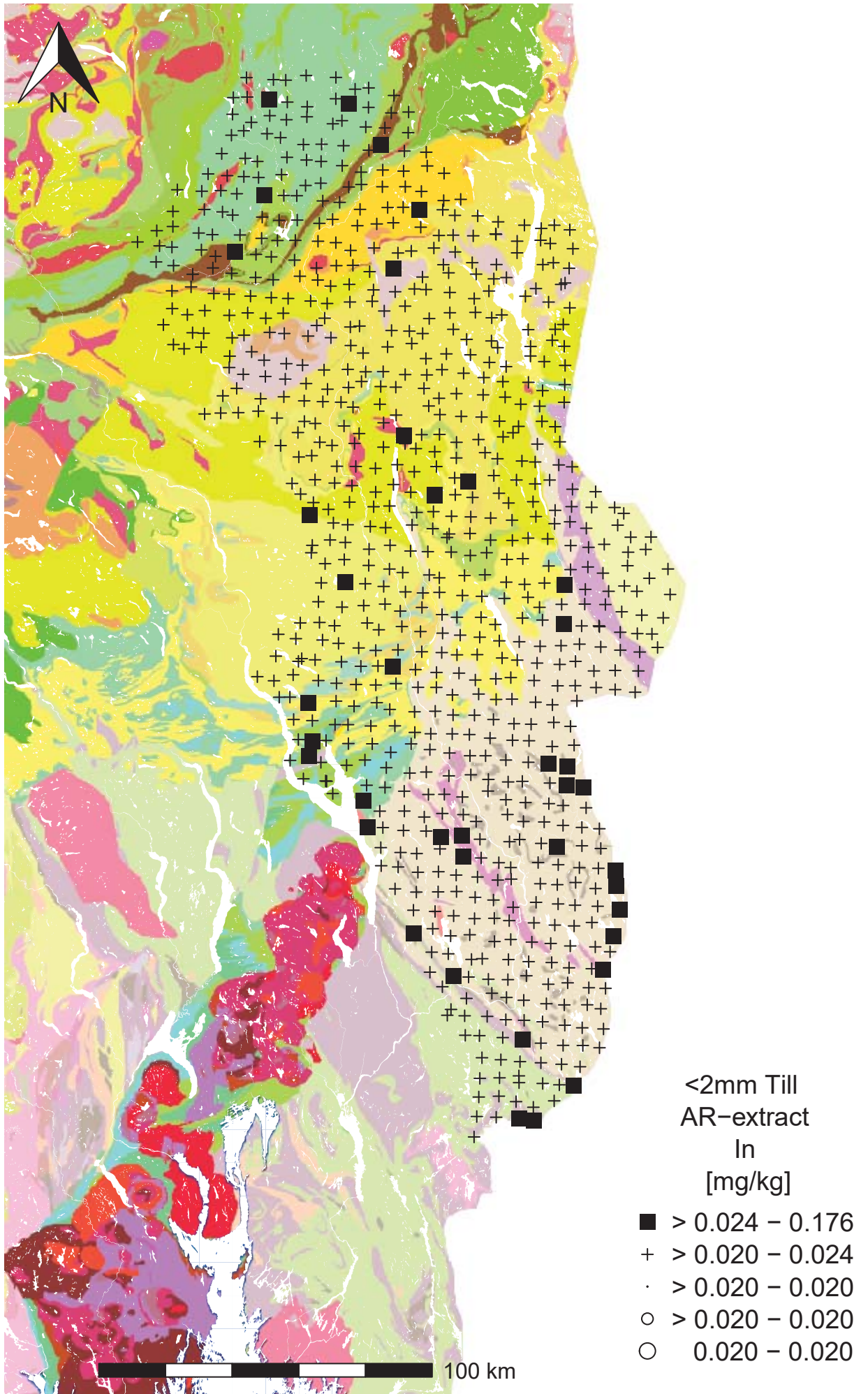


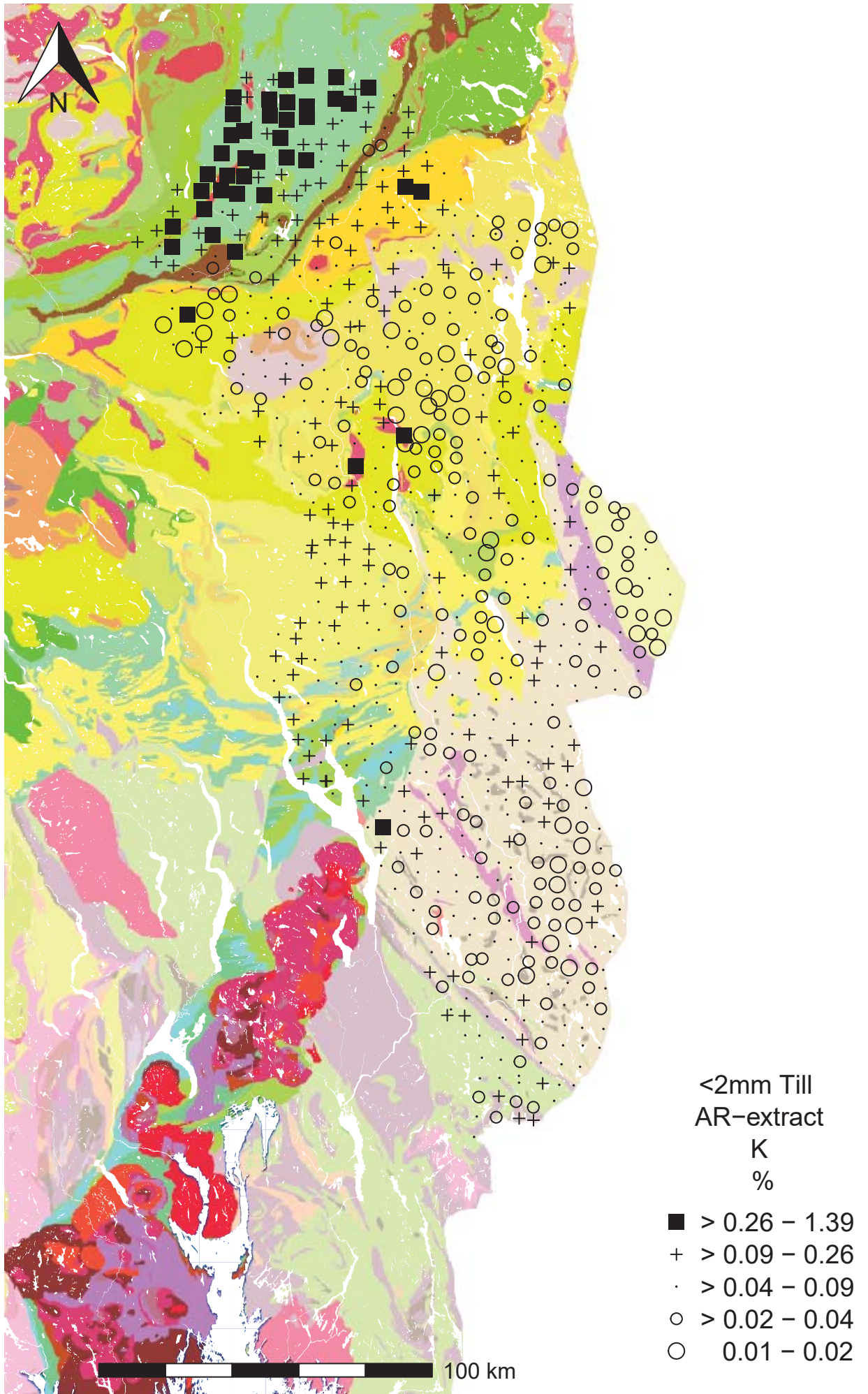




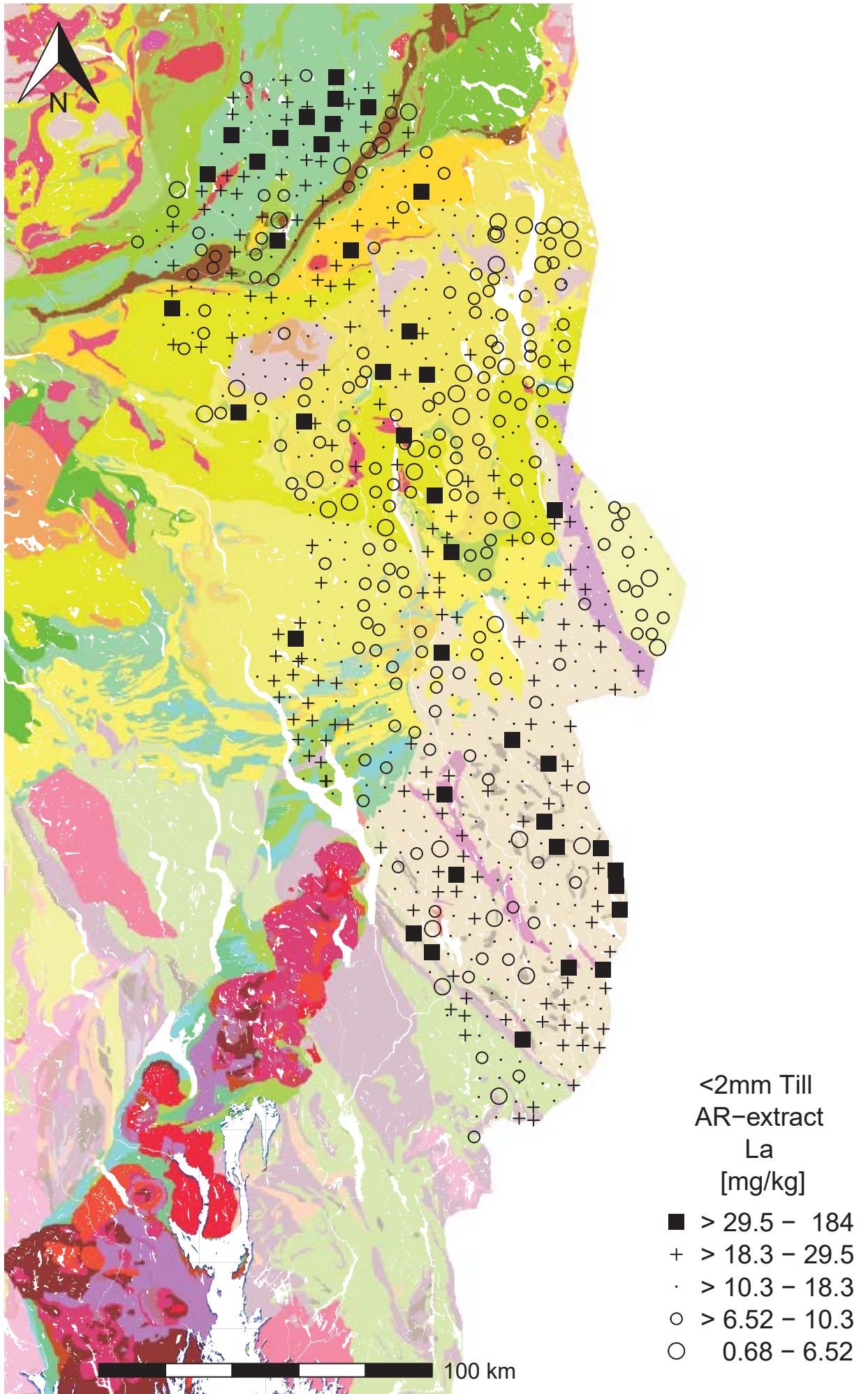


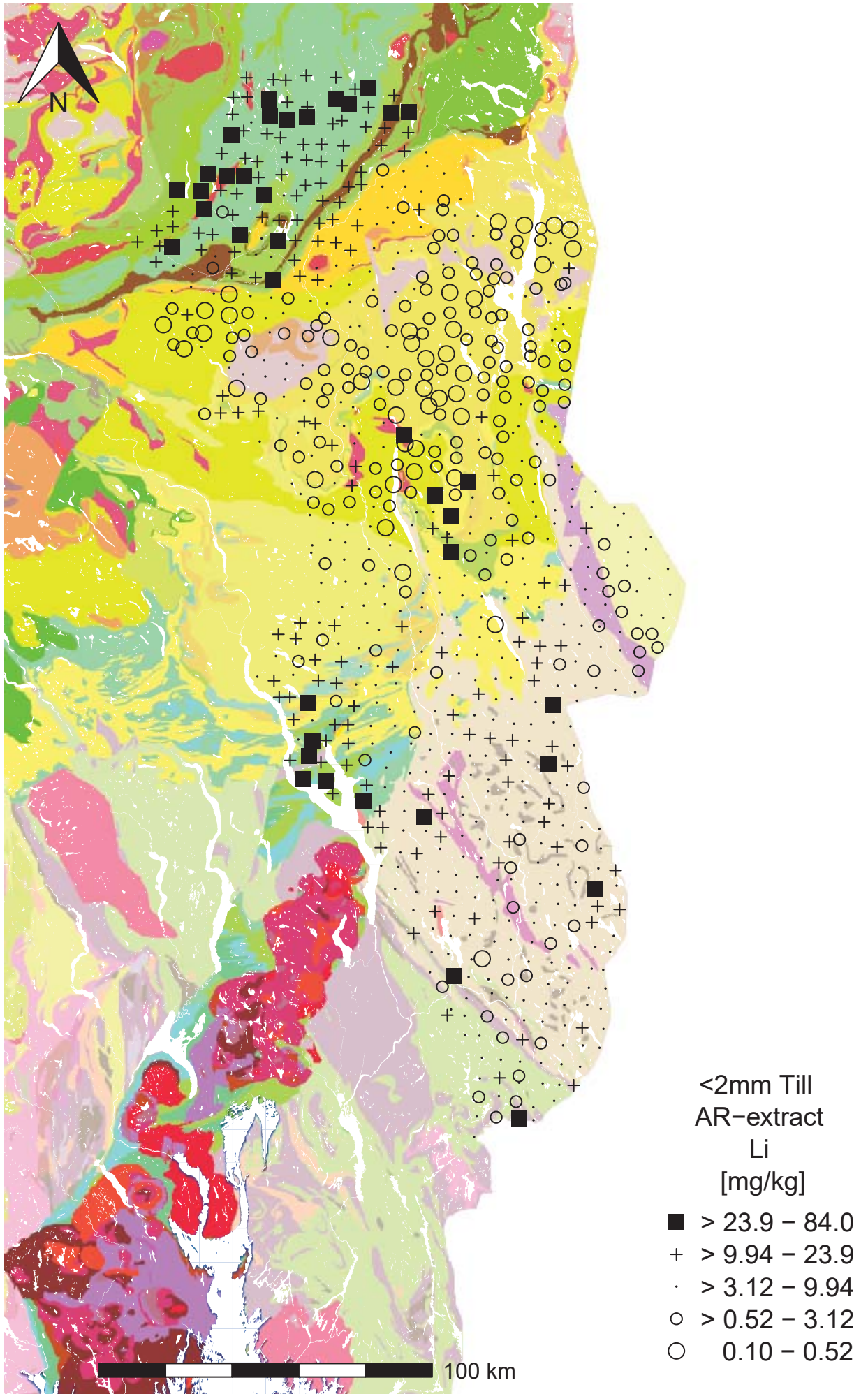




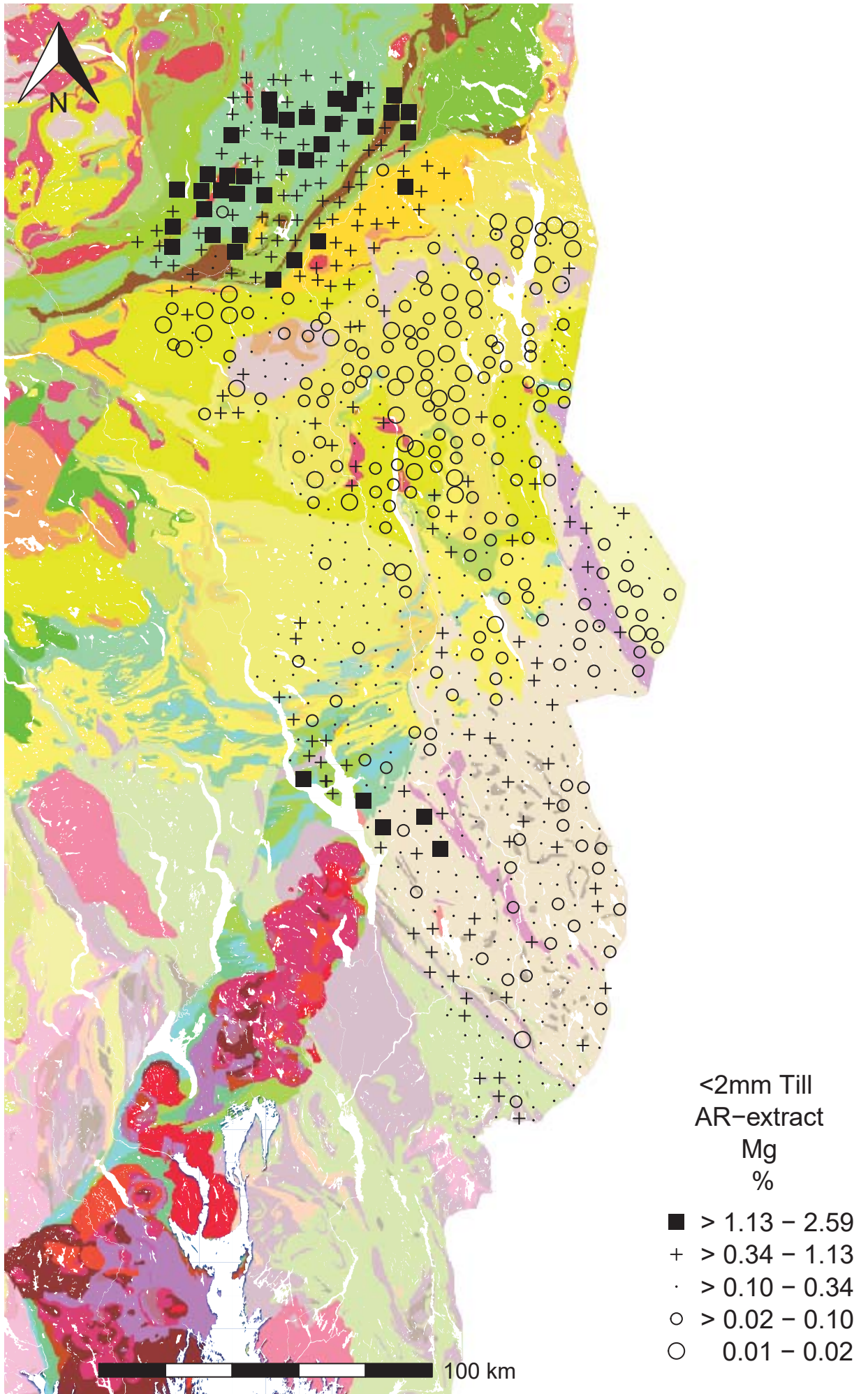


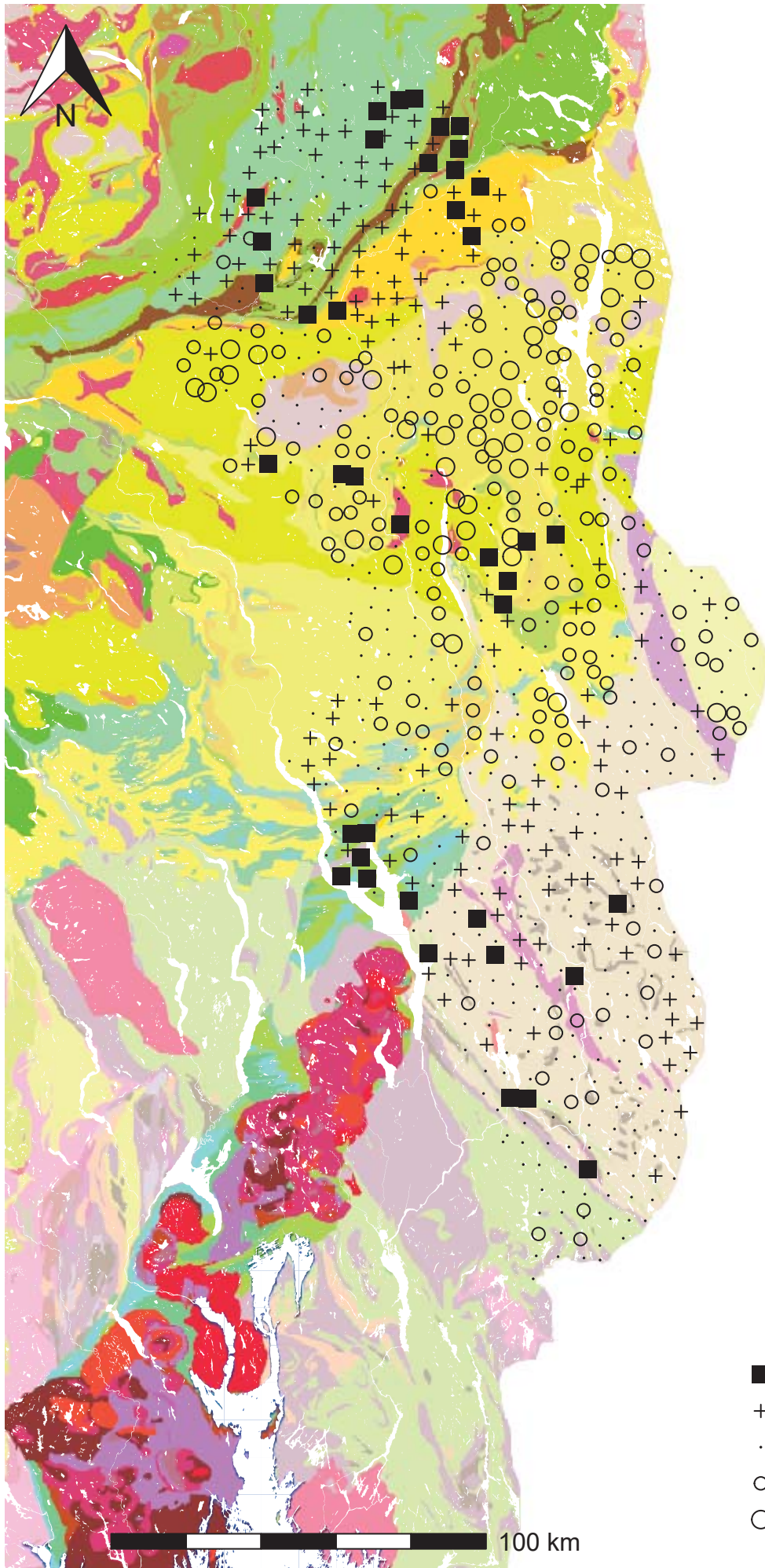




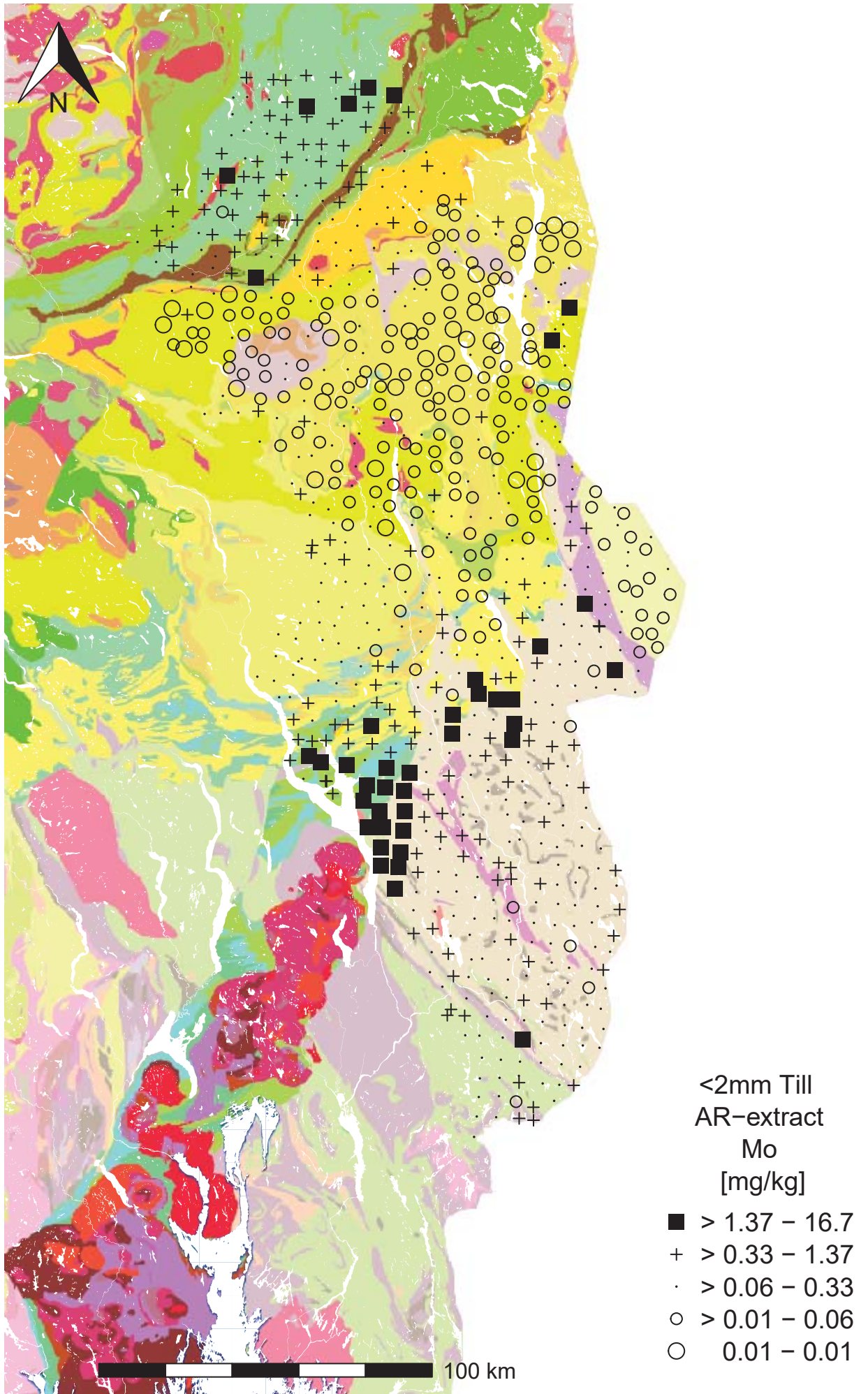


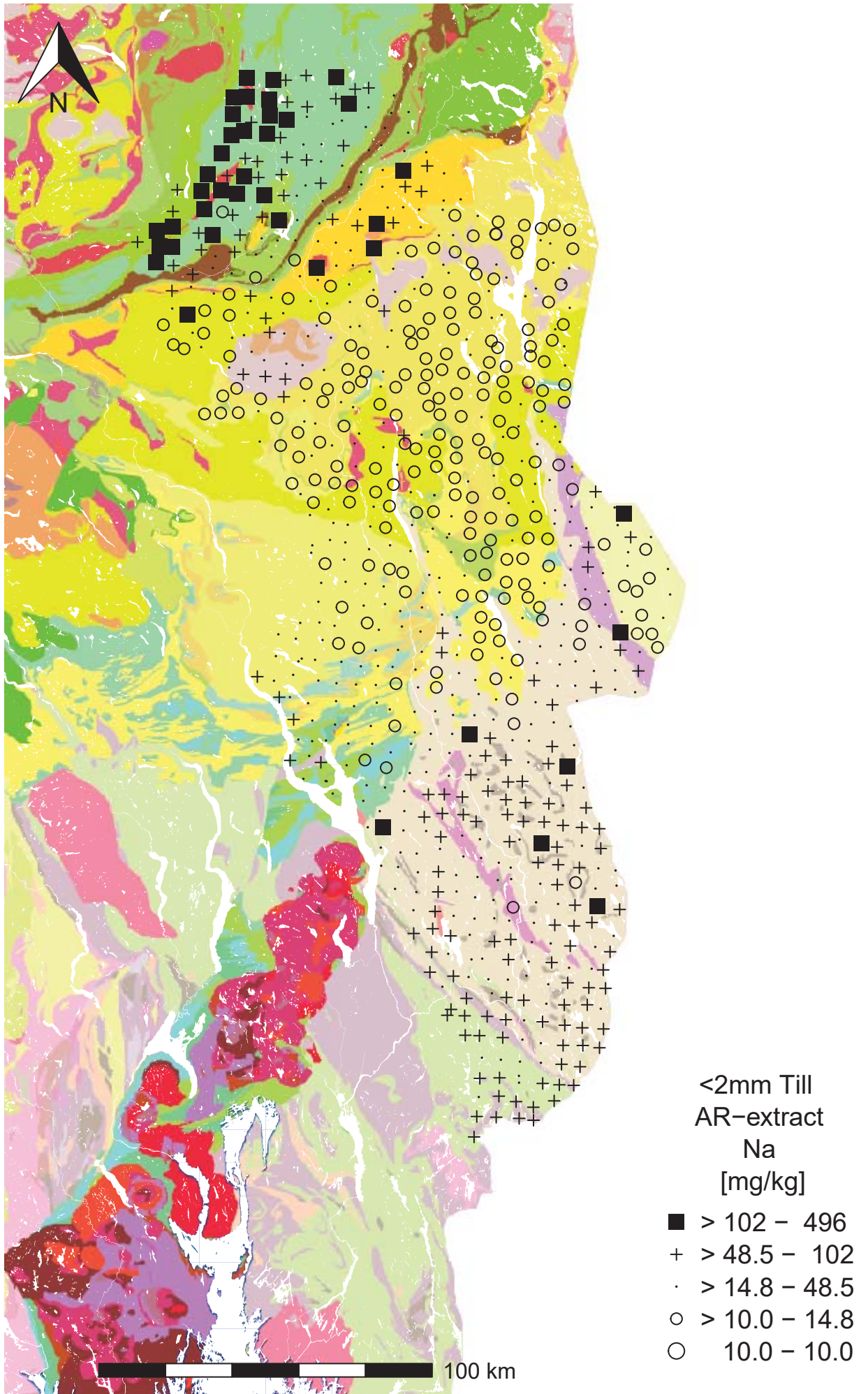




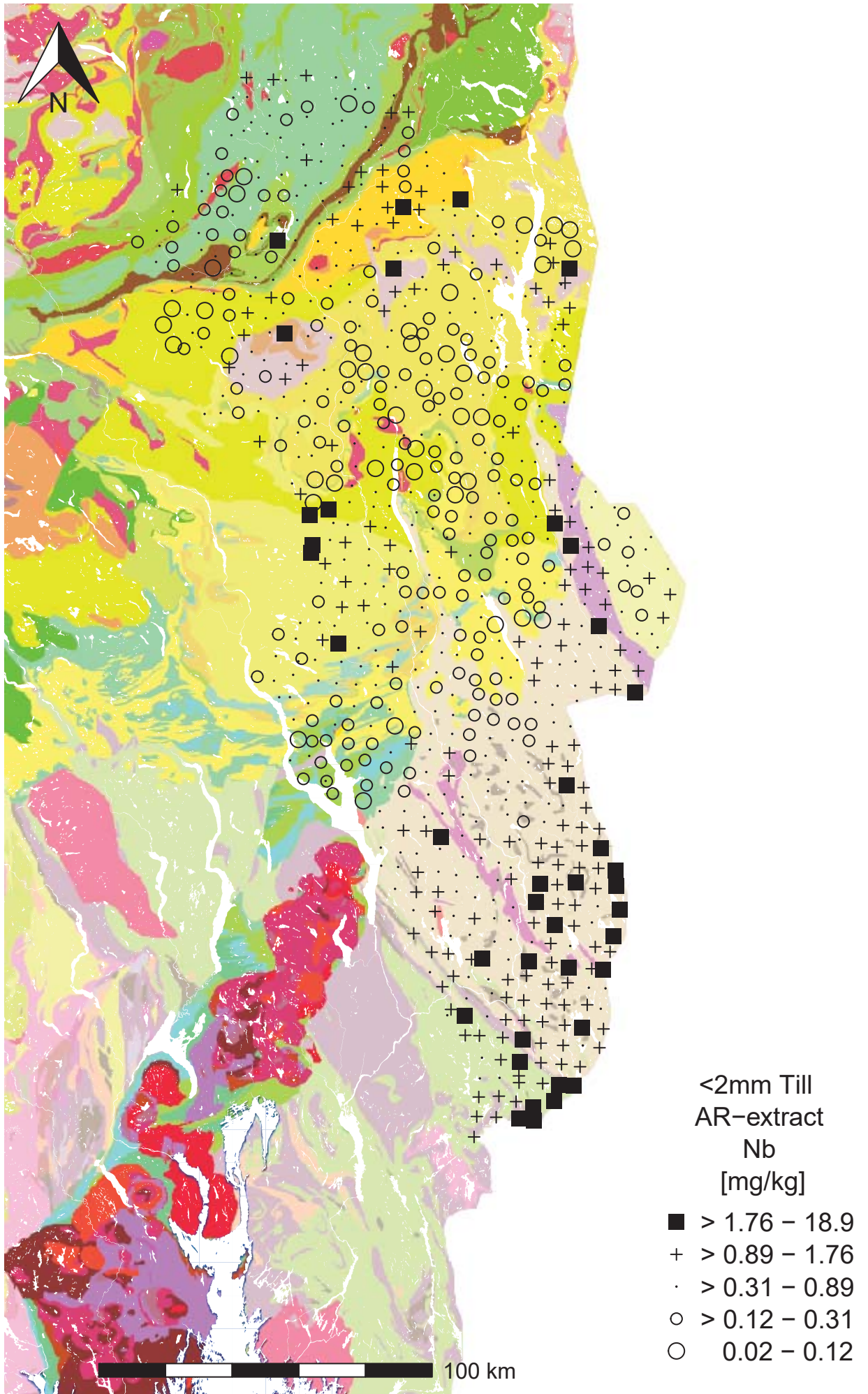


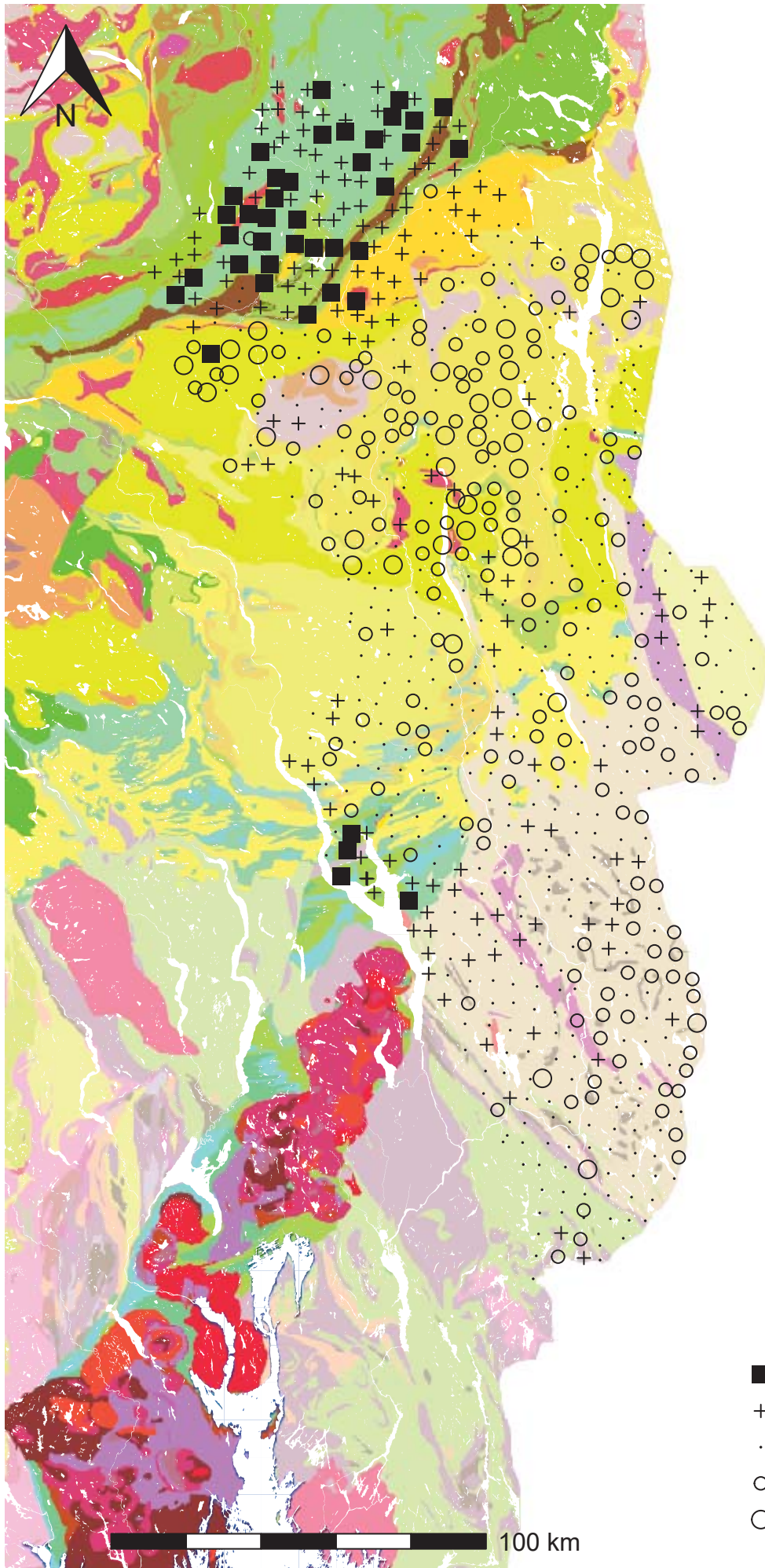




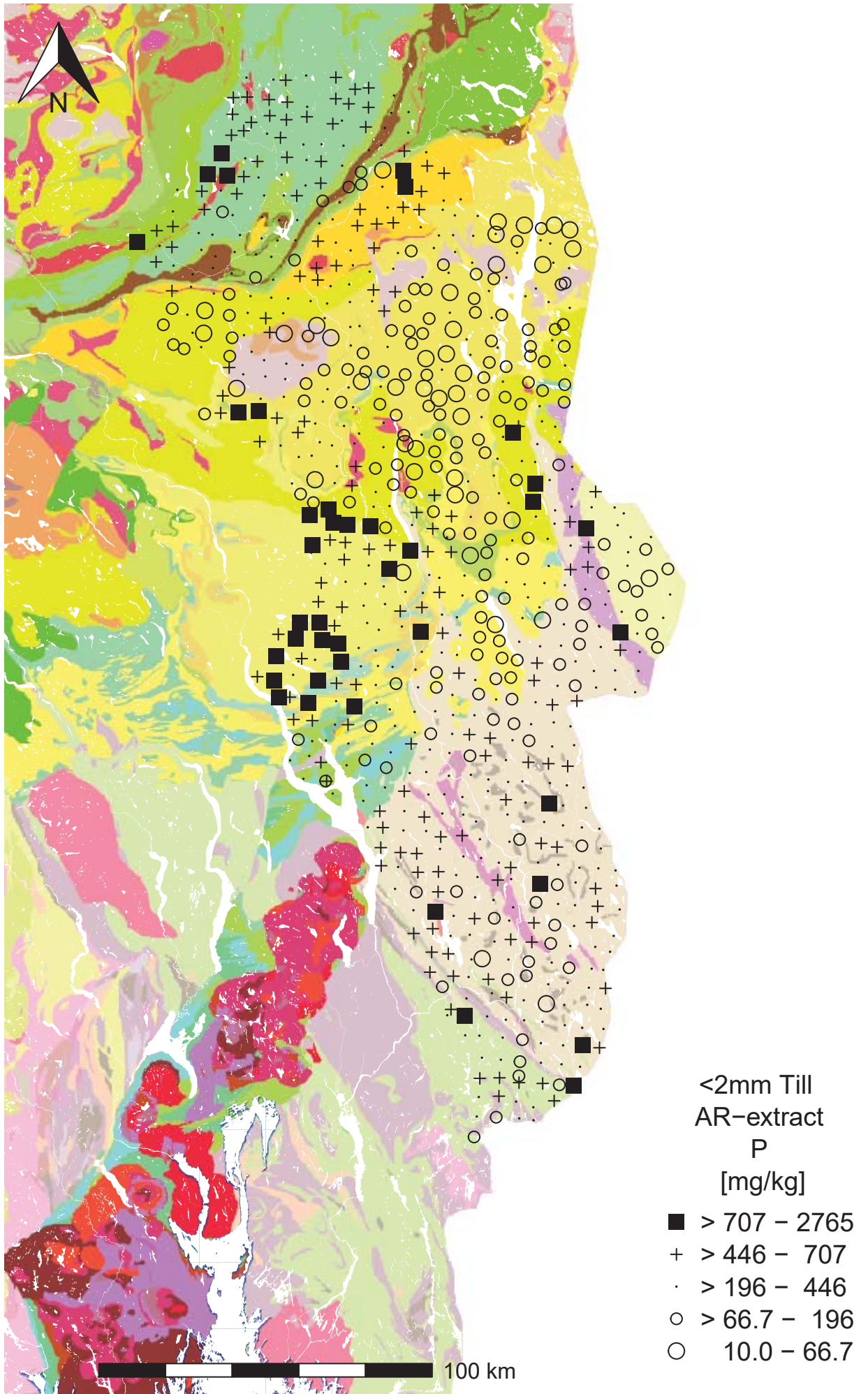




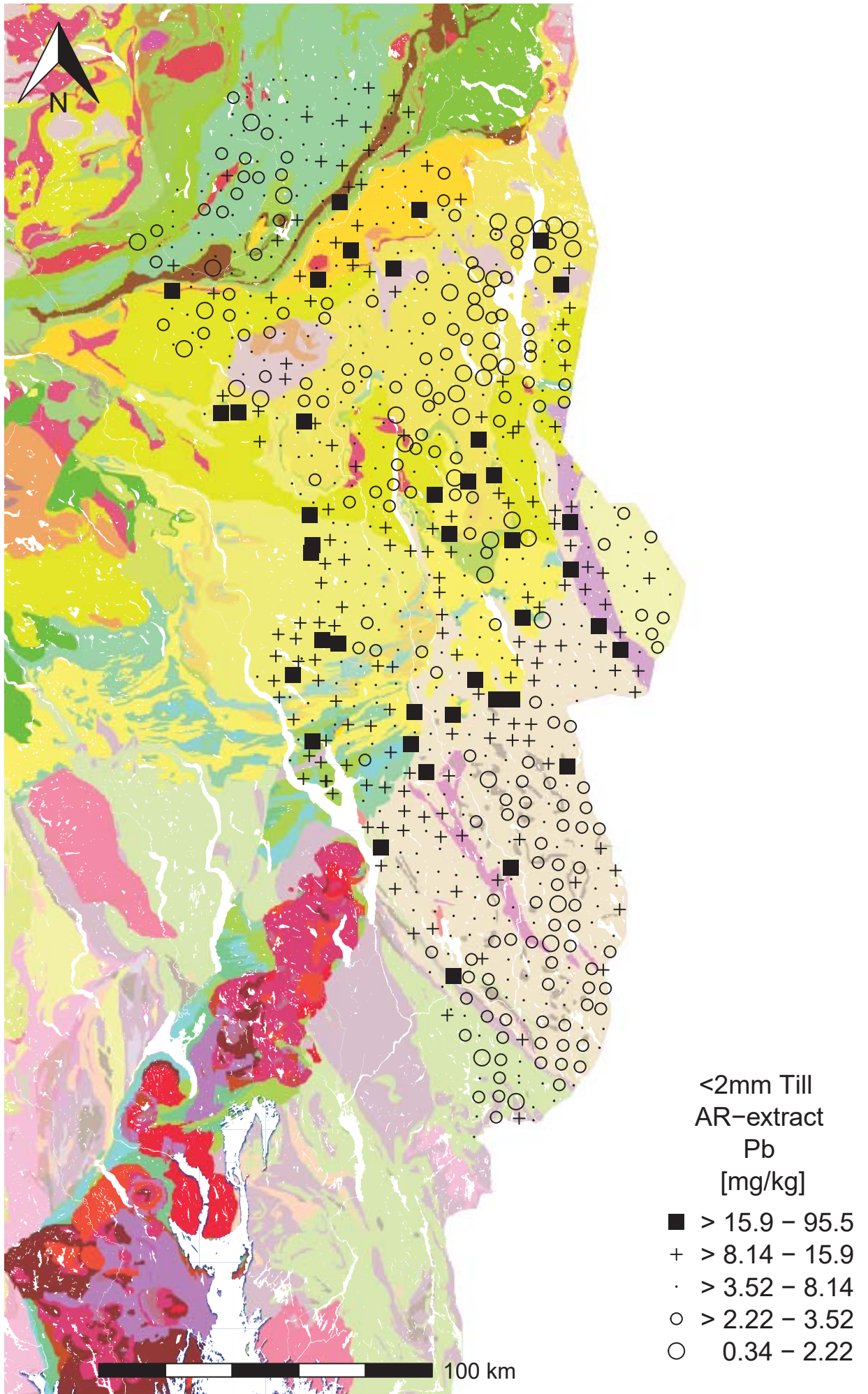


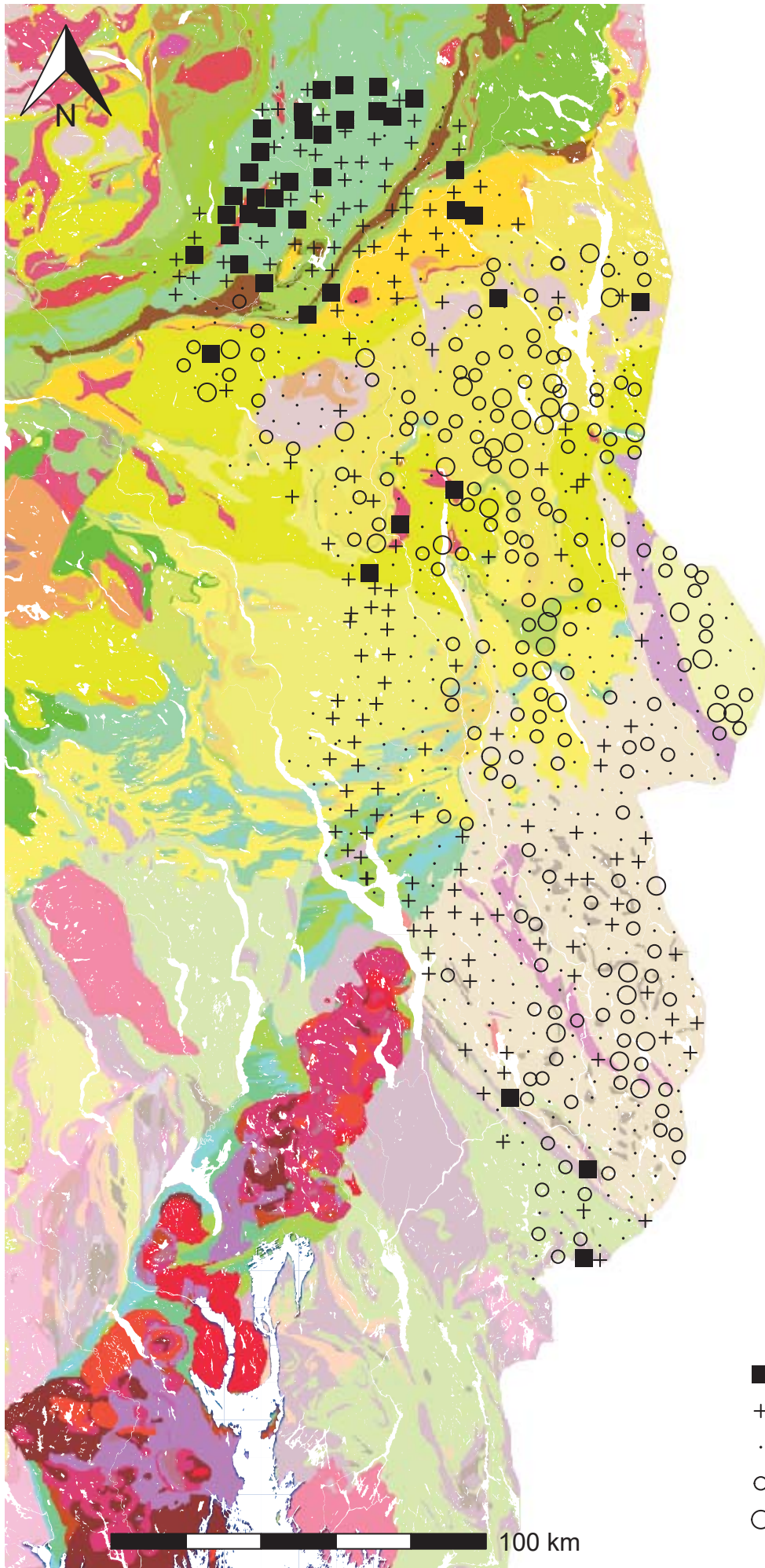




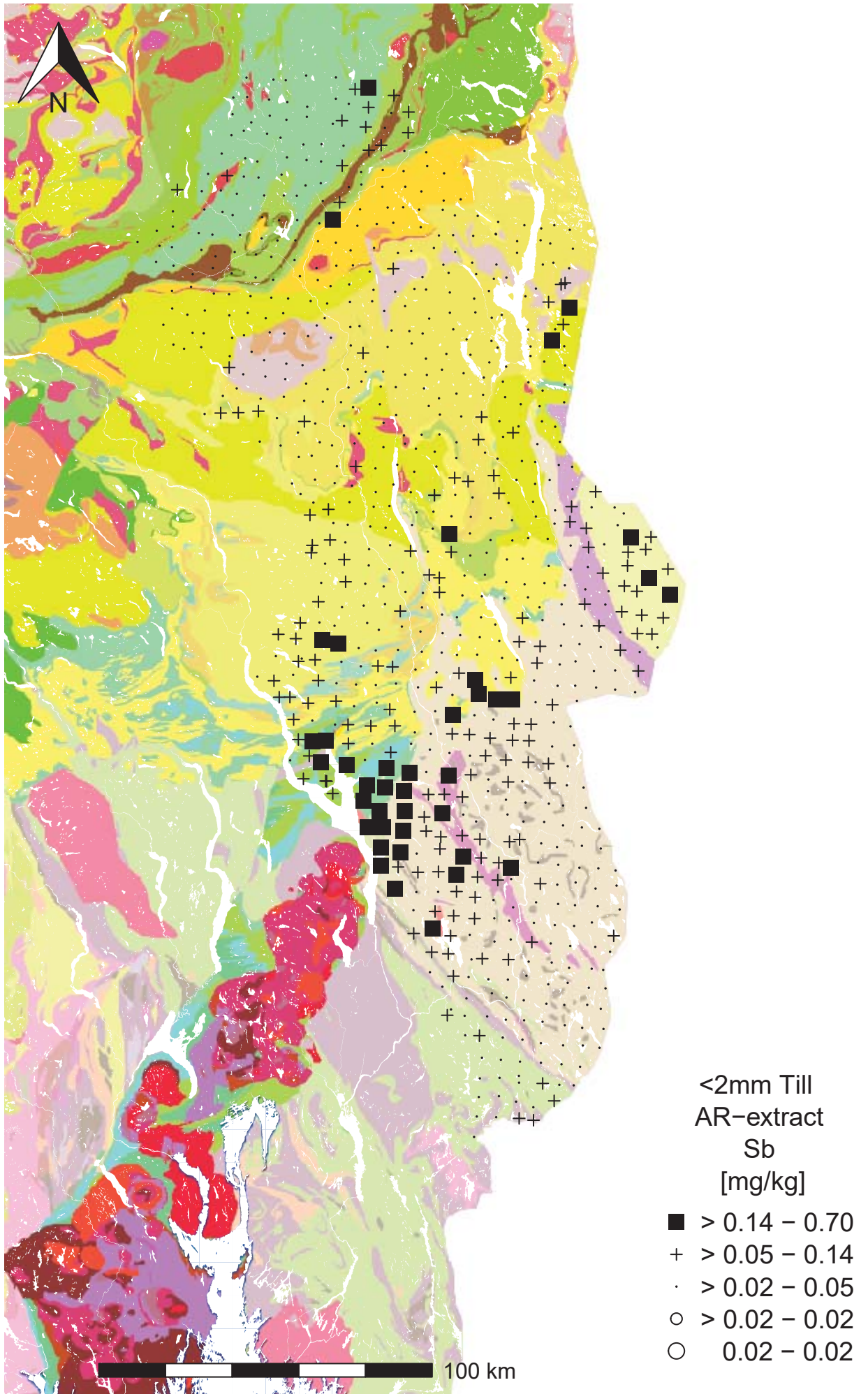


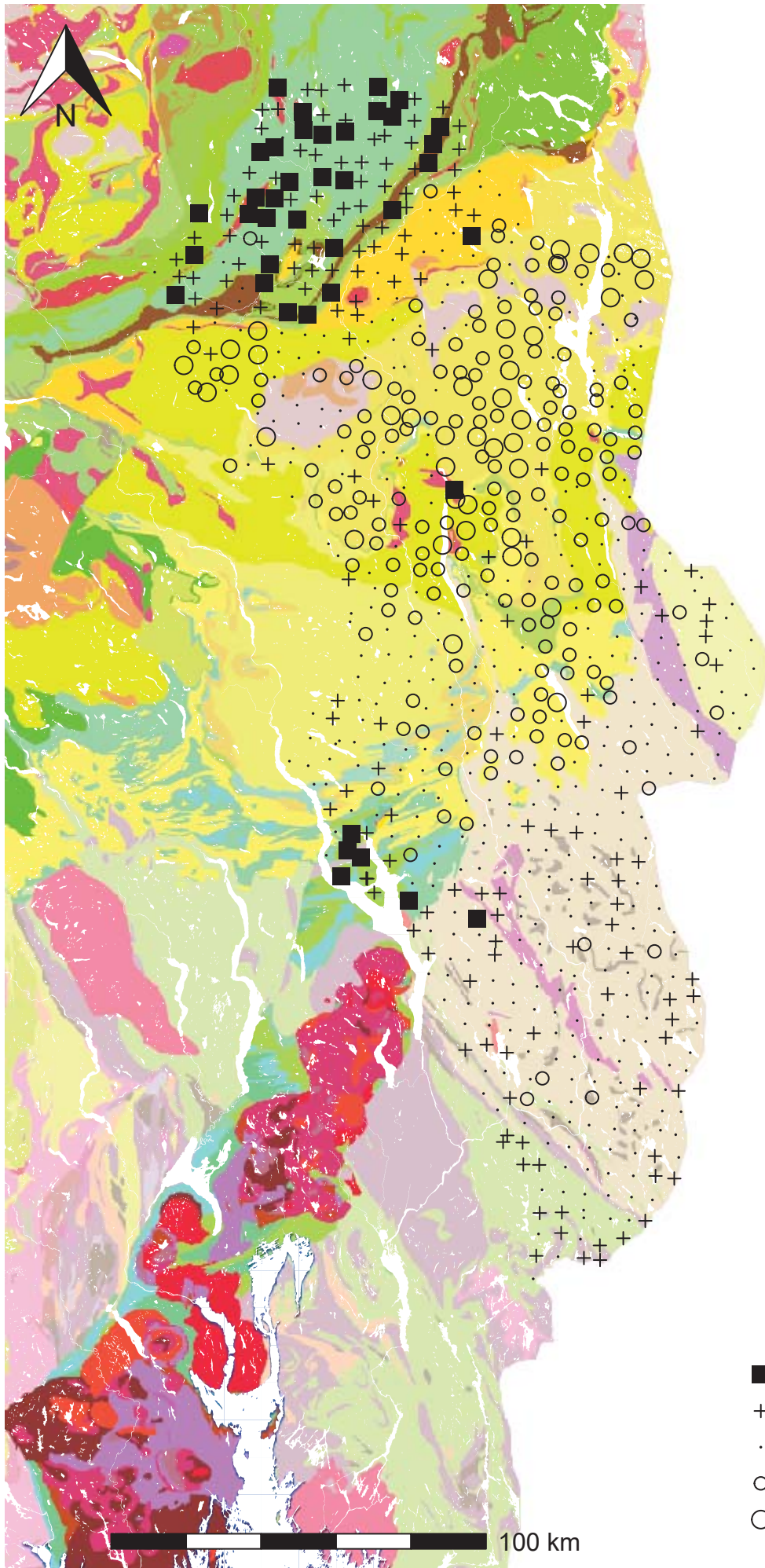




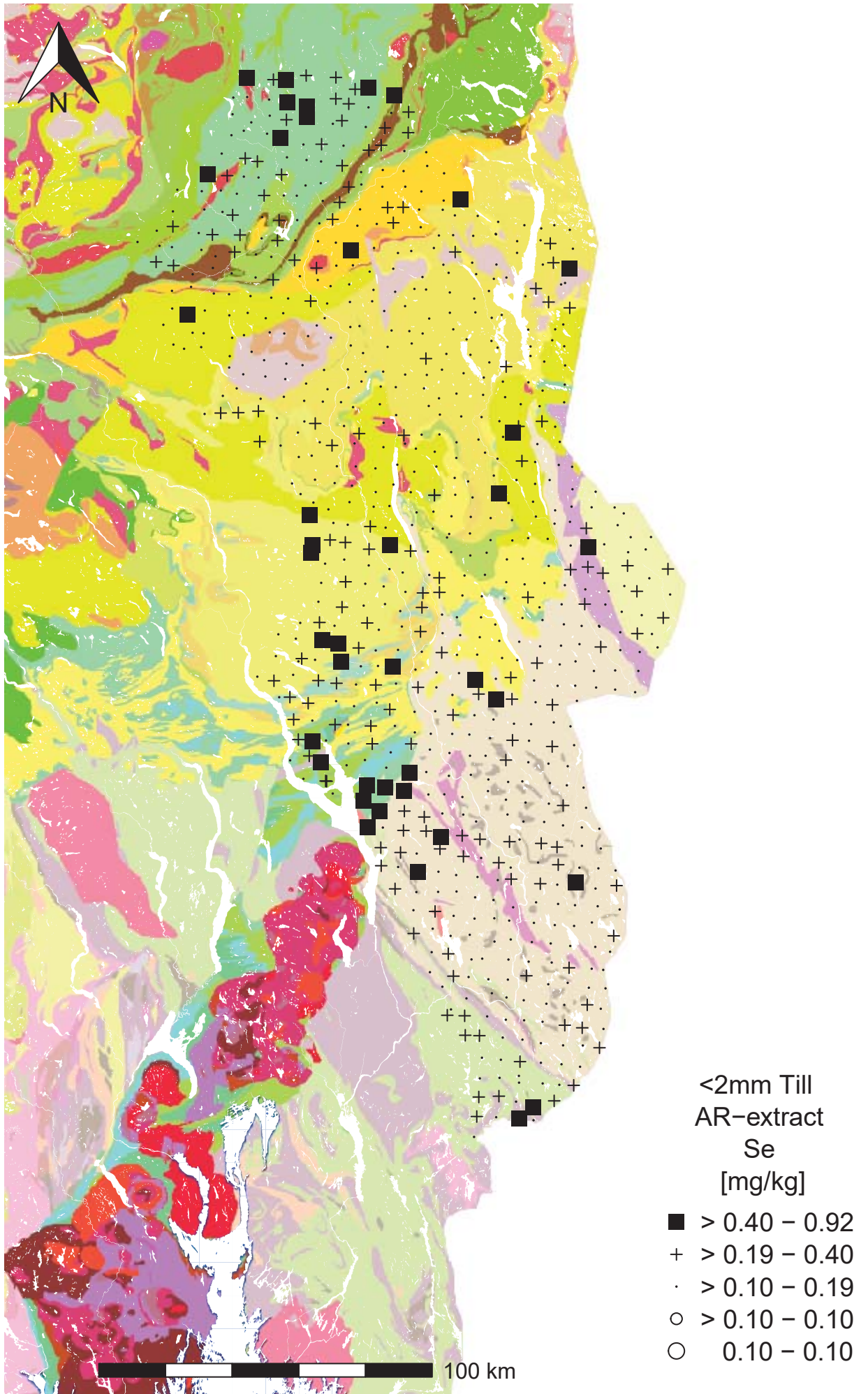




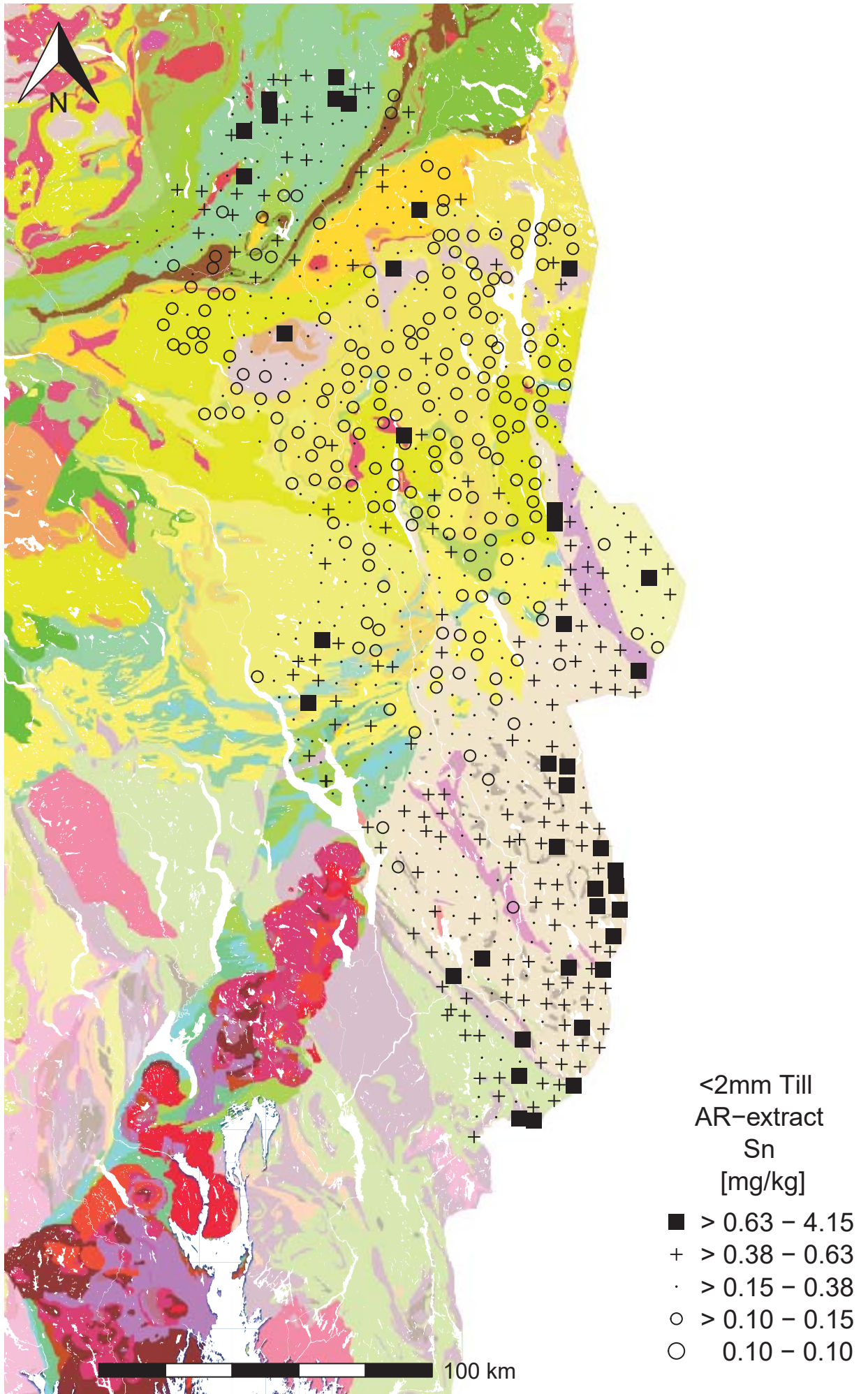


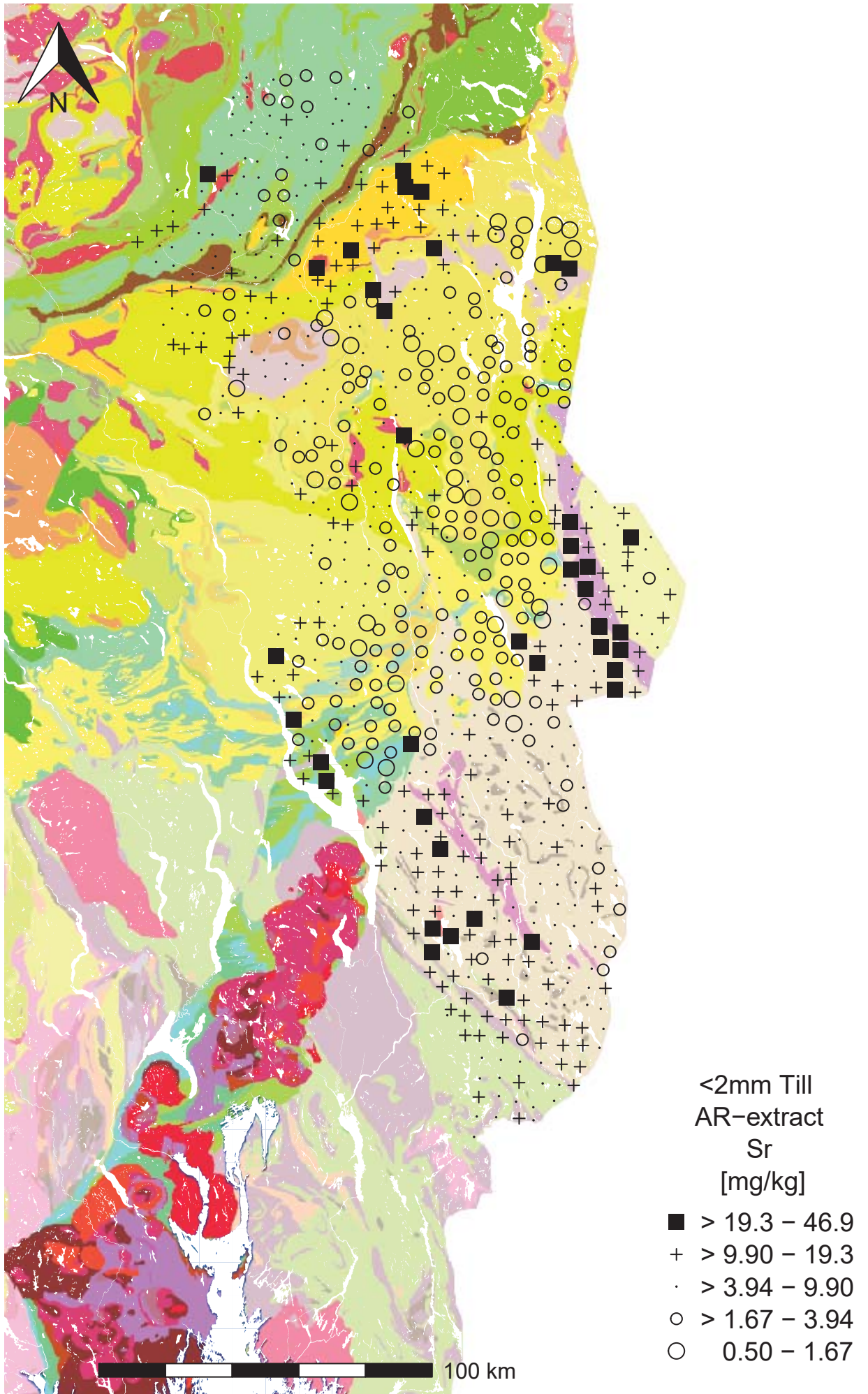




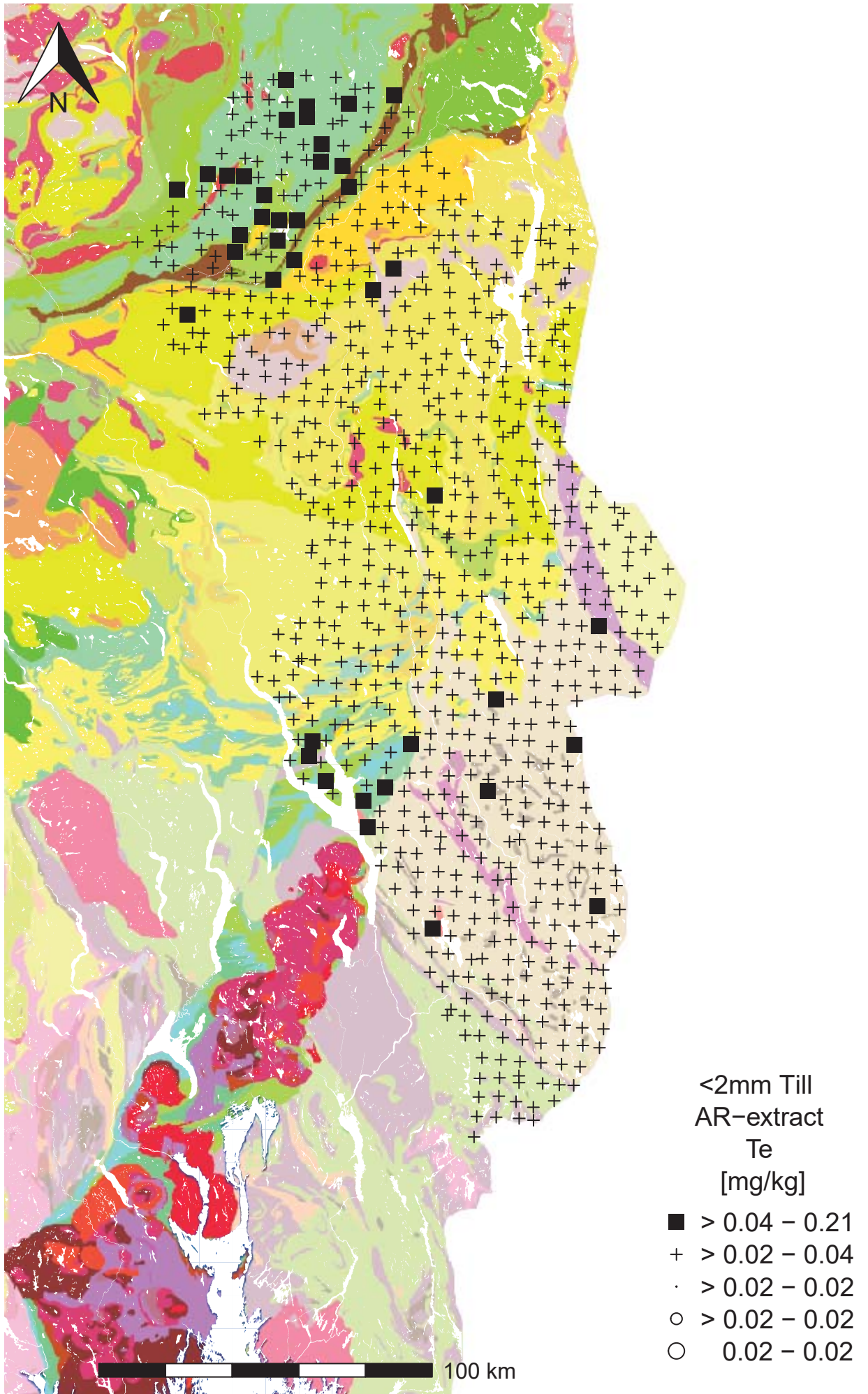


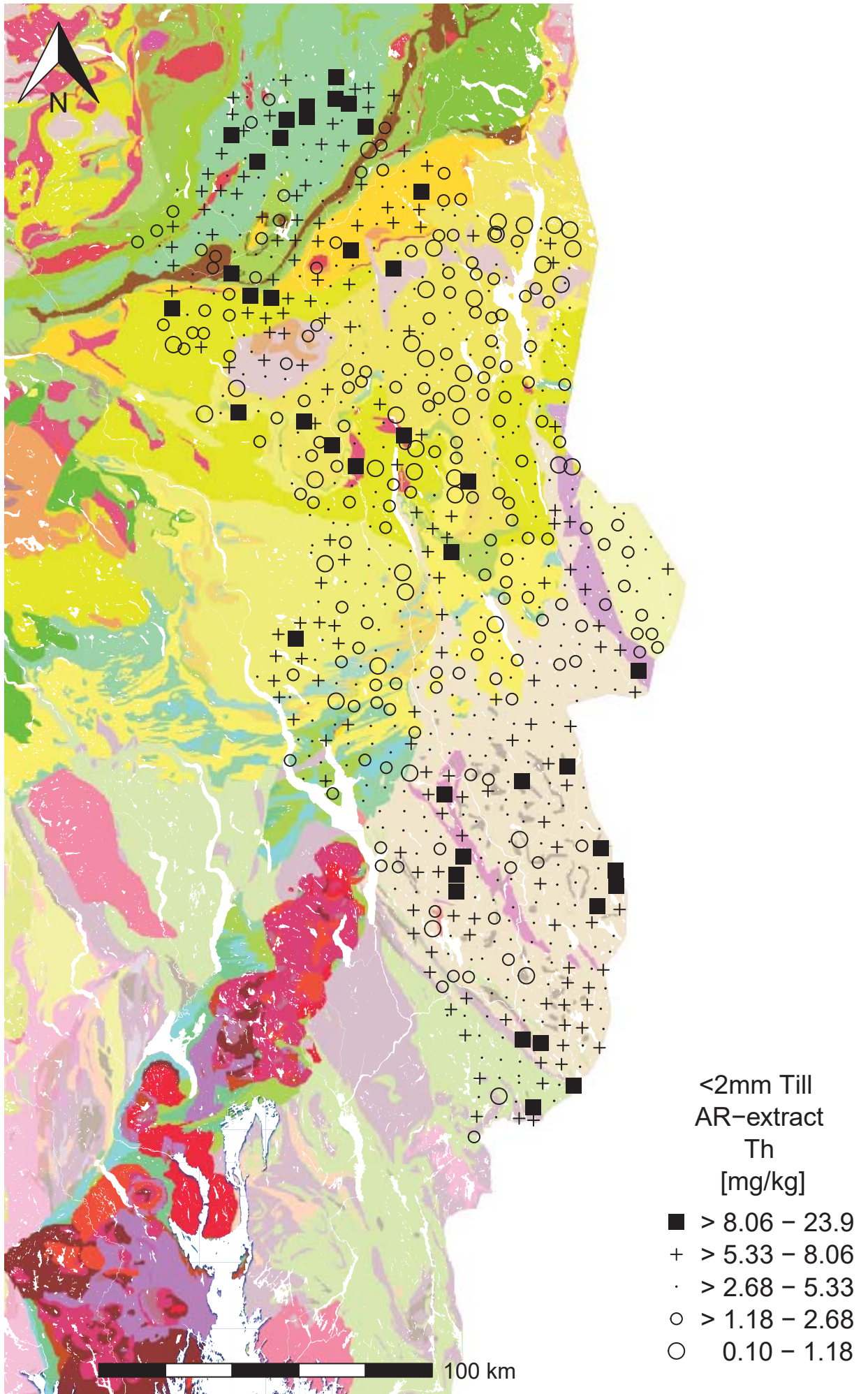




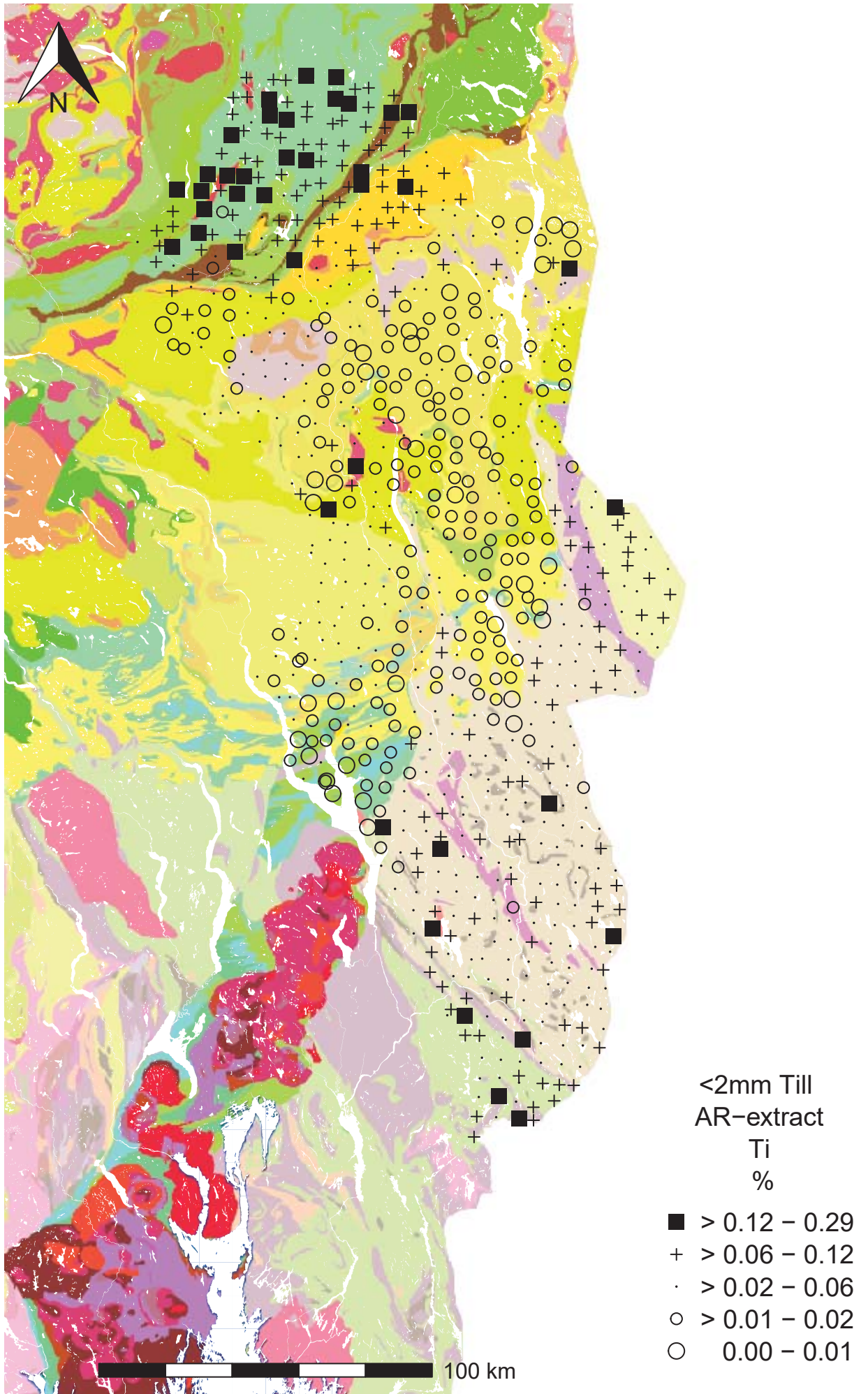




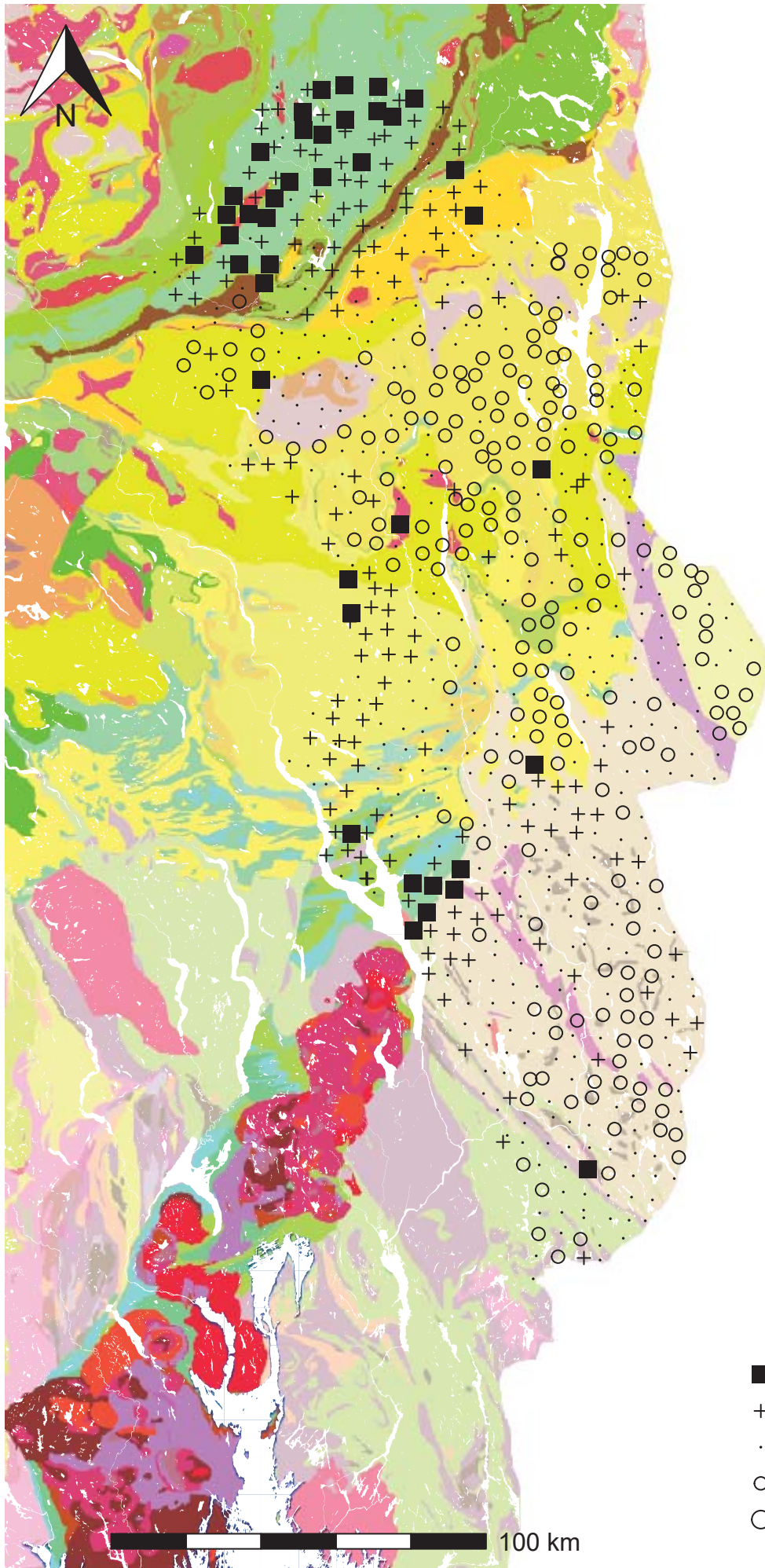


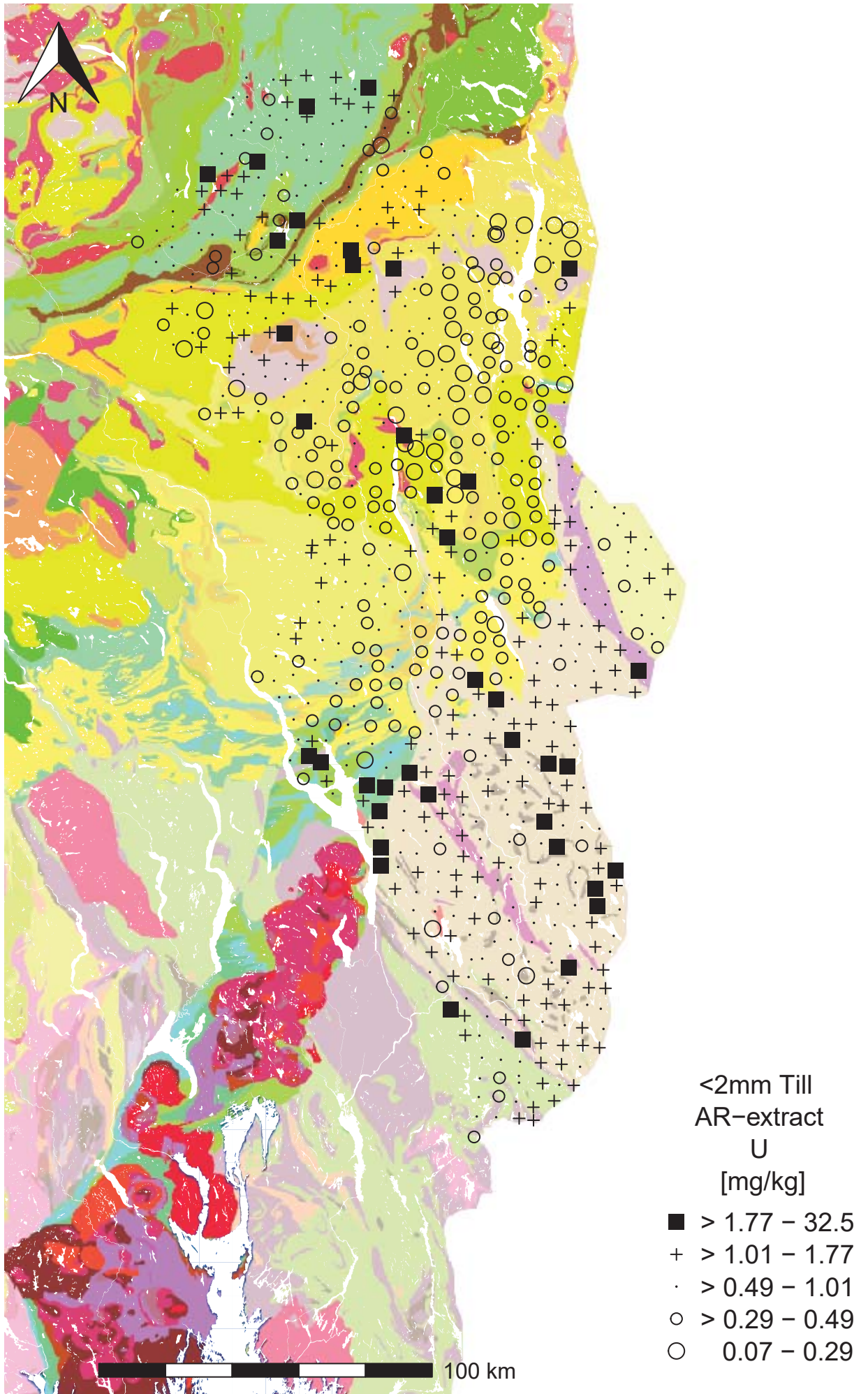




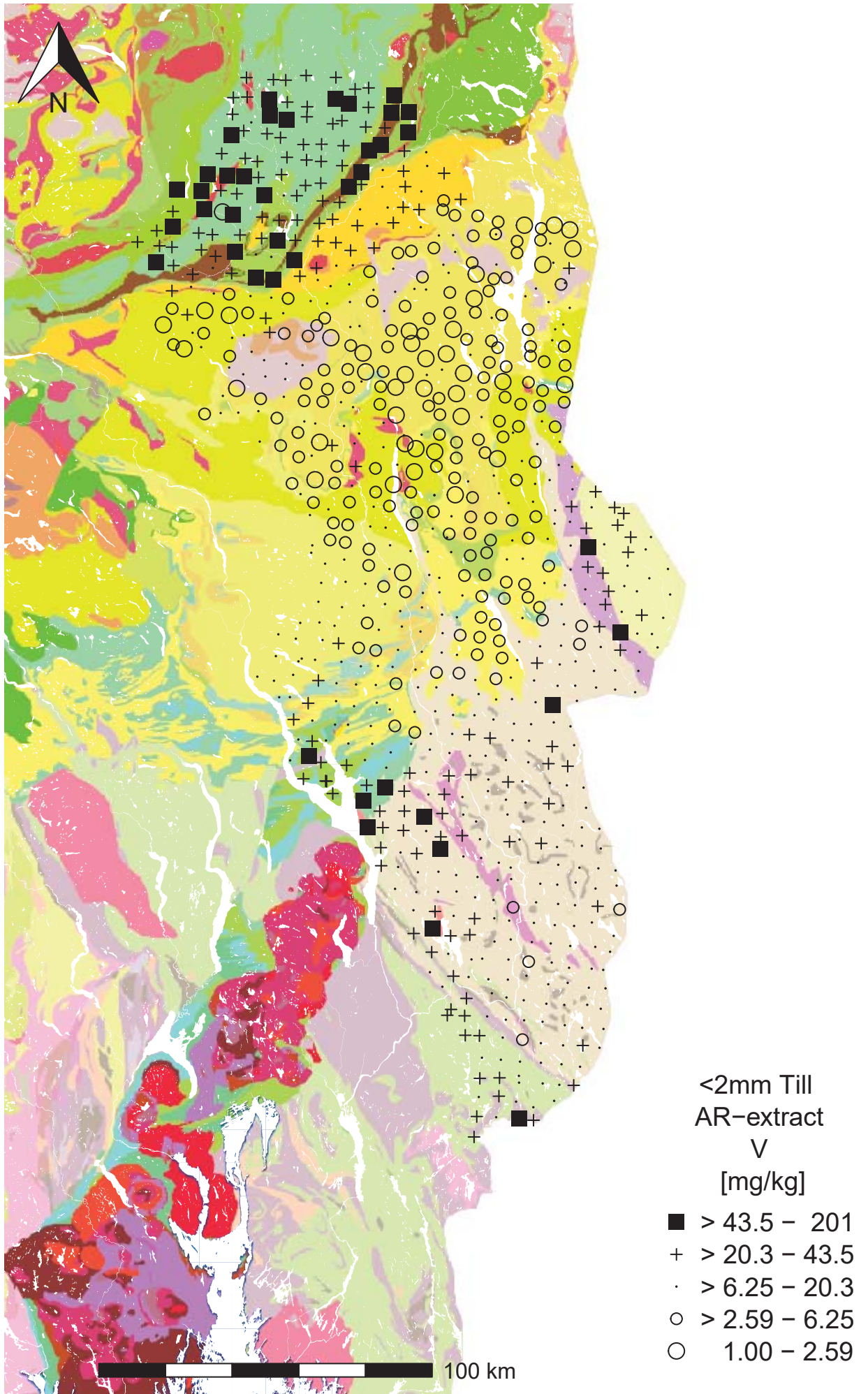


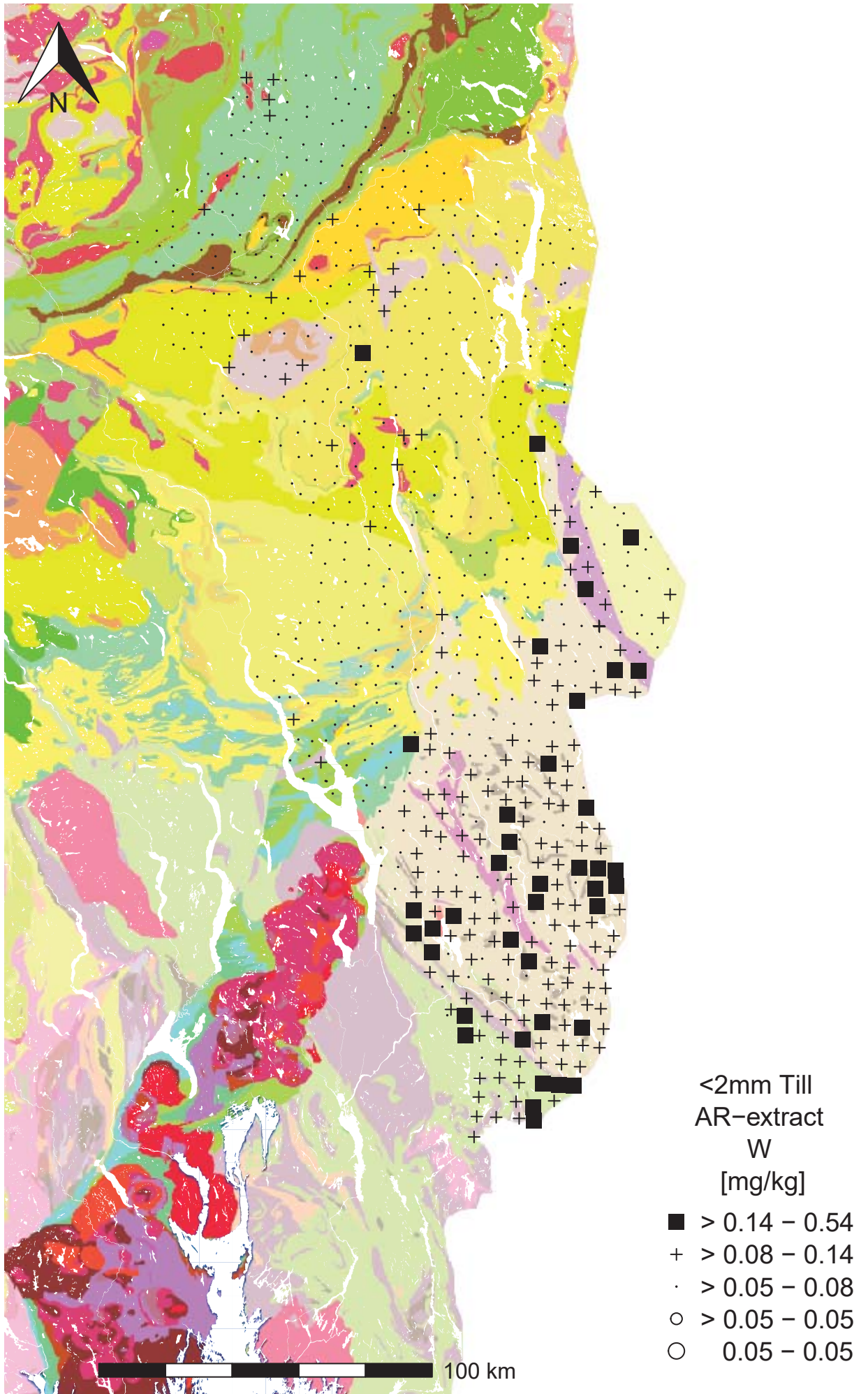




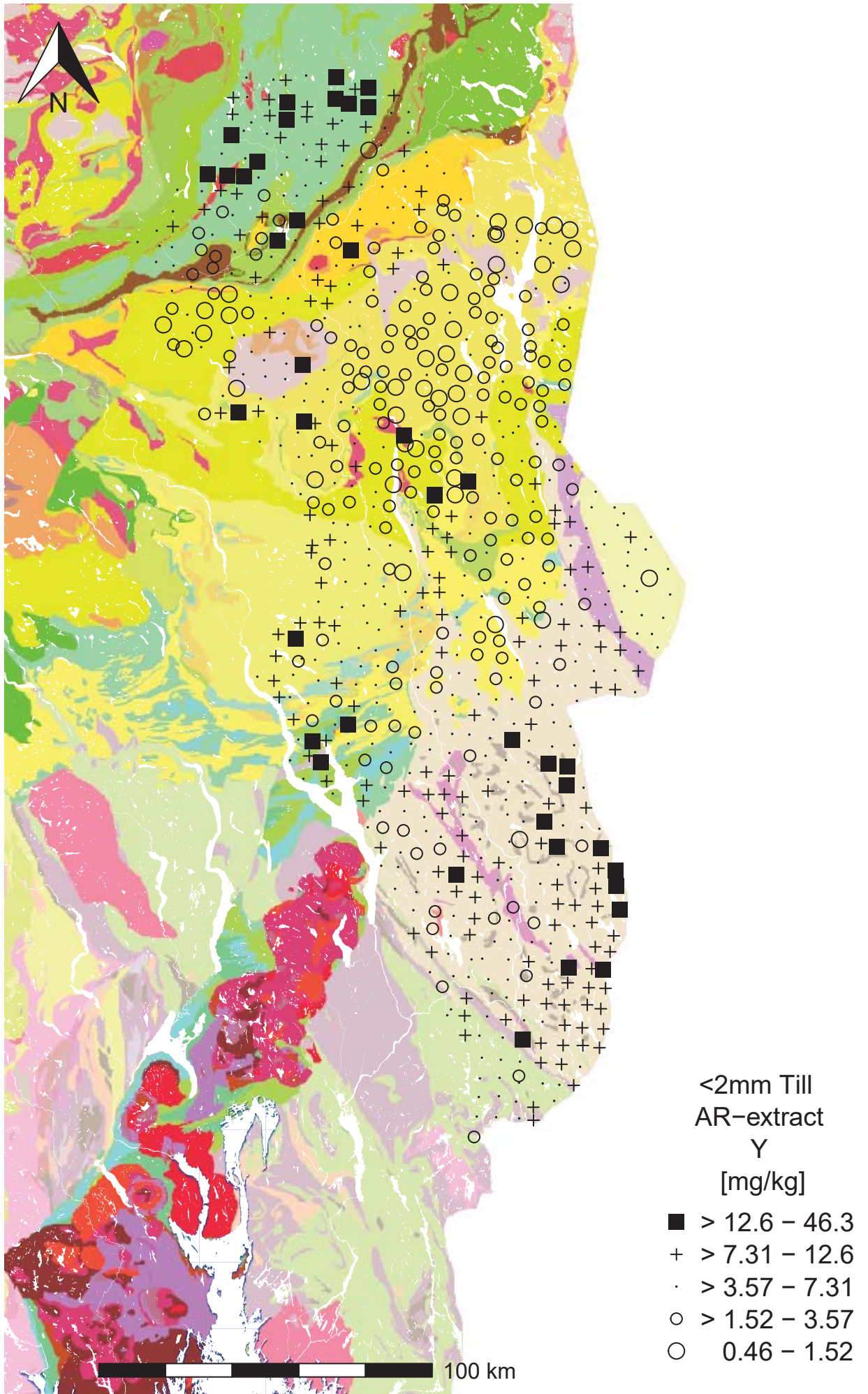


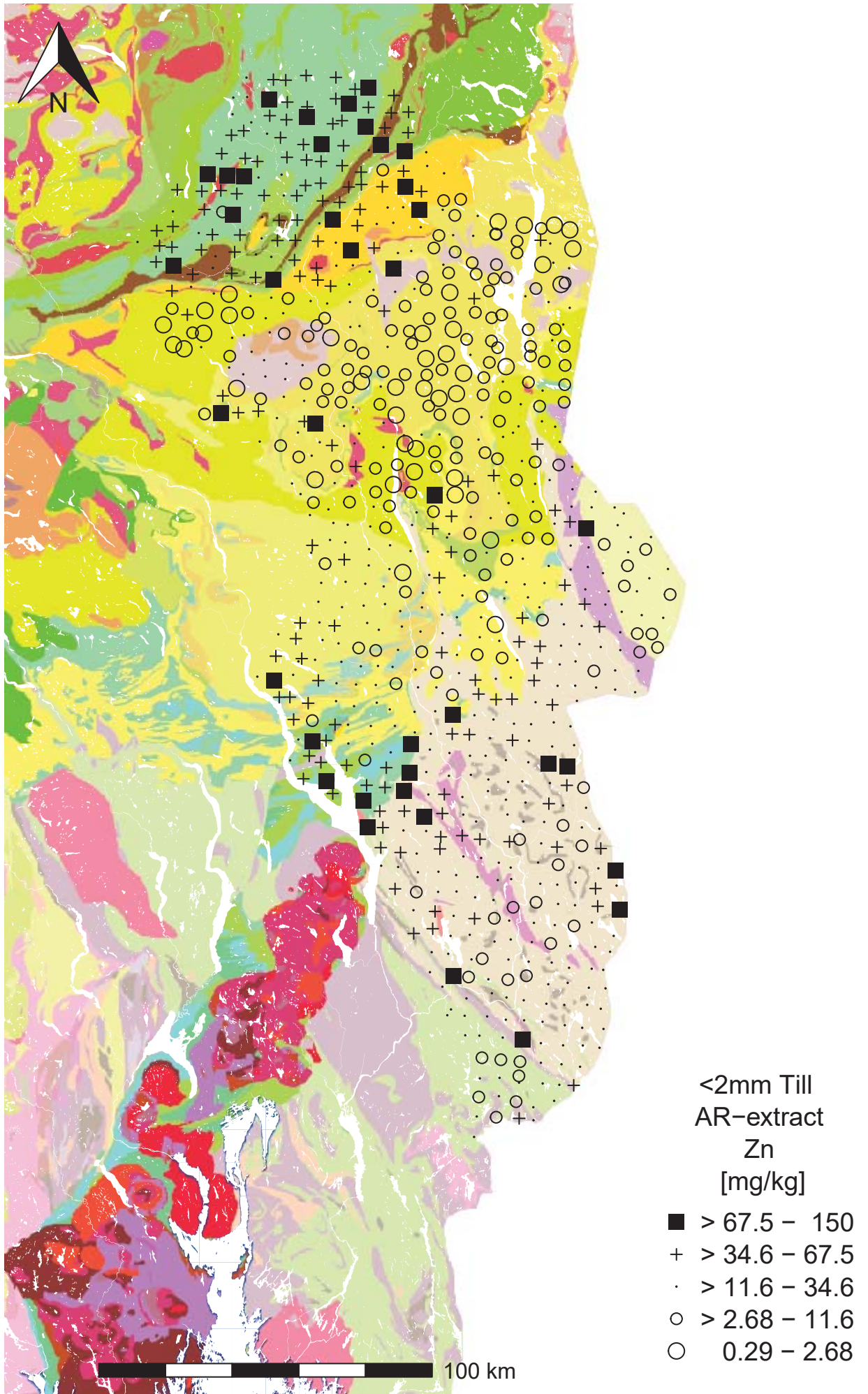




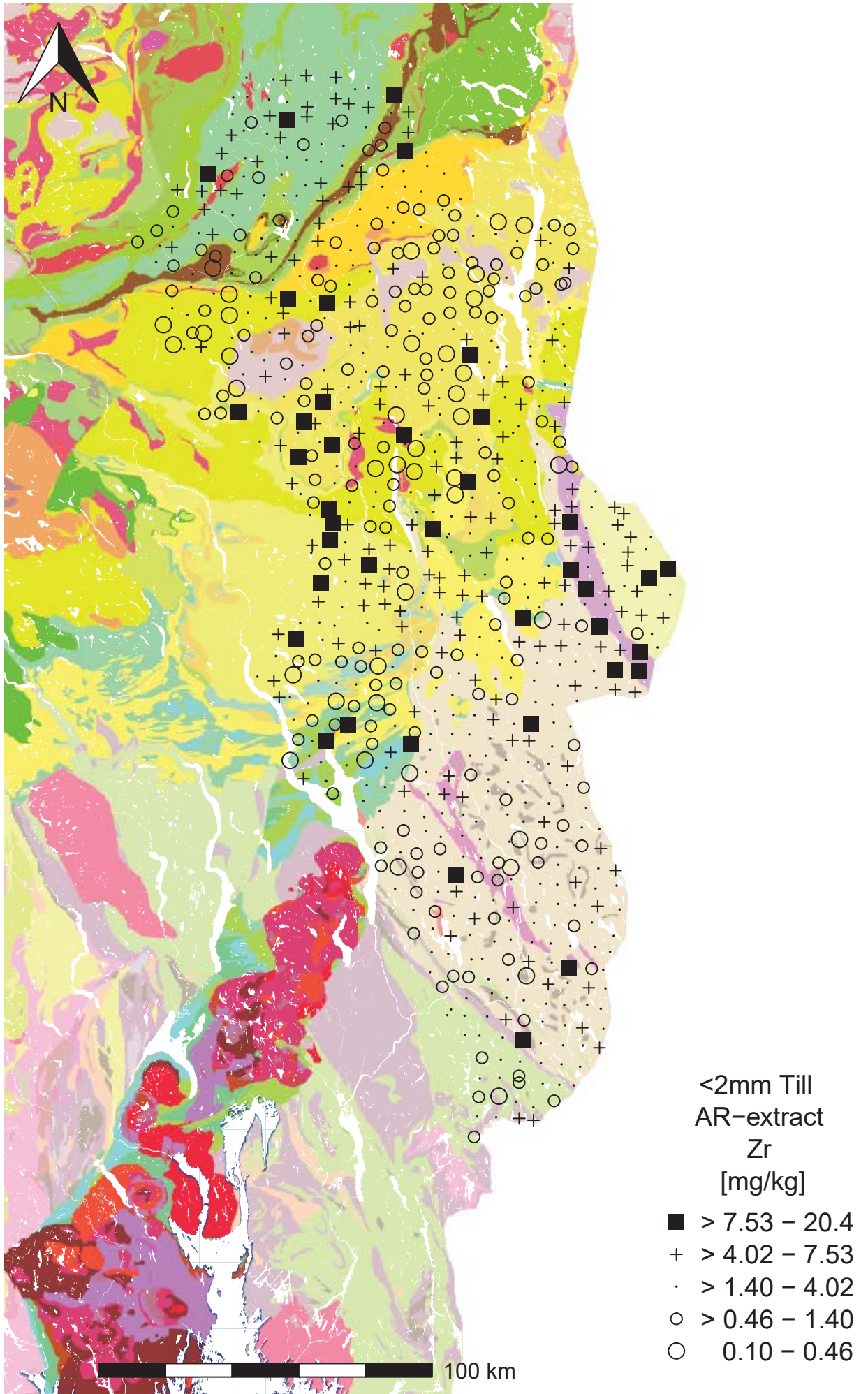


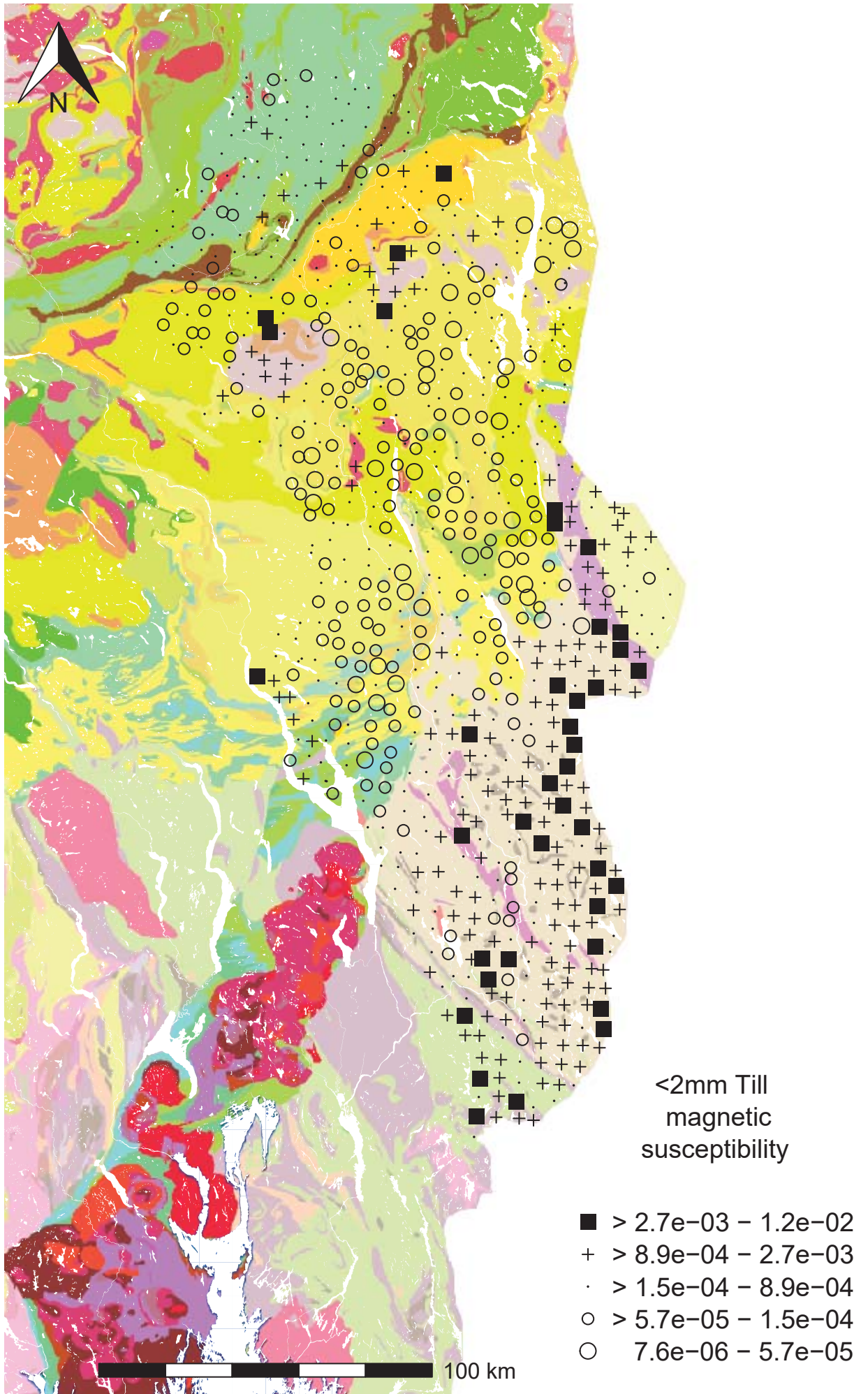
















GEOLOGICAL  
SURVEY OF  
NORWAY

· NGU ·

Geological Survey of Norway  
PO Box 6315, Sluppen  
N-7491 Trondheim, Norway

Visitor address  
Leiv Eirikssons vei 39  
7040 Trondheim

Tel (+ 47) 73 90 40 00  
E-mail [ngu@ngu.no](mailto:ngu@ngu.no)  
Web [www.ngu.no/en-gb/](http://www.ngu.no/en-gb/)